

Housheng Su
Xiaofan Wang

Pinning Control of Complex Networked Systems

Synchronization, Consensus and Flocking
of Networked Systems via Pinning



上海交通大学出版社
SHANGHAI JIAO TONG UNIVERSITY PRESS



Springer

Pinning Control of Complex Networked Systems

Housheng Su • Xiaofan Wang

Pinning Control of Complex Networked Systems

Synchronization, Consensus and Flocking
of Networked Systems via Pinning



上海交通大学出版社
SHANGHAI JIAO TONG UNIVERSITY PRESS

 Springer

Housheng Su
Department of Control Science
and Engineering
Huazhong University of Science
and Technology
Wuhan, People's Republic of China

Xiaofan Wang
Department of Automation
Shanghai Jiao Tong University
Shanghai, People's Republic of China

ISBN 978-3-642-34577-7

ISBN 978-3-642-34578-4 (eBook)

DOI 10.1007/978-3-642-34578-4

Springer Heidelberg New York Dordrecht London

Jointly published with Shanghai Jiao Tong University Press, Shanghai

ISBN: 978-7-313-09022-5 Shanghai Jiao Tong University Press, Shanghai

Library of Congress Control Number: 2012955134

© Shanghai Jiao Tong University Press, Shanghai and Springer-Verlag Berlin Heidelberg 2013

This work is subject to copyright. All rights are reserved by the Publisher, whether the whole or part of the material is concerned, specifically the rights of translation, reprinting, reuse of illustrations, recitation, broadcasting, reproduction on microfilms or in any other physical way, and transmission or information storage and retrieval, electronic adaptation, computer software, or by similar or dissimilar methodology now known or hereafter developed. Exempted from this legal reservation are brief excerpts in connection with reviews or scholarly analysis or material supplied specifically for the purpose of being entered and executed on a computer system, for exclusive use by the purchaser of the work. Duplication of this publication or parts thereof is permitted only under the provisions of the Copyright Law of the Publisher's location, in its current version, and permission for use must always be obtained from Springer. Permissions for use may be obtained through RightsLink at the Copyright Clearance Center. Violations are liable to prosecution under the respective Copyright Law.

The use of general descriptive names, registered names, trademarks, service marks, etc. in this publication does not imply, even in the absence of a specific statement, that such names are exempt from the relevant protective laws and regulations and therefore free for general use.

While the advice and information in this book are believed to be true and accurate at the date of publication, neither the authors nor the editors nor the publisher can accept any legal responsibility for any errors or omissions that may be made. The publisher makes no warranty, express or implied, with respect to the material contained herein.

Printed on acid-free paper

Springer is part of Springer Science+Business Media (www.springer.com)

*To my parents Zhongzhi Su and Dongmei
Wang*

—Housheng Su

*To my wife Hong Liu and daughter Rong
Wang*

—Xiaofan Wang

Preface

One of the main purposes for the study of complex network topology and modeling is to understand the influence of network structure on its function and consequently to find effective ways to improve network performance. In practice, directly controlling every node in a dynamical network with a huge number of nodes might be impossible but might also be unnecessary. Therefore, a pinning control strategy, that is, to achieve the goal of control by directly adding control input to a fraction of nodes selected from the network, is very important for the control of networked systems.

This monograph intends to investigate the synchronization, consensus and flocking of networked systems via pinning control strategy, which aims to control the whole dynamical network via imposing controllers on only a fraction of nodes. For a dynamical network with fixed and connected topology, the feasibility and effectiveness of different pinning control strategies are investigated. For a dynamical network with time-varying and possibly disconnected topology, consensus and flocking control of mobile multi-agent systems with limited communication capabilities are studied. Research on pinning control of networked systems can not only help better understand the mechanisms of natural collective phenomena, but also benefit the applications in mobile sensor/robot networks.

This monograph is organized as follows. Chapter 1 overviews recent research in pinning control of complex networked systems. Chapters 2 and 3 introduce synchronization of complex dynamical networks via pinning, including pinning control for complete synchronization and pinning control for cluster synchronization. Chapters 4 and 5 study consensus of multi-agent systems via pinning, including distributed pinning-controlled second-order consensus of multi-agent systems and distributed pinning-controlled consensus in a heterogeneous influence network. The pinning-controlled flocking of multi-agent systems is investigated with a virtual leader in Chap. 6 and with preserved network connectivity in Chap. 7, respectively.

We would like to thank those colleagues who have helped us on the topics of this book. They are Professor Guanrong Chen of City University of Hong Kong, Professor Zongli Lin of University of Virginia, Professor Xiang Li of Fudan University, Professor Michael Zhiqiang Chen of the University of Hong Kong, Professor Zhi-

hai Rong of Donghua University and Doctor Wen Yang of East China University of Science and Technology. We gratefully acknowledge the support of the National Natural Science Foundation of China under Grant Nos. 61074125 and 61104140, the Research Fund for the Doctoral Program of Higher Education (RFDP) under Grant No. 20100142120023, the Natural Science Foundation of Hubei Province of China under Grant No. 2011CDB042.

Wuhan, China
Shanghai, China

Housheng Su
Xiaofan Wang

Contents

- 1 Overview 1**
 - 1.1 Introduction 1
 - 1.2 Synchronization of Complex Dynamical Networks via Pinning . . . 3
 - 1.2.1 Stability Conditions for Complete Synchronization 4
 - 1.2.2 Stability Conditions for Cluster Synchronization 5
 - 1.2.3 Selective Strategies of Pinning Control 7
 - 1.2.4 Controllable Regions 8
 - 1.2.5 Control Methodologies 8
 - 1.3 Consensus and Flocking of Multi-Agent Systems via Pinning . . . 9
 - 1.3.1 Single Virtual Leader Case 9
 - 1.3.2 Multiple Virtual Leaders Case 10
 - 1.3.3 Connectivity Maintenance 10
 - 1.4 Conclusions and Notes 11
 - References 11

- 2 Pinning Control for Complete Synchronization of Complex Dynamical Networks 17**
 - 2.1 Complex Network Models 17
 - 2.1.1 ER Random Network Model 17
 - 2.1.2 BA Scale-Free Network Model 19
 - 2.1.3 A Directed Scale-Free Network Model 20
 - 2.2 Stability Conditions for Complete Synchronization of Complex Dynamical Networks 20
 - 2.2.1 Global Stability Conditions 24
 - 2.2.2 Local Stability Conditions 25
 - 2.3 Virtual Control of Pinned Complex Dynamical Networks 27
 - 2.4 Selective Strategies of Pinning Control 32
 - 2.4.1 Pinning Control Based on Node-Degree 32
 - 2.4.2 Pinning Control Based on ControlRank 37
 - 2.5 Conclusions and Notes 41
 - References 42

3	Pinning Control for Cluster Synchronization of Complex Dynamical Networks	45
3.1	Problem Statement	45
3.2	Decentralized Adaptive Pinning Control Scheme	46
3.2.1	Algorithm Description	46
3.2.2	Main Results and Theoretical Analysis	46
3.2.3	Complete Synchronization Case	52
3.3	Simulation Study	53
3.3.1	Example 1: Three Clusters	54
3.3.2	Example 2: One Cluster	56
3.4	Conclusions and Notes	59
	References	59
4	Distributed Pinning-Controlled Second-Order Consensus of Multi-Agent Systems	61
4.1	Consensus Without Connectivity Assumptions	61
4.1.1	Problem Statement	62
4.1.2	Consensus Without a Leader	63
4.1.3	Consensus with a Leader	67
4.1.4	Simulation Study	70
4.2	Consensus with Preserved Network Connectivity	71
4.2.1	Problem Statement	72
4.2.2	Algorithm Design and Main Results	73
4.2.3	Consensus with a Virtual Leader	78
4.2.4	Simulation Study	83
4.3	Adaptive Consensus of Networked Mobile Agents with Nonlinear Dynamics	89
4.3.1	Problem Statement	90
4.3.2	Main Results	91
4.3.3	Simulation Study	96
4.4	Conclusions and Notes	99
	References	99
5	Distributed Pinning-Controlled Consensus in a Heterogeneous Influence Network	103
5.1	Backgrounds and Problem Statement	103
5.2	Consensus in a Heterogeneous Influence Network	104
5.3	Pinning Controlled Consensus in a Heterogeneous Influence Network	107
5.4	Conclusions and Notes	110
	References	110
6	Distributed Pinning-Controlled Flocking with a Virtual Leader	111
6.1	Introduction	111
6.2	Backgrounds and Problem Statement	113
6.3	Flocking with a Fraction of Informed Agents	115

6.3.1	Algorithm Description and Main Results	115
6.3.2	Cohesive Analysis	117
6.3.3	Velocity Matching Analysis	118
6.3.4	Collision Avoidance Analysis	123
6.4	Flocking with a Virtual Leader of Varying Velocity	123
6.4.1	Algorithm Description and Main Result	123
6.4.2	Theoretical Analysis	125
6.5	Simulation Study	128
6.5.1	Flocking with a Fraction of Informed Agents	128
6.5.2	Flocking with a Virtual Leader of Varying Velocity	130
6.5.3	Flocking with a Fraction of Informed Agents and a Virtual Leader of Varying Velocity	131
6.6	Conclusions and Notes	133
	References	135
7	Distributed Pinning-Controlled Flocking with Preserved Network Connectivity	137
7.1	Flocking Based only on Position Measurements	137
7.1.1	Background and Problem Statement	138
7.1.2	Fundamental Flocking Algorithm	138
7.1.3	Flocking with a Virtual Leader	143
7.1.4	Simulation Study	145
7.2	Adaptive Flocking of Multiple Agents Governed by Nonlinear Dynamics	149
7.2.1	Preliminaries and Problem Statement	150
7.2.2	Main Results	151
7.2.3	Simulation Study	156
7.3	Conclusions and Notes	158
	References	159
	Index	161

Chapter 1

Overview

Abstract This chapter overviews recent research results in pinning control of complex networked systems, which are roughly categorized as synchronization of complex dynamical networks via pinning, and consensus and flocking of multi-agent systems via pinning. Some background and motivation for pinning control of complex networked systems is provided. Theoretical and simulation analysis results regarding pinning control of networks with fixed and switching topologies are summarized. Finally, some future directions are pointed out.

Keywords Pinning control · Complex networked systems · Synchronization · Complex dynamical networks · Consensus · Flocking · Multi-agent systems

1.1 Introduction

Automatic control theory deals with influencing the behavior of dynamical systems, which is an interdisciplinary subfield of science. Many control strategies are proposed for different specific control systems, such as adaptive control, hierarchical control, intelligent control, optimal control, robust control, stochastic control, and distributed control.

With the rapid development in network theory, computer technology, and communication technology, the investigation of control theory is recently being further extended from a single dynamical system to multiple interconnected systems. In particular, the problem of coordinated control of multi-agent systems has received increasing interest in different fields including biology, physics, computer science, and control engineering, partly due to the wide applications in many control areas, including cooperative control of mobile robots and design of mobile sensor networks [1]. Coordinated control of multi-agent systems means that a large number of agents, relying only on its neighbors' local information, reach a coordinated motion, which are characterized by distributed control, local interactions and self-organization. Indeed, the spirit of coordinated control protocol is inspired by the pioneering models of Reynolds [2] and Vicsek [3]. Many versions of distributed coordinated control protocols have been proposed, including consensus, swarming, flocking, and rendezvous.

In recent years, there has also been increasing interest in the study of complex dynamical networks, which is partially spurred by the discovery of the small-world and scale-free properties of many natural and artificial complex networks [4]. In 1998, a small-world network model was proposed by Watts and Strogatz [5], which has the properties of a small average path length and a large clustering coefficient. The connectivity distribution of a small-world network peaks at an average value and decays exponentially. In the following year, a scale-free network model was proposed by Barabási and Albert [6]. Unlike the homogeneous distributions of small-world networks, scale-free networks have inhomogeneous degree distributions in a power-law form.

Synchronization phenomena are ubiquitous in nature. There has been significant interest in the study of synchronization from different fields (see, for example, [7, 8] and the references therein). Two main lines of research on the problems of synchronization have emerged from this study. On the one hand, the two pioneering papers on synchronization in coupled systems [9] and synchronization in chaotic systems [10] have stimulated a great deal of interest in the study of complete synchronization of coupled nonlinear dynamical systems. On the other hand, there has been much interest in the study of synchronization in dynamical networks with complex topologies in the past decade [4, 11].

Control will be a necessary means for guiding or forcing the network to achieve desired synchronization if a given network of dynamical systems is not synchronizable or if the synchronized state is not the desired state. In practice, directly controlling every node in a dynamical network with huge number of nodes might be impossible but might also be unnecessary. Therefore, a pinning control strategy, that is, to achieve the goal of control by directly adding control inputs to a fraction of nodes selected from the network, is very important for the control of networked systems. A pinning control algorithm was studied to suppress spatial chaos in coupled map lattices and multi-mode laser systems [12–14]. Wang and Chen firstly studied the control of a scale-free dynamical network to its equilibrium via pinning [15]. Li, Wang, and Chen further specified the stable conditions and bridged the pinning control with virtual control propagation to explore the efficiency of selective pinning strategies [16]. Since then, many researchers have contributed to the fruitful understandings in this topic, including complete synchronization, cluster synchronization, selective strategies, controllable regions, and control methodologies for different specific scenes. Recently, some experiments were proposed to illustrate the effectiveness of the pinning control strategy [17].

Subsequently, the idea of pinning control has also been applied to coordinated control of multi-agent systems. From the viewpoint of complex network theory, one of the main challenges with coordinated control of multi-agent systems is that the topology of the corresponding dynamical network is time-varying which depends on the states of all the agents in the network. Furthermore, connectivity of the initial network cannot guarantee connectivity of the network all the time. One way to overcome this difficulty is to assume that there is a real or virtual leader and that every agent is an informed agent which has the information of the leader so that a navigational feedback term could be added to every agent. In this way, all agents could

remain cohesive and asymptotically move with the same desired velocity no matter whether the initial network is connected or not. However, this assumption is in contrast with some nature examples and may be difficult to implement in engineering applications. Therefore, by using pinning control strategy, coordinated control of multi-agent systems with only a fraction of informed agents is more practical.

In this chapter, we overview recent research results in pinning control for synchronization of complex dynamical networks, and consensus and flocking of multi-agent systems via pinning, which include the following topics:

- (i) Stability conditions for synchronization of complex dynamical networks via pinning. It has been well known that the stability conditions for synchronization of complex dynamical networks via pinning depend on the intrinsic dynamics of the nodes and the topology of the network. Various methods have been investigated towards finding sufficient conditions for global or local asymptotic stability of the pinning process.
- (ii) Selective strategies of pinning control. The efficiency to fulfill different specifications varies from the network considered and the pinning strategies chosen. Selective pinning strategies play an important role to achieve better efficiency for stabilizing a complex networked system.
- (iii) Controllable regions. By evaluating the pinning controllable regions of a given complex dynamical network, one could decide on the effectiveness of a selective pinning strategy and select the best selective pinning strategy.
- (iv) Control methodologies. In order to adapt the different specifications in realistic scenario, many control methodologies have been introduced for the pinning control of complex dynamical networks, including adaptive control, intermittent control, impulsive control, stochastic control, finite-time control, and control with time delays.
- (v) Consensus and flocking of multi-agent systems with real or virtual leaders. Leaders are commonly adopted to help the agents achieve a desired common velocity or arrive at a desired destination. In switching multi-agent networks, many versions of distributed coordinated control protocols have been investigated towards finding what sufficient conditions can guarantee the stability of the multi-agent systems and what agents should be chosen as pinned candidates.
- (vi) Connectivity maintenance. One effective way to achieve coordinated control is to design a protocol which could preserve connectivity of the network during the evolution. In this way, a single informed agent is enough to guide all other agents in the network.

1.2 Synchronization of Complex Dynamical Networks via Pinning

Consider a complex network consisting of N identical linearly and diffusively coupled nodes of n -dimensional dynamical system described by

$$\dot{x}_i(t) = f(x_i(t), t) + \sum_{j=1, j \neq i}^N c_{ij} a_{ij} \Gamma(x_j(t) - x_i(t)), \quad i = 1, \dots, N, \quad (1.1)$$

where $x_i = [x_i^1, \dots, x_i^n]^T \in \mathbf{R}^n$ is the state vector of the i th node, $t \in [0, +\infty)$ is continuous time, $f: \mathbf{R}^n \times [0, +\infty) \rightarrow \mathbf{R}^n$ is a continuous map, and c_{ij} denote the coupling strengths between node i and node j , $\Gamma = (\tau_{ij}) \in \mathbf{R}^{n \times n}$ is a matrix linking coupled variables, and if some pairs (i, j) , $1 \leq i, j \leq n$, with $\tau_{ij} \neq 0$, then it means two coupled nodes are linked through their i th and j th state variables, respectively.

1.2.1 Stability Conditions for Complete Synchronization

Network (1.1) is said to realize complete synchronization if

$$\lim_{t \rightarrow \infty} \|x_i(t) - x_j(t)\| = 0$$

for all i and j . The problem of pinning control for synchronization of network (1.1) is to directly control a fraction of nodes in the network to achieve

$$\lim_{t \rightarrow \infty} \|x_i(t) - \bar{x}(t)\| = 0, \quad i = 1, \dots, N,$$

where the homogeneous stationary state satisfies

$$f(\bar{x}(t), t) = 0. \quad (1.2)$$

The controlled network is described with a local negative feedback control law as follows:

$$\begin{aligned} \dot{x}_i(t) &= f(x_i(t), t) + \sum_{j=1, j \neq i}^N c_{ij} a_{ij} \Gamma(x_j(t) - x_i(t)) + h_i c_i \Gamma(\bar{x}(t) - x_i(t)), \\ i &= 1, \dots, N, \end{aligned} \quad (1.3)$$

where c_i is the feedback gain. If node i can obtain information from node j , then $a_{ij} = 1$; otherwise, $a_{ij} = 0$. If node i is selected for feedback, then $h_i = 1$; otherwise, $h_i = 0$.

Pinning control for synchronization of complex dynamical networks was firstly investigated in [15] for the stabilization of a scale-free dynamical network. A simple criterion for the local stabilization of complex dynamical networks was proposed, which depends on the topology of the network, the feedback gain, and the node intrinsic dynamics [15]. Li, Wang, and Chen further investigated both the global and local stabilization of complex dynamical networks via the pinning control strategy [16]. Sufficient conditions were presented to guarantee the convergence of complex dynamical networks locally and globally by pinning only one node [18]. Pinning control based on the Lyapunov V-stability approach was investigated, which

converts the network stability problem into the measurement of the negative definiteness of one simple matrix that characterizes the topology of the network [19]. Pinning-controlled networks were analyzed via a renormalization approach, which included two operations, edge weighting, and node reduction [20]. Based on the Lyapunov V-stability approach, a sufficient condition for the pinning control of uncertain complex networks was derived in terms of linear matrix inequalities [21]. In [22], the authors studied pinning control of complex dynamical networks with asymmetric and heterogeneous coupling. A low-dimensional condition without the pinning controllers involved for the pinning control of complex dynamical networks was proposed in [23]. By using the local pinning control algorithm, some sufficient conditions concerning the global stability of controlling a complex network with digraph topology to a homogeneous trajectory of the uncoupled system were derived in [24]. The authors proposed some low-dimensional pinning criteria for global synchronization of both directed and undirected complex networks [25]. Several pinning criteria were proposed to guarantee synchronization for the controlled dynamical network with uncertainties [26].

Due to the finite speeds of transmission and spreading as well as traffic congestions, in reality there usually are time delays in spreading and communication. Both delay-independent and delay-dependent asymptotical stability criteria were derived for a weighted general undirected complex dynamical network with constant time delay [27]. Some generic stability criteria ensuring delay-independent stability were derived for pinning control of complex dynamical networks with heterogeneous delays in both continuous-time and discrete-time domains [28]. By adding linear and adaptive feedback controllers to a fraction of nodes, some sufficient conditions for the global synchronization were obtained without assuming the symmetry of the coupling matrix [29]. Both linear and adaptive feedback schemes were used to pin a complex delayed dynamical network to a homogeneous trajectory [30]. The delayed dynamical network was theoretically proved to be asymptotically synchronized with linear feedback control, and to be exponentially asymptotically synchronized with adaptive feedback controllers [30]. Some less conservative criteria for both continuous-time and discrete-time complex dynamical networks with time delay were obtained by solving optimal problems of a series of linear matrix inequalities [31]. Some stability conditions were attained for pinning control of time-varying polytopic directed stochastic networks [32]. Several adaptive synchronization criteria were obtained for a given complex dynamical network with both delayed and non-delayed couplings [33]. In [34], the authors proposed some local stability conditions for pinning control of fractional-order weighted complex networks. Some criteria were derived for pinning stabilization of linearly coupled stochastic neural networks [35].

1.2.2 Stability Conditions for Cluster Synchronization

Suppose d nonempty subsets (clusters) $\{G_1, \dots, G_d\}$ form a partition of the index set $\{1, 2, \dots, N\}$, where $\bigcup_{l=1}^d G_l = \{1, 2, \dots, N\}$ and $G_l \neq \emptyset$. A network with N

nodes is said to realize d -cluster synchronization if

$$\lim_{t \rightarrow \infty} \|x_i(t) - x_j(t)\| = 0$$

for all i and j in the same cluster, and

$$\lim_{t \rightarrow \infty} \|x_i(t) - x_j(t)\| \neq 0$$

for all i and j in different clusters.

The problem of pinning control for d -cluster synchronization is to directly control a small fraction of nodes in network (1.1) to achieve

$$\lim_{t \rightarrow \infty} \sum_{l=1}^d \sum_{i \in G_l} \|x_i(t) - \bar{x}_l(t)\| = 0,$$

where $\bar{x}_l(t)$ is the desired state of the l th cluster G_l , which naturally is required to satisfy

$$\dot{\bar{x}}_l(t) = f(\bar{x}_l(t), t), \quad l = 1, \dots, d, \quad (1.4)$$

where $\bar{x}_l(t)$ is an equilibrium of the node system. The controlled network is described as follows:

$$\begin{aligned} \dot{x}_i(t) &= f(x_i(t), t) + \sum_{j=1, j \neq i}^N c_{ij} a_{ij} \Gamma(x_j(t) - x_i(t)) + h_i c_i \Gamma(\bar{x}_{\hat{i}}(t) - x_i(t)), \\ i &= 1, \dots, N, \end{aligned} \quad (1.5)$$

where \hat{i} is the subscript of the subset for which $i \in G_{\hat{i}}$. If node i is selected to be pinned, then $h_i = 1$; otherwise, $h_i = 0$.

Due to the specific goals in practice, many biological, social, and technological networks functionally divide into communities. Therefore, cluster synchronization of complex dynamical networks has received increasing interest and had many applications in practice. For example, two subgroups will be naturally formed in social networks when a crowd of people choose to accept or reject an opinion according to their preference. When a group of robots are to carry out a complex task, subtasks will divide the robot network into communities, and consensus should be achieved within each community. By introducing the inhibitory coupling to the coupling matrix, some sufficient conditions were presented to guarantee the cluster synchronization of linearly coupled complex networks under pinning control [36]. In [37], the authors investigated both local and global stability conditions for cluster synchronization of complex dynamical networks, in which at least those nodes with direct connections between groups in a network with community structure should be pinned. By introducing local adaptive strategies for both coupling strengths and feedback gains, it was shown that the collective dynamics of the underlying complex network can be controlled to its heterogeneous stationary states without requiring

global information of the network [38]. By proposing an adaptive pinning feedback to the coupling strength, the authors of [39] derived sufficient conditions for cluster synchronization with nonlinearly coupled nonidentical dynamical systems and asymmetrical coupling matrix. In [40], some sufficient conditions were derived to guarantee global cluster synchronization by using intermittent pinning control. In [41], several sufficient conditions were proposed to guarantee cluster synchronization of complex dynamical networks via the free matrix approach and stochastic analysis techniques, when at least one node in each cluster was pinned. Cluster synchronization of complex dynamical networks with community structure and non-identical nodes was studied via pinning control and adaptive coupling strength [42].

1.2.3 Selective Strategies of Pinning Control

Exploring network topology is crucial for understanding and predicting network dynamics. For example, using the inhomogeneous nature of scale-free networks, specifically applications, such as target immunization against epidemic spread [43] and high degree seeking algorithm in routing and searching [44], the performance is much better than that of random methods regardless of the topological characteristic of networks. An important topic in pinning control of complex dynamical networks is to study the relationship between network topology and effective pinning strategy. In [15], the authors showed that pinning the high-degree nodes is more efficient than pinning randomly chosen ones in an unweighted symmetrical scale-free network, but there is no significant difference between a random pinning scheme and a high-degree pinning scheme in a random network. In [16], the authors further proposed the concept of virtual control and showed why a high-degree pinning scheme is more effective than a random pinning one in a scale-free network. In order to increase the synchronization performance, it was shown that the nodes adjacent to the highest degree node are good candidates to be pinned [45]. The authors of [46] showed that a max-degree pinning scheme is better than a random pinning one in a disassortative network, while the combination of the two schemes is more effective in an assortative network. In [47], the authors illustrated that pinning the small nodes is better than pinning the big nodes when the portion of pinned nodes is relatively large in an unweighted symmetrical scale-free network, but pinning the big nodes is, in fact, always better than pinning the small ones in normalized weighted scale-free networks. The investigation in [48] showed that pinning the nodes with high betweenness centrality is usually more effective than pinning the ones with high degree, partly due to the fact that betweenness centrality contains more information with the degree as well as the shortest path. The authors illustrated that for any network structure, the pinning control performance was maximized via uniform pinning of all the network nodes [49]. For a scale-free directed dynamical network, it was shown that pinning a vertex with the largest ControlRank is much more effective than pinning a vertex with the largest out-degree [50]. The authors modified the traditional degree-based strategy, and used a decrease-and-conquer approach to

assign the best control strengths to the pinned highest-degree nodes, which provides better control performance than conventional methods, based on degree, betweenness centrality, and closeness [51].

1.2.4 Controllable Regions

It is very important for a complex dynamical system to evaluate the controllable regions of the system, which can help deciding on the effectiveness of a pinning control strategy, the number of nodes to be pinned, and the location of the pinned nodes in the entire network. Based on the eigenvalue analysis, the authors obtained the controllable regions directly in the control parameter space for both the diagonal coupling and nondiagonal couplings [52]. An extension of the master stability function approach was proposed for the controllability of networks under pinning control schemes, in which the controllable regions of the system were characterized by the coupling gain, the control gain, and the number of pinned nodes [53]. Several manageable criteria were proposed, and the effects of the network topology, the location and number of pinned nodes, and the nodes' intrinsic dynamics on the global pinning-controllability were analyzed for global pinning-controllability of complex networks [54]. In [55], the stable regions of the coupled network were clarified and the eigenvalue distribution of the asymmetric coupling and control matrices were specified for asymmetric complex dynamical networks.

1.2.5 Control Methodologies

In order to fulfill different specifications varying from model to model, different control methodologies were adopted for pinning control of complex dynamical networks. Based on a centralized adaptive strategy, it is possible to control the collective dynamics of a complex network with a weak coupling strength to a desired state by pinning only one single node [18]. In [36], the centralized adaptive strategy for complete synchronization of complex dynamical networks in [18] was extended to the case of adaptive cluster synchronization. By introducing local adaptive strategy on the feedback gains, several adaptive synchronization criteria were attained for weighted complex dynamical networks [56] and general complex dynamical networks [57]. A fully decentralized adaptive pinning control scheme for cluster synchronization of undirected complex dynamical networks by introducing local adaptive strategies to both coupling strengths and feedback gains was considered in [58, 59]. An adaptive pinning control scheme was investigated for a class of uncertain complex networks against network deterioration [60]. In order to achieve finite-time synchronization, discontinuous pinning controllers were designed for coupled neural networks [61]. Without traditional assumptions on control width, a pinning periodically intermittent scheme was designed for pinning control of complex delayed dynamical networks [62]. In order to be effective on the dynamical systems

which are subject to instantaneous perturbations at certain instants, pinning control of complex delayed dynamical networks was investigated by a single impulsive controller [63]. The synchronization of stochastic discrete-time networks was investigated via impulsive pinning controllers [64].

1.3 Consensus and Flocking of Multi-Agent Systems via Pinning

Consider a multi-agent system consisting of N agents of an n -dimensional dynamical system described by

$$\dot{x}_i(t) = f(x_i, u_i), \quad i = 1, \dots, N, \quad (1.6)$$

where $x_i = [x_i^1, \dots, x_i^n]^T \in \mathbf{R}^n$ is the state vector of the i th agent, f is a smooth vector field representing its dynamics, $u_i = [u_i^1, \dots, u_i^m]^T \in \mathbf{R}^m$ is the control input which can only use the states of its neighbors.

1.3.1 Single Virtual Leader Case

The problem of consensus with a virtual leader is to design control input u_i , $i = 1, 2, \dots, N$, such that

$$\lim_{t \rightarrow \infty} \|x_i(t) - x_\gamma(t)\| = 0, \quad (1.7)$$

for all $i = 1, 2, \dots, N$, where x_γ is the state of the virtual leader, which satisfies

$$\dot{x}_\gamma = f(x_\gamma). \quad (1.8)$$

If the state of each agent is composed of its position and velocity, then $x_i = [q_i, p_i]^T$, where q_i is the position of the i th agent and p_i is the velocity of the i th agent. The problem of flocking with a virtual leader is to design control input u_i , $i = 1, 2, \dots, N$, such that each agent can asymptotically approach the velocity of the virtual leader, the distance between any two agents is asymptotically stabilized, and collisions among the agents can be avoided.

Based on the artificial potential function method, the coordinated control of multiple autonomous agents was investigated with a virtual leader in [65]. The multi-agent consensus problem with an active leader and variable interconnection topology was studied via a neighbor-based state-estimation strategy in [66]. Consensus algorithms with a time-varying virtual leader were investigated for vehicles modeled by single integrator dynamics in [67]. Second-order consensus of multi-agent systems with a bounded control input and a fraction of informed agents was studied in [68]. Based on the contraction analysis and multiple Lyapunov functions, the consensus of multi-agent systems with general nonlinear coupling was investigated in [69]. The consensus problem for directed networks was investigated

via distributed nonlinear protocols [70]. Distributed discrete-time consensus with a time-varying reference state was studied in [71]. Second-order consensus of multi-agent systems was investigated with a virtual leader and nonlinear dynamics [72]. By introducing some predictive mechanism into a few pinning agents, consensus of multi-agent systems can be substantially accelerated [73]. The finite-time distributed consensus of multi-agent systems with a virtual leader was investigated by using a binary consensus protocol [74]. Second-order consensus of multi-agent systems with an active virtual leader and time-varying delays coupling was studied in [75]. Distributed coordinated tracking with reduced interaction was investigated via a variable structure method [76]. Consensus of multi-agent systems with a varying-velocity leader and input saturation was studied in [77]. Flocking of multi-agent systems with a virtual leader was investigated by incorporating information feedback into a few pinning agents [78].

1.3.2 Multiple Virtual Leaders Case

Most tracking problems in consensus and flocking of multi-agent systems are related to a single virtual leader. However, there are many missions in reality which include multiple goal seeking [79]. In the nest-building example, both birds, executing gender-specific networks, exhibit social nesting and feeding behavior directed toward multiple goal seeking [79]. Many social organisms move in groups when they forage or migrate. Within such a group, there are a few subgroups of informed individuals, each subgroup has a preferred direction of motion (representative of knowledge of location of food or migration route) [79, 80]. The flocking problem of controlling a group of mobile autonomous agents to track multiple virtual leaders with varying velocities was investigated in [81]. Second-order consensus of multi-agent systems on digraphs with multiple leaders was studied via pinning control [82]. Distributed containment control and surrounding control of multi-agent systems were investigated in [83] and [84], respectively.

1.3.3 Connectivity Maintenance

In coordinative control of a network of multi-agent systems, to guarantee the stability of the coordinated motion, a basic assumption typically is that the underlying topology of the network can maintain its connectivity frequently enough during the motion evolution. However, for a given set of initial conditions, this assumption is very difficult to satisfy and verify. In particular, the connectivity of the initial network generally cannot guarantee the connectivity of the network throughout the evolution. Ji and Egerstedt [85] proposed a hysteresis in adding new links and a special potential function to achieve rendezvous while preserving the network connectivity. Zavlanos, Jadbabaie, and Pappas [86] used the hysteresis and potential function

method to study a flocking problem combined with the network connectivity for double-integrator dynamics to achieve velocity alignment. Based on the bounded potential function method, rendezvous of multiple mobile agents was studied with preserved network connectivity [87]. A connectivity-preserving flocking algorithm for multi-agent systems based only on position measurements was proposed in [88]. By introducing local adaptive strategies to both the coupling strength and feedback gain, connectivity-preserving consensus and flocking algorithms were proposed for multi-agent nonlinear systems in [89] and [90], respectively.

1.4 Conclusions and Notes

In this chapter, we have reviewed some recent advances in pinning control of complex networked systems. However, there are also some unsolved challenging theoretical problems, including controllability and dynamical mechanisms. Also, we still lack a deep understanding of the relationship between the effectiveness of pinning control and the structure properties of a network. For example, we still do not know very well how to utilize the community structure to achieve better pinning control.

The idea of pinning control could also be applied to some other areas. One possible application is opinion formation in social networks. People form opinions over various issues and some issues such as how to educate children do not have an obvious best solution. Individuals try to engage in communication with their neighbors in order to learn from their experiences. Recently, Jadbabaie and his colleagues proposed a non-Bayesian learning rule which combines their personal experience and the views of their neighbors [91]. Under mild assumptions, agents could eventually aggregate information and reach the true underlying state of the world. Based on the idea of pinning control, we may ask a number of questions. For example, what is the influence of the positions of those most informed agents who have best prior views on the convergence speed and robustness of the algorithm. If only a fraction of agents are informed agents or even just one agent is informed agent, can the goal of social learning still be achieved? We expect better understanding of all these questions.

References

1. Ren W, Beard R, Atkins E (2007) Information consensus in multivehicle cooperative control: collective group behavior through local interaction. *IEEE Control Syst Mag* 27:71–82
2. Reynolds CW (1987) Flocks, herds, and schools: a distributed behavioral model. *Comput Graph* 21:25–34
3. Vicsek T, Cziro'ok A, Ben-Jacob E, Cohen Q, Shochet I (1995) Novel type of phase transition in a system of self-driven particles. *Phys Rev Lett* 75:1226–1229
4. Wang X, Chen G (2003) Complex networks: small-world, scale-free and beyond. *IEEE Circuits Syst Mag* 3:6–20

5. Watts DJ, Strogatz SH (1998) Collective dynamics of small world networks. *Nature* 393:440–442
6. Barabási AL, Albert R (1999) Emergence of scaling in random networks. *Science* 286:509–512
7. Wang X (2002) Complex networks: topology, dynamics, and synchronization. *Int J Bifurc Chaos* 12:885–916
8. Wu CW (2002) Synchronization in coupled chaotic circuits and systems. World Scientific, Singapore
9. Fujisaka H, Yamada T (1983) Stability theory of synchronized motion in coupled-oscillator systems. *Prog Theor Phys* 69:32–47
10. Pecora LM, Carroll TL (1990) Synchronization in chaotic systems. *Phys Rev Lett* 64:821–824
11. Wang X, Chen G (2002) Synchronization in scale-free dynamical networks: robustness and fragility. *IEEE Trans Circuits Syst I, Fundam Theory Appl* 49:54–62
12. Roy R, Murphy TW, Maier TDJ, Gills Z (1992) Dynamical control of a chaotic laser: experimental stabilization of a globally coupled system. *Phys Rev Lett* 68:1259–1262
13. Hu G, Qu ZL (1994) Controlling spatiotemporal chaos in coupled map lattice systems. *Phys Rev Lett* 72:68–71
14. Grigoriev RO, Cross MC, Schuster HG (1997) Pinning control of spatiotemporal chaos. *Phys Rev Lett* 79:2795–2798
15. Wang X, Chen G (2002) Pinning control of scale-free dynamical networks. *Physica A* 310:521–531
16. Li X, Wang X, Chen G (2004) Pinning a complex dynamical network to its equilibrium. *IEEE Trans Circuits Syst I, Fundam Theory Appl* 51:2074–2087
17. Porfiri M, Fiorilli F (2010) Experiments on node-to-node pinning control of Chua's circuits. *Physica D* 239:454–464
18. Chen T, Liu X, Lu W (2007) Pinning complex networks by a single controller. *IEEE Trans Circuits Syst I, Fundam Theory Appl* 54:1317–1326
19. Xiang J, Chen G (2007) On the V-stability of complex dynamical networks. *Automatica* 43:1049–1057
20. Xiang J, Chen G (2009) Analysis of pinning-controlled networks: a renormalization approach. *IEEE Trans Autom Control* 54:1869–1875
21. Wu Y, Wei W, Li G, Xiang J (2009) Pinning control of uncertain complex networks to a homogeneous orbit. *IEEE Trans Circuits Syst II, Express Briefs* 56:235–239
22. Xiang L, Liu Z, Chen Z, Chen F, Yuan Z (2007) Pinning control of complex dynamical networks with general topology. *Physica A* 379:298–306
23. Yu W, Chen G, Lü J (2009) On pinning synchronization of complex dynamical networks. *Automatica* 45:429–435
24. Lu W, Li X, Rong Z (2010) Global stabilization of complex directed networks with a local pinning algorithm. *Automatica* 46:116–121
25. Song Q, Cao J (2010) On pinning synchronization of directed and undirected complex dynamical networks. *IEEE Trans Circuits Syst I, Fundam Theory Appl* 57:672–680
26. Wang L, Sun Y (2010) Robustness of pinning a general complex dynamical network. *Nonlinear Dyn* 374:1699–1703
27. Liu Z, Chen Z, Yuan Z (2007) Pinning control of weighted general complex dynamical networks with time delay. *Physica A* 375:345–354
28. Xiang L, Liu Z, Chen Z, Chen F, Yuan Z (2008) Pinning control of complex dynamical networks with heterogeneous delays. *Comput Math Appl* 56:1423–1433
29. Guo W, Austin F, Chen S, Sun W (2009) Pinning synchronization of the complex networks with non-delayed and delayed coupling. *Phys Lett A* 373:1565–1572
30. Zhao J, Lu J, Zhang Q (2009) Pinning a complex delayed dynamical network to a homogeneous trajectory. *IEEE Trans Circuits Syst II, Express Briefs* 56:514–518
31. Xu D, Su Z (2009) Synchronization criterions and pinning control of general complex networks with time delay. *Appl Math Comput* 215:1593–1608

32. Xiong W, Ho D, Huang C (2010) Pinning synchronization of time-varying polytopic directed stochastic networks. *Phys Lett A* 374:439–447
33. Wang Z, Huang L, Wang Y, Zuo Y (2010) Synchronization analysis of networks with both delayed and non-delayed couplings via adaptive pinning control method. *Commun Nonlinear Sci Numer Simul* 15:4202–4208
34. Tang Y, Wang Z, Fang J (2009) Pinning control of fractional-order weighted complex networks. *Chaos* 19:013112
35. Lu J, Ho D, Wang Z (2008) Pinning stabilization of linearly coupled stochastic neural networks via minimum number of controllers. *IEEE Trans Neural Netw* 20:1617–1629
36. Wu W, Zhou W, Chen T (2009) Cluster synchronization of linearly coupled complex networks under pinning control. *IEEE Trans Circuits Syst I, Fundam Theory Appl* 56:829–839
37. Li K, Small M, Fu X (2008) Generation of clusters in complex dynamical networks via pinning control. *J Phys A, Math Theor* 41:505101
38. Su H, Rong Z, Chen MZQ, Wang X, Chen G, Wang H (2012) Decentralized adaptive pinning control for cluster synchronization of complex dynamical networks. *IEEE Trans Syst Man Cybern. Part B: Cybernetics*. doi:[10.1109/TSMCB.2012.2202647](https://doi.org/10.1109/TSMCB.2012.2202647)
39. Wang J, Feng J, Xu C, Zhao Y (2012) Cluster synchronization of nonlinearly-coupled complex networks with nonidentical nodes and asymmetrical coupling matrix. *Phys Lett A* 67:1635–1646
40. Liu X, Chen T (2011) Cluster synchronization in directed networks via intermittent pinning control. *IEEE Trans Neural Netw* 22:1009–1021
41. Li L, Cao J (2011) Cluster synchronization in an array of coupled stochastic delayed neural networks via pinning control. *Neurocomputing* 74:846–856
42. Wu Z, Fu X (2012) Pinning control of uncertain complex networks to a homogeneous orbit. *Commun Nonlinear Sci Numer Simul* 17:1628–1636
43. Pastor-Satorras R, Vespignani A (2001) Immunization of complex networks. *Phys Rev Lett* 65:036134
44. Adamic LA, Lukose R, Puniyani A (2001) Search in power-law networks. *Phys Rev Lett* 64:461351
45. Turci L, Macau E (2011) Performance of pinning-controlled synchronization. *Phys Rev E* 84:011120
46. Miao Q, Rong Z, Tang Y, Fang J (2008) Effects of degree correlation on the controllability of networks. *Physica A* 387:6225–6230
47. Zou Y, Chen G (2009) Choosing effective controlled nodes for scale-free network synchronization. *Physica A* 388:2931–2940
48. Rong Z, Li X, Lu W (2010) Pinning a complex network through the betweenness centrality strategy. In: *The IEEE international symposium on circuits and systems*, pp 1689–1692
49. Porfiri M, Fiorilli F (2009) Node-to-node pinning control of complex networks. *Chaos* 19:013122
50. Lu Y, Wang X (2008) Pinning control of directed dynamical networks based on ControlRank. *Int J Comput Math* 85:1279–1286
51. Tang W, Ng K, Jia Q (2010) A degree-based strategy for constrained pinning control of complex networks. *Int J Bifurc Chaos* 20:1533–1539
52. Zhan M, Gao J, Wu Y, Xiao J (2007) Chaos synchronization in coupled systems by applying pinning control. *Phys Rev E* 76:036203
53. Sorrentino F, Bernardo M, Garofalo F, Chen G (2007) Controllability of complex networks via pinning. *Phys Rev E* 75:046103
54. Porfiri M, Bernardo M (2008) Criteria for global pinning-controllability of complex networks. *Automatica* 44:3100–3106
55. Xiang L, Chen Z, Liu Z, Chen F, Yuan Z (2009) Stability and controllability of asymmetric complex dynamical networks: eigenvalue analysis. *Int J Mod Phys C* 20:237–252
56. Wang L, Dai H, Dong H, Cao Y, Sun Y (2008) Adaptive synchronization of weighted complex dynamical networks through pinning. *Eur Phys J B* 61:335–342

57. Zhou J, Lu J, Lü J (2008) Pinning adaptive synchronization of a general complex dynamical network. *Automatica* 44:996–1003
58. Delellis P, Bernardo M, Turci F (2010) Fully adaptive pinning control of complex networks. In: *Proceedings of 2010 IEEE international symposium on circuits and systems*, pp 685–688
59. Su H, Rong Z, Wang X, Chen G (2010) On decentralized adaptive pinning synchronization of complex dynamical networks. In: *Proceedings of 2010 IEEE international symposium on circuits and systems*, pp 417–420
60. Jin X, Yang G (2011) Adaptive synchronization of a class of uncertain complex networks against network deterioration. *IEEE Trans Circuits Syst I, Fundam Theory Appl* 58:1396–1409
61. Shen J, Cao J (2011) Finite-time synchronization of coupled neural networks via discontinuous controllers. *Cogn Neurodyn* 5:373–385
62. Cai S, Hao J, He Q, Liu Z (2011) Exponential synchronization of complex delayed dynamical networks via pinning periodically intermittent control. *Phys Lett A* 375:1965–1971
63. Zhou J, Wu Q, Xiang L (2011) Pinning complex delayed dynamical networks by a single impulsive controller. *IEEE Trans Circuits Syst I, Fundam Theory Appl* 58:2882–2893
64. Tang Y, Leung S, Wong W, Fang J (2010) Impulsive pinning synchronization of stochastic discrete-time networks. *Neurocomputing* 73:2132–2139
65. Leonard N, Frierelli E (2001) Virtual leaders, artificial potentials and coordinated control of groups. In: *Proc of the 40th IEEE conference on decision and control*, pp 2968–2973
66. Hong Y, Hu J, Gao L (2006) Tracking control for multi-agent consensus with an active leader and variable topology. *Automatica* 42:1177–1182
67. Ren W (2007) Multi-vehicle consensus with a time-varying reference state. *Syst Control Lett* 56:474–483
68. Ren W (2008) On consensus algorithms for double-integrator dynamics. *IEEE Trans Autom Control* 53:1503–1509
69. Chen F, Chen Z, Xiang L, Liu Z, Yuan Z (2009) Reaching a consensus via pinning control. *Automatica* 45:1215–1220
70. Liu X, Chen T, Lu W (2009) Consensus problem in directed networks of multi-agents via nonlinear protocols. *Phys Lett A* 373:3122–3127
71. Cao Y, Ren W, Li Y (2009) Distributed discrete-time coordinated tracking with a time-varying reference state and limited communication. *Automatica* 45:1299–1305
72. Song Q, Cao J, Yu W (2010) Second-order leader-following consensus of nonlinear multi-agent systems via pinning control. *Syst Control Lett* 59:553–562
73. Zhang H, Chen MZQ, Stan G (2011) Fast consensus via predictive pinning control. *IEEE Trans Circuits Syst I, Fundam Theory Appl* 58:2247–2258
74. Chen G, Lewis F, Xie L (2011) Finite-time distributed consensus via binary control protocols. *Automatica* 47:1962–1968
75. Lu X, Austin F, Chen S (2011) Flocking in multi-agent systems with active virtual leader and time-varying delays coupling. *Commun Nonlinear Sci Numer Simul* 16:1014–1026
76. Cao Y, Ren W (2012) Distributed coordinated tracking with reduced interaction via a variable structure approach. *IEEE Trans Autom Control* 57:33–48
77. Peng K, Su H, Yang Y (2009) Coordinated control of multi-agent systems with a varying-velocity leader and input saturation. *Commun Theor Phys* 5(2):449–456
78. Su H, Wang X, Lin Z (2009) Flocking of multi-agents with a virtual leader. *IEEE Trans Autom Control* 54:293–307
79. Portegys TE (2001) Goal-Seeking Behavior in a Connectionist model. *Artif Intell Rev* 16:225–253
80. Couzin ID, Krause J, Franks NR, Levin SA (2005) Effective leadership and decision-making in animal groups on the move. *Nature* 433:513–516
81. Su H, Wang X, Yang W (2008) Flocking in multi-agent systems with multiple virtual leaders. *Asian J Control* 10:238–245
82. Chen G, Lewis F (2012) Coordination of networked systems on digraphs with multiple leaders via pinning control. *Int J Syst Sci* 43:368–384

83. Cao Y, Stuart D, Ren W, Meng Z (2011) Distributed containment control for multiple autonomous vehicles with double-integrator dynamics: Algorithms and Experiments. *IEEE Trans Control Syst Technol* 19:929–938
84. Chen F, Ren W, Cao Y (2010) Surrounding control in cooperative agent networks. *Syst Control Lett* 59:704–712
85. Ji M, Egerstedt M (2007) Distributed coordination control of multiagent systems while preserving connectedness. *IEEE Trans Robot* 23:693–703
86. Zavlanos MM, Jadbabaie A, Pappas GJ (2007) Flocking while preserving network connectivity. In: *Proc of the 46th IEEE conference on decision and control*, pp 2919–2924
87. Su H, Wang X, Chen G (2010) Rendezvous of multiple mobile agents with preserved network connectivity. *Syst Control Lett* 59:313–322
88. Su H, Wang X, Chen G (2009) A connectivity-preserving flocking algorithm for multi-agent systems based only on position measurements. *Int J Control* 82:1334–1343
89. Su H, Chen G, Wang X, Lin Z (2011) Adaptive second-order consensus of networked mobile agents with nonlinear dynamics. *Automatica* 47:368–375
90. Su H, Chen G, Wang X, Lin Z (2010) Adaptive flocking with a virtual leader of multiple agents governed by nonlinear dynamics. In: *The 29th Chinese control conference*, pp 5827–5832
91. Jadbabaie A, Sandroni A, Tahbaz-Salehi A (2012) Non-Bayesian social learning. *Games Econ Behav* 76:210–225

Chapter 2

Pinning Control for Complete Synchronization of Complex Dynamical Networks

Abstract This chapter first introduces some complex network models and then gives both local and global stability conditions for complete synchronization of complex dynamical networks. In addition, the concept of virtual control of pinned complex dynamical networks is introduced to illustrate the principle of pinning control. The main reason is explained for why significantly less local controllers are required by specifically pinning the most highly connected nodes in a scale-free network than those required by the randomly pinning scheme, and why there is no significant difference between specifically and randomly pinning schemes for controlling random dynamical networks. Finally, a novel pinning scheme based on ControlRank (CR) is introduced, which is a vertex centrality index exploring the link structure of the directed networks. Moreover, it is shown that pinning the vertex with largest CR is much more effective than pinning the vertex with largest out-degree.

Keywords Complete synchronization · Virtual control · Complex network · ControlRank

2.1 Complex Network Models

In this section, we will introduce three complex network models, that is, ER random network model, BA scale-free network model and a new directed scale-free network model, which will be used in this chapter.

2.1.1 ER Random Network Model

The basic ER random network model is defined as a random graph of labeled N nodes connected by n edges, which are chosen randomly from all the $N(N - 1)/2$ possible edges. The network evolution is uniform: Starting with N nodes, every pair of nodes are connected with the same probability p (Fig. 2.1).

The main goal of the random graph theory is to determine in what connection probability p a particular property of a graph will likely arise. For a large N , the

Fig. 2.1 [1] Evolution of an ER random graph. One starts with $N = 10$ isolated nodes in (a), and connects every pair of nodes with probability (b) $p = 0.1$, (c) $p = 0.15$, and (d) $p = 0.25$, respectively

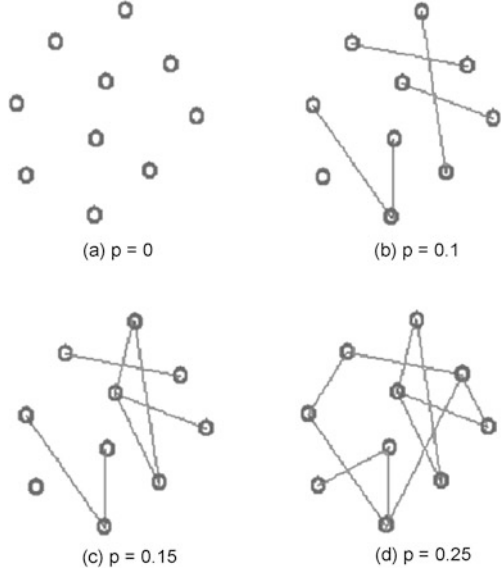
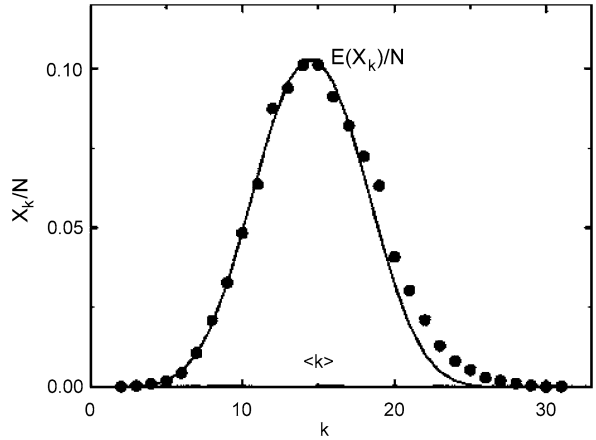


Fig. 2.2 [1] Degree distribution that results from the numerical simulation of an ER random network, which is generated with $N = 10000$ and connection probability $p = 0.0015$. (After Albert and Barabási [2])



ER model generates a homogeneous random network, whose connectivity approximately follows a Poisson distribution described by (Fig. 2.2)

$$P(k) \approx e^{-\langle k \rangle} \frac{\langle k \rangle^k}{k!} \quad (2.1)$$

where $\langle k \rangle$, the so-called average degree of the network, is the average of k_i over all i nodes in the network. With this connectivity distribution, nodes in the network are quite uniformly spread out, which is known as a homogeneous feature of the distribution.

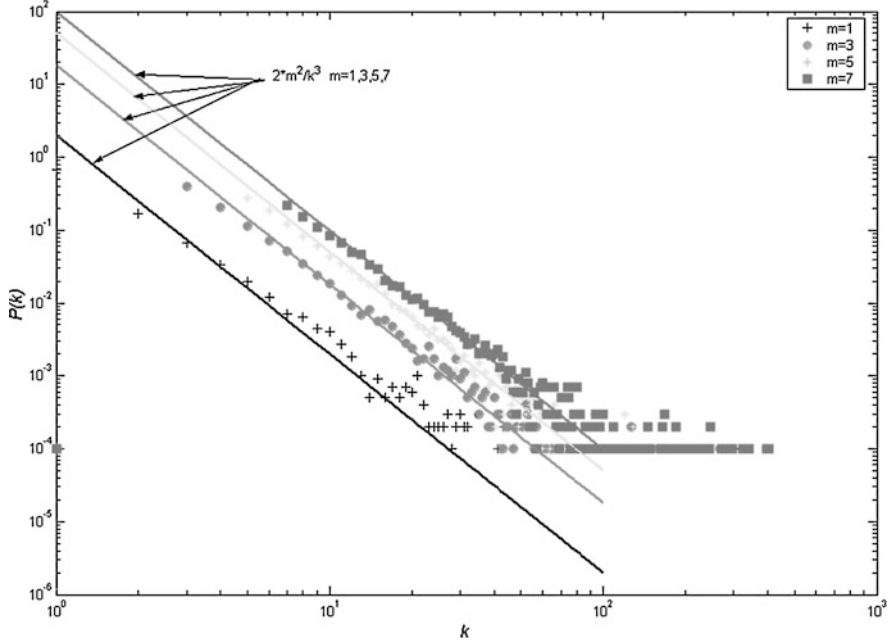


Fig. 2.3 [1] Degree distribution $P(k)$ of a BA scale-free model, with $N = m_0 + t = 10000$ and $m = m_0 = 1, 3, 5, 7$, respectively

2.1.2 BA Scale-Free Network Model

The BA scale-free model is generated as follows [1].

1. *Growth*: Starting with a small number (m_0) of nodes, at every time step, add a new node with $m (\leq m_0)$ edges that link the new node to m different nodes already presented in the network.
2. *Preferential attachment*: When choosing the nodes to which the new node connects, assume that the probability $\Pi(k_i)$ that a new node will be connected to node i depends on the degree k_i of node i , in such way that

$$\Pi(k_i) = \frac{k_i}{\sum_j k_j}. \quad (2.2)$$

After t time steps, we get a network having $N = t + m_0$ nodes and mt edges. This network evolves into a scale-invariant state with the probability that a node has k edges following a power-law distribution $P(k) \sim 2m^2k^{-\gamma_{\text{BA}}}$ with an exponent $\gamma_{\text{BA}} = 3$ (Fig. 2.3), where the scaling exponent γ_{BA} is independent of m , i.e., γ_{BA} is scale-invariant, and in this sense the network is said to be scale-free.

It has been suggested that the BA scale-free network model has captured the basic mechanisms, growth, and preferential attachment, responsible for the scale-free feature and “rich gets richer” phenomenon in many real-life complex networks [2–5].

2.1.3 A Directed Scale-Free Network Model

It has been demonstrated that many real complex networks display a scale-free feature [2, 5–7]. Since the BA model describes undirected scale-free networks [7, 8], some researchers have investigated models of directed scale-free networks [9–11].

Based on the Tadic model [11], a new directed scale-free network model was proposed in this subsection. Except for the power law property of its degree distribution, the directed model is also strongly connected, following the rules as follows:

1. *Strongly Connected.* At a unique time t , one vertex i ($i = t$) is added. Meanwhile, two old vertices n ($n \leq t$) and k ($k \leq t$) are selected connecting i by two directed links $n \rightarrow i$ and $i \rightarrow k$.
2. *Growth and Rearrangements.* When i is added, $M(t)(M(t) > 2)$ new links are distributed between all vertices. The first two links are added using following rule 1, then the other $M(t) - 2$ new links are added, in which $\alpha(M(t) - 2)$ ($0 \leq \alpha \leq 1$) new links are between i and the old vertices, whereas the rest $(1 - \alpha)(M(t) - 2)$ are links updated between the old vertices.
3. *Preferential Attachment.* The probability Π_{in} that the new link $n \rightarrow i$ going from an old vertex n depends on the in-degree $d_{\text{in}}(n, t)$ of n at t is

$$\Pi_{\text{in}} = \frac{\alpha(M(t) - 2) + d_{\text{in}}(n, t)}{(1 + \alpha)(M(t) - 2) \times t};$$

while the probability Π_{out} that the new link $i \rightarrow k$ pointing to an old vertex k depends on the out-degree $d_{\text{out}}(k, t)$ of vertex k at t is

$$\Pi_{\text{out}} = \frac{\alpha(M(t) - 2) + d_{\text{out}}(k, t)}{(1 + \alpha)(M(t) - 2) \times t}.$$

4. *Preferential Update.* Link $n \rightarrow k$ is established between two old vertices n and k , which are selected with probabilities Π_{out} and Π_{in} defined above.

As a result, a directed scale-free network is obtained, whose in-degree and out-degree both follow power law distribution (Fig. 2.4(a)–(b)), and the accumulation distribution of ControlRank is neither exponential distribution nor power law distribution, which follows a stretched exponential distribution (Fig. 2.4(c)). A proof of the power law distribution of the in-degree and out-degree can be found in [10, 11].

2.2 Stability Conditions for Complete Synchronization of Complex Dynamical Networks

Before stating the main results of this section, we need the following definitions and lemmas, which are taken from [13–16].

Definition 2.1 A function $\phi : \mathbf{R}^n \times \mathbf{R} \rightarrow \mathbf{R}^n$ is increasing if $(x - y)^T(\phi(x, t) - \phi(y, t)) \geq 0$ for all x, y, t .

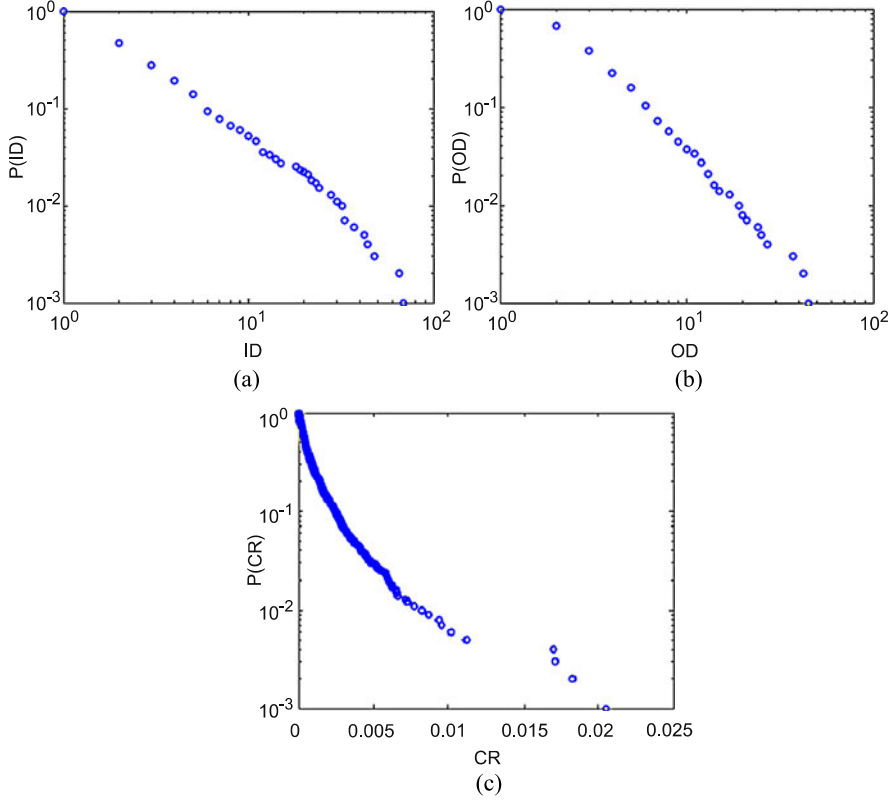


Fig. 2.4 [12] Accumulation distributions of in-degree (a), out-degree (b), and ControlRank (c) for a network of $N = 1000$ vertices with parameters $\alpha = 0.5$, $m_0 = 3$; $M(t) = M = 3$ directed links are added per time unit

Definition 2.2 A function $\phi : \mathbf{R}^n \times \mathbf{R} \rightarrow \mathbf{R}^n$ is uniformly increasing if there exists $c > 0$ such that for all x, y, t

$$(x - y)^T (\phi(x, t) - \phi(y, t)) \geq c \|x - y\|^2.$$

Definition 2.3 Given a square matrix V , a function $\phi : \mathbf{R}^n \times \mathbf{R} \rightarrow \mathbf{R}^n$ is V -uniformly increasing if $V\phi$ is uniformly increasing.

Definition 2.4 A function $\phi : \mathbf{R}^n \times \mathbf{R} \rightarrow \mathbf{R}^n$ is (V -uniformly) decreasing if $-\phi$ is (V -uniformly) increasing.

Definition 2.5 A function $f(x, t)$ is Lipschitz continuous in x with Lipschitz constant L_C^f if $\|f(x, t) - f(y, t)\| \leq L_C^f \|x - y\|$ for all x, y, t .

Lemma 2.1 If $f(x, t)$ is V -uniformly decreasing for a symmetric and positive definite matrix V , then $\dot{x} = f(x, t) + \eta(t)$ is asymptotically stable for all $\eta(t)$,

in the sense that $\|x - y\| \rightarrow 0$ as $t \rightarrow \infty$ where $\dot{x} = f(x, t)$, $x(t_0) = x_0$ and $\dot{y} = f(y, t)$, $y(t_0) = y_0$. Consequently, the zero solution of the error dynamics

$$\dot{e} = f(x, t) - f(y, t), \quad e(t_0) = x_0 - y_0$$

is asymptotically stable.

Lemma 2.2 Suppose $f(x, t)$ is Lipschitz continuous in x with Lipschitz constant $L_C^f > 0$ and V is symmetric and positive definite. If $\alpha > (L_C^f)/(\lambda_{\min}(V)) > 0$ where $\lambda_{\min}(V)$ is the smallest eigenvalue of V , then $\dot{x} = f(x, t) - \alpha V$ is asymptotically stable.

Definition 2.6 A matrix A is reducible if there exists a permutation matrix P such that PAP^T is of the form $\begin{pmatrix} B & C \\ 0 & D \end{pmatrix}$, where B and D are square matrices. Matrix A is irreducible if it is not reducible.

Definition 2.7

1. Let M_1 be the class of matrices such that their row i consists of zeros except for one entry α_i and one entry $-\alpha_i$ for some nonzero α_i .
2. The set W consists of all matrices with zero row sums, which have only nonpositive off-diagonal elements. The set W_i consists of all irreducible matrices in W .

Lemma 2.3 If A is a symmetric matrix in W , then A is positive semi-definite and has a zero eigenvalue associated with the eigenvector $(1, 1, \dots, 1)$. Furthermore, A can be decomposed as $A = M^T M$, where M is a matrix in M_1 . Furthermore, if A is irreducible, then the zero eigenvalue has multiplicity 1.

Definition 2.8 The Kronecker product of matrices A and B is defined as

$$A \otimes B = \begin{pmatrix} a_{11}B & \dots & a_{1m}B \\ \vdots & \ddots & \vdots \\ a_{n1}B & \dots & a_{nm}B \end{pmatrix}$$

where if A is an $n \times m$ matrix and B is a $p \times q$ matrix, then $A \otimes B$ is an $np \times mq$ matrix.

Definition 2.9 Vector $A \otimes f(x_i, t)$ is defined as

$$A \otimes f(x_i, t) = \begin{pmatrix} a_{11}f(x_1, t) + a_{12}f(x_2, t) + \dots + a_{1m}f(x_m, t) \\ \vdots \\ a_{n1}f(x_1, t) + a_{n2}f(x_2, t) + \dots + a_{nm}f(x_m, t) \end{pmatrix}$$

where if A is an $n \times m$ matrix and f is a $p \times 1$ function, then $A \otimes f(x_i, t)$ is a $np \times 1$ vector.

Suppose that a complex network consists of N identical linearly and diffusively coupled nodes, with each node being an n -dimensional dynamical system. In network (1.1), letting $a_{ii} = -\sum_{j=1, j \neq i}^N a_{ij}$, the coupling matrix $A = (a_{ij}) \in \mathbf{R}^{N \times N}$ represents the coupling configuration of the network, which is assumed in this section as a random network described by the ER model or a scale-free network described by the BA model. Then, the coupling matrix A is symmetric and the matrix $-A$ is in W (Definition 2.7).

Suppose the network is connected in the sense of having no isolated clusters. Then, the symmetric matrix A is irreducible. From Lemma 2.3, we know that zero is an eigenvalue of $-A$ with multiplicity 1, and other eigenvalues of $-A$ are strictly positive.

Suppose that we want to stabilize network (1.1) onto a homogeneous stationary state (1.2). To achieve the goal (1.2), we apply the pinning control strategy on a small fraction δ ($0 < \delta \ll 1$) of the nodes in network (1.1). Suppose that nodes i_1, i_2, \dots, i_l are selected, where $l = [\delta N]$ stands for the largest integer smaller than the real number δN . This controlled network can be described as

$$\begin{aligned} \dot{x}_{ik} &= f(x_{ik}) + \sum_{j=1, j \neq i_k}^N c_{ikj} a_{ikj} \Gamma(x_j - x_{ik}) + u_{ik}, \quad k = 1, 2, \dots, l, \\ \dot{x}_{ik} &= f(x_{ik}) + \sum_{j=1, j \neq i_k}^N c_{ikj} a_{ikj} \Gamma(x_j - x_{ik}), \quad k = l+1, l+2, \dots, N. \end{aligned} \quad (2.3)$$

For simplicity, we use the local linear negative feedback control law as follows:

$$u_{ik} = -c_{ik i_k} d_{ik} \Gamma(x_{ik} - \bar{x}), \quad k = 1, 2, \dots, l \quad (2.4)$$

where the coupling strength $c_{ik i_k}$ satisfies $c_{ik i_k} a_{ik i_k} + \sum_{j=1, j \neq i_k}^N c_{ikj} a_{ikj} = 0$, and the feedback gain $d_{ik} > 0$.

Without loss of generality, we rearrange the order of nodes in the network such that the pinned nodes $i_k, k = 1, 2, \dots, l$, are the first l nodes in the rearranged network.

Define the following two matrices:

$$\begin{aligned} D &= \text{diag}(d_1, d_2, \dots, d_l, 0, \dots, 0) \in \mathbf{R}^{N \times N}, \\ D' &= \text{diag}(c_{11}d_1, c_{22}d_2, \dots, c_{ll}d_l, 0, \dots, 0) \in \mathbf{R}^{N \times N}. \end{aligned}$$

Substituting (2.4) into (2.3), we can rearrange the controlled network (2.3) and write it by using the Kronecker product (Definition 2.9) as

$$\begin{aligned} \dot{x} &= f(x) - [(G + D') \otimes \Gamma]x + (D' \otimes \Gamma)\bar{X} \\ &= I_N \otimes f(x_i) - [(G + D') \otimes \Gamma]x + (D' \otimes \Gamma)\bar{X} \end{aligned} \quad (2.5)$$

where $\bar{X} = [\bar{x}^T, \dots, \bar{x}^T]^T$, and the elements g_{ij} of the symmetric irreducible matrix $G = (g_{ij}) \in \mathbf{R}^{N \times N}$ are defined as

$$g_{ij} = -c_{ij} a_{ij}. \quad (2.6)$$

It is easy to see that G is positive semi-definite, and $G + D'$ is positive definite with the minimal eigenvalue $\lambda_{\min}(G + D') > 0$.

2.2.1 Global Stability Conditions

Theorem 2.1 Suppose that Γ is symmetric positive semi-definite. Let T be a matrix such that $f(x) + Tx$ is V -uniformly decreasing for some symmetric positive definite matrix V . The controlled network (2.5) is globally stable about the homogeneous state \bar{x} if there exists a positive definite diagonal matrix U such that the matrix

$$(U \otimes V)[(G + D') \otimes \Gamma + I \otimes T] \quad (2.7)$$

is positive definite.

Proof Construct a Lyapunov function $g(\tilde{x}) = \frac{1}{2}\tilde{x}^T(U \otimes V)\tilde{x}$, which is radially unbounded with respect to \tilde{x} , where $\tilde{x} = x - \bar{x}$. The derivative of $g(\tilde{x})$ along the trajectories of the controlled network (2.5) is

$$\begin{aligned} \dot{g}(\tilde{x}) &= \tilde{x}^T(U \otimes V)\dot{\tilde{x}} \\ &= \tilde{x}^T(U \otimes V)[f(x) - f(\bar{x}) + (I \otimes T)\tilde{x} \\ &\quad - [(G + D') \otimes \Gamma + I \otimes T]\tilde{x}]. \end{aligned} \quad (2.8)$$

Hence, $\tilde{x}^T(U \otimes V)[f(x) - f(\bar{x}) + (I \otimes T)\tilde{x}]$ in (2.8) is non-positive because of the V -uniformly decreasing property of $f(x) + Tx$. From (2.7), $\tilde{x}^T(U \otimes V)[(G + D') \otimes \Gamma + I \otimes T]\tilde{x}$ is positive. Therefore, this theorem is proved by Lyapunov's direct method. \square

Theorem 2.2 Assume that $f(x)$ is Lipschitz continuous in x with a Lipschitz constant $L_C^f > 0$. If Γ is symmetric and positive definite, then the controlled dynamical network (2.5) is globally stable about the homogeneous state \bar{x} , provided that there exists a constant $\alpha = (L_C^f)/(\lambda_{\min}(\Gamma)) > 0$ such that

$$\lambda_{\min}(G + D') > \alpha \quad (2.9)$$

where $\lambda_{\min}(\Gamma)$ and $\lambda_{\min}(G + D)$ are the minimal eigenvalues of matrices Γ and $G + D$, respectively.

Proof With Lemma 2.2, there exists a constant $\alpha = (L_C^f)/(\lambda_{\min}(\Gamma))$ such that for any $\varepsilon > 0$ small enough, the trajectories of $\dot{x} = f(x) - (\alpha + \varepsilon)\Gamma x$ are uniformly decreasing. Denote $\lambda_{\min}(G + D') = \alpha + \delta > \alpha + \varepsilon$ with some $\delta > 0$. We can select

$U = I$, $V = I$, and $T = -(\alpha + \varepsilon)\Gamma$, so that the matrix

$$(U \otimes V)[(G + D') \otimes \Gamma + I \otimes T] = [G + D' - (\alpha + \varepsilon)I] \otimes \Gamma \quad (2.10)$$

is positive definite. Therefore, by Theorem 2.1, the controlled dynamical network (2.5) is globally stable about the homogeneous state \bar{x} , and this completes the proof of Theorem 2.2. \square

Theorem 2.2 gives a sufficient condition, inequality (2.9), for the existence of the coupling strength matrix $C_{\text{couple}} = (c_{ij})^{N \times N}$ that can stabilize the dynamical network (2.5). By making some further simplifications, we have the following constructive corollary.

Corollary 2.1 *Suppose that $c_{ij} = c$ and $d_i = cd$. The controlled dynamical network (2.5) is globally stable about the homogeneous state \bar{x} if*

$$c > \frac{L_C^f}{\lambda_{\min}(-A + \text{diag}(d, \dots, d, 0, \dots, 0)) \cdot \lambda_{\min}(\Gamma)}. \quad (2.11)$$

Remark 2.1 If we assume that Γ is only a constant 0–1 matrix, then using the Gershgorin theorem we can verify that only $\Gamma = \text{diag}(1, \dots, 1, 0, \dots, 0)_{n \times n}$ can satisfy the condition as a symmetric and positive semi-definite matrix described in Theorem 2.1, and Γ will be I_n for the symmetric and positive definite matrix described in Theorem 2.2. Hence, condition (2.11) in Corollary 2.1 can be simplified as

$$c > \frac{L_C^f}{\lambda_{\min}(-A + \text{diag}(d, \dots, d, 0, \dots, 0))}. \quad (2.12)$$

If the oscillator $\dot{x}_i = f(x_i)$ is chaotic, then the Lipschitz constant L_C^f of function f also means that for two arbitrary, different initial values x_i^1 and x_i^2 , the corresponding different trajectories should satisfy $\|f(x_i^1) - f(x_i^2)\| < L_C^f \|x_i^1 - x_i^2\|$ for all time t . Another more precise concept for a chaotic system is the Lyapunov exponent (LE). However, the relationship between the LEs of the coupled network (1.1) and those of uncoupled chaotic nodes is nontrivial, and only in some simplified coupling the relationship can be easily analyzed.

2.2.2 Local Stability Conditions

Theorem 2.3 *Consider the controlled network (2.3). Suppose that there exists a constant $\rho > 0$ such that $[Df(\bar{x}) - \rho]$ is a Hurwitz matrix, $c_{ij} = c$, $d_i = cd$, $\Gamma = I_n$.*

Let $\lambda_1 = \lambda_{\min}(-A + \text{diag}(d, \dots, d, 0, \dots, 0))$. If

$$c\lambda_1 \geq \rho, \quad (2.13)$$

then the homogeneous stationary state \bar{x} of the controlled network (2.3) is locally exponentially stable.

Proof Because $c_{ij} = c, d_i = cd, \Gamma = I_n$, we can simplify the controlled network (2.5) as

$$\begin{aligned} \dot{x}_i &= f(x_i) + c \sum_{j=1}^N a_{ij} x_j - cd(x_i - \bar{x}), \quad i = 1, 2, \dots, l, \\ \dot{x}_i &= f(x_i) + c \sum_{j=1}^N a_{ij} x_j, \quad i = l+1, l+2, \dots, N. \end{aligned} \quad (2.14)$$

Linearizing the controlled network (2.14) on the homogeneous stationary state \bar{x} leads to

$$\dot{\eta} = \eta [Df(\bar{x})] - cB\eta \quad (2.15)$$

where $D(f(\bar{x})) \in \mathbf{R}^{n \times n}$ is the Jacobian of f at \bar{x} , $\eta = (\eta_1, \eta_2, \dots, \eta_N)^T \in \mathbf{R}^{Nn}$, with $\eta_i(t) = x_i(t) - \bar{x}, i = 1, 2, \dots, N$, and $B = -A + \text{diag}(d, \dots, d, 0, \dots, 0)$.

Obviously, B is symmetric and positive definite, so all of its eigenvalues are positive, denoted as

$$0 < \lambda_{\min}(-A + \text{diag}(d, \dots, d, 0, \dots, 0)) = \lambda_1 < \lambda_2 < \dots < \lambda_N \quad (2.16)$$

with their corresponding (generalized) eigenvectors $\Phi = [\phi_1, \phi_2, \dots, \phi_N] \in \mathbf{R}^{N \times N}$ which satisfy

$$B\phi_k = \lambda_k \phi_k, \quad k = 1, 2, \dots, N.$$

Similarly, (2.15) can be expanded in the basis Φ into the following linear time-varying system:

$$\dot{v}_k^T = [Df(\bar{x}) - c\lambda_k] v_k^T, \quad k = 1, 2, \dots, N \quad (2.17)$$

where $\eta = \Phi v$ and v_k is the k th row of v , which is equivalent to condition (2.13). \square

Theorem 2.4 Assume that the node $\dot{x}_i = f(x_i)$ is chaotic for all $i = 1, 2, \dots, N$, with the maximum positive LE $h_{\max} > 0$. If $c_{ij} = c, d_i = cd, \Gamma = I_n$, then the controlled network (2.3) is locally asymptotically stable about the homogeneous state \bar{x} , provided that

$$c > \frac{h_{\max}}{\lambda_{\min}(-A + \text{diag}(d, \dots, d, 0, \dots, 0))}. \quad (2.18)$$

Proof Recall the concept of TLEs [17–19] for (2.15), denoted by $\mu_i(\lambda_k)$, for each $\lambda_k, k = 1, 2, \dots, N$, defined by

$$\mu_i(\lambda_k) = h_i - c\lambda_k, \quad i = 1, 2, \dots, m. \quad (2.19)$$

The TLEs characterize the behavior of the infinitesimal vectors, and determine the stability of the controlled states. Hence, the local stability of the controlled network (2.14) about the homogeneous state \bar{x} is converted into the negative TLEs of (2.17). Due to the order of $0 < \lambda_1 < \lambda_2 \leq \dots \leq \lambda_N$, it is obvious that the following condition must be satisfied:

$$\mu_{\max}(\lambda_2) = h_{\max} - c\lambda_1 < 0, \quad (2.20)$$

which is equivalent to condition (2.18). \square

2.3 Virtual Control of Pinned Complex Dynamical Networks

Let the coupling strength $c_{ij} = c$ and the feedback gain $d_i = cd$, as was in Corollary 2.1, and further set Γ as a 0–1 matrix. Rearranging the order of the nodes in the controlled dynamical network (2.3), and ordering the pinned nodes $i_k, k = 1, 2, \dots, l$, as the first l nodes, we have

$$\begin{aligned} \dot{x}_i &= f(x_i) + c \sum_{j=1}^N a_{ij} \Gamma x_j - cd \Gamma (x_i - \bar{x}), \quad i = 1, 2, \dots, l, \\ \dot{x}_i &= f(x_i) + c \sum_{j=1}^N a_{ij} \Gamma x_j, \quad i = l+1, l+2, \dots, N. \end{aligned} \quad (2.21)$$

From the stability conditions (2.11) and (2.12) [or (2.18)], the dynamical network (2.21) will be globally (or locally asymptotically) stable about the homogeneous stationary state \bar{x} , if

$$\begin{cases} \Gamma = I_m, \\ c > \frac{C}{\lambda_{\min}(-A + \text{diag}(d, \dots, d, 0, \dots, 0))}. \end{cases} \quad (2.22)$$

Here, C equals the L_C^f in Theorem 2.2 or the h_{\max} in Theorem 2.4.

Owing to the local error-feedback nature of each pinned node, it is guaranteed that, as the feedback control gain limit $d \rightarrow \infty$, the states of the controlled nodes can be pinned to the homogeneous target state \bar{x} . Hence, the pinning control stability of network (2.21) is converted to that of the following controlled network:

$$\begin{aligned} x_i &= \bar{x}, \quad i = 1, 2, \dots, l, \\ \dot{x}_i &= f(x_i) + c \sum_{j=l+1}^N a_{ij} \Gamma x_j + c \sum_{j=1}^l a_{ij} \Gamma \bar{x}, \quad i = l+1, l+2, \dots, N. \end{aligned} \quad (2.23)$$

Since

$$a_{ii} = \sum_{j=1, j \neq i}^N a_{ij} = - \left(\sum_{j=l+1, j \neq i}^N a_{ij} + \sum_{j=1}^l a_{ij} \right), \quad i = l+1, l+2, \dots, N, \quad (2.24)$$

network (2.23) can be equivalently rewritten in the form with a virtual control as

$$\begin{aligned} x_i &= \bar{x}, \quad i = 1, 2, \dots, l, \\ \dot{x}_i &= f(x_i) + c \sum_{j=l+1}^N \tilde{b}_{ij} \Gamma x_j + \tilde{u}_i, \quad i = l+1, l+2, \dots, N, \end{aligned} \quad (2.25)$$

where the virtual control laws are taken as

$$\tilde{u}_i = -c \tilde{d}_i (x_i - \bar{x}), \quad i = l+1, l+2, \dots, N, \quad (2.26)$$

with the virtual control feedback gains $\tilde{d}_i = \sum_{j=1}^l a_{ij}$.

Denote $\tilde{B} = (\tilde{b}_{ij}) \in \mathbf{R}^{(N-l) \times (N-l)}$ as

$$\begin{aligned} \tilde{b}_{ij} &= a_{ij}, \quad j \neq i, \quad j = l+1, \dots, N, \quad i = l+1, l+2, \dots, N, \\ \tilde{b}_{ii} &= - \sum_{j=1, j \neq i}^N a_{ij}, \end{aligned} \quad (2.27)$$

which is symmetric. Here, the matrix $-\tilde{B}$ is in W . It should be noted that a_{ij} in (2.27) are the rearranged elements in the original adjacency matrix A .

Given a pinning control strategy, that is, supposing that the nodes i_1, i_2, \dots, i_l are selected to be under pinning control, and $\tilde{A} \in \mathbf{R}^{(N-l) \times (N-l)}$ is a minor matrix of A with respect to the pinning control scheme, which is obtained by removing the i_1, i_2, \dots, i_l row-column pairs from A , we have

$$\tilde{A} = \tilde{B} + \text{diag}(\tilde{d}_{l+1}, \tilde{d}_{l+2}, \dots, \tilde{d}_N). \quad (2.28)$$

Recall that we have let the coupling strength be $c_{ij} = c$ and Γ be a 0–1 matrix.

Corollary 2.2 *If \tilde{A} is irreducible, then the dynamical network (2.25) with the virtual control (2.26) is globally (or locally asymptotically) stable about homogeneous state \bar{x} , provided that $\Gamma = I_m$ and*

$$c > \frac{C}{\lambda_{\min}(-\tilde{A})} \quad (2.29)$$

with C being the L_C^f in Theorem 2.2 (or the h_{\max} in Theorem 2.4).

Remark 2.2 If \tilde{A} is reducible, then, following Definition 2.6, \tilde{A} can be blocked into a series of irreducible matrices $\tilde{A}_1, \dots, \tilde{A}_n$. In this case, the corresponding subnet-

works will be globally (or locally asymptotically) stable about homogeneous state \bar{x} , provided that

$$c > \frac{C}{\max\{\lambda_{\min}(-\tilde{A}_j) \mid j = 1, 2, \dots, n\}} \quad (2.30)$$

with C being the L_C^f in Theorem 2.2 (or the h_{\max} in Theorem 2.4).

Clearly, we have the following order of the stable conditions (2.22), (2.29)–(2.30):

$$\begin{aligned} 0 &= \lambda_{\min}(-A) < \lambda_{\min}(-A + \text{diag}(d, \dots, d, 0, \dots, 0)) \\ &< \lim_{d \rightarrow \infty} \lambda_{\min}(-A + \text{diag}(d, \dots, d, 0, \dots, 0)) \\ &= \lambda_{\min}(-\tilde{A}) \\ &\leq \max\{\lambda_{\min}(-\tilde{A}_j) \mid j = 1, 2, \dots, m\}. \end{aligned} \quad (2.31)$$

With Lemma 2.1, it can be verified that the stable condition (2.29) in Corollary 2.2 for network (2.23) is the same as that for synchronizing the following network:

$$\dot{x}_i = f(x_i) + c \sum_{j=l+1}^N a_{ij} \Gamma x_j, \quad i = l+1, l+2, \dots, N. \quad (2.32)$$

Luckily, condition (2.29) is exactly the stable condition for synchronizing network (2.32). Hence, the whole pinned network, controlled by the small amount of local feedback controllers and those virtual controllers, is stabilized onto the homogeneous state \bar{x} via synchronization. This phenomenon will be visually illustrated in the simulation study below.

Pinning strategies mainly include random pinning and specific pinning schemes. In the random pinning scheme, we apply local feedback injections to a fraction δ of randomly selected nodes. While in the specific pinning scheme, we first pin the node of the highest degree, and then continue to select and pin the other nodes in a monotonically decreasing order of degrees.

In a star-like structure of a dynamical network, the kernel node is specifically selected to control for stabilizing the whole network. While in a ring or lattice, only specifically pinning a small amount of nodes is not sufficient to stabilize the whole ring, other factors such as the pinning distribution should also be taken into account. It was proposed in [20] that to stabilize a scale-free dynamical network, the specific pinning scheme requires much fewer local controllers than the random pinning scheme. To study the dynamics spreading in such complex networks in this section, we further perform a simulation-based topological analysis on the virtual control effect in different pinning strategies of complex networks, using the ER random network model and BA scale-free network model as prototypes.

Figure 2.5 is a mini-illustration of the virtual control process in the specific pinning scheme on a network generated by the BA scale-free model with $N = 10$,

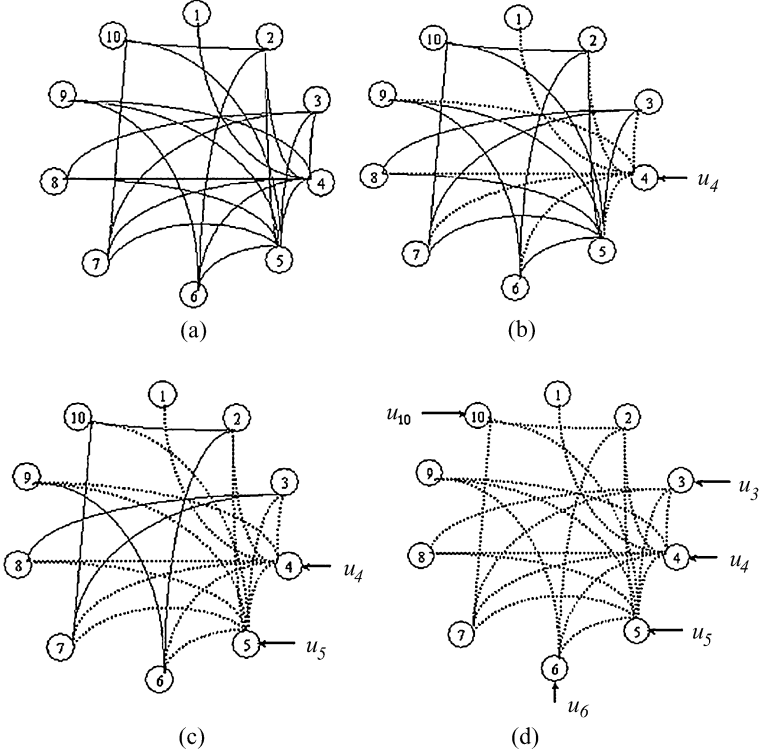


Fig. 2.5 [1] Illustration of virtual control (dotted line) in the specific pinning control of a network generated by BA scale-free model with $N = 10$, $m_0 = m = 3$

$m = m_0 = 3$. It can be observed that while the pinned nodes are stabilized onto the homogeneous state \bar{x} , their dynamics spread in the network as shown by the dotted lines, which is the virtual control. On the other hand, it can be found in Fig. 2.5(b) that the whole ten-node original network was broken into two parts: An isolated first node, which is only connected with the fourth node, and the remaining 8-node sub-network. While increasing the pinning fraction of nodes, this subnetwork continues to shrink, and finally reaches the case as shown in Fig. 2.5(d): every unpinned node is ‘isolated’ and virtually controlled by other pinned and also stabilized nodes.

It can be observed that the virtual control mainly affects the pinned network in two aspects: the percentage of the network that are virtually controlled, and the subnetwork scale that is virtually divided by those pinned nodes.

We have numerically analyzed the effect of virtual control in different pinning schemes for different topological networks. In the simulation, scale-free networks were generated by the BA scale-free model with $N = 3000$ and $m = m_0 = 3$, and random networks were generated by the ER random model containing 3000 nodes with 9000 connections.

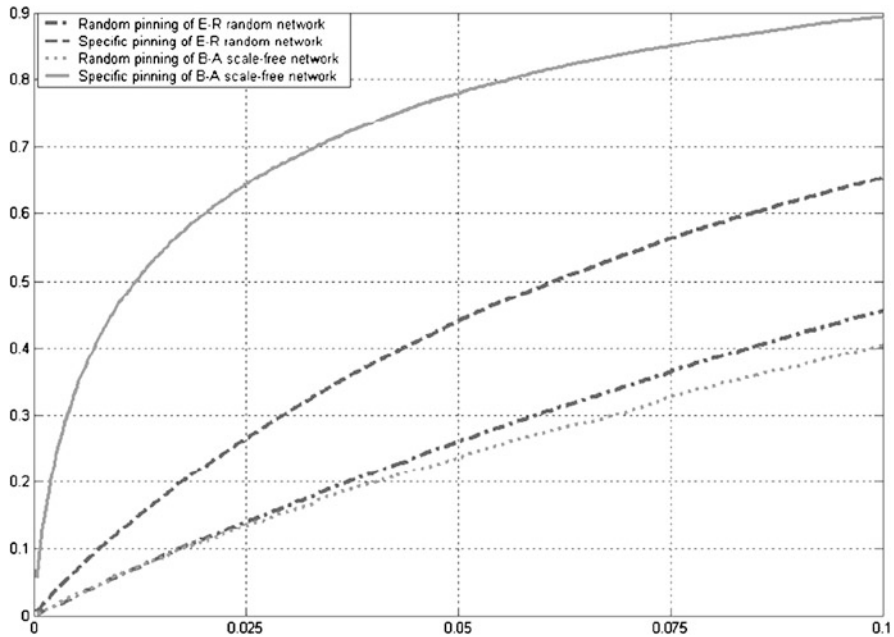


Fig. 2.6 [1] Virtually controlled percentage after pinning a fraction δ of nodes in the networks (10 random groups average output)

Figure 2.6 shows the percentage of those stabilized pinning-controlled nodes in the whole network, after pinning a fraction δ of nodes in an ER random network and in a BA scale-free network. It can be observed that, due to its extremely nonhomogeneous nature, almost 80 % of the nodes have been ‘virtually controlled’ by only 5 % of specifically pinned nodes in the 3000-node scale-free network. If randomly pinning 5 % of nodes, less than 30 % of nodes could be “virtually controlled.” The homogeneous nature of random networks results in the phenomenon that there is no significant difference between the random and specific pinning control schemes for the ER random networks.

Figure 2.7 shows the percentage of the largest cluster in the whole pinning-controlled network, after pinning a fraction δ of nodes in an ER random network and a BA scale-free network. If specifically pinning only 5 % of the “biggest” nodes in a scale-free network, the whole network could be virtually broken into many small clusters. Hence, with the ordered stable conditions (2.31), a smaller coupling strength threshold is required in the specific pinning scheme than that in the random pinning scheme for stabilizing scale-free networks. On the other hand, the whole random network was not dramatically disturbed as compared to the scale-free networks by randomly or specifically pinning a small fraction of nodes.

Hence, for random networks, there is no significant difference in its dynamics spreading when the specific pinning or the random pinning scheme is used. After stabilizing those pinned nodes by these two pinning schemes, the dynamics spread-

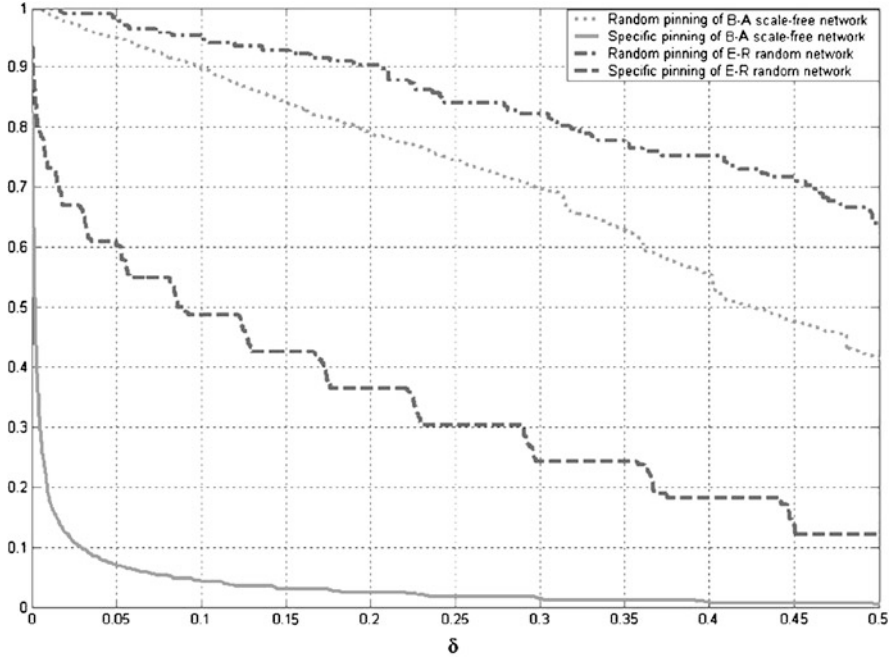


Fig. 2.7 [1] Largest cluster percentage after pinning a fraction δ of nodes in the networks (ten random groups average output)

ing behaviors are almost the same. On the other hand, much fewer local controllers will be required to control a scale-free network by the specific pinning scheme than that by the random pinning scheme. Furthermore, the dynamics of those specifically pinned nodes, which simply are the homogeneous states \bar{x} here, spread in the scale-free networks significantly faster than those of randomly pinned nodes. This phenomenon also reflects the ‘robustness and yet fragility’ property of scale-free networks.

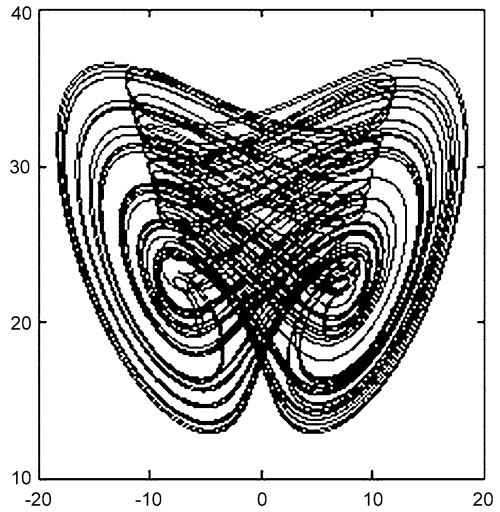
2.4 Selective Strategies of Pinning Control

2.4.1 Pinning Control Based on Node-Degree

Consider a scale-free dynamical network of the chaotic Chen’s oscillators. A single Chen’s oscillator is described in the dimensionless form by

$$\begin{pmatrix} \dot{x}_1 \\ \dot{x}_2 \\ \dot{x}_3 \end{pmatrix} = \begin{pmatrix} p_1(x_2 - x_1) \\ (p_3 - p_2)x_1 - x_1x_3 + p_3x_2 \\ x_1x_2 - p_2x_3 \end{pmatrix}. \quad (2.33)$$

Fig. 2.8 [1] The x_1 - x_3 plot of Chen's attractor



If the system parameters are selected as $p_1 = 35$, $p_2 = 3$, $p_3 = 28$, then the single Chen's system (2.33) has a chaotic attractor [21], as shown in Fig. 2.8. In this set of system parameters, one unstable equilibrium point of the oscillator (2.33) is $x^+ = [7.9373, 7.9373, 21]^T$.

Suppose that in each pair two connected Chen's oscillators are linked together through their identical sub-state variables, i.e., $\Gamma = \text{diag}(1, 1, 1)$. The entire dynamical network is described by the following state equations:

$$\begin{pmatrix} \dot{x}_{i1} \\ \dot{x}_{i2} \\ \dot{x}_{i3} \end{pmatrix} = \begin{pmatrix} p_1(x_{i2} - x_{i1}) + c \sum_{j=1}^N a_{ij}x_{j1} \\ (p_3 - p_2)x_{i1} - x_{i1}x_{i3} + p_3x_{i2} + c \sum_{j=1}^N a_{ij}x_{j2} \\ x_{i1}x_{i2} - p_2x_{i3} + c \sum_{j=1}^N a_{ij}x_{j3} \end{pmatrix}, \quad i = 1, 2, \dots, N. \quad (2.34)$$

We want to stabilize network (2.34) onto the originally unstable equilibrium point $\bar{x} = x^+$ by applying the local linear feedback pinning control to a small fraction δ of nodes. The equations of the controlled network are

$$\begin{pmatrix} \dot{x}_{i1} \\ \dot{x}_{i2} \\ \dot{x}_{i3} \end{pmatrix} = \begin{pmatrix} p_1(x_{i2} - x_{i1}) + c \sum_{j=1}^N a_{ij}x_{j1} + u_{i1} \\ (p_3 - p_2)x_{i1} - x_{i1}x_{i3} + p_3x_{i2} + c \sum_{j=1}^N a_{ij}x_{j2} + u_{i2} \\ x_{i1}x_{i2} - p_2x_{i3} + c \sum_{j=1}^N a_{ij}x_{j3} + u_{i3} \end{pmatrix}, \quad i = 1, 2, \dots, N, \quad (2.35)$$

where

$$u_{ij} = \begin{cases} -cd(x_{ij} - x^+), & i = i_1, i_2, \dots, i_l, j = 1, 2, 3, \\ 0 & \text{otherwise.} \end{cases}$$

It can be easily checked that the Lipschitz constant for the system is larger than 100, while the maximum positive LE is about 2.01745. In the simulation, we set $C = 2.01745$ and $d = 1000$ according to the stable condition (2.22).

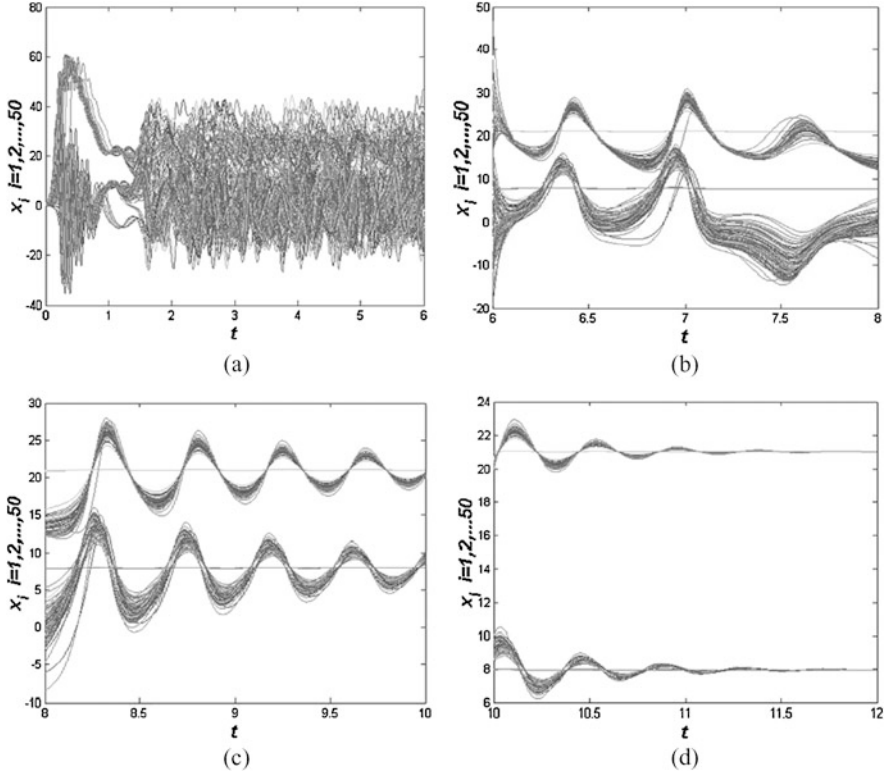


Fig. 2.9 [1] Specifically pinning the biggest node of 19 degrees in a 50-node network generated by the BA scale-free model: (a)–(d) are stabilizing phases with different coupling strengths; (a) $c = 0$, $d = 0$; (b) $c = 10$, $d = 1000$; (c) $c = 15$, $d = 1000$; (d) $c = 20$, $d = 1000$

Figure 2.9 visualizes the process of controlling a 50-node network generated by the BA scale-free model, where only the “biggest” node is pinned, which has 19 degrees, and the corresponding stable threshold of the coupling strength c is 6.2765. Figure 2.10 is the same stabilization process with two “biggest” nodes pinned, which have 19 degrees and 17 degrees, respectively, yielding a smaller threshold for the coupling strength $c = 3.4862$. It can be observed that increasing the pinning fraction δ will accelerate the convergence of the network stabilization, as shown in Fig. 2.11, though we also know that a bigger δ means more controllers are used.

Figure 2.12 is the counterpart by random pinning. If only randomly selecting two nodes as the same small fraction as in the previous specific pinning scheme, two nodes with 6 degrees and 9 degrees, respectively, are chosen for this round, and the corresponding stable condition threshold for the coupling strength c is 8.0895 with $d = 1000$. However, to achieve the stabilization of the whole network onto the same unstable equilibrium point x^+ , a much larger value of the coupling strength c is required in the random pinning scheme than that of the specific pinning scheme, as shown in Fig. 2.12(b)–(c). Increasing the pinning fraction to 10 % (5 nodes)

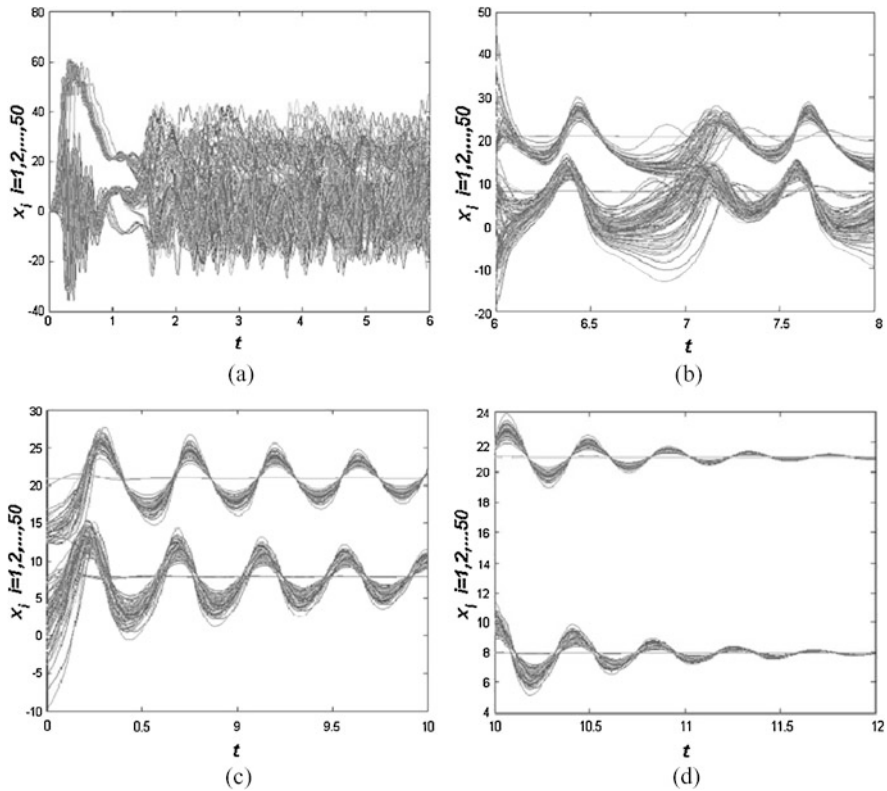


Fig. 2.10 [1] Specifically pinning two biggest nodes of 19 and 17 degrees, respectively, in the same 50-node network as in Fig. 2.9: (a)–(d) are stabilizing phases with different coupling strengths; (a) $c = 5$, $d = 0$; (b) $c = 5$, $d = 1000$; (c) $c = 8$, $d = 1000$; (d) $c = 10$, $d = 1000$

helps stabilize the whole network faster. This time, five nodes having 3, 3, 9, 3, 4, degrees, respectively, are selected for control, resulting in a corresponding threshold 5.4537. Figure 2.12(d) shows the stabilization process with the coupling strength $c = 15$. Hence, for the random pinning scheme, to achieve the same stabilization process as that by the specific pinning scheme, the costs are increasing in both the coupling strength and the pinning fraction. That is to say, to control such a scale-free dynamical network, random pinning control is much more “expensive” than specific pinning control, as compared to Fig. 2.13.

A common feature in this subsection is the synchronization phenomenon in the pinning-controlled dynamical networks, regardless of being stabilized onto the homogeneous state x^+ or not. The oscillation behavior of the smallest node in different pinning-controlled networks is a reflection of the dynamics spreading in scale-free networks, as shown in Figs. 2.11 and 2.13.

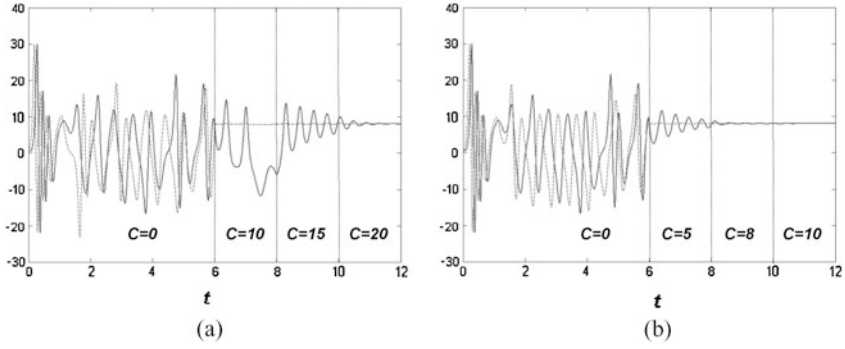


Fig. 2.11 [1] The convergence comparison of the smallest node for different specific pinning fractions. (a) Specifically pinning the biggest node: $N = 50$, the biggest node (—) and the smallest node (---). (b) Specifically pinning two biggest nodes: $N = 50$, the biggest node (—) and the smallest node (---)

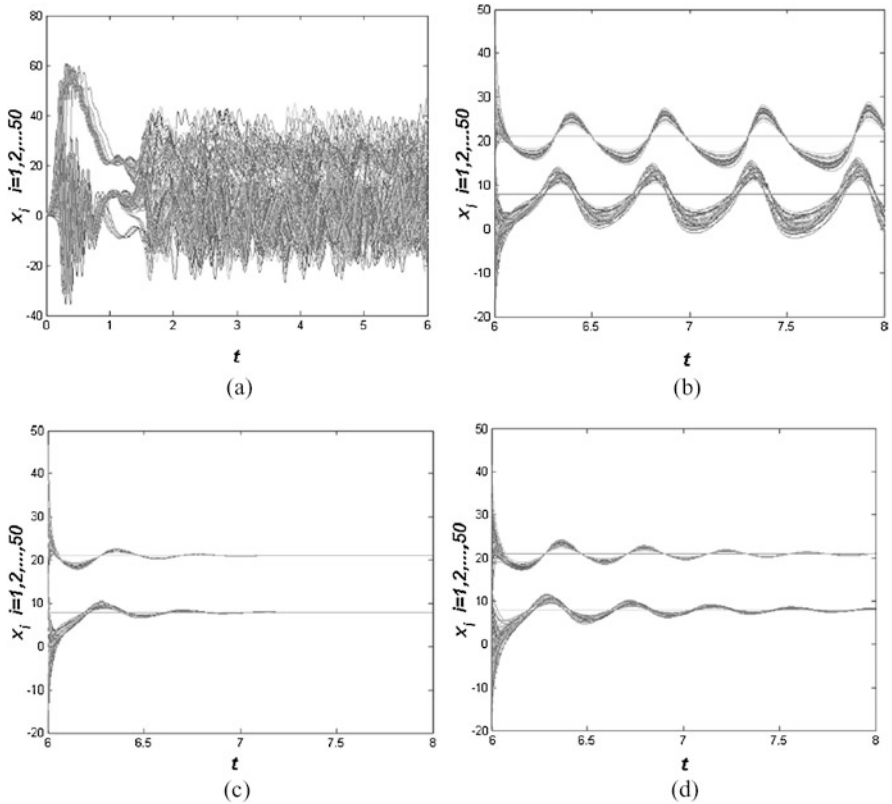


Fig. 2.12 [1] Randomly pinning some nodes in the same 50-node network as in Fig. 2.9. In (b) and (c), two nodes having 6 degrees and 9 degrees, respectively, are randomly selected for control with feedback gain $d = 1000$ and the coupling strength $c = 15, 30$, respectively. In (d), five nodes are randomly selected for the feedback control with gain $d = 1000$ and coupling strength $c = 15$

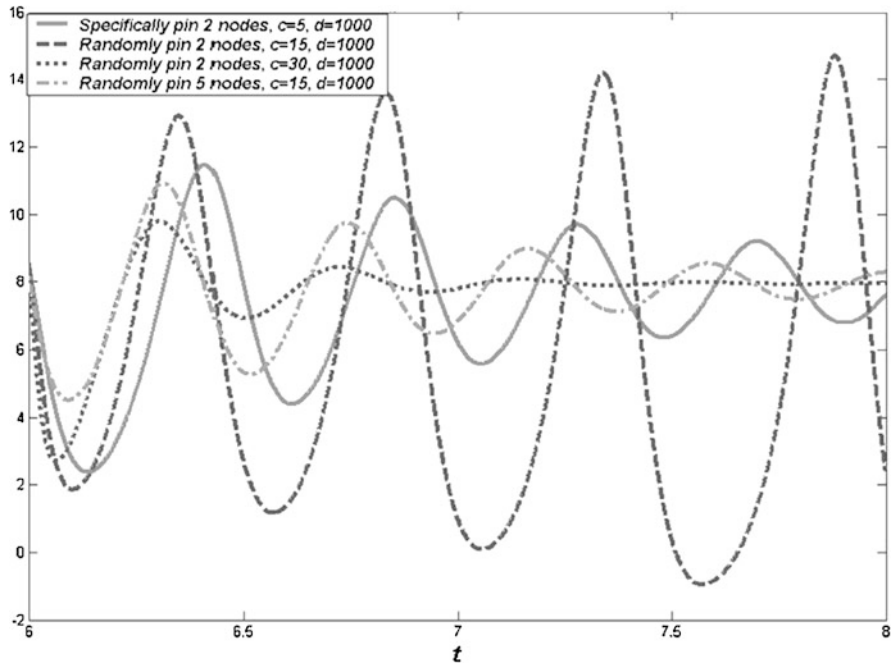


Fig. 2.13 [1] Stabilization process of the smallest node: comparison of the dynamics spreading and controllers' costs by using different pinning schemes

2.4.2 Pinning Control Based on ControlRank

It has been shown for a class of undirected dynamical networks that applying local linear feedback injections to a small fraction of the most highly connected vertices is much more effective than pinning the same number of randomly selected vertices [1, 20, 22]. However, vertex degree as a general index has exploited only little information of the relationships among vertices. Here, the purpose is trying to develop a new effective pinning scheme for directed networks.

In order to efficiently explore the implicative control ability of vertices in dynamical networks, we propose a new vertex centrality index called ControlRank (CR). CR is inspired by PageRank [23, 24], which is used in Google search engine for scoring and ranking web pages from link analysis. CR does not only depend on out-degrees but also makes full use of the link structure of networks. Meanwhile, factors affecting CR are related to the lower bound of pinning stabilizability in dynamical networks [25]. For a class of directed scale-free dynamical networks which are strongly connected, if the vertex of the largest CR is pinned, then the whole graph can be synchronized to its equilibrium better than when using the pinning strategy based on largest out-degree.

Suppose that we want to stabilize network (1.1) onto a homogeneous stationary state (1.2). Assume the coupling strengths in network (1.1) are the same, $c_{ij} = c$ and $d_i = cd$.

Synchronization can be achieved by pinning only if the network is strongly connected and the coupling strength is sufficiently large [26, 27]. Recently, rigorous mathematical proof demonstrates that such a stabilization goal can be achieved by pinning even a single vertex [28], and the bounds of the stabilizability are analytically estimated as well [25].

The Laplacian matrix of a directed network is defined as $L = ID - \bar{A}$, where $ID = \text{diag}(ID'_1, ID'_2, \dots, ID'_N)$ is the diagonal matrix of vertex in-degrees and \bar{A} is the adjacency matrix of the directed network. Clearly, L is a zero row sums matrix with non-positive off-diagonal elements and thus $e = [1, \dots, 1]^T$ is a right-eigenvector of L corresponding to its largest eigenvalue zero. Suppose that the vertices i_1, i_2, \dots, i_l are selected as pinned vertices, and let $\tilde{L} \in \mathbf{R}^{(N-l) \times (N-l)}$ be the minor matrix of L with respect to the pinning strategies, which is obtained by removing the i_1, i_2, \dots, i_l row-column pairs of L .

The network is synchronizable if [25]

$$c > \frac{\rho}{\text{Re } \lambda_1(\tilde{L})}, \quad (2.36)$$

here, ρ is a positive constant which guarantees a construct matrix to be an M-matrix for proof of the criterion. $\text{Re } \lambda_1(\tilde{L})$ is the smallest real part of the eigenvalues of \tilde{L} . In criterion (2.36), $\text{Re } \lambda_1(\tilde{L})$ is required to be a positive real number if and only if all vertices in the underlying network can be accessed by a certain vertex [27]. The lower bound of $\text{Re } \lambda_1(\tilde{L})$ can be directly obtained [25] from Schur Complement [29] and the results in [30]:

$$\text{Re } \lambda_1(\tilde{L}) \geq \frac{1}{2} \left\{ 2 \left[k + \frac{1}{2} (2k)^{-d} \right] \right\}^{-d} \quad (2.37)$$

where k is the largest out-degree of pinned vertices i_1, i_2, \dots, i_l , and d is the largest distance from the pinned vertices set to the unpinned set. Hence, a good pinning strategy should take into account the two factors of bound estimation, the out-degree in the pinned vertex set and the largest distance from the pinned to unpinned vertices.

CR is a vertex centrality index mining link structure of the directed networks, which is defined as follows

$$CR_i = \sum_{j \rightarrow i} \frac{CR_j}{ID_j}, \quad i = 1, 2, \dots, N, \quad (2.38)$$

where CR_i is the CR of vertex i , and ID_j is the in-degree of vertex j . Denoting $CR = (CR_1, CR_2, \dots, CR_N)$, we have the matrix form of (2.38) as follows:

$$CR = CR \times ID^{-1} \times \bar{A} \quad (2.39)$$

where each row of $ID^{-1} \times \bar{A}$ sums to 1 in a strongly connected network.

As a comparison, the PageRank (PR) vector used in Google is defined as [31, 32]:

$$PR = A \times OD^{-1} \times PR, \quad (2.40)$$

here, the column vector $PR = (PR_1, PR_2, \dots, PR_N)^T$, PR_i stands for the PR of vertex i , and OD is the diagonal matrix of the vertex out-degrees and each column of $\bar{A} \times OD^{-1}$ sums to 1 in a strongly connected network. Comparing (2.39) with (2.40), we can see a duality between CR and PR vectors: the CR vector of a graph is just the PR vector of the reversal graph, which is obtained by reversing direction of all links in the original graph. Just as PR is the right dominant eigenvector of $\bar{A} \times OD^{-1}$ associated with its largest eigenvalue 1, CR is the left dominant eigenvector of $ID^{-1} \times \bar{A}$ associated with its largest eigenvalue 1.

Suppose the network is strongly connected, then \bar{A} is primitive and irreducible. Meanwhile, $ID^{-1} \times \bar{A}$ is a row normalized stochastic matrix. As a result, $ID^{-1} \times \bar{A}$ has a unique dominant eigenvector, CR, which can be obtained by power iteration from any initial $CR^{(0)}$:

$$CR^{(k)} = CR^{(k-1)} \times ID^{-1} \times \bar{A}. \quad (2.41)$$

Obtain from link analysis of the whole graph, CR contains much more implicative topology information than out-degree and quantitatively measures vertex controllability in the network. On the one hand, CR is a vector of the vertices hub scores in PageRank and obtained by In-link normalization method [32]. As discussed in [32], CR has an obvious positive correlation with out-degrees. On the other hand, CR of a vertex is related to the largest distance from it to all the other vertices. At each iteration in (2.41), vertex j will contribute $CR_j \times \frac{1}{ID_j}$ to each in-degree neighbors, which is in direct ratio to $\frac{1}{ID_j}$. Then if there is a path of length two from vertex p to j through vertex i , j will contribute $CR_j \times \frac{1}{ID_i} \times \frac{1}{ID_j}$ to p indirectly through i in direct ratio to $\frac{1}{ID_i} \times \frac{1}{ID_j}$. Hence, the contribution of CR from j to p attenuates with increment of the length of path from p to j .

In sum, CR depends not only on the out-degree of the vertex, but also on the largest distance to other vertices from it, as illustrated in Fig. 2.14:

In the directed network as shown in Fig. 2.14, vertex 4 has the highest CR, which is of the largest out-degree, and can access the vertex of largest distance through a path of the smallest length.

Remarkably, the lower bound of pinning stability criterion (2.37) is specified by k and d , the largest out-degree of the pinned vertices and the largest distance from pinned vertices to those unpinned. Since CR will be affected by both factors, an intuitive consideration is that pinning a vertex of the largest CR will be a better strategy than pinning a vertex of the largest out-degree [22].

We illustrate the efficiency of the novel pinning strategy using the chaotic Lorenz oscillator [33] as a dynamical vertex in the directed scale-free network. Suppose that two coupled Lorenz oscillators are linked together through the first state variable, i.e., $\Gamma = \text{diag}(1, 0, 0)$. State equations of the network are described by

$$\begin{pmatrix} \dot{x}_{i1} \\ \dot{x}_{i2} \\ \dot{x}_{i3} \end{pmatrix} = \begin{pmatrix} -ax_{i1} + ax_{i2} + c \sum_{j=1}^N a_{ij} \Gamma x_{j1} \\ rx_{i1} - x_{i2} - x_{i1}x_{i3} \\ x_{i1}x_{i2} - bx_{i3} \end{pmatrix}, \quad i = 1, 2, \dots, N, \quad (2.42)$$

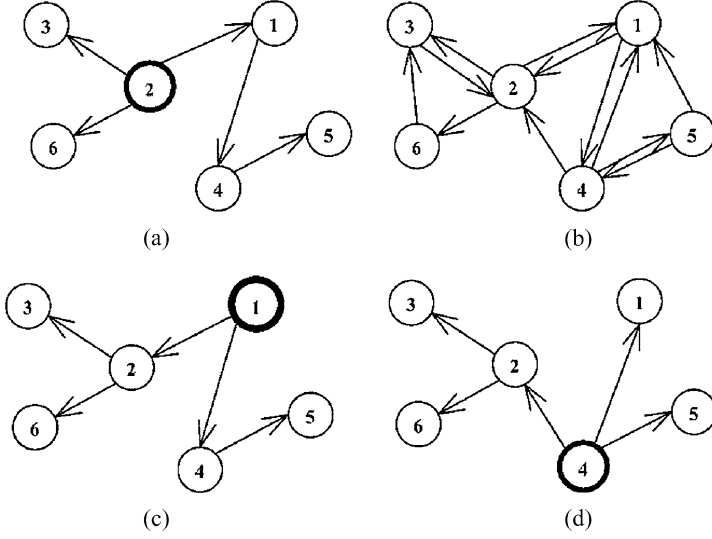


Fig. 2.14 [12] The original directed network is shown in (a); vertices 1, 2, and 4 are considered in (b), (c), and (d). For (b), vertex 1 with $OD_1 = 2$, $d_1 = 2$, $CR_1 = 0.2182$; for (c), vertex 2 with $OD_2 = 3$, $d_2 = 3$, $CR_2 = 0.1091$; for (d), vertex 4 with $OD_4 = 3$, $d_4 = 2$, $CR_4 = 0.3636$. OD_i and d_i , respectively, stand for the out-degree of vertex i and the largest distance from i to the other vertices

in which $a = 10$, $b = 8$, $r = 28$. For these parameters, an isolated oscillator has three unstable equilibriums as follows:

$$x^\pm = [\pm 8.4853 \quad \pm 8.4853 \quad 27]^T, \quad x^0 = [0 \quad 0 \quad 0]^T.$$

Suppose that we want to stabilize network (2.42) onto the homogeneous state x^- . The state equations of the pinned scale-free network are

$$\begin{pmatrix} \dot{x}_{i1} \\ \dot{x}_{i2} \\ \dot{x}_{i3} \end{pmatrix} = \begin{pmatrix} -ax_{i1} + ax_{i2} + c \sum_{j=1}^N a_{ij} \Gamma x_{j1} + u_i \\ rx_{i1} - x_{i2} - x_{i1}x_{i3} \\ x_{i1}x_{i2} - bx_{i3} \end{pmatrix}, \quad i = 1, 2, \dots, N, \quad (2.43)$$

where

$$u_i = \begin{cases} cd(x_1^- - x_{i1}), & i = i_1, i_2, \dots, i_l, \\ 0, & \text{otherwise,} \end{cases} \quad (2.44)$$

with the coupling strength c and feedback gain d .

Figure 2.15 visualizes the process of controlling a directed scale-free network of 100 vertices, where only one vertex is pinned with the given coupling strength $c = 70$ and feedback gain $d = 1000$. Figure 2.15(a) is the stabilization process with one randomly selected vertex pinned, and Figs. 2.15(b)–(c) are with one vertex of largest out-degree and largest CR, respectively. It can be observed that the specific pinning (Figs. 2.15(b) and 2.15(c)) stabilizes the whole network much faster than the random pinning strategy (Fig. 2.15(a)). Furthermore, considering the control performance

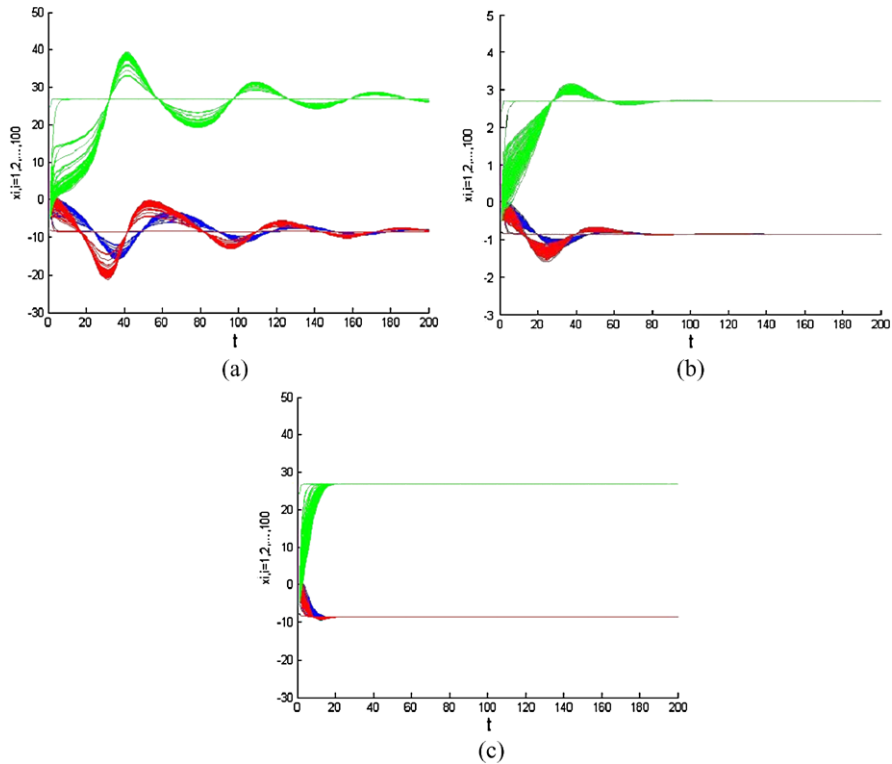


Fig. 2.15 [12] Pinning one vertex in the same 100-vertex network with the same coupling strength $c = 70$ and feedback gain $d = 1000$: (a) random pinning; (b) pinning one vertex of largest out-degree; (c) pinning one vertex of largest CR

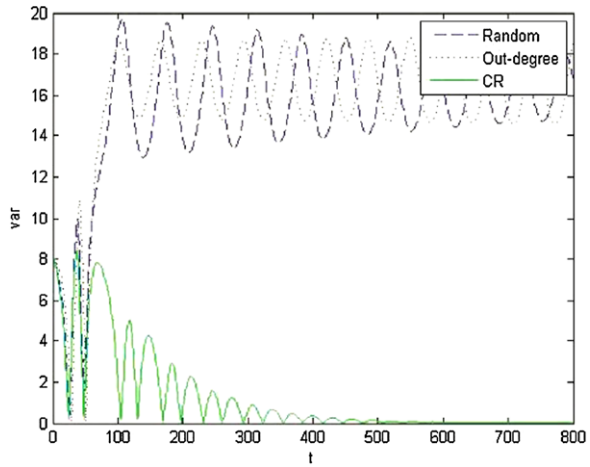
indices like rising time, peak time, and overshoot, Figs. 2.15(b) and 2.15(c) imply that CR-based pinning strategy yields better performance than that of the degree-based pinning strategy.

In the following simulation, we take $N = 1000$ and $m_0 = 3$, $M(t) = M = 3$, namely, the original network contains 1000 vertices with about 3000 links. We use variance $\text{var} = \frac{\sum_{i=1}^N (x_{i1}(t) - \bar{x}_{i1})^2}{N}$ to measure synchronization capacity, as shown in Fig. 2.16, which indicates that only the pinning strategy based on the largest CR can stabilize the given network. Therefore, the new pinning strategy is more effective even in large-scale networks.

2.5 Conclusions and Notes

In this chapter, we have derived some conditions for stabilizing a complex dynamical network onto its homogeneous state by only pinning a small fraction of the

Fig. 2.16 [12] Convergence comparison of the variance for different pinning strategies in the same directed scale-free network of 1000 Lorenz oscillators: coupling strength $c = 150$, feedback gain $d = 1000$. The *blue dashed line* is for the random pinning strategy, the *red dotted line* is for the specific strategy pinning vertex of the largest out-degree, and the *green solid line* is for the specific strategy pinning vertex of the largest CR (Color figure online)



network nodes using local feedback controllers. The placement of the local controllers is affected by the topology of the network. Based on the concept of virtual control, the pinned nodes virtually control other dynamical nodes through the connections among them. Furthermore, the whole network is virtually broken into parts of subnetworks, when those pinned nodes have been stabilized onto the homogeneous state by their local feedback controllers. Owing to the nonhomogeneous nature of scale-free networks, it is much easier to stabilize a scale-free network by specifically placing the local controllers on the big nodes with high degrees than by randomly placing these local controllers into the network. In contrast, to stabilize homogeneous networks such as random graphs, randomly pinning a fraction of network nodes will have no significant difference from specifically pinning those relatively big nodes. Since many real-life complex networks have scale-free features, maintaining the stability of their big nodes is the key to keep the stability of the whole network. On the other hand, for homogeneous networks, randomly stabilizing a fraction of nodes may help control the dynamics of the whole network effectively. Finally, we proposed a new pinning control strategy based on a new vertex centrality index ControlRank for directed dynamical networks. The CR vector is a dual form of the PR vector used in Google search engine for ranking vertices. An important future research topic is how to generalize the CR-based pinning strategy to directed networks which are not strongly connected. Moreover, the relationship between CR and the stabilizability criterion needs rigorous theoretic analysis.

References

1. Li X, Wang X, Chen G (2004) Pinning a complex dynamical network to its equilibrium. *IEEE Trans Circuits Syst I, Fundam Theory Appl* 51:2074–2087
2. Albert R, Barabási AL (2002) Statistical mechanics of complex networks. *Rev Mod Phys* 74:47–97

3. Dorogovtsev SN, Mendes JFF (2002) Evolution of networks. *Adv Phys* 51:1079–1187
4. Li X, Chen G (2003) A local-world evolving network model. *Physica A* 328:274–286
5. Newman MEJ (2003) The structure and function of complex networks. *SIAM Rev* 45:167–256
6. Albert R, Jeong H, Barabási AL (1999) Diameter of the World Wide Web. *Nature* 401:130–131
7. Barabási AL, Albert R (1999) Emergence of scaling in random networks. *Science* 286:509–512
8. Barabási AL, Albert R, Jeong H (2000) Scale-free characteristics of random networks: the topology of the World-Wide Web. *Physica A* 281:69–77
9. Bollobas B, Borgs C, Chayes J, Riordan O (2003) Directed scale-free graph. In: *Proc of the 14th ACM-SIAM symposium on discrete algorithms*, pp 132–139
10. Dorogovtsev SN, Mendes JFF, Samukhin AN (2000) Structure of growing networks with preferential linking. *Phys Rev Lett* 85:4633–4636
11. Tadic B (2011) Dynamics of directed graphs: the World-Wide Web. *Physica A* 293:273–284
12. Lu Y, Wang X (2008) Pinning control of directed dynamical networks based on ControlRank. *Int J Comput Math* 85:1279–1286
13. Wu CW (2002) *Synchronization in coupled chaotic circuits and systems*. World Scientific, Singapore
14. Wu CW, Chua LO (1995) Synchronization in an array of linearly coupled dynamical systems. *IEEE Trans Circuits Syst I, Fundam Theory Appl* 42:430–447
15. Wu CW, Chua LO (1995) Application of Kronecker products to the analysis of systems with uniform linear coupling. *IEEE Trans Circuits Syst I, Fundam Theory Appl* 42:775–778
16. Chua LO, Green DN (1976) A qualitative analysis of the behavior of dynamic nonlinear networks: stability of autonomous networks. *IEEE Trans Circuits Syst* 23:355–379
17. Ding MZ, Yang YM (1997) Stability of synchronous chaos and on–off intermittency in coupled map lattices. *Phys Rev E* 56:4009–4016
18. Li X, Chen G (2003) Synchronization and desynchronization of complex dynamical networks: an engineering viewpoint. *IEEE Trans Circuits Syst I, Fundam Theory Appl* 50:1381–1390
19. Rangarajan G, Ding MZ (2002) Stability of synchronized chaos in coupled dynamical systems. *Phys Lett A* 296:204–209
20. Wang X, Chen G (2002) Pinning control of scale-free dynamical networks. *Physica A* 310:521–531
21. Chen G, Ueta T (1999) Yet another chaotic attractor. *Int J Bifurc Chaos* 9:1465–1466
22. Xiang L, Liu Z, Chen Z, Chen F, Yuan Z (2007) Pinning control of complex dynamical networks with general topology. *Physica A* 379:298–306
23. Brin S, Page L (1998) The anatomy of a large-scale hypertextual web search engine. In: *Proceedings of the seventh international World Wide Web conference*, pp 14–18
24. Brin S, Page L (1999) The pagerank citation ranking: bringing order to the web. Technical Report, Computer Science Department, Stanford University, 1999–0120
25. Lu W, Li X, Rong Z (2010) Global stabilization of complex directed networks with a local pinning algorithm. *Automatica* 46:116–121
26. Wu CW (2005) Synchronization in networks of nonlinear dynamical systems coupled via a directed graph. *Nonlinearity* 18:1057–1064
27. Wu CW (2005) On Rayleigh–Ritz ratios of a generalized Laplacian matrix of directed graphs. *Linear Algebra Appl* 402:207–227
28. Chen T, Liu X, Lu W (2007) Pinning complex networks by a single controller. *IEEE Trans Circuits Syst I, Fundam Theory Appl* 54:1317–1326
29. Boyd S, Ghaoui L, Feron E, Balakrishnan V (1994) *Linear matrix inequalities in system and control theory*. Studies in applied mathematics, vol 15. Society for Industrial and Applied Mathematics (SIAM), Philadelphia
30. Wu CW (2005) On bounds of extremal eigenvalues of irreducible and m -reducible matrices. *Linear Algebra Appl* 402:29–45

31. Langville AN, Meyer CD (2006) Google's PageRank and beyond: the science of search engine rankings. Princeton University Press, Princeton
32. Ding C, He X, Husbands P, Zha H, Simon H (2002) PageRank, HITS and a unified framework for link analysis. In: Proceedings of the 25th annual international ACM SIGIR conference on research and development in information retrieval, pp 249–253
33. Ramirez JA (1994) Nonlinear feedback for controlling the Lorenz equation. Phys Rev E 50:2339–2342

Chapter 3

Pinning Control for Cluster Synchronization of Complex Dynamical Networks

Abstract This chapter introduces decentralized adaptive pinning control for cluster synchronization of complex networks. Unlike most existing pinning control algorithms with or without an adaptive strategy, which require global information of the underlying network such as the eigenvalues of the coupling matrix of the whole network or a centralized adaptive control scheme, we propose a novel decentralized adaptive pinning control scheme for cluster synchronization of undirected networks using a local adaptive strategy on both coupling strengths and feedback gains. By introducing this local adaptive strategy on each node, we show that the network can synchronize using weak coupling strengths and small feedback gains.

Keywords Cluster synchronization · Decentralized adaptive pinning control · Complex dynamical networks

3.1 Problem Statement

Cluster synchronization of complex dynamical networks aims to make nodes synchronize with each other in the same cluster, but desynchronize with each other among different clusters, where clusters represent subgroups of the coupled oscillators in a network. In this chapter, by introducing local adaptive strategies to both coupling strengths and feedback gains, we develop a decentralized adaptive pinning control scheme for cluster synchronization of undirected complex dynamical networks without using any global information on the underlying network. Generally speaking, the chapter extends the centralized adaptive strategies in [1, 2] to the decentralized case, and extends the decentralized adaptive complete synchronization in [3–5] to the decentralized adaptive cluster synchronization. In contrast to the centralized adaptive strategies developed in [1, 2], each node only acquires the state information from its neighbors and only selects those few nodes that have the information of their desired heterogeneous stationary states. This is a significant improvement upon the existing centralized algorithms. Different from the known results on adaptive complete synchronization in [3–5], we investigate the adaptive cluster synchronization problem here. The cluster synchronization problem cannot be viewed as a simple collective form for the independent complete synchronization problems. This is because, unlike complete synchronization, each node is affected

not only by the nodes in the same cluster but also by the nodes in different clusters, which have different synchronized states, therefore there is no guarantee that a node will definitely synchronize with the nodes in the same cluster. In order to achieve cluster synchronization, unlike the traditional definition of the coupling matrix of the network, inhibitory coupling is introduced to the coupling matrix in our network. Thus, the decentralized adaptive algorithms derived in [3–5] cannot solve the cluster synchronization problems formulated here. To overcome this difficulty, unlike the results presented in [3–5], pinning control for cluster synchronization of complex dynamical networks is investigated here and local adaptive strategies are introduced to only parts of edges in the graph, which calls for a more delicate treatment.

In this chapter, an adaptive pinning control scheme is developed for cluster synchronization of network (1.5). The approach is to use a decentralized method, that is, each node only needs the state information of its neighbors and only selects those few nodes that have the information of their desired states. The main advantage of the proposed scheme over the existing centralized algorithms is that it does not need to acquire or use state information from all nodes in the network.

3.2 Decentralized Adaptive Pinning Control Scheme

3.2.1 Algorithm Description

The proposed adaptive strategy for node i is designed as

$$\begin{aligned}\dot{x}_i(t) &= f(x_i(t), t) + \sum_{j=1, j \neq i}^N c_{ij}(t) a_{ij} (x_j(t) - x_i(t)) + h_i c_i(t) (\bar{x}_{\hat{i}}(t) - x_i(t)), \\ \dot{c}_{ij}(t) &= h_{ij} a_{ij} k_{ij} (x_i(t) - x_j(t))^T P (x_i(t) - x_j(t)), \\ \dot{c}_i(t) &= h_i k_i (x_i(t) - \bar{x}_{\hat{i}}(t))^T P (x_i(t) - \bar{x}_{\hat{i}}(t)),\end{aligned}\tag{3.1}$$

where $c_{ij}(0) = c > 0$, $c_i(0) \geq 0$, $\Gamma = I_n$ in network (1.5) and a positive-definite diagonal matrix $P = \text{diag}\{p_1, \dots, p_n\}$. The positive constants $k_{ij} = k_{ji}$ and k_i are the weights of the adaptive laws for parameters $c_{ij}(t)$ and $c_i(t)$, respectively. If nodes i and j are in the same cluster, then $h_{ij} = 1$; otherwise, $h_{ij} = 0$. Clearly, the adaptive parameters $c_{ij}(t)$ for node i only contain the state information of its neighbors.

3.2.2 Main Results and Theoretical Analysis

The following assumption and lemmas are needed for our main result.

Assumption 3.1 ([1]) For any $x, y \in \mathbf{R}^n$, the continuous map $f : \mathbf{R}^n \times [0, +\infty) \rightarrow \mathbf{R}^n$ satisfies

$$(x - y)^T P \{ [f(x, t) - f(y, t)] - \Delta(x - y) \} \leq -\omega(x - y)^T (x - y) \quad (3.2)$$

for a diagonal matrix $\Delta = \text{diag}\{\delta_1, \dots, \delta_n\}$, and a positive constant $\omega > 0$.

It is assumed in [2] that for an $N \times N$ symmetric matrix

$$A = \begin{bmatrix} A_{11} & A_{12} & \cdots & A_{1d} \\ A_{21} & A_{22} & \cdots & A_{2d} \\ \vdots & \vdots & \ddots & \vdots \\ A_{d1} & A_{d2} & \cdots & A_{dd} \end{bmatrix}, \quad (3.3)$$

where $A = (a_{ij}) \in \mathbf{R}^{N \times N}$, each block $A_{uv} = (z_{ij}) \in \mathbf{R}^{k_u \times k_v}$ ($u, v = 1, \dots, d$) is a zero-row-sum matrix, that is, $\sum_{j=1}^{k_v} z_{ij} = 0$, and each block $A_{uu} = (s_{ij}) \in \mathbf{R}^{k_u \times k_u}$ satisfies $s_{ii} = -\sum_{j=1, j \neq i}^{k_u} s_{ij}$ where $s_{ij} = s_{ji} \geq 0$ ($i \neq j$) and k_u and k_v are the numbers of nodes in the subset u and v , respectively.

Note also that, unlike the traditional definition of the coupling matrix of the network, the element a_{ij} with $i \in G_u$ and $j \in G_v$ in (3.3) may be negative here, which is called an inhibitory coupling [2]. This provides a mechanism to desynchronize two nodes belonging to two different clusters.

Lemma 3.1 [1] If $L = (l_{ij}) \in \mathbf{R}^{N \times N}$ is a symmetric irreducible matrix with $l_{ii} = -\sum_{j=1, j \neq i}^N l_{ij}$, $l_{ij} = l_{ji} \geq 0$ ($i \neq j$), then for any matrix $E = \text{diag}(e, 0, \dots, 0)$ with $e > 0$, all eigenvalues of the matrix $(L - E)$ are negative.

Lemma 3.2 [2] For any $x \in \mathbf{R}^p$, $y \in \mathbf{R}^q$, and matrix $M = (m_{ij}) \in \mathbf{R}^{p \times q}$,

$$x^T M y \leq (1/2) \max[p, q] \cdot \max_{i,j} |m_{ij}| (x^T x + y^T y).$$

Lemma 3.3 Let matrix A be given as in (3.3). Then, under the adaptive strategy (3.1),

$$B = (a_{ij} c_{ij}(t)) = \begin{bmatrix} B_{11} & B_{12} & \cdots & B_{1d} \\ B_{21} & B_{22} & \cdots & B_{2d} \\ \vdots & \vdots & \ddots & \vdots \\ B_{d1} & B_{d2} & \cdots & B_{dd} \end{bmatrix} \in \mathbf{R}^{N \times N}$$

is a symmetric matrix, in which each block B_{uv} ($u, v = 1, \dots, d$) is a zero-row-sum matrix and each block B_{uu} is with $a_{ii} c_{ii}(t) = -\sum_{j=1, j \neq i}^{k_u} a_{ij} c_{ij}(t)$, $a_{ij} c_{ij}(t) = a_{ji} c_{ji}(t) \geq 0$ ($i \neq j$), where k_u is the number of nodes in the subset u .

Proof If nodes i and j are not in the same cluster, then by the adaptive strategy (3.1), one has

$$\dot{c}_{ij}(t) = 0.$$

If nodes i and j are in the same cluster, then by the adaptive strategy (3.1), one has

$$\dot{c}_{ij}(t) = \dot{c}_{ji}(t).$$

Therefore, B is a symmetric irreducible matrix. Similar to (3.3), each block $B_{uv}(u, v = 1, \dots, d)$ is a zero-row-sum matrix and each block B_{uu} is with $a_{ii}c_{ii}(t) = -\sum_{j=1, j \neq i}^{k_u} a_{ij}c_{ij}(t)$, $a_{ij}c_{ij}(t) = a_{ji}c_{ji}(t) \geq 0$ ($i \neq j$), where k_u is the number of nodes in the subset u . \square

Lemma 3.4 *Let matrix A be given as in (3.3). Then*

$$\begin{aligned} & \sum_{i=1}^N (x_i - \bar{x}_{\hat{i}})^T P \sum_{j=1, \hat{i}=\hat{j}, j \neq i}^N a_{ij}c_{ij}(x_i - x_j) \\ &= \frac{1}{2} \sum_{i=1}^N \sum_{j=1, j \neq i}^N h_{ij}a_{ij}c_{ij}(x_i - x_j)^T P (x_i - x_j). \end{aligned}$$

Proof Note that, if $\hat{i} = \hat{j}$, then nodes i and j are in the same cluster, so

$$\sum_{i=1}^N (x_i - \bar{x}_{\hat{i}})^T P \sum_{j=1, \hat{i}=\hat{j}, j \neq i}^N a_{ij}c_{ij}(x_i - x_j) = \sum_{i=1}^N \tilde{x}_i^T P \sum_{j=1, \hat{i}=\hat{j}, j \neq i}^N a_{ij}c_{ij}(\tilde{x}_i - \tilde{x}_j) \quad (3.4)$$

and

$$\begin{aligned} & \frac{1}{2} \sum_{i=1}^N \sum_{j=1, j \neq i}^N h_{ij}a_{ij}c_{ij}(x_i - x_j)^T P (x_i - x_j) \\ &= \frac{1}{2} \sum_{i=1}^N \sum_{j=1, \hat{i}=\hat{j}, j \neq i}^N a_{ij}c_{ij}(\tilde{x}_i - \tilde{x}_j)^T P (\tilde{x}_i - \tilde{x}_j), \end{aligned} \quad (3.5)$$

where $\tilde{x}_i = x_i - \bar{x}_{\hat{i}}$. Thus, by using the results in Lemma 3.3, we have

$$\begin{aligned} & \frac{1}{2} \sum_{i=1}^N \sum_{j=1, \hat{i}=\hat{j}, j \neq i}^N a_{ij}c_{ij}(\tilde{x}_i - \tilde{x}_j)^T P (\tilde{x}_i - \tilde{x}_j) \\ &= \frac{1}{2} \sum_{i=1}^N \sum_{j=1, \hat{i}=\hat{j}, j \neq i}^N a_{ij}c_{ij}\tilde{x}_i^T P (\tilde{x}_i - \tilde{x}_j) - \frac{1}{2} \sum_{i=1}^N \sum_{j=1, \hat{i}=\hat{j}, j \neq i}^N a_{ij}c_{ij}\tilde{x}_j^T P (\tilde{x}_i - \tilde{x}_j) \\ &= \frac{1}{2} \sum_{i=1}^N \sum_{j=1, \hat{i}=\hat{j}, j \neq i}^N a_{ij}c_{ij}\tilde{x}_i^T P (\tilde{x}_i - \tilde{x}_j) + \frac{1}{2} \sum_{j=1}^N \sum_{i=1, \hat{i}=\hat{j}, j \neq i}^N a_{ji}c_{ji}\tilde{x}_j^T P (\tilde{x}_j - \tilde{x}_i) \end{aligned} \quad (3.6)$$

$$= \sum_{i=1}^N \sum_{j=1, \hat{i}=\hat{j}, j \neq i}^N a_{ij} c_{ij} \tilde{x}_i^T P (\tilde{x}_i - \tilde{x}_j). \quad (3.7)$$

Since $a_{ij} c_{ij} = a_{ji} c_{ji}$ and $\tilde{x}_i - \tilde{x}_j = -(\tilde{x}_j - \tilde{x}_i)$, we have switched the order of the summation signs in the second term in the first equality to obtain (3.6) and have switched the dummy variables i and j in the second term in (3.6) to obtain (3.7).

Therefore, from (3.4), (3.5), and (3.7),

$$\begin{aligned} & \sum_{i=1}^N (x_i - \bar{x}_i)^T P \sum_{j=1, \hat{i}=\hat{j}, j \neq i}^N a_{ij} c_{ij} (x_i - x_j) \\ &= \frac{1}{2} \sum_{i=1}^N \sum_{j=1, j \neq i}^N h_{ij} a_{ij} c_{ij} (x_i - x_j)^T P (x_i - x_j). \end{aligned}$$

□

Lemma 3.5 [6] *If a scalar function $V(x, t)$ satisfies the following conditions:*

- (a) $V(x, t)$ is lower bounded;
- (b) $\dot{V}(x, t)$ is negative semi-definite;
- (c) $\dot{V}(x, t)$ is uniformly continuous in t ;

then $\dot{V}(x, t) \rightarrow 0$, as $t \rightarrow \infty$.

Note that, Lemma 3.5 is, in fact, an extension of Barbalat's Lemma. More details about Lemma 3.5 can be seen in [6, Lemma 4.3 (Lyapunov-like Lemma)].

Theorem 3.1 *Consider network (1.1), where each node is steered by the adaptive strategy (3.1). Suppose that Assumption 3.1 holds, and at least one node in each cluster is selected to be controlled. Let matrix A be given as in (3.3). Then, all clusters asymptotically synchronize to their given heterogeneous stationary states, namely,*

$$\lim_{t \rightarrow \infty} \sum_{l=1}^d \sum_{i \in G_l} \|x_i(t) - \bar{x}_l(t)\| = 0.$$

Proof Define the Lyapunov functional candidate as

$$V(t) = \frac{1}{2} \sum_{i=1}^N \left[(x_i - \bar{x}_i)^T P (x_i - \bar{x}_i) + \sum_{j=1, j \neq i}^N \frac{(c_{ij} - m)^2}{2k_{ij}} + \frac{(c_i - m)^2}{k_i} \right], \quad (3.8)$$

where the positive constant

$$m I_{k_u} > \left(\delta_r + (d-1) \max_{u,v} [k_u, k_v] \cdot \max_{i,j} |a_{ij} c_{ij}| \right) I_{k_u} (H_{uu} - A_{uu})^{-1}.$$

Differentiating $V(t)$ gives

$$\begin{aligned}
\dot{V}(t) &= \sum_{i=1}^N \tilde{x}_i^T P \left[f(x_i, t) - f(\bar{x}_i, t) - \sum_{j=1, j \neq i}^N a_{ij} c_{ij} (\tilde{x}_i - \tilde{x}_j) - h_i c_i \tilde{x}_i \right] \\
&\quad + \frac{1}{2} \sum_{i=1}^N \sum_{j=1, j \neq i}^N h_{ij} a_{ij} (c_{ij} - m) (\tilde{x}_i - \tilde{x}_j)^T P (\tilde{x}_i - \tilde{x}_j) \\
&\quad + \sum_{i=1}^N h_i (c_i - m) \tilde{x}_i^T P \tilde{x}_i \\
&\leq \sum_{i=1}^N \tilde{x}_i^T P \left[\Delta \tilde{x}_i - \sum_{j=1, j \neq i}^N a_{ij} c_{ij} (\tilde{x}_i - \tilde{x}_j) - h_i c_i \tilde{x}_i \right] - \sum_{i=1}^N \omega \tilde{x}_i^T \tilde{x}_i \\
&\quad + \frac{1}{2} \sum_{i=1}^N \sum_{j=1, j \neq i}^N h_{ij} a_{ij} (c_{ij} - m) (\tilde{x}_i - \tilde{x}_j)^T P (\tilde{x}_i - \tilde{x}_j) \\
&\quad + \sum_{i=1}^N h_i (c_i - m) \tilde{x}_i^T P \tilde{x}_i \\
&= - \sum_{i=1}^N \omega \tilde{x}_i^T \tilde{x}_i + \sum_{r=1}^n p_r \sum_{i=1}^N \tilde{x}_i^T \left[\delta_r \tilde{x}_i^r - \sum_{j=1, j \neq i}^N a_{ij} c_{ij} (\tilde{x}_i^r - \tilde{x}_j^r) - h_i c_i \tilde{x}_i^r \right] \\
&\quad + \frac{1}{2} \sum_{r=1}^n p_r \sum_{i=1}^N \sum_{j=1, j \neq i}^N h_{ij} a_{ij} (c_{ij} - m) (\tilde{x}_i^r - \tilde{x}_j^r)^T (\tilde{x}_i^r - \tilde{x}_j^r) \\
&\quad + \sum_{r=1}^n p_r \sum_{i=1}^N h_i (c_i - m) \tilde{x}_i^T \tilde{x}_i^r \\
&= - \sum_{i=1}^N \omega \tilde{x}_i^T \tilde{x}_i + \sum_{r=1}^n p_r \left[m \sum_{u=1}^d x^{urT} (A_{uu} - H_{uu}) x^{ur} + \delta_r \sum_{u=1}^d x^{urT} x^{ur} \right] \\
&\quad + \sum_{r=1}^n p_r \left[\sum_{u=1}^d \sum_{v \neq u} x^{urT} B_{uv} x^{vr} \right] \\
&\leq - \sum_{i=1}^N \omega \tilde{x}_i^T \tilde{x}_i + \sum_{r=1}^n p_r \left[\sum_{u=1}^d x^{urT} (m A_{uu} - m H_{uu} + \delta_r I_{k_u}) x^{ur} \right] \\
&\quad + \sum_{r=1}^n p_r \left[(1/2) \max_{u,v} [k_u, k_v] \cdot \max_{i,j} |a_{ij} c_{ij}| \sum_{u=1}^d \sum_{v \neq u} (x^{urT} x^{ur} + x^{vrT} x^{vr}) \right]
\end{aligned}$$

$$\begin{aligned}
&\leq - \sum_{i=1}^N \omega \tilde{x}_i^T \tilde{x}_i + \sum_{r=1}^n p_r \left[\sum_{u=1}^d x^{urT} (mA_{uu} - mH_{uu} + \delta_r I_{k_u}) x^{ur} \right] \\
&\quad + \sum_{r=1}^n p_r \left[(d-1) \max_{u,v} [k_u, k_v] \cdot \max_{i,j} |a_{ij} c_{ij}| \sum_{u=1}^d x^{urT} x^{ur} \right], \tag{3.9}
\end{aligned}$$

where $x^r = [x_1^r, \dots, x_N^r]^T = [x^{1r}, \dots, x^{ur}, \dots, x^{dr}]^T \in \mathbf{R}^N$, $x^{ur} \in \mathbf{R}^{k_u}$ is the vector in the u th cluster, and

$$H = \begin{bmatrix} H_{11} & 0 & \cdots & 0 \\ 0 & H_{22} & \cdots & 0 \\ \vdots & \vdots & \ddots & \vdots \\ 0 & 0 & \cdots & H_{dd} \end{bmatrix}.$$

According to (3.3), and at least one node in each cluster is selected to be controlled, from Lemmas 3.1 and 3.3, it can be verified that $(A_{uu} - H_{uu})$ is negative-definite. Since the positive constant

$$mI_{k_u} > \left(\delta_r + (d-1) \max_{u,v} [k_u, k_v] \cdot \max_{i,j} |a_{ij} c_{ij}| \right) I_{k_u} (H_{uu} - A_{uu})^{-1},$$

one has

$$\dot{V}(t) \leq - \sum_{i=1}^N \omega \tilde{x}_i^T \tilde{x}_i.$$

Thus, $\dot{V}(t)$ is negative semi-definite. From the definition of $V(t)$, it is obvious that $V(t)$ is lower bounded. According to Assumption 3.1 and (3.9), $\dot{V}(t)$ is uniformly continuous in t . Therefore, Lemma 3.5 can be applied here. It is obvious that $\dot{V}(t) = 0$ if and only if $\tilde{x}_i = 0, i = 1, 2, \dots, n$. The set $S = \{\tilde{x} \in \mathbf{R}^{Nn}, c \in \mathbf{R}^N, \tilde{c} \in \mathbf{R}^{N^2} : \tilde{x} = 0, c = c_0, \tilde{c} = \tilde{c}_0\}$, where $c = [c_1, c_2, \dots, c_N]^T$, $\tilde{c} = [\tilde{c}_{11}, \tilde{c}_{12}, \dots, \tilde{c}_{NN}]^T$, c_0 and \tilde{c}_0 are positive constant vectors, is the largest invariant set contained in $M = \{\dot{V}(t) = 0\}$ for system (3.1). According to Lemma 3.5, the trajectories of the system (3.1) converge asymptotically to the set S , that is, $\tilde{x} \rightarrow 0$, $c \rightarrow c_0$ and $\tilde{c} \rightarrow \tilde{c}_0$ as $t \rightarrow \infty$.

Thus,

$$\lim_{t \rightarrow \infty} \sum_{l=1}^d \sum_{i \in G_l} \|x_i(t) - \bar{x}_l(t)\| = 0.$$

This completes the proof of Theorem 3.1. \square

In order to achieve pinning control for d -cluster synchronization of complex dynamical networks, an adaptive strategy to node i was designed in [2] as

$$\begin{aligned}\dot{x}_i(t) &= f(x_i(t), t) + \sum_{j=1, j \neq i}^N m_{ij}(x_j(t) - x_i(t)) + h_i c(t)(\bar{x}_i(t) - x_i(t)), \\ \dot{c}(t) &= \frac{\alpha}{2} \sum_{i=1}^N (x_i(t) - \bar{x}_i(t))^T P (x_i(t) - \bar{x}_i(t)),\end{aligned}\tag{3.10}$$

where

$$M(t) = (m_{ij}(t))_{N \times N} = \begin{bmatrix} c(t)A_{11} & A_{12} & \cdots & A_{1d} \\ A_{21} & c(t)A_{22} & \cdots & A_{2d} \\ \vdots & \vdots & \ddots & \vdots \\ A_{d1} & A_{d2} & \cdots & c(t)A_{dd} \end{bmatrix}.$$

Remark 3.1 Under the assumption that there is at least one single controller in each cluster, Assumption 3.1 and (3.3) hold, and d -cluster synchronization of complex networks was established in [2], where, however, the adaptive parameter at each node requires the state information from all nodes and the information on the heterogeneous stationary states over the whole networks. Unlike protocol (3.10), each node in protocol (3.1) only has the state information of its neighbors and only selects those few nodes that have the information on the heterogeneous stationary states.

3.2.3 Complete Synchronization Case

When there is only one cluster in the network, the protocol (3.1) can also be used to realize complete synchronization of the network. The adaptive strategy for node i in this case can be rewritten as

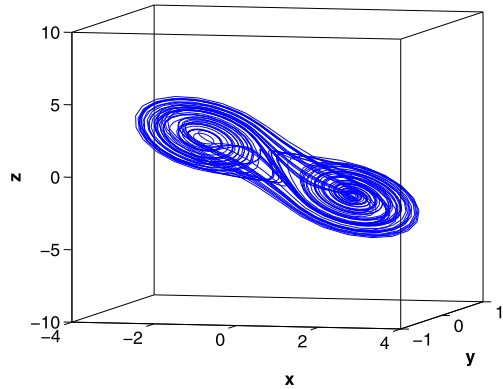
$$\begin{aligned}\dot{x}_i(t) &= f(x_i(t), t) + \sum_{j=1, j \neq i}^N c_{ij}(t)a_{ij}(x_j(t) - x_i(t)) + h_i c_i(t)(\bar{x}(t) - x_i(t)), \\ \dot{c}_{ij}(t) &= a_{ij}k_{ij}(x_i(t) - x_j(t))^T P (x_i(t) - x_j(t)), \\ \dot{c}_i(t) &= h_i k_i(x_i(t) - \bar{x}(t))^T P (x_i(t) - \bar{x}(t)).\end{aligned}\tag{3.11}$$

The graph Laplacian of the connected network naturally satisfies (3.3).

Lemma 3.6 *For a one-cluster connected network,*

$$\sum_{i=1}^N (x_i - \bar{x})^T P \sum_{j=1, j \neq i}^N a_{ij}c_{ij}(x_i - x_j) = \frac{1}{2} \sum_{i=1}^N \sum_{j=1, j \neq i}^N a_{ij}c_{ij}(x_i - x_j)^T P (x_i - x_j).$$

Fig. 3.1 A chaotic Chua circuit



Proof The proof is similar to that of Lemma 3.4. \square

Corollary 3.1 Consider network (1.1) with a single cluster, where each node is steered by the adaptive strategy (3.11). Suppose that the whole network is connected, Assumption 3.1 holds, and at least one node is selected to be controlled. Then, all nodes asymptotically synchronize to the given homogeneous stationary state, namely,

$$\lim_{t \rightarrow \infty} \|x_i(t) - \bar{x}(t)\| = 0.$$

Proof This is a special case of Theorem 3.1. \square

Remark 3.2 A similar argument follows as in Remark 3.1.

3.3 Simulation Study

In this section, numerical examples are given to verify and illustrate the theoretical results. In the following simulations, each node is a chaotic Chua circuit (see Fig. 3.1 [7]),

$$\begin{cases} \dot{x}^1 = 10(x^2 - x^1 + f(x^1)), \\ \dot{x}^2 = x^1 - x^2 + x^3, \\ \dot{x}^3 = -15x^2 - 0.0385x^3, \end{cases} \quad (3.12)$$

where

$$f(x^1) = \begin{cases} -bx^1 - a + b, & x^1 > 1, \\ -ax^1, & |x^1| \leq 1, \\ -bx^1 + a - b, & x^1 < -1, \end{cases}$$

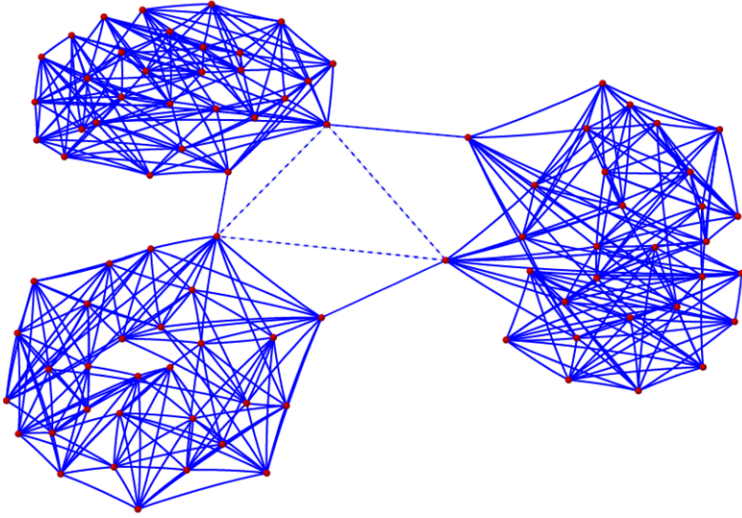


Fig. 3.2 The network example with $N = 90$ in 3 clusters

where $a = -1.27$ and $b = -0.68$. The Chua circuit (3.12) has three unstable equilibrium points: $[1.8586, 0.0048, -1.8539]^T$, $[0, 0, 0]^T$, and $[-1.8586, -0.0048, 1.8539]^T$.

3.3.1 Example 1: Three Clusters

Simulations were performed with protocol (3.1) applied to 90 nodes grouped in 3 clusters. Each cluster is a homogeneous small-world network, which starts from a nearest-neighbor lattice with 30 nodes and an average degree $k = 10$. Two edges were randomly selected and then swapped, forbidding duplicate connections, until p percent of edges had been swapped. Through this reconnection, one can obtain a homogeneous small-world network with a high clustering coefficient and a short average path length without altering the connection distribution of the original network [8]. In this example, three homogeneous small-world clusters are generated randomly with swapping probability $p = 0.1$ and they are linked by a few random edges (see Fig. 3.2). The coupling matrix of the network satisfies (3.3). Initial states of the 90 nodes were chosen randomly from the cube $[-1, 1] \times [-1, 1] \times [-1, 1]$. The heterogeneous stationary states are the three unstable equilibrium points of the Chua circuit (3.12). There is only one node in each cluster that is chosen randomly to be controlled. The adaptive parameters are set as $c_{ij}(0) = 1$ and $c_i(0) = 0$, the weights $k_{ij} = 1$ and $k_i = 1$, and the matrix $P = \text{diag}\{1, 1, \dots, 1\}$.

In Fig. 3.3, plots (a), (b), and (c) show the convergence of states on the x^1 -axis, x^2 -axis and x^3 -axis, respectively; plot (d) depicts the mean squared errors σ_i

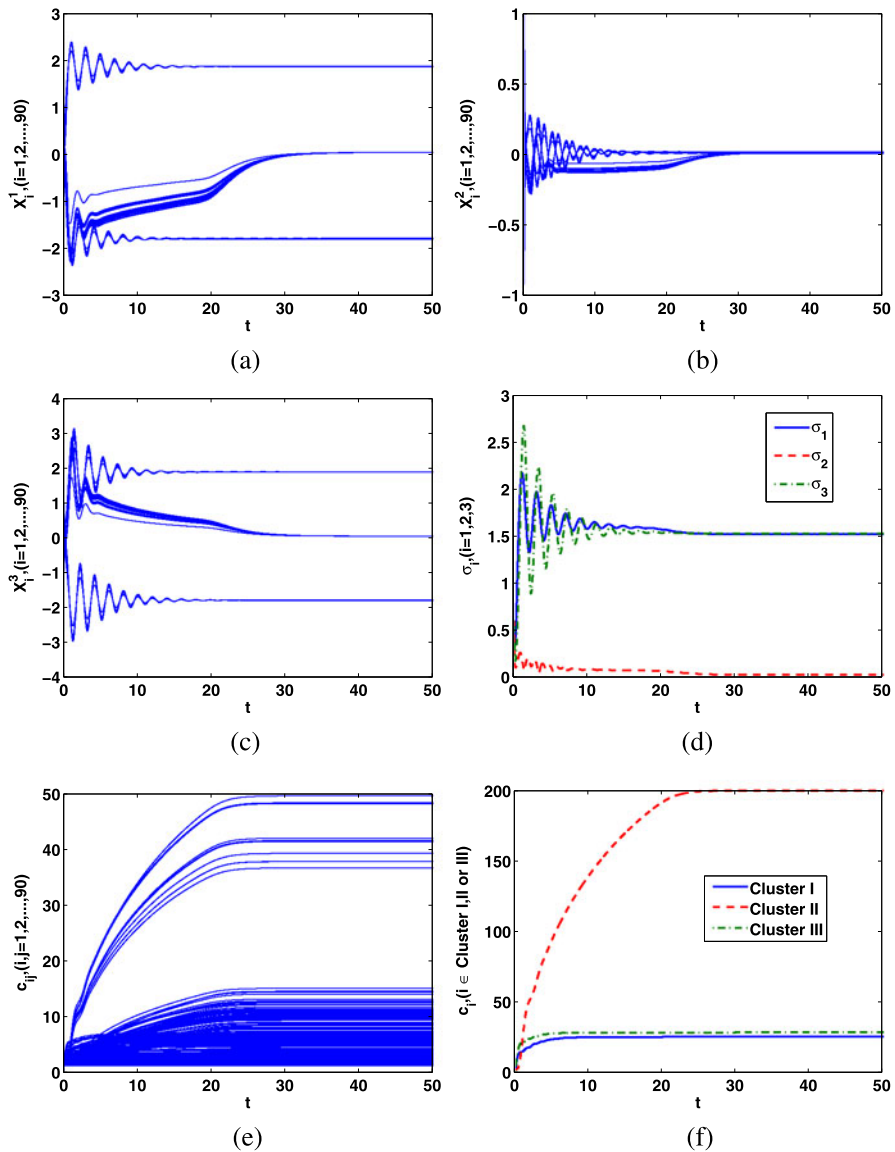


Fig. 3.3 [7] Pinning control of 90 nodes under protocol (3.1)

for the x^i -axis, where $\sigma_i = \sqrt{\frac{1}{N-1} \sum_{j=1}^N (x_j^i - \frac{1}{N} \sum_{j=1}^N x_j^i)^2}$; plot (e) represents the adaptive coupling strengths which eventually approach constants; plot (f) depicts the adaptive feedback gains which eventually approach constants.

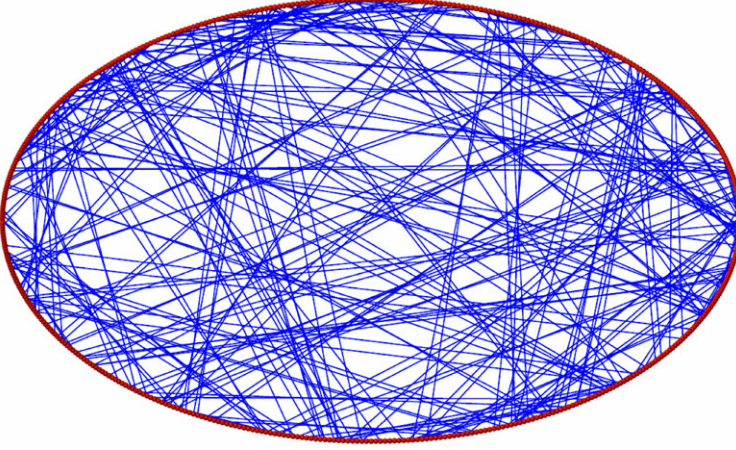


Fig. 3.4 The WS small-world network with $N = 500$, probability $p = 0.1$ and an average degree $k = 10$

3.3.2 Example 2: One Cluster

Simulations were performed by applying protocol (3.11) to a homogeneous network of 500 nodes with swapping probability $p = 0.1$ and an average degree $k = 10$ [8] (see Fig. 3.4). The clustering coefficient of this small-world network $C = 0.4857$. The average path length of this small-world network $L = 4.0652$. Initial states of the 500 nodes were chosen randomly from the cube $[-1, 1] \times [-1, 1] \times [-1, 1]$. The homogeneous stationary state $\bar{x} = [1.8586, 0.0048, -1.8539]$. There is only one node which is chosen randomly from the network to be controlled. The adaptive parameters are set as $c_{ij}(0) = 0.01$ and $c_i(0) = 0$, the weights $k_{ij} = 1$ and $k_i = 1$, and the matrix $P = \text{diag}\{1, 1, \dots, 1\}$.

In Fig. 3.5, plots (a), (b), and (c) show the convergence of states on the x^1 -axis, x^2 -axis and x^3 -axis, respectively; plot (d) depicts the mean squared errors σ_i for the x^i -axis; plot (e) represents the maximum adaptive coupling strength which eventually tends to a constant; plot (f) depicts the adaptive feedback gain which eventually tends to a constant.

For the same initial conditions of the states, we now make a comparison of the control gains among the nonadaptive pinning control algorithm (1.5), the centralized pinning control algorithm in [1], and the decentralized pinning control algorithm (3.11). To ensure the fairness of the comparison, we select the same nodes to apply the pinning control. We use a more reasonable index, that is, the average value of all the coupling strengths and feedback gains,

$$\text{Ave}(c) = \frac{1}{\sum_{i=1}^N ((\sum_{j=1, j \neq i}^N a_{ij}) + h_i)} \sum_{i=1}^N \left(\left(\sum_{j=1, j \neq i}^N a_{ij} c_{ij} \right) + h_i c_i \right),$$

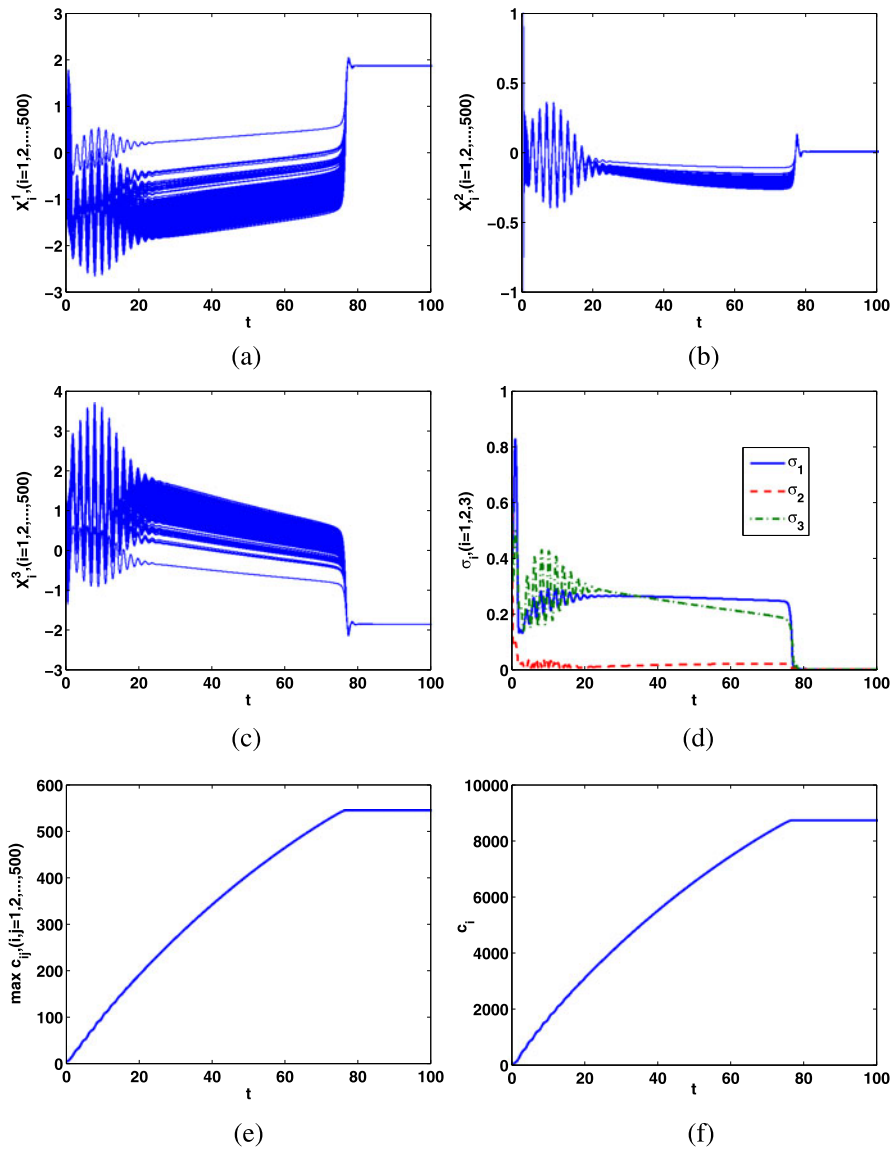
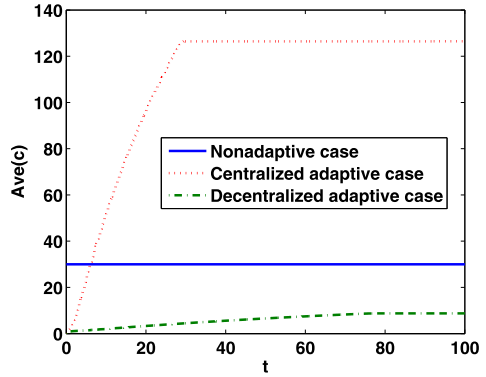


Fig. 3.5 [7] Pinning control of 500 nodes under protocol (3.11)

to measure the control gains. Since the size of the network is very large, we cannot assign different least coupling strengths or feedback gains to different edges artificially for the nonadaptive pinning control algorithm (1.5). Therefore, we choose the same value for all the coupling strengths and feedback gains when the nonadaptive pinning control algorithm (1.5) is applied, that is, all the coupling strengths

Fig. 3.6 [7] The comparison of the control gains



and feedback gains are equal to the average value of all the coupling strengths and feedback gains. We choose the control gain $\text{Ave}(c) = 20$ and 30 for the nonadaptive pinning control algorithm (1.5), respectively. The network cannot be synchronized for the case of the control gain $\text{Ave}(c) = 20$, but can be synchronized for the case of $\text{Ave}(c) = 30$. We then compare the decentralized pinning control algorithm (3.11) against the nonadaptive pinning control algorithm (1.5) with $\text{Ave}(c) = 30$ and the centralized pinning control algorithm in [1] in Fig. 3.6. It is demonstrated by Fig. 3.6 that the practical average value of all the coupling strengths and feedback gains of the decentralized adaptive case is much less than the other two cases. The reason can be analyzed as follows. For a given large complex network, it is difficult or impossible to know which edges need larger coupling or control gains even if the initial states of all nodes are known. Therefore, we cannot assign different least coupling strengths or feedback gains to different edges in order to satisfy the theoretical least coupling and control gains for the synchronization of the network. For the nonadaptive algorithm, one optional method is to assign a uniform coupling and control gain, which must be larger than or equal to the largest value in the theoretical least coupling and control gains for the synchronization of the network, to all the coupling strengths or feedback gains so as to satisfy theoretical least coupling and control gains for the synchronization of the network. The centralized adaptive algorithm also has a common coupling and control gain for all edges, which should be larger than or equal to the largest value in the theoretical least coupling and control gains for the synchronization of the network. However, the decentralized adaptive algorithm can adjust each coupling strength or feedback gain to its proper value through local interactions with neighbors, in which the gains for some edges may be smaller than the largest value in the theoretical least coupling and control gains for the synchronization of the network. Therefore, it is reasonable that the practical average value of all the coupling strengths and feedback gains of the decentralized adaptive case is much less than the other two cases.

3.4 Conclusions and Notes

In this chapter, we have investigated the pinning control problem for cluster synchronization of complex dynamical networks. By introducing local adaptive strategies for both coupling strengths and feedback gains, it was shown that the collective dynamics of the underlying complex network can be controlled to its heterogeneous stationary states without requiring global information of the network. This is superior to the existing protocols for the same problem since global information of the underlying network is not acquired or used. Simulations showed that, by employing the proposed decentralized adaptive pinning control scheme, it is possible to control the collective dynamics of a complex network to the desired heterogeneous stationary states in different clusters with only weak coupling strengths and small feedback gains, demonstrating a clear advantage of the approach developed in this chapter.

References

1. Chen T, Liu X, Lu W (2007) Pinning complex networks by a single controller. *IEEE Trans Circuits Syst I, Fundam Theory Appl* 54:1317–1326
2. Wu W, Zhou W, Chen T (2009) Cluster synchronization of linearly coupled complex networks under pinning control. *IEEE Trans Circuits Syst I, Fundam Theory Appl* 56:829–839
3. Delellis P, Bernardo M, Garofalo F (2008) Synchronization of complex networks through local adaptive coupling. *Chaos* 18:037110
4. Delellis P, Bernardo M, Garofalo F (2009) Novel decentralized adaptive strategies for the synchronization of complex networks. *Automatica* 45:1312–1318
5. Delellis P, Bernardo M, Turci F (2010) Fully adaptive pinning control of complex networks. In: *Proceedings of 2010 IEEE international symposium on circuits and systems*, pp 685–688
6. Slotine JJE, Li W (1991) *Applied nonlinear control*. Prentice Hall, Englewood Cliffs
7. Su H, Rong Z, Chen MZQ, Wang X, Chen G, Wang H (2012) Decentralized adaptive pinning control for cluster synchronization of complex dynamical networks. *IEEE Trans Syst Man Cybern, Part B, Cybern.* doi:[10.1109/TSMCB.2012.2202647](https://doi.org/10.1109/TSMCB.2012.2202647)
8. Santos FC, Rodrigues JF, Pacheco JM (2005) Epidemic spreading and cooperation dynamics on homogeneous small-world networks. *Phys Rev E* 72:056128

Chapter 4

Distributed Pinning-Controlled Second-Order Consensus of Multi-Agent Systems

Abstract This chapter introduces second-order consensus of multi-agent systems. We first revisit the second-order consensus problems for coupled harmonic oscillators in a dynamic proximity network. Unlike many existing algorithms for distributed control of complex dynamical networks that require explicit assumptions on the network connectivity, we show that the coupled harmonic oscillators with or without a leader can always be synchronized, without imposing any network connectivity assumption. We then introduce a second-order consensus algorithm with connectivity preservation. This algorithm can enable the group of mobile agents to converge to the same position and move with the same velocity while preserving the connectivity of the whole network during the evolution if the initial network is connected. We find that there is a trade-off between the maximum overshoot and the settling time of the velocity convergence. We also introduce the second-order consensus protocol with a virtual leader and show that all agents can asymptotically attain a desired velocity even if only one agent in the team has information about the virtual leader. Finally, we study second-order consensus of multiple nonlinear dynamical mobile agents with a virtual leader in a dynamic proximity network. Under the assumption that the initial network is connected, we introduce local adaptation strategies for both the weights on the velocity navigational feedback and the velocity coupling strengths that enable all agents to synchronize with the virtual leader even when only one agent is informed, without requiring any knowledge of the agent dynamics.

Keywords Second-order consensus · Dynamic proximity network · Connectivity preservation · Virtual leader

4.1 Consensus Without Connectivity Assumptions

In the synchronization [1], second-order consensus [2–4], and flocking [5–9] algorithms, certain network connectivity assumptions play a crucial role in the stability analysis. This is because exchanging sufficient information among agents is necessary for cooperation. However, in practice, such kinds of network connectivity assumptions are usually very difficult to verify and may not hold even if the initial network is well connected. On the other hand, we observe that the intrinsic dynam-

ics of the harmonic oscillators will cause the agents to meet with each other from time to time, even if the initial velocities and positions are different. Motivated by this observation and inspired by the recent work [1], we revisit in this section the coupled second-order linear harmonic oscillator models in a dynamic proximity network. The topology of proximity network depends on the relative distances of the harmonic oscillators. The harmonic oscillators are coupled by their velocity information. We will examine the synchronization of coupled harmonic oscillators in the dynamic proximity network without any connectivity assumption. We will also examine the synchronization of coupled harmonic oscillators with a leader and in the absence of any connectivity assumption on the followers.

4.1.1 Problem Statement

We consider N agents moving in a one-dimensional Euclidean space. The behavior of each agent is described by a harmonic oscillator of the form

$$\begin{aligned}\dot{q}_i &= p_i, \\ \dot{p}_i &= -\omega^2 q_i + u_i, \quad i = 1, 2, \dots, N,\end{aligned}\tag{4.1}$$

where $q_i \in \mathbf{R}$ is the position of agent i , $p_i \in \mathbf{R}$ is its velocity vector, $u_i \in \mathbf{R}$ is its control input, and ω is the frequency of the oscillator. For notational convenience, we also define

$$q = \begin{bmatrix} q_1 \\ q_2 \\ \vdots \\ q_N \end{bmatrix}, \quad p = \begin{bmatrix} p_1 \\ p_2 \\ \vdots \\ p_N \end{bmatrix}.$$

The problem of synchronization is to design a control input u_i to cause

$$\lim_{t \rightarrow \infty} \|q_i(t) - q_j(t)\| = 0$$

and

$$\lim_{t \rightarrow \infty} \|p_i(t) - p_j(t)\| = 0$$

for all i and j . In the situation where a leader, labeled as agent $N + 1$, is present, the goal is then to design a control input u_i to cause

$$\lim_{t \rightarrow \infty} \|q_i(t) - q_\gamma(t)\| = 0$$

and

$$\lim_{t \rightarrow \infty} \|p_i(t) - p_\gamma(t)\| = 0$$

for all i , where q_γ and p_γ are the position and velocity of the leader, respectively. The dynamic of the leader satisfies

$$\begin{aligned}\dot{q}_\gamma &= p_\gamma, \\ \dot{p}_\gamma &= -\omega^2 q_\gamma.\end{aligned}\tag{4.2}$$

In [1], N coupled harmonic oscillators are connected by dampers, i.e.,

$$u_i = - \sum_{j=1}^N a_{ij}(t)(p_i - p_j), \quad i = 1, 2, \dots, N, \quad (4.3)$$

where $a_{ij}(t)$ characterizes the interaction between agents i and j at time t . Under certain network connectivity assumptions and the influence of the control input (4.3), synchronization of the positions and velocities in both fixed and switching networks was established in [1].

We investigate the system in a dynamic proximity network. Each agent has a limited communication capability which allows it to communicate only with agents within its neighborhood. The neighboring agents of agent i at time t is denoted as:

$$\mathcal{N}_i(t) = \{j : \|q_i - q_j\| < r, j = 1, 2, \dots, N, j \neq i\},$$

where $\|\cdot\|$ is the Euclidean norm. In the above definition, we have assumed that all agents have an identical influencing/sensing radius r . During the course of motion, the relative distances between agents may vary with time, so the neighbors of each agent may change. We define the neighboring graph $\mathcal{G}(t) = \{\mathcal{V}, \mathcal{E}(t)\}$ to be an undirected graph consisting of a set of vertices $\mathcal{V} = \{1, 2, \dots, N\}$, whose elements represent agents in the group, and a set of edges $\mathcal{E}(t) = \{(i, j) \in \mathcal{V} \times \mathcal{V} : i \sim j\}$, containing unordered pairs of vertices that represent neighboring relations at time t . Vertices i and j are said to be adjacent at time t if $(i, j) \in \mathcal{E}(t)$. A path of length l between vertices i and j is a sequence of $l + 1$ distinct vertices starting with i and ending with j such that consecutive vertices in the sequence are adjacent.

4.1.2 Consensus Without a Leader

Let the control input for agent i be given by

$$u_i = - \sum_{j \in \mathcal{N}_i(t)} a_{ij}(q)(p_i - p_j), \quad i = 1, 2, \dots, N, \quad (4.4)$$

where $A(q) = (a_{ij}(q))_{N \times N}$ is the adjacency matrix which is defined in [5] as

$$a_{ij}(q) = \begin{cases} 0 & \text{if } j = i, \\ \rho_h(\|q_j - q_i\|_\sigma / \|r\|_\sigma) & \text{if } j \neq i, \end{cases}$$

with the bump function $\rho_h(z)$, $h \in (0, 1)$, being

$$\rho_h(z) = \begin{cases} 1 & \text{if } z \in [0, h), \\ 0.5[1 + \cos(\pi \frac{z-h}{1-h})] & \text{if } z \in [h, 1], \\ 0, & \text{otherwise,} \end{cases}$$

where the σ -norm $\|\cdot\|_\sigma$, defined for a general n -dimensional vector as a map $\mathbf{R}^n \rightarrow \mathbf{R}_{\geq 0}$,

$$\|z\|_\sigma = \frac{1}{\varepsilon} \left[\sqrt{1 + \varepsilon \|z\|^2} - 1 \right],$$

for some constant $\varepsilon > 0$. It is clear that $a_{ij}(q) = a_{ji}(q) > 0$ if $(j, i) \in \mathcal{E}(t)$ and $a_{ij}(q) = a_{ji}(q) = 0$ if $j \neq i$ but $(j, i) \notin \mathcal{E}(t)$. Note that the adjacency matrix $A(q)$ is continuous even if the network is switching. We define the Laplacian of graph $\mathcal{G}(t)$ with adjacency matrix $A(q)$ as $L(q) = \Delta(A(q)) - A(q)$, where the degree matrix $\Delta(A(q))$ is a diagonal matrix with the i th diagonal element being $\sum_{j=1}^N a_{ij}(q)$. Denote the eigenvalues of $L(q)$ as $\lambda_1(L(q)) \leq \lambda_2(L(q)) \leq \dots \leq \lambda_N(L(q))$. Then, $\lambda_1(L(q)) = 0$ and $(1, 1, \dots, 1)^T \in \mathbf{R}^N$ is the corresponding eigenvector. Moreover, if $\mathcal{G}(t)$ is a connected graph, then $\lambda_2(L(q)) > 0$ [10]. Denote the position and velocity of the center of mass (COM) of all agents in the group as

$$\bar{q} = \frac{\sum_{i=1}^N q_i}{N}, \quad \bar{p} = \frac{\sum_{i=1}^N p_i}{N}.$$

Theorem 4.1 Consider a system of N mobile agents with dynamics (4.1), each being steered by the control input (4.4). Then,

$$q_i(t) \rightarrow \bar{q}(0) \cos(\omega t) + \frac{1}{\omega} \bar{p}(0) \sin(\omega t)$$

and

$$p_i(t) \rightarrow -\omega \bar{q}(0) \sin(\omega t) \bar{q}(0) + \bar{p}(0) \cos(\omega t),$$

as $t \rightarrow \infty$, where $\bar{q}(0)$ and $\bar{p}(0)$ are respectively the initial position and velocity of the COM of the group.

Proof Denote the position difference and the velocity difference between agent i and the COM as $\tilde{q}_i = q_i - \bar{q}$ and $\tilde{p}_i = p_i - \bar{p}$, respectively. Then,

$$\begin{aligned} \dot{\tilde{q}}_i &= \tilde{p}_i, \\ \dot{\tilde{p}}_i &= -\omega^2 \tilde{q}_i - \sum_{j \in \mathcal{N}_i(t)} a_{ij}(\tilde{q})(\tilde{p}_i - \tilde{p}_j). \end{aligned}$$

For notational convenience, we also define

$$\tilde{q} = \begin{bmatrix} \tilde{q}_1 \\ \tilde{q}_2 \\ \vdots \\ \tilde{q}_N \end{bmatrix}, \quad \tilde{p} = \begin{bmatrix} \tilde{p}_1 \\ \tilde{p}_2 \\ \vdots \\ \tilde{p}_N \end{bmatrix}.$$

Consider the Lyapunov function candidate

$$Q(\tilde{q}, \tilde{p}) = \frac{1}{2} \omega^2 \tilde{q}^T \tilde{q} + \frac{1}{2} \tilde{p}^T \tilde{p},$$

which is a positive definite function and radially unbounded with respect to \tilde{p} and \tilde{q} .

The derivative of Q along the trajectories of the agents is given by

$$\begin{aligned} \dot{Q} &= \omega^2 \tilde{p}^T \tilde{q} + \tilde{p}^T \dot{\tilde{p}} \\ &= \omega^2 \tilde{p}^T \tilde{q} + \tilde{p}^T (-\omega^2 \tilde{q} - L(\tilde{q}) \tilde{p}) \\ &= -\tilde{p}^T L(\tilde{q}) \tilde{p} \leq 0. \end{aligned}$$

It then follows from the LaSalle Invariance Principle [11] that all trajectories of the agents converge to the largest invariant set inside the region

$$S = \{[\tilde{q}^T, \tilde{p}^T]^T \in \mathbf{R}^{2N} : \dot{Q} = 0\}.$$

We now consider the trajectories that lie entirely in S . Suppose that $\mathcal{G}(t)$ consists of $n(t)$, $1 \leq n(t) \leq N$, connected subgraphs and there are $N_k(t)$ agents in the k th, $1 \leq k \leq n(t)$, connected subgraph at time t . For any time t , there exists an orthogonal permutation matrix $P(t) \in \mathbf{R}^{N \times N}$ such that $L(\tilde{q})$ can be transformed into a block diagonal matrix as follows,

$$\begin{aligned} \check{L}(\tilde{q}) &= P(t)L(\tilde{q})P^T(t) \\ &= \begin{bmatrix} L_1(\tilde{q}) & \dots & 0 & \dots & 0 \\ \vdots & \ddots & \vdots & \vdots & \vdots \\ 0 & \dots & L_k(\tilde{q}) & \dots & 0 \\ \vdots & \vdots & \vdots & \ddots & \vdots \\ 0 & \dots & 0 & \dots & L_{n(t)}(\tilde{q}) \end{bmatrix}, \end{aligned}$$

where $L_k(\tilde{q}) \in \mathbf{R}^{N_k(t) \times N_k(t)}$ is the Laplacian matrix associated with the k th connected subgraph of the graph $\mathcal{G}(t)$. The indices of the state vector can be rearranged such that

$$\check{p} = \begin{bmatrix} \check{p}^1 \\ \check{p}^2 \\ \vdots \\ \check{p}^{n(t)} \end{bmatrix} = P(t)\tilde{p}, \quad \check{p}^k = \begin{bmatrix} \check{p}_1^k \\ \check{p}_2^k \\ \vdots \\ \check{p}_{N_k(t)}^k \end{bmatrix},$$

where \check{p}^k is the velocity difference vector of the $N_k(t)$ agents within the k th connected subgraph. Therefore,

$$\begin{aligned} -\tilde{p}^T L(\tilde{q}) \tilde{p} &= -\check{p}^T \check{L}(\tilde{q}) \check{p} \\ &= -[(\check{p}^1)^T \dots (\check{p}^k)^T \dots (\check{p}^{n(t)})^T]^T \\ &\quad \times \begin{bmatrix} L_1(\tilde{q}) & \dots & 0 & \dots & 0 \\ \vdots & \ddots & \vdots & \vdots & \vdots \\ 0 & \dots & L_k(\tilde{q}) & \dots & 0 \\ \vdots & \vdots & \vdots & \ddots & \vdots \\ 0 & \dots & 0 & \dots & L_{n(t)}(\tilde{q}) \end{bmatrix} \begin{bmatrix} \check{p}^1 \\ \vdots \\ \check{p}^k \\ \vdots \\ \check{p}^{n(t)} \end{bmatrix}. \end{aligned}$$

Clearly, $-\tilde{p}^T L(\tilde{q}) \tilde{p} = 0$ if and only if

$$(\check{p}^k)^T (L_k(\tilde{q})) \check{p}^k = 0, \quad k = 1, 2, \dots, n(t). \quad (4.5)$$

By the sum of squares property [5],

$$(\check{p}^k)^T (L_k(\tilde{q})) \check{p}^k = \frac{1}{2} \sum_{(i,j) \in \mathcal{E}(t)} a_{ij}(\tilde{q}) \|\check{p}_i^k - \check{p}_j^k\|^2.$$

Therefore, (4.5) is equivalent to

$$\check{p}_1^k = \check{p}_2^k = \cdots = \check{p}_{N_k(t)}^k, \quad k = 1, 2, \dots, n(t), \quad (4.6)$$

which implies that the velocities of the agents in the same subgroup are synchronized.

We next show that $n(t) = 1$. This would imply that all agents approach the same velocity asymptotically. From (4.1), (4.4), and (4.6), we have

$$\begin{aligned} \dot{q}_i &= p_i, \\ \dot{p}_i &= -\omega^2 q_i, \quad i = 1, 2, \dots, N, \end{aligned} \quad (4.7)$$

from which we obtain

$$q_i(t) = c_{1i} \cos(\omega t) + c_{2i} \sin(\omega t) \quad (4.8)$$

and

$$p_i(t) = -c_{1i} \omega \sin(\omega t) + c_{2i} \omega \cos(\omega t), \quad (4.9)$$

where c_{1i} and c_{2i} depend on the initial positions and velocities of all the agents in the group. From (4.8), every pair of agents in the group must collide during each uniformly bounded time-interval

$$[t_i, t_{i+1}), \quad t_{i+1} - t_i = \frac{\pi}{\omega}.$$

Assume that there are at least two connected subgroups in the system. Then, from earlier analysis, we know that agents from two different connected subgroups must collide at some time t' , i.e., at time t' , an agent i is connected with another agent j . In this case, we have $\tilde{p}_i(t') \neq \tilde{p}_j(t')$. It then follows from (4.5) that

$$\dot{Q}(t') < 0,$$

which contradicts with the fact that $\dot{Q}(t) = 0$. Thus, we conclude that the interaction network will not switch for all t . Consequently, $n(t) = 1$ for all t , i.e.,

$$\tilde{p}_1 = \tilde{p}_2 = \cdots = \tilde{p}_N = 0,$$

or

$$p_1 = p_2 = \cdots = p_N = \bar{p},$$

which implies that

$$\dot{p}_1 = \dot{p}_2 = \cdots = \dot{p}_N.$$

Then, from (4.1) and (4.4)

$$q_1 = q_2 = \cdots = q_N.$$

It follows from (4.1), (4.4), and the symmetry of $A(t)$ that

$$\dot{\bar{p}} = \frac{\sum_{i=1}^N \dot{p}_i}{N} = -\omega^2 \bar{q},$$

which in turn implies that

$$\begin{cases} \dot{\bar{q}} = \bar{p}, \\ \dot{\bar{p}} = -\omega^2 \bar{q}. \end{cases} \quad (4.10)$$

The solution of (4.10) can be obtained as

$$\bar{q}(t) = \bar{q}(0) \cos(\omega t) + \frac{1}{\omega} \bar{p}(0) \sin(\omega t),$$

and

$$\bar{p}(t) = -\omega \bar{q}(0) \sin(\omega t) + \bar{p}(0) \cos(\omega t).$$

In conclusion, it follows from the LaSalle Invariance Principle that

$$q_i(t) \rightarrow \bar{q}(0) \cos(\omega t) + \frac{1}{\omega} \bar{p}(0) \sin(\omega t)$$

and

$$p_i(t) \rightarrow -\omega \bar{q}(0) \sin(\omega t) + \bar{p}(0) \cos(\omega t),$$

as $t \rightarrow \infty$. □

Remark 4.1 Unlike many existing algorithms, Theorem 4.1 shows that the coupled harmonic oscillators can be synchronized even without any network connectivity assumption. This is because there exist an infinite sequence of contiguous, nonempty, and uniformly bounded time-intervals $[t_j, t_{j+1})$, $j = 0, 1, 2, \dots$, such that across each time interval each pair of agents in the group must naturally collide, that is, they exchange velocity information with each other when the relative distances between them are within the influencing/sensing radius r across each time interval.

4.1.3 Consensus with a Leader

In this subsection, we investigate the synchronization algorithm for the situation when a leader is present. In this case, the control input for agent i is given by

$$u_i = - \sum_{j \in \mathcal{N}_i(t)} a_{ij}(q)(p_i - p_j) - a_{i\gamma}(q)(p_i - p_\gamma), \quad i = 1, 2, \dots, N. \quad (4.11)$$

Theorem 4.2 Consider a system of N mobile agents with dynamics (4.1) and a leader with dynamic (4.2). Let each follower be steered by the control input (4.11). Then,

$$q_i(t) \rightarrow q_\gamma(0) \cos(\omega t) + \frac{1}{\omega} p_\gamma(0) \sin(\omega t)$$

and

$$p_i(t) \rightarrow -\omega q_\gamma(0) \sin(\omega t) + p_\gamma(0) \cos(\omega t),$$

as $t \rightarrow \infty$, where $q_\gamma(0)$ and $p_\gamma(0)$ are respectively the initial position and velocity of the leader.

Proof Denote the position difference and the velocity difference between agent i and the leader as $\tilde{q}_i = q_i - q_\gamma$ and $\tilde{p}_i = p_i - p_\gamma$, respectively. Then

$$\begin{aligned}\dot{\tilde{q}}_i &= \tilde{p}_i, \\ \dot{\tilde{p}}_i &= -\omega^2 \tilde{q}_i - \sum_{j \in \mathcal{N}_i(t)} a_{ij}(\tilde{q})(\tilde{p}_i - \tilde{p}_j) - a_{i\gamma}(\tilde{q})\tilde{p}_i.\end{aligned}\quad (4.12)$$

For notational convenience, we also define

$$\tilde{q} = \begin{bmatrix} \tilde{q}_1 \\ \tilde{q}_2 \\ \vdots \\ \tilde{q}_N \end{bmatrix}, \quad \tilde{p} = \begin{bmatrix} \tilde{p}_1 \\ \tilde{p}_2 \\ \vdots \\ \tilde{p}_N \end{bmatrix}.$$

Consider the Lyapunov function candidate

$$Q(\tilde{q}, \tilde{p}) = \frac{1}{2} \omega^2 \tilde{q}^T \tilde{q} + \frac{1}{2} \tilde{p}^T \tilde{p},$$

which is positive definite function and radially unbounded with respect to \tilde{p} and \tilde{q} .

The derivative of Q along the trajectories of the agents is given by,

$$\begin{aligned}\dot{Q} &= \omega^2 \tilde{p}^T \tilde{q} + \tilde{p}^T (-\omega^2 \tilde{q} - L(\tilde{q})\tilde{p} - H(\tilde{q})\tilde{p}) \\ &= -\tilde{p}^T (L(\tilde{q}) + H(\tilde{q}))\tilde{p} \leq 0,\end{aligned}$$

where

$$H(\tilde{q}) = \begin{bmatrix} a_{1\gamma}(\tilde{q}) & 0 & \dots & 0 \\ 0 & a_{2\gamma}(\tilde{q}) & \dots & 0 \\ \vdots & \vdots & \ddots & \vdots \\ 0 & 0 & \dots & a_{N\gamma}(\tilde{q}) \end{bmatrix}.$$

It then follows from the LaSalle Invariance Principle [11] that all trajectories of the agents converge to the largest invariant set inside the region

$$S = \{[\tilde{q}^T, \tilde{p}^T]^T \in \mathbf{R}^{2N} : \dot{Q} = 0\}.$$

We now consider the trajectories that lie entirely in S . Suppose that $\mathcal{G}(t)$ consists of $n(t)$, $1 \leq n(t) \leq N$, connected subgraphs and there are $N_k(t)$ agents in the k th, $1 \leq k \leq n(t)$, connected subgraph at time t . Similar to the analysis in the proof of Theorem 4.1, we have

$$\begin{aligned}& -\tilde{p}^T (L(\tilde{q}) + H(\tilde{q}))\tilde{p} \\ &= -[(\check{p}^1)^T \quad \dots \quad (\check{p}^k)^T \quad \dots \quad (\check{p}^{n(t)})^T]^T\end{aligned}$$

$$\begin{aligned}
& \times \begin{bmatrix} L_1(\tilde{q}) & \dots & 0 & \dots & 0 \\ \vdots & \ddots & \vdots & \vdots & \vdots \\ 0 & \dots & L_k(\tilde{q}) & \dots & 0 \\ \vdots & \vdots & \vdots & \ddots & \vdots \\ 0 & \dots & 0 & \dots & L_{n(t)}(\tilde{q}) \end{bmatrix} \begin{bmatrix} \check{p}^1 \\ \vdots \\ \check{p}^k \\ \vdots \\ \check{p}^{n(t)} \end{bmatrix} \\
& - [(\check{p}^1)^T \dots (\check{p}^k)^T \dots (\check{p}^{n(t)})^T]^T \\
& \times \begin{bmatrix} H_1(\tilde{q}) & \dots & 0 & \dots & 0 \\ \vdots & \ddots & \vdots & \vdots & \vdots \\ 0 & \dots & H_k(\tilde{q}) & \dots & 0 \\ \vdots & \vdots & \vdots & \ddots & \vdots \\ 0 & \dots & 0 & \dots & H_{n(t)}(\tilde{q}) \end{bmatrix} \begin{bmatrix} \check{p}^1 \\ \vdots \\ \check{p}^k \\ \vdots \\ \check{p}^{n(t)} \end{bmatrix},
\end{aligned}$$

where \check{p}^k is the velocity difference within the k th connected subgraph. Clearly, $-\check{p}^T(L(\tilde{q}) + H(\tilde{q}))\check{p} = 0$ if and only if

$$(\check{p}^k)^T (L_k(\tilde{q}) + H_k(\tilde{q}))\check{p}^k = 0, \quad k = 1, 2, \dots, n(t), \quad (4.13)$$

which implies that if one agent in the subgroup k is the neighbor of the leader, then the velocity difference between the agents in this subgroup and the virtual leader is zero, otherwise, the velocity difference between the agents in this subgroup is synchronized but may not be zero. As in the proof of Theorem 4.1, we can show that $n(t) = 1$, and the leader is a neighbor of the agents of the connected group. From (4.13),

$$\tilde{p}_1 = \tilde{p}_2 = \dots = \tilde{p}_N = 0, \quad (4.14)$$

from which it follows that

$$\dot{\tilde{p}}_1 = \dot{\tilde{p}}_2 = \dots = \dot{\tilde{p}}_N = 0.$$

Then, from (4.12) it follows that

$$\tilde{q}_1 = \tilde{q}_2 = \dots = \tilde{q}_N = 0. \quad (4.15)$$

Finally, from (4.2), (4.14), and (4.15), we have

$$q_i(t) \rightarrow q_\gamma(0) \cos(\omega t) + \frac{1}{\omega} p_\gamma(0) \sin(\omega t),$$

and

$$p_i(t) \rightarrow -\omega q_\gamma(0) \sin(\omega t) + p_\gamma(0) \cos(\omega t),$$

as $t \rightarrow \infty$. □

Remark 4.2 Unlike many existing algorithms with a leader, Theorem 4.2 shows that all harmonic oscillators can asymptotically attain the position and velocity of the leader even without any connectivity assumption on the followers. This is

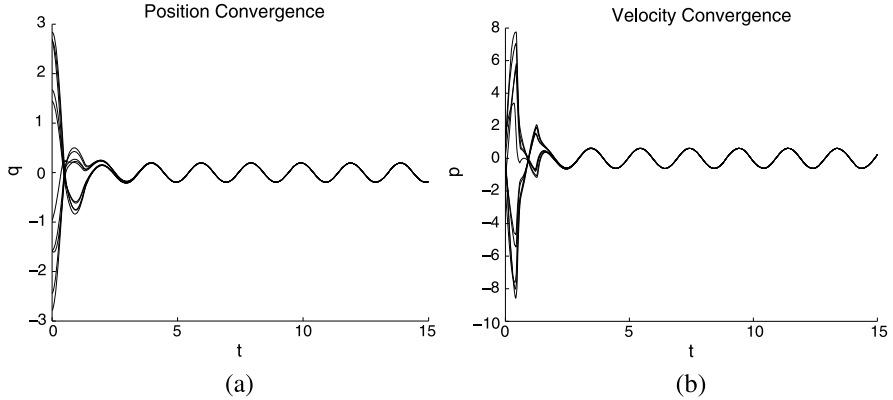


Fig. 4.1 [12] Synchronization of 10 agents under control input (4.4)

because there exists an infinite sequence of contiguous, nonempty and uniformly bounded time-intervals $[t_j, t_{j+1})$, $j = 0, 1, 2, \dots$, such that during each time interval all agents in the group and the leader must naturally collide, that is, each agent in the group exchanges velocity information with the leader when the relative distance between them is below the influencing/sensing radius r across each time interval.

4.1.4 Simulation Study

All the simulations are performed with 10 agents whose initial positions and velocities are randomly chosen within $[-4, 4]$ and $[-2, 2]$, respectively. In the simulation, we choose the influencing/sensing radius $r = 0.5$, the parameter $\omega = 3.162$, and $\varepsilon = 0.1$ for the σ -norm.

Figure 4.1 shows the synchronization of coupled harmonic oscillators under control input (4.4). In particular, plots (a) and (b) are respectively the evolutions of the position and velocity of the ten agents. It is obvious from these plots that the control input (4.4) is capable of achieving stable synchronization motion in the absence of any network connectivity assumption.

Figure 4.2 shows the synchronization with a leader of coupled harmonic oscillators under control input (4.11). In this figure, initial position and velocity of the leader are set to be $q_\gamma(0) = 1$ and $p_\gamma(0) = 1$. Shown in plots (a) and (b) are respectively the evolution of the position difference and velocity differences between the ten agents and the leader. These simulation results show that all agents asymptotically attain the position and velocity of the leader in the absence of any connectivity assumption on the followers.

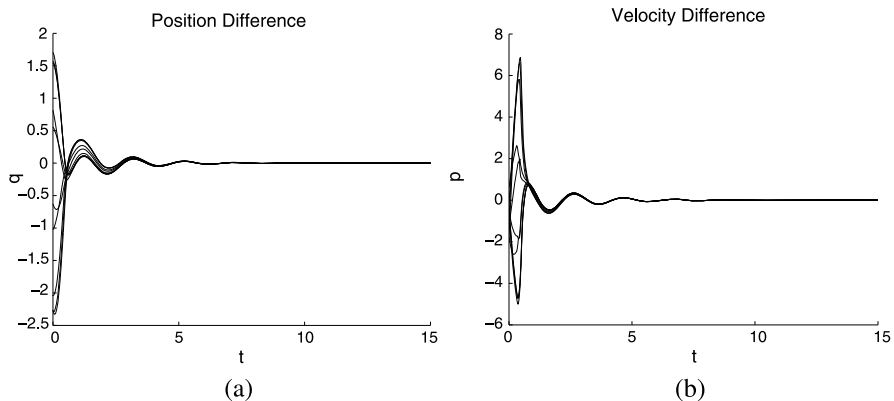


Fig. 4.2 [12] Synchronization with a leader of 10 agents under control input (4.11)

4.2 Consensus with Preserved Network Connectivity

Subjected to limited sensing and communication capabilities of agents, the interaction topology among agents may change over time. A basic assumption made in most previous works on stability analysis of collective dynamics is that the underlying topology can remain connected enough frequently during the motion evolution. However, for a given set of initial states and parameters, it is very difficult or even impossible to satisfy and verify this assumption in practice. In fact, the connectivity of the initial network generally cannot guarantee the connectivity of the whole network throughout a long process of motion. For example, the consensus algorithm proposed in [13], the flocking algorithms in [5], and the rendezvous algorithm in [14] have all been known to possibly result in fragmentation even if the initial network is connected.

Recently, some efforts had been made to preserve the connectivity of the networks. For example, Cortes, Martinez, and Bullo [15] proposed a circumcenter algorithm to avoid losing existing connections. Degennaro and Jadbabaie [16] suggested an iterative decentralized algorithm to maximize the smallest nonzero eigenvalue of the Laplacian matrix for the connectivity control. Spanos and Murray [17] used a measure of local connectivity to ensure the global connectivity of a network. Dimarogonas and Kyriakopoulos [18, 19] used potential functions to maintain the network connectivity for rendezvous and swarming. Ji and Egerstedt [20] proposed a hysteresis in adding new links and a special potential function to achieve rendezvous while preserving the network connectivity. However, all these works are concerned with agents described by single-integrator dynamics. Recently, Zavlanos, Jadbabaie, and Pappas [21] used the hysteresis and potential function method to study a flocking problem combining with the network connectivity for double-integrator dynamics to achieve velocity alignment.

In this section, we investigate the second-order consensus problem with connectivity preservation for double-integrator dynamics, also employing hysteresis in

adding new links and using the potential function method. It should be noted, however, that in [20] and [21], two specific potential functions are constructed for single-integrator dynamics and double-integrator dynamics, respectively, which tend to infinity as the distance between two already connected agents tends to the sensing radius, which is rather impractical. In this section, we construct a general class of bounded potential functions that can preserve the network connectivity for double-integrator dynamics and the aforementioned divergence problem can be avoided. We also investigate the consensus protocol with a virtual leader and show that all agents can asymptotically attain a desired velocity even if only one agent in the team has communication with, hence has information about the virtual leader.

4.2.1 Problem Statement

Consider N agents moving in an n -dimensional Euclidean space. The motion of each agent is described by a double-integrator equation of the form

$$\begin{aligned}\dot{q}_i &= p_i, \\ \dot{p}_i &= u_i, \quad i = 1, \dots, N,\end{aligned}\tag{4.16}$$

where $q_i \in \mathbf{R}^n$ is the position vector of agent i , $p_i \in \mathbf{R}^n$ is its velocity vector, and $u_i \in \mathbf{R}^n$ is the (force) control input acting on agent i , $i = 1, \dots, N$.

Suppose that all agents have the same influencing/sensing radius r . Let $\varepsilon \in (0, r]$ and $\varepsilon_0 \in (0, r)$ be the given constants and $\varepsilon_0 \leq \varepsilon$. Call $G(t) = (V, E(t))$ a undirected dynamic graph consisting of a set of vertices $V = \{1, 2, \dots, N\}$ indexed by the set of agents and a time-varying set of links $E(t) = \{(i, j) | i, j \in V\}$ such that

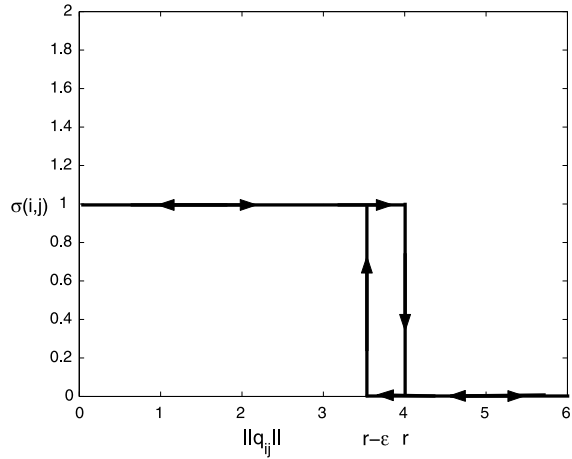
- (i) Initial links are generated by $E(0) = \{(i, j) | \|q_i(0) - q_j(0)\| < r - \varepsilon_0, i, j \in V\}$.
- (ii) If $(i, j) \notin E(t^-)$ and $\|q_i(t) - q_j(t)\| < r - \varepsilon$, then (i, j) is a new link being added to $E(t)$.
- (iii) If $\|q_i(t) - q_j(t)\| \geq r$, then $(i, j) \notin E(t)$.

Throughout this chapter, $\|\cdot\|$ denotes the Euclidean norm. One can use a symmetric indicator function $\sigma(i, j) \in \{0, 1\}$ to describe whether there is a link between agent i and agent j at time t , which is defined as

$$\sigma(i, j)[t] = \begin{cases} 0 & \text{if } ((\sigma(i, j)[t^-] = 0) \cap (\|q_i(t) - q_j(t)\| \geq r - \varepsilon)) \cup \\ & ((\sigma(i, j)[t^-] = 1) \cap (\|q_i(t) - q_j(t)\| \geq r)), \\ 1 & \text{if } ((\sigma(i, j)[t^-] = 1) \cap (\|q_i(t) - q_j(t)\| < r)) \cup \\ & ((\sigma(i, j)[t^-] = 0) \cap (\|q_i(t) - q_j(t)\| < r - \varepsilon)). \end{cases}$$

One can see from Fig. 4.3 that there is a hysteresis in the indicator function for adding new links to the graph [20, 21]. When $\varepsilon = r$, no new links can be added to the graph. Moreover, one will see that the selection of the parameter ε (ε_0) is a trade-off between the maximum overshoot and the settling time of velocity convergence

Fig. 4.3 [22] Indicator function $\sigma(i, j)$



(the feasible energy and the radius of the initial network): the smaller the value of ε (ε_0), the larger the maximum overshoot and the smaller the settling time (the larger the magnitude of the potential function and the radius of the initial network).

Our objective is to make all agents converge to the same position and move with the same velocity under the assumption that the initial network is connected. To achieve this goal, we choose the control law u_i for agent i in (4.16) to be

$$u_i = \alpha_i + \beta_i, \quad (4.17)$$

where α_i is the gradient-based term, which is designed to enforce the position of each agent to a common value and also to maintain the connectivity of the network, and β_i is the consensus term, which regulates the velocity of each agent to a common value.

In some cases, the regulation of agents is for certain purposes, e.g., achieving a desired common velocity or arriving at a desired destination. In the situation where there is a virtual leader, we modify the control law (4.17) to

$$u_i = \alpha_i + \beta_i + \gamma_i, \quad (4.18)$$

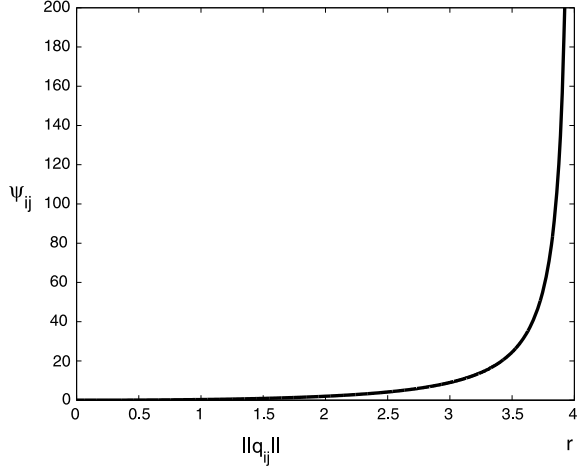
where γ_i is the navigational feedback term, which drives agent i to track the virtual leader.

4.2.2 Algorithm Design and Main Results

We now specify an explicit control input in Eq. (4.17) as

$$u_i = - \underbrace{\sum_{j \in N_i(t)} \nabla_{q_i} \psi(\|q_{ij}\|)}_{\alpha_i} - \underbrace{\sum_{j \in N_i(t)} w_{ij}(p_i - p_j)}_{\beta_i}. \quad (4.19)$$

Fig. 4.4 [22] The potential function (4.21)



Here, $q_{ij} = q_i - q_j$, the constant $w_{ji} = w_{ji} > 0$ is bounded for all $i, j \in V$, $N_i(t)$ is the neighborhood region of agent i at time t defined as

$$N_i(t) = \{j \mid \sigma(i, j)[t] = 1, j \neq i, j = 1, \dots, N\}. \quad (4.20)$$

The nonnegative potential $\psi(\|q_{ij}\|)$ is defined to be a function of the distance $\|q_{ij}\|$ between agent i and agent j , differentiable with respect to $\|q_{ij}\| \in [0, r]$ such that

- (i) $\frac{\partial \psi(\|q_{ij}\|)}{\partial \|q_{ij}\|} > 0$ for $\|q_{ij}\| \in (0, r)$.
- (ii) $\lim_{\|q_{ij}\| \rightarrow 0} \left(\frac{\partial \psi(\|q_{ij}\|)}{\partial \|q_{ij}\|} \cdot \frac{1}{\|q_{ij}\|} \right)$ is nonnegative and bounded.
- (iii) $\psi(r) = \hat{Q} \in [Q_{\max}, +\infty)$, where $Q_{\max} \triangleq \frac{1}{2} \sum_{i=1}^N p_i^T(0) p_i(0) + \frac{N(N-1)}{2} \psi \times (\|r - \varepsilon_0\|)$.

Condition (i) illustrates that the potential between the two agents is an increasing function of their distance, which makes two agents attract each other; Condition (ii) requires that the magnitude of gradient between two agents is the same or a higher-order term of their distance when the two agents converge to the same position; Condition (iii) states that the potential between two agents will be sufficiently large when the distance between the two agents reaches the sensing radius, which guarantees that all existing edges will not be lost. One example of such a potential function is the following (see Fig. 4.4):

$$\psi(\|q_{ij}\|) = \frac{\|q_{ij}\|^2}{r - \|q_{ij}\| + \frac{r^2}{\hat{Q}}}, \quad \|q_{ij}\| \in [0, r]. \quad (4.21)$$

Note that in [20] and [21], only two specific potential functions are proposed: in [20],

$$\psi(\|q_{ij}\|) = \frac{\|q_{ij}\|^2}{r - \|q_{ij}\|}, \quad \|q_{ij}\| \in [0, r), \quad (4.22)$$

and in [21],

$$\psi(\|q_{ij}\|) = \frac{1}{\|q_{ij}\|^2} + \frac{1}{r^2 - \|q_{ij}\|^2}, \quad \|q_{ij}\| \in (0, r). \quad (4.23)$$

Potential function (4.22) satisfies Conditions (i) and (ii) but does not satisfy Condition (iii) of our general definition of the potential function, and potential function (4.23) does not satisfy any of the three conditions. In particular, potential functions (4.22) and (4.23) tend to infinity when the distance between two agents i and j tends to r , which may not be practical since it will require extremely large control input. If the hysteresis parameter $\varepsilon = 0$, from simple calculation, $\hat{Q} = +\infty$ in the potential function (4.21). Therefore, the potential function (4.21) is the same as the potential function (4.22). Note that, here as well as in [20, 21], without the hysteresis mechanism (see Fig. 4.3), no new links will be added to the network. This is because the potential force is so big as to prevent the addition of new links when the distance between two agents i and j tends to r .

The sum of the total artificial potential energy and the total kinetic energy is defined as follows:

$$Q = \frac{1}{2} \sum_{i=1}^N \left(\sum_{j \in N_i(t)} \psi(\|q_{ij}\|) + p_i^T p_i \right), \quad (4.24)$$

with the initial energy $Q_0 = Q(q(0), p(0))$. Clearly, Q is a positive semi-definite function.

The adjacency matrix $A(t) = (a_{ij}(t))$ of the above graph $G(t)$ is defined as

$$a_{ij}(t) = \begin{cases} w_{ij}, & (i, j) \in E(t), \\ 0, & \text{otherwise.} \end{cases}$$

The corresponding Laplacian is $L(t) = \Delta(A(t)) - A(t)$, where the degree matrix $\Delta(A(t))$ is a diagonal matrix with the i th diagonal element equal to $\sum_{j=1, j \neq i}^N a_{ij}(t)$. The corresponding n -dimensional graph Laplacian is defined as $\hat{L}(t) = L(t) \otimes I_n$, where I_n is the identity matrix of order n and \otimes stands for the Kronecker product. This multi-dimensional Laplacian satisfies the following sum-of-squares property [5]:

$$z^T \hat{L}(t) z = \frac{1}{2} \sum_{(i,j) \in E} a_{ij}(t) \|z_j - z_i\|^2,$$

where $z = [z_1^T, z_2^T, \dots, z_N^T]^T \in \mathbf{R}^{Nn}$ and $z_i \in \mathbf{R}^n$ for all i .

Denote the position and velocity of the center of mass (COM) of all agents in the group by

$$\bar{q} = \frac{\sum_{i=1}^N q_i}{N}, \quad \bar{p} = \frac{\sum_{i=1}^N p_i}{N}.$$

The main results of this section are given in the following theorem:

Theorem 4.3 Consider a system of N mobile agents with dynamics (4.16), each steered by protocol (4.19). Suppose that the initial network $G(0)$ is connected and the initial energy Q_0 is finite. Then, the following hold:

- (i) $G(t)$ is connected for all $t \geq 0$.
- (ii) All agents asymptotically converge to the same position and move with the same velocity.
- (iii) The velocity $\bar{p}(t)$ of the COM is invariant for all $t \geq 0$.

Proof Proof of part (i)

Assume that $G(t)$ switches at time t_k ($k = 1, 2, \dots$), otherwise $G(t)$ is a fixed graph in each time-interval $[t_{k-1}, t_k)$. Note that Q_0 is finite and the time derivative of $Q(t)$ in $[t_0, t_1)$ is

$$\begin{aligned} \dot{Q}(t) &= \frac{1}{2} \sum_{i=1}^N \sum_{j \in N_i} \dot{\psi}(\|q_{ij}\|) + \sum_{i=1}^N p_i^T \dot{p}_i \\ &= \sum_{i=1}^N p_i^T \sum_{j \in N_i} \nabla_{q_i} \psi(\|q_{ij}\|) \\ &\quad + \sum_{i=1}^N p_i^T \left(- \sum_{j \in N_i} \nabla_{q_i} \psi(\|q_{ij}\|) - \sum_{j \in N_i} w_{ij} (p_i - p_j) \right) \\ &= -p^T [L(t) \otimes I_n] p. \end{aligned}$$

Since $L(t)$ is positive semi-definite [10], $\dot{Q}(t) \leq 0$ in $[t_0, t_1)$, which implies that

$$Q(t) \leq Q_0 < Q_{\max} \quad \text{for } t \in [t_0, t_1).$$

From the definition of the potential function, one has $\psi(r) > Q_{\max} > Q_0$. Therefore, no edge-distances will tend to r for $t \in [t_0, t_1)$, which implies that no existing edges will be lost at time t_1 . Hence, new edges must be added in the interaction network at the switching time t_1 . Without loss of generality, assume that there are m_1 new links being added to the interaction network at time t_1 . Clearly, $0 < m_1 \leq M$ and $M \triangleq \frac{(N-1)(N-2)}{2}$, thus, $Q(t_1) = Q_0 + m_1 \psi(\|r - \varepsilon\|) \leq Q_{\max}$.

Similar to the aforementioned analysis, the time derivative of $Q(t)$ in $[t_{k-1}, t_k)$ is

$$\dot{Q}(t) = -p^T [L(t) \otimes I_n] p \leq 0, \quad (4.25)$$

which implies that

$$Q(t) \leq Q(t_{k-1}) < Q_{\max} \quad \text{for } t \in [t_{k-1}, t_k), \quad k = 1, 2, \dots \quad (4.26)$$

Therefore, no edge-distances will tend to r for $t \in [t_{k-1}, t_k)$, which implies that no edges will be lost at time t_k and $Q(t_k) \leq Q_{\max}$.

Since $G(0)$ is connected and no edges in $E(0)$ will be lost, $G(t)$ will be connected for all $t \geq 0$.

Proof of parts (ii) and (iii)

Assume that there are m_k new links being added to the interaction network at time t_k . Clearly, $0 < m_k \leq M$. From (4.24) and (4.26), one has

$$Q(t_k) \leq Q_0 + (m_1 + \cdots + m_k)\psi(\|r - \varepsilon\|) \leq Q_{\max}.$$

Since there are at most M new links that can be added to $G(t)$, one has $k \leq M$ and $Q(t) \leq Q_{\max}$ for all $t \geq 0$. Therefore, the number of switching times k of the system (4.16) is finite, which implies the interaction network $G(t)$ eventually becomes fixed. Thus, the rest discussions can be restricted on the time interval (t_k, ∞) . Note that the distance of edge is not longer than $\psi^{-1}(Q_{\max})$. Hence, the set

$$\Omega = \{\hat{q} \in D_g, p \in \mathbf{R}^{Nn} \mid Q(\hat{q}, p) \leq Q_{\max}\}, \quad (4.27)$$

is positively invariant, where $D_g = \{\hat{q} \in \mathbf{R}^{N^2n} \mid \|q_{ij}\| \in [0, \psi^{-1}(Q_{\max})], \forall (i, j) \in E(t)\}$, $\hat{q} = [q_{11}^T, \dots, q_{1N}^T, \dots, q_{N1}^T, \dots, q_{NN}^T]^T$, and $p = [p_1^T, p_2^T, \dots, p_N^T]^T$.

Since $G(t)$ is connected for all $t \geq 0$, one has $\|q_{ij}\| < (N-1)r$ for all i and j . Since $Q(t) \leq Q_{\max}$, one has $p_i^T p_i \leq 2Q_{\max}$, and thus $\|p_i\| \leq \sqrt{2Q_{\max}}$. Therefore, the set Ω satisfying $Q(t) \leq Q_{\max}$ is closed and bounded, hence compact. Note that system (4.16) with control input (4.19) is an autonomous system, at least on the concerned time interval (t_k, ∞) . Therefore, the LaSalle's invariance principle [11] can be applied to infer that if the initial conditions of the system lies in Ω , its trajectories will converge to the largest invariant set inside the region $S = \{\hat{q} \in D_g, p \in \mathbf{R}^{Nn} \mid \dot{Q} = 0\}$.

From (4.25), one has

$$\dot{Q} = -p^T(L(t) \otimes I_n)p = \frac{1}{2} \sum_{(i,j) \in E} w_{ij} \|p_j - p_i\|^2. \quad (4.28)$$

Therefore, $\dot{Q} = 0$ if and only if $p_1 = \cdots = p_N$, which implies that all agents asymptotically move with the same velocity.

Since $\psi(\|q_{ij}\|) = \psi(\|q_{ji}\|)$ and $w_{ij} = w_{ji}$, from the control input (4.19), one has

$$\bar{u} = \dot{\bar{p}} = \frac{\sum_{i=1}^N u_i}{N} = -\frac{1}{N} \sum_{i=1}^N \left(\sum_{j \in N_i(t)} \nabla_{q_i} \psi(\|q_{ij}\|) + \sum_{j \in N_i(t)} w_{ij} (p_i - p_j) \right) = 0, \quad (4.29)$$

which implies that the velocity of the COM is invariant for all $t \geq 0$.

In steady state, $p_1 = \cdots = p_N = \bar{p}$, so that $\dot{p}_i = \dot{\bar{p}} = 0, \forall i \in V$. From (4.19), one has

$$u_i = \dot{p}_i = - \sum_{j \in N_i(t)} \nabla_{q_i} \psi(\|q_{ij}\|) = - \sum_{j \in N_i(t)} \frac{\partial \psi(\|q_{ij}\|)}{\partial \|q_{ij}\|} \cdot \frac{1}{\|q_{ij}\|} (q_i - q_j) = 0, \quad i = 1, \dots, N. \quad (4.30)$$

Rewrite (4.30) in a matrix form as

$$-(\hat{L}(t) \otimes I_n)q = 0,$$

where $q^T = [q_1^T, \dots, q_N^T]$ and $\hat{L}(t) = [\hat{l}_{ij}]$ is a matrix with

$$\hat{l}_{ii} = - \sum_{j=1, j \neq i}^N \left(\frac{\partial \psi(\|q_{ij}\|)}{\partial \|q_{ij}\|} \cdot \frac{1}{\|q_{ij}\|} \right)$$

and

$$\hat{l}_{ij} = \frac{\partial \psi(\|q_{ij}\|)}{\partial \|q_{ij}\|} \cdot \frac{1}{\|q_{ij}\|}, \quad \text{for } i \neq j.$$

From the definition, $\frac{\partial \psi(\|q_{ij}\|)}{\partial \|q_{ij}\|} \cdot \frac{1}{\|q_{ij}\|}$ is positive and uniformly bounded for $\|q_{ij}\| \in (0, \psi^{-1}(Q_{\max}))$ and $\lim_{\|q_{ij}\| \rightarrow 0} (\frac{\partial \psi(\|q_{ij}\|)}{\partial \|q_{ij}\|} \cdot \frac{1}{\|q_{ij}\|})$ is nonnegative and bounded. Since the dynamic network is connected all the time, from the property of the Laplacian matrix $\hat{L}(t) \otimes I_n$ [10], q converges asymptotically to $\text{span}\{1\}$, which implies that $q_1 = q_2 = \dots = q_N$. \square

In this following, we present some qualitative analysis of the convergence rate of the system. From (4.25), the decay rate of the total energy Q is influenced by the topology of the interaction network. From (4.28), $\dot{Q} = 0$ if and only if $p_1 = \dots = p_N$. Since the interaction network is connected all the time, from the matrix theory [23] and (4.25), one has

$$-\lambda_N(L(t))p^T p \leq \dot{Q}(t) \leq -\lambda_2(L(t))p^T p. \quad (4.31)$$

Thus, $\lambda_2(L(t))$ characterizes the convergence rate of the system. Therefore, we conclude that the convergence rate of the system relies on the smallest nonzero eigenvalue of the Laplacian of the interaction network. For an undirected graph, adding edges increases the smallest nonzero eigenvalue $\lambda_2(L(t))$, and $\lambda_2(L(t))$ attains its maximum value N when the topology of the network is fully connected [24]. Thus, $\lambda_2(L(0)) \leq \lambda_2(L(t)) \leq N$, showing that $\lambda_2(L(0))$ characterizes the bound of the convergence rate of the system.

4.2.3 Consensus with a Virtual Leader

In nature, few individuals have some pertinent information, such as knowledge of the location of a food source or of a migration route [25]. Here, we assume that only one agent is informed about the virtual leader. Certainly, the result can be generalized to the case with multiple informed agents, which may lead to faster convergence. Suppose that velocity of the virtual leader can be received by the informed agent through some designed mechanism, such as broadcasting. The control input to agent i is designed as

$$u_i = - \underbrace{\sum_{j \in N_i(t)} \nabla_{q_i} \psi(\|q_{ij}\|)}_{\alpha_i} - \underbrace{\sum_{j \in N_i(t)} w_{ij}(p_i - p_j)}_{\beta_i} - \underbrace{h_i c_1(p_i - p_\gamma)}_{\gamma_i}, \quad c_1 > 0, \quad (4.32)$$

where p_γ is a desired constant velocity of the virtual leader. If agent i is the informed agent, then $h_i = 1$; otherwise, $h_i = 0$. Without loss of generality, assume that the first agent is the informed agent, that is, $h_i = 1$ for $i = 1$ and $h_i = 0$ for all the others.

Define the sum of the total artificial potential energy and the total relative kinetic energy between all agents and the virtual leader as follows:

$$U = \frac{1}{2} \sum_{i=1}^N \left(\sum_{j \in N_i(t)} \psi(\|q_{ij}\|) + (p_i - p_\gamma)^T (p_i - p_\gamma) \right). \quad (4.33)$$

Clearly, U is a positive semi-definite function. Here, the potential function ψ should satisfy Conditions (i)–(iii) defined in the last section with Q_{\max} in Condition (iii) being replaced by

$$U_{\max} \triangleq \frac{1}{2} \sum_{i=1}^N (p_i(0) - p_\gamma(0))^T (p_i(0) - p_\gamma(0)) + \frac{N(N-1)}{2} \psi(\|r - \varepsilon_0\|).$$

Our main results on tracking the virtual leader can be stated in the following theorem.

Theorem 4.4 *Consider a system of N mobile agents with dynamics (4.16), each steered by protocol (4.32). Suppose that the initial network $G(0)$ is connected and the initial energy U_0 is finite. Then, the following hold:*

- (i) $G(t)$ is connected for all $t \geq 0$.
- (ii) All agents asymptotically converge to the same position and move with the desired velocity p_γ .

Proof We first prove part (i) of Theorem 4.4.

Denote the position difference vector and the velocity difference vector between agent i and the virtual leader by $\tilde{q}_i = q_i - p_\gamma t$ and $\tilde{p}_i = p_i - p_\gamma$, respectively. Then,

$$\begin{aligned} \dot{\tilde{q}}_i &= \tilde{p}_i, \\ \dot{\tilde{p}}_i &= u_i, \quad i = 1, \dots, N. \end{aligned} \quad (4.34)$$

By the definition of $\psi(\|q_{ij}\|)$, where $q_{ij} = q_i - q_j$, we have, for $\tilde{q}_{ij} = \tilde{q}_i - \tilde{q}_j$,

$$\psi(\|q_{ij}\|) = \psi(\|\tilde{q}_{ij}\|). \quad (4.35)$$

Thus, the control input (4.32) for agent i can be rewritten as

$$u_i = - \sum_{j \in N_i(t)} \nabla_{\tilde{q}_i} \psi(\|\tilde{q}_{ij}\|) - \sum_{j \in N_i(t)} w_{ij} (\tilde{p}_i - \tilde{p}_j) - h_i c_1 \tilde{p}_i, \quad (4.36)$$

and the positive semi-definite energy function (4.33) can be rewritten as

$$U = \frac{1}{2} \sum_{i=1}^N (\psi(\|\tilde{q}_{ij}\|) + \tilde{p}_i^T \tilde{p}_i). \quad (4.37)$$

Similar to the proof of part (i) of Theorem 4.3, we can show that the time derivative of $U(t)$ in $[t_{k-1}, t_k)$ is

$$\dot{U}(t) = \frac{1}{2} \sum_{i=1}^N \sum_{j \in N_i(t)} \dot{\psi}(\|\tilde{q}_{ij}\|) + \sum_{i=1}^N \tilde{p}_i^T \dot{\tilde{p}}_i = -\tilde{p}^T[(L(t) + c_1 H) \otimes I_n] \tilde{p} \leq 0. \quad (4.38)$$

Since $H = \text{diag}(h_1, h_2, \dots, h_N)$ is positive semi-definite, $\dot{U}(t) \leq 0$ in $[t_{k-1}, t_k)$, which implies that

$$U(t) \leq U(t_{k-1}) < U_{\max} \quad \text{for } t \in [t_{k-1}, t_k), \quad k = 1, 2, \dots \quad (4.39)$$

Therefore, no edge-distance will tend to r for $t \in [t_{k-1}, t_k)$, which implies that no edge will be lost at time t_k , and $U(t_k) \leq U_{\max}$. Since $G(0)$ is connected and no edges in $E(0)$ will be lost, $G(t)$ will remain to be connected for all $t \geq 0$.

We now prove part (ii) of Theorem 4.4.

Similar to the proof of part (ii) of Theorem 4.3, the set

$$\Omega = \{\hat{q} \in D_g, \tilde{p} \in \mathbf{R}^{Nn} \mid U(\hat{q}, \tilde{p}) \leq U_{\max}\}, \quad (4.40)$$

is compact, where $D_g = \{\hat{q} \in \mathbf{R}^{N^2n} \mid \|\tilde{q}_{ij}\| \in [0, \psi^{-1}(U_{\max})], \forall (i, j) \in E(t)\}$, $\hat{q} = [\hat{q}_{11}^T, \dots, \hat{q}_{1N}^T, \dots, \hat{q}_{N1}^T, \dots, \hat{q}_{NN}^T]^T$ and $\tilde{p} = [\tilde{p}_1^T, \tilde{p}_2^T, \dots, \tilde{p}_N^T]^T$. From LaSalle's invariance principle [11], we have

$$\dot{U} = -\tilde{p}^T[(L(t) + c_1 H) \otimes I_n] \tilde{p} = -\tilde{p}^T(L(t) \otimes I_n) \tilde{p} - c_1 \tilde{p}^T(H \otimes I_n) \tilde{p} = 0, \quad (4.41)$$

which implies that $\tilde{p}_1 = \dots = \tilde{p}_N$ and $\tilde{p}_1 = 0$, i.e., $p_1 = \dots = p_N = p_\gamma$. This also implies that, in steady state, $u_i = \dot{p}_i = \dot{p}_\gamma = 0$. Thus, from (4.32),

$$u_i = \dot{p}_i = - \sum_{j \in N_i(t)} \nabla_{q_i} \psi(\|q_{ij}\|) = - \sum_{j \in N_i(t)} \frac{\partial \psi(\|q_{ij}\|)}{\partial \|q_{ij}\|} \cdot \frac{1}{\|q_{ij}\|} (q_i - q_j) = 0, \quad i = 1, \dots, N. \quad (4.42)$$

Similar to the proof of part (ii) of Theorem 4.3, we have $q_1 = q_2 = \dots = q_N$. \square

In general, all agents asymptotically converge to the desired velocity p_γ , which implies that the velocity $\bar{p}(t)$ of the COM asymptotically converge to the desired velocity p_γ . From the control input (4.32),

$$\dot{\bar{p}} = \frac{\sum_{i=1}^N u_i}{N} = -c_1 \frac{1}{N} \sum_{i=1}^N h_i (p_i - p_\gamma) = 0. \quad (4.43)$$

Even if only one agent in the group is not the informed agent, it is difficult to explicitly estimate the convergence rate of the COM. However, one can get a bound for the convergence rate of the system. From (4.38), the decay rate of the total energy U is influenced by the topology of the interaction network and the coeffi-

cient c_1 . From (4.41), $\dot{U} = 0$ if and only if $p_1 = \dots = p_N = p_\gamma$. Similar to (4.31), one has

$$-(\lambda_N(L(t)) + c_1)\tilde{p}^T \tilde{p} \leq \dot{U}(t) \leq -\lambda_2(L(t))\tilde{p}^T \tilde{p}. \quad (4.44)$$

Thus, $\lambda_2(L(t))$ characterizes the convergence rate of the system. Therefore, we conclude that the convergence rate of the system relies on the smallest nonzero eigenvalue of the Laplacian of the interaction network. Thus,

$$\lambda_2(L(0)) \leq \lambda_2(L(t)) \leq N.$$

When all agents have reached the common desired velocity, the velocity of COM must reach the desired velocity. Then, the convergence rate of the system is not faster than the convergence rate of COM. Therefore, $\lambda_2(L(0))$ characterizes the bound of the convergence rate of COM.

In the situation where each agent is an informed agent and the velocity $p_\gamma(t)$ of the virtual leader varies with time, we propose the following protocol:

$$u_i = - \underbrace{\sum_{j \in N_i(t)} \nabla_{q_i} \psi(\|q_{ij}\|)}_{\alpha_i} - \underbrace{\sum_{j \in N_i(t)} w_{ij}(p_i - p_j)}_{\beta_i} + \underbrace{\dot{p}_\gamma - c_1(p_i - p_\gamma)}_{\gamma_i}. \quad (4.45)$$

In practical implementation, the derivative of the velocity of the virtual leader can be calculated by numerical differentiation. The results on tracking the virtual leader with a varying velocity can then be stated in the following theorem.

Theorem 4.5 *Consider a system of N mobile agents with dynamics (4.16), each steered by protocol (4.45). Suppose that the initial network $G(0)$ is connected and the initial energy U_0 is finite. Then, the following hold:*

- (i) $G(t)$ is connected for all $t \geq 0$.
- (ii) All agents asymptotically converge to the same position and move with the desired velocity p_γ .
- (iii) If the initial velocity of the COM, $\bar{p}(0)$, is equal to the initial velocity of virtual leader, $p_\gamma(0)$, then $\bar{p}(t)$ is equal to the desired velocity $p_\gamma(t)$ for all $t \geq 0$; otherwise $\bar{p}(t)$ will exponentially converge to the desired velocity $p_\gamma(t)$ with a time constant $c_1 s$.

Proof Denote the position difference vector and the velocity difference vector between agent i and the virtual leader as $\tilde{q}_i = q_i - p_\gamma t$ and $\tilde{p}_i = p_i - p_\gamma$, respectively. Then,

$$\begin{aligned} \dot{\tilde{q}}_i &= \tilde{p}_i, \\ \dot{\tilde{p}}_i &= u_i - \dot{p}_\gamma, \quad i = 1, \dots, N. \end{aligned} \quad (4.46)$$

Similar to the proof of part (i) of Theorem 4.4, the time derivative of $U(t)$ in $[t_{k-1}, t_k)$ is

$$\dot{U}(t) = \frac{1}{2} \sum_{i=1}^N \sum_{j \in N_i(t)} \dot{\psi}(\|\tilde{q}_{ij}\|) + \sum_{i=1}^N \tilde{p}_i^T \dot{\tilde{p}}_i = -\tilde{p}^T[(L(t) + c_1 I_N) \otimes I_n] \tilde{p} \leq 0, \quad (4.47)$$

which implies that

$$U(t) \leq U(t_{k-1}) < U_{\max} \quad \text{for } t \in [t_{k-1}, t_k), \quad k = 1, 2, \dots \quad (4.48)$$

Therefore, no edge-distances will tend to r for $t \in [t_{k-1}, t_k)$, which implies that no edges will be lost at time t_k , and $U(t_k) \leq U_{\max}$. Since $G(0)$ is connected and no edges in $E(0)$ will be lost, $G(t)$ will be connected for all $t \geq 0$.

We now prove part (ii) of Theorem 4.5.

Similar to the proof of part (ii) of Theorem 4.4, the set

$$\Omega = \{\tilde{q} \in D_g, \tilde{p} \in \mathbf{R}^{Nn} \mid U(\tilde{q}, \tilde{p}) \leq U_{\max}\} \quad (4.49)$$

is compact. From LaSalle's invariance principle [11],

$$\dot{U} = -\tilde{p}^T[(L(t) + c_1 I_N) \otimes I_n] \tilde{p} = -\tilde{p}^T(L(t) \otimes I_n) \tilde{p} - c_1 \tilde{p}^T \tilde{p} = 0, \quad (4.50)$$

which implies that $\tilde{p}_1 = \dots = \tilde{p}_N = 0$, i.e., $p_1 = \dots = p_N = p_\gamma$. This also implies that, in steady state, $u_i = \dot{p}_i = \dot{p}_\gamma$. From (4.45),

$$u_i - \dot{p}_\gamma = - \sum_{j \in N_i(t)} \nabla_{q_i} \psi(\|q_{ij}\|) = - \sum_{j \in N_i(t)} \frac{\partial \psi(\|q_{ij}\|)}{\partial \|q_{ij}\|} \cdot \frac{1}{\|q_{ij}\|} (q_i - q_j) = 0, \quad i = 1, \dots, N. \quad (4.51)$$

Similar to the proof of part (ii) of Theorem 4.4, $q_1 = q_2 = \dots = q_N$.

Finally, we prove part (iii) of Theorem 4.5.

Since $\psi(\|q_{ij}\|) = \psi(\|q_{ji}\|)$ and $w_{ij} = w_{ji}$, from the control protocol (4.45),

$$\begin{aligned} \dot{\tilde{p}} - \dot{p}_\gamma &= -\frac{1}{N} \sum_{i=1}^N \left(\sum_{j \in N_i(t)} \nabla_{q_i} \psi(\|q_{ij}\|) - \sum_{j \in N_i(t)} w_{ij} (p_i - p_j) - c_1 (p_i - p_\gamma) \right) \\ &= -c_1 \tilde{p} + c_1 p_\gamma. \end{aligned} \quad (4.52)$$

By solving (4.52),

$$\tilde{p} = p_\gamma + (\tilde{p}(0) - p_\gamma(0))e^{-c_1 t}. \quad (4.53)$$

Thus, it follows that if $\tilde{p}(0) = p_\gamma(0)$ then $\tilde{p}(t) = p_\gamma$ for all $t \geq 0$; otherwise, $\tilde{p}(t)$ will exponentially converge to the desired velocity with a time constant, c_1 s. \square

4.2.4 Simulation Study

We consider 10 agents moving in a 2-dimensional plane under the influence of the control protocol (4.19). The influencing/sensing radius is chosen as $r = 4$. Initial positions and initial velocities of the 10 agents are chosen randomly from the boxes $[0, 8] \times [0, 8]$ and $[0, 4] \times [0, 4]$, respectively. Here, the initial interaction network is set to be connected. Potential function (4.21) is selected for the protocol (4.19). If we choose $\varepsilon_0 = \varepsilon$, then

$$\begin{aligned} Q_{\max} &= \frac{1}{2} \sum_{i=1}^N p_i^T(0) p_i(0) + \frac{N(N-1)}{2} \psi(\|r - \varepsilon\|) \\ &\leq \frac{N(N-1)}{2} \psi(\|r - \varepsilon\|) + \frac{N}{2} \max(p_i^T(0) p_i(0)) \\ &= \frac{N(N-1)}{2} \frac{(r - \varepsilon)^2}{\varepsilon + \frac{r^2}{Q_{\max}}} + \frac{N}{2} \max(p_i^T(0) p_i(0)). \end{aligned} \quad (4.54)$$

Note that we can evaluate Q_{\max} by using an estimate of the bound of the initial velocities of all agents. Under the same initial positions and velocities, the simulations are performed with $\varepsilon = 0.01$ and $\varepsilon = 1.0$, respectively. From (4.54), we have $Q_{\max} \leq 70122.2$ for $\varepsilon = 0.01$ and $Q_{\max} \leq 471.7$ for $\varepsilon = 1.0$. If we choose $\hat{Q} = 72000$, then the potential function (4.21) can be explicitly described as

$$\psi(\|q_{ij}\|) = \frac{\|q_{ij}\|^2}{r - \|q_{ij}\| + \frac{1}{4500}}, \quad \|q_{ij}\| \in [0, 4]. \quad (4.55)$$

In Fig. 4.5, potential function (4.55) was selected for the algorithm (4.19) and $\varepsilon_0 = 0.01$. Figure 4.5(a) shows the initial states of the agents, where the solid lines represent the neighboring relations, and the solid lines with arrows represent the directions of velocities; Figure 4.5(b) depicts the motion trajectories of all agents from $t = 0$ to 7 s; Figures 4.5(c)–(d) and (e)–(f) show the convergence of positions for $\varepsilon = 0.01$ and $\varepsilon = 1.0$, respectively, from which one can see that all agents eventually achieve the same position; Figures 4.5(g)–(h) and (i)–(j) show the convergence of velocities for $\varepsilon = 0.01$ and $\varepsilon = 1.0$, respectively. If we choose the percentage set for the settling time as $c_{ts} = 0.04$, then the settling times in Figs. 4.5(g)–(j) are 2.7, 3.2, 5.6, and 6.6 s, respectively.

We find that the smaller the value of the constant ε , the larger the maximum overshoot and the smaller the settling time of the velocity. Therefore, there exists a fundamental trade-off between maximum overshoot and settling time for choosing the parameter ε . This is due to the fact that a smaller ε corresponds to a larger potential force, but also leads to earlier adding of edges.

In the following, we present simulation results for the situation without adding new edges to the network ($\varepsilon = 4$). In the simulation, potential function (4.55) was selected for the algorithm (4.19), and the initial states of the agents and all parameters were chosen the same as those in Fig. 4.5. Figures 4.6(a)–(b) show the convergence of positions over the x -axis and the y -axis, respectively; Figures 4.6(c)–(d) show the

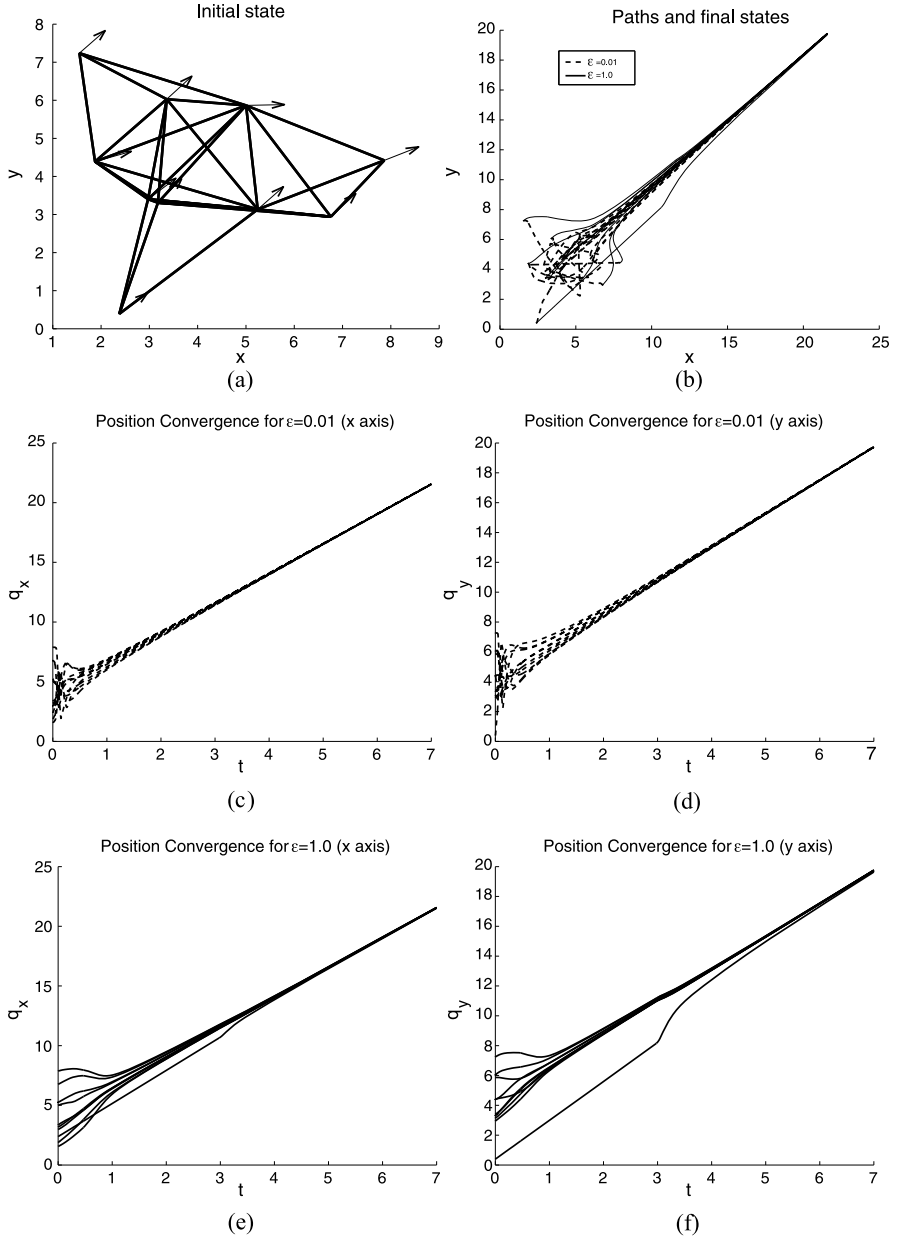


Fig. 4.5 [22] Consensus of 10 agents under algorithm (4.19)

convergence of velocities over the x -axis and the y -axis, respectively. One can see that all agents eventually reach the same position and velocity. This is because that initial network is connected and no existing edges are lost. Compared to both cases

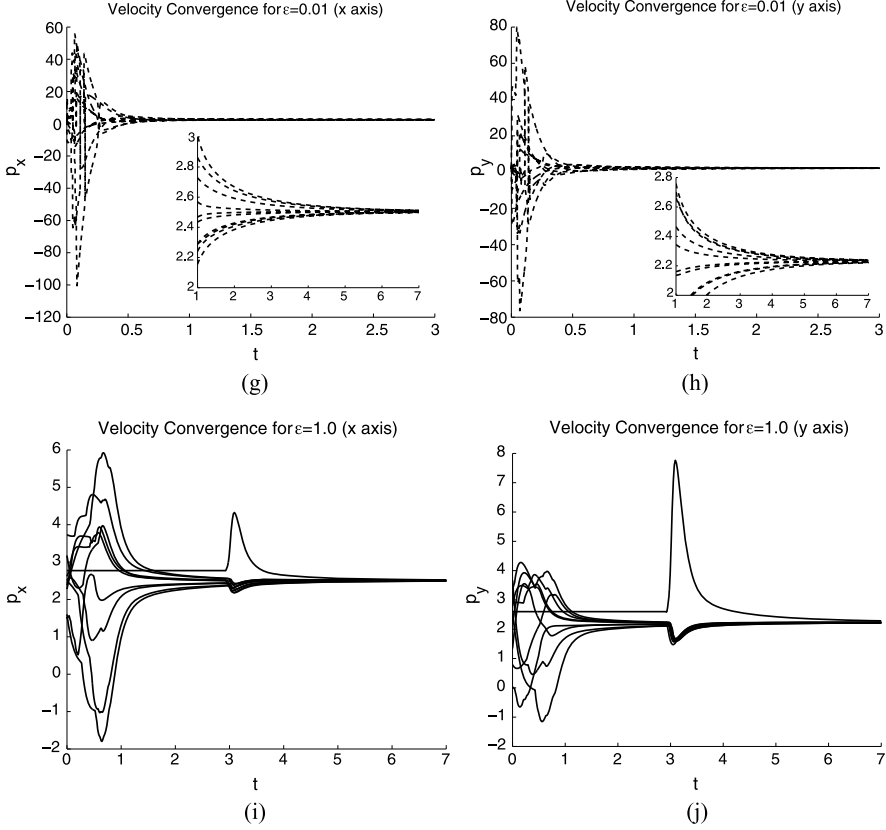


Fig. 4.5 (Continued)

in Fig. 4.5, the maximum overshoot becomes smaller but the settling time becomes larger. This is due to the fact that no new edges are added to the network.

Simulations on protocol (4.32) and on protocol (4.45) are performed with 50 agents moving in a 2-dimensional plane. In both simulations, $r = 4$ and $\epsilon = \epsilon_0 = 0.5$. Initial positions and velocities of the 50 agents are chosen randomly from the boxes $[0, 15] \times [0, 15]$ and $[0, 4] \times [0, 4]$, respectively. Once again, the initial interaction network is set to be connected. The desired velocity of the virtual leader is chosen as $p_\gamma = [3, 3]$, and potential function (4.21) is selected for both protocol (4.32) and protocol (4.45). We have

$$\begin{aligned}
 U_{\max} &= \frac{1}{2} \sum_{i=1}^N \tilde{p}_i^T(0) \tilde{p}_i(0) + \frac{N(N-1)}{2} \psi(\|r - \epsilon\|) \\
 &\leq \frac{N(N-1)}{2} \psi(\|r - \epsilon\|) + \frac{N}{2} \max(\tilde{p}_i^T(0) \tilde{p}_i(0))
 \end{aligned}$$

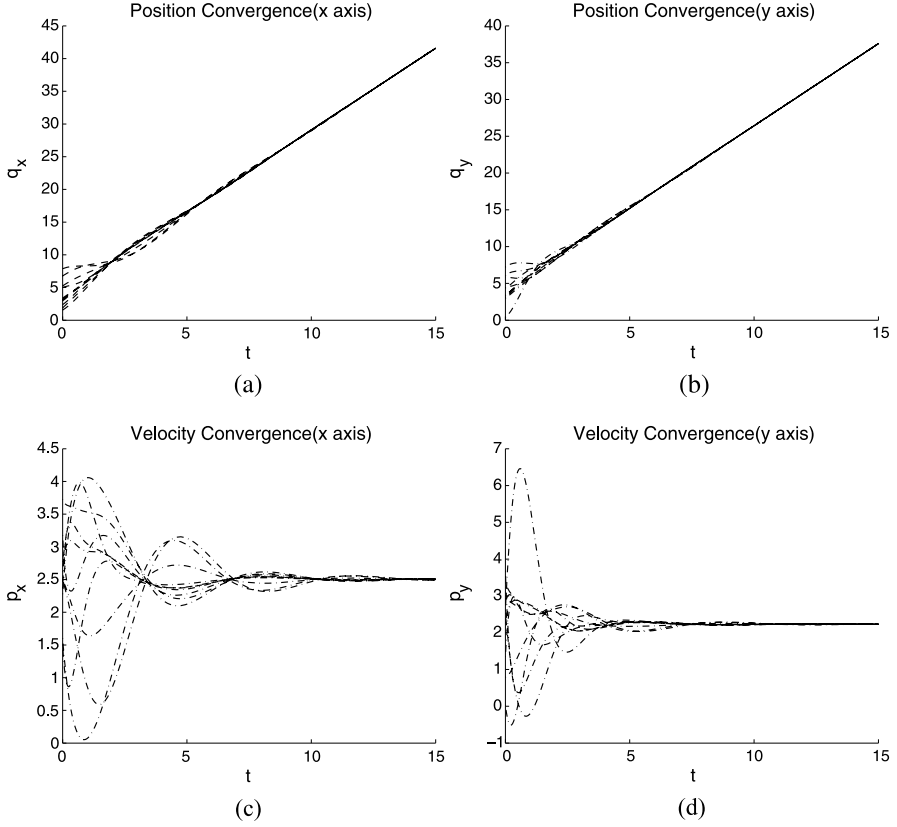


Fig. 4.6 [22] Consensus of 10 agents without adding new edges under algorithm (4.19)

$$= \frac{N(N-1)}{2} \frac{(r-\varepsilon)^2}{\varepsilon + \frac{r^2}{U_{\max}}} + \frac{N}{2} \max(\tilde{p}_i^T(0) \tilde{p}_i(0)). \quad (4.56)$$

From (4.56), $U_{\max} \leq 30205.7$. If we choose $\hat{U} = 32000$, then the potential function (4.21) can be explicitly described as

$$\psi(\|q_{ij}\|) = \frac{\|q_{ij}\|^2}{r - \|q_{ij}\| + \frac{1}{2000}}, \quad \|q_{ij}\| \in [0, 4]. \quad (4.57)$$

In Fig. 4.7, the informed agent is chosen randomly from the group and marked with a star; Figure 4.7(a) shows the initial states of the agents; Figure 4.7(b) depicts the motion trajectories of all agents from $t = 0$ to 35 s; Figures 4.7(c)–(d) show the convergence of positions over the x -axis and the y -axis, respectively; Figures 4.7(e)–(f) show the convergence of velocities over the x -axis and the y -axis, respectively. One can see that all agents eventually reach the same position and velocity. The final common velocity is equal to the desired velocity p_γ .

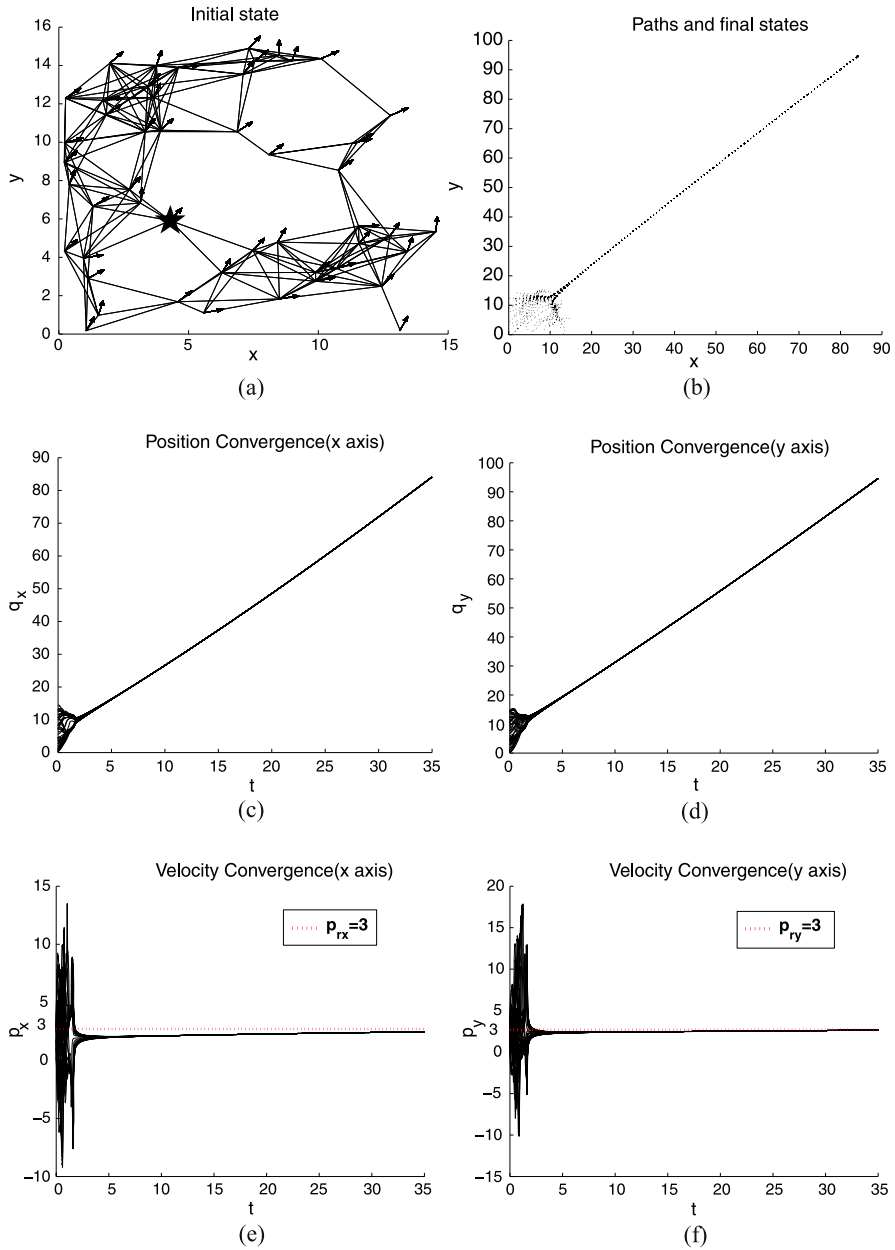


Fig. 4.7 [22] Consensus of 50 agents under algorithm (4.32)

Figure 4.8(a) shows the initial states of the agents; Figure 4.8(b) depicts the motion trajectories of all agents from $t = 0$ to $t = 5$ s; Figures 4.8(c)–(d) show the convergence of positions over the x -axis and the y -axis, respectively; Figures 4.8(e)–(f)

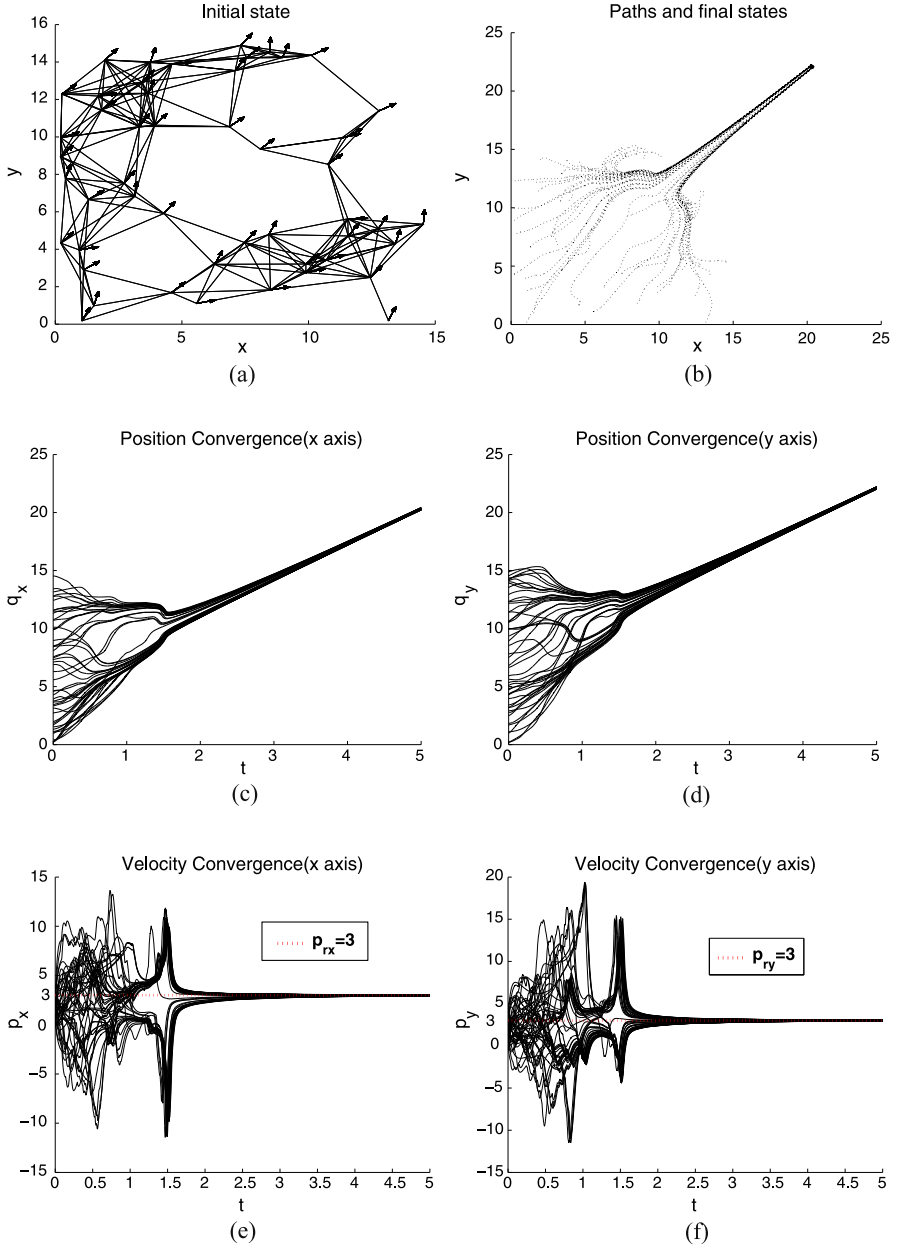


Fig. 4.8 [22] Consensus of 50 agents under algorithm (4.45)

show the convergence of velocities over the x -axis and the y -axis, respectively. One can see that all agents eventually reach the same position and velocity. The final common velocity is equal to the desired velocity p_y . One can clearly see that the

group using control protocol (4.32) needs a longer convergence time than that using control protocol (4.45).

4.3 Adaptive Consensus of Networked Mobile Agents with Nonlinear Dynamics

Many works on second-order consensus problems [2–4, 14, 26], or first-order consensus problems (see, e.g., [27]), focus on agents described by double-integrator or single-integrator dynamics. However, in reality, mobile agents may be governed by more complicated intrinsic dynamics. Indeed, nonlinear dynamics are commonly considered in synchronization problems on complex networks (see, e.g., [28, 29]). Second-order consensus-type problems with nonlinear agent dynamics have recently been investigated in fixed networks [30, 31].

A (virtual) leader–follower approach is commonly adopted to help the agents achieve a desired common velocity or arrive at a desired destination [5, 7, 8, 32, 33]. In this section, we investigate second-order consensus of multi-agent systems with a virtual leader in a dynamic proximity network. In order to avoid fragmentation, we extend the connectivity-preserving strategy in the system of the first-order dynamics without a virtual leader developed in [20] to the case of the second-order dynamics with a virtual leader considered in this section. A connectivity-preserving flocking algorithm [9] was concerned with agents described by double-integrator dynamics. In this section, we consider a class of multi-agent systems where the intrinsic dynamics of the agents are nonlinear. In this case, unlike in most existing works on second-order consensus-type problems, the equilibrium of velocities is time-varying due to the nonlinear intrinsic dynamics. More specifically, the convergence of those existing second-order consensus-type algorithms on an undirected network depends only on the topology of the network. However, due to the nonlinearity in the intrinsic dynamics of the agents, three factors including the velocity coupling strengths, the weights on the velocity navigational feedbacks and the topology of the network, play important roles in the convergence of the second-order consensus algorithms. Due to the nonlinearity in the intrinsic dynamics of the agents, the algorithm derived in [9] cannot be used to solve the flocking problems under the assumptions in this section.

In addition, similar to the pinning control problems on complex dynamical networks [34–36], we assume that only a fraction of agents in the group are informed agents that have access to information about the position and velocity of the virtual leader through, for example, certain pre-designed communication mechanism such as wireless broadcasting or sensing. In fact, every informed agent is applied a pinning controller, which is an effective method to control the collective dynamics of a complex network to a desired state. By introducing local adaptation strategies for both the weights on the velocity navigational feedback and the velocity coupling strengths, we establish that all agents in the group can synchronize with the virtual leader even when only one agent in the team has access to the information of the virtual leader. Compared to the results in [5, 7, 8, 33], the algorithm developed in this

chapter requires fewer informed agents. Like most existing works on synchronization and control problems on complex networks with nonlinear dynamics (see, e.g., [28, 29, 34–36]) and second-order consensus-type problems with nonlinear agent dynamics (see, e.g., [30, 31]), all agents and the virtual leader share the same intrinsic dynamics and their intrinsic dynamics satisfy a Lipschitz-like condition. Unlike the results on those references, the convergent condition here does not require any knowledge of the nonlinear agent dynamics, thanks to the adaptation strategies.

4.3.1 Problem Statement

Consider N agents, labeled as $1, 2, \dots, N$, moving in an n -dimensional Euclidean space. The motion of each agent is governed by

$$\begin{aligned}\dot{q}_i &= p_i, \\ \dot{p}_i &= f(p_i) + u_i,\end{aligned}\tag{4.58}$$

where $q_i \in \mathbf{R}^n$ is the position vector of agent i , $p_i \in \mathbf{R}^n$ is its velocity vector, $f(p_i) \in \mathbf{R}^n$ is its intrinsic dynamics, and $u_i \in \mathbf{R}^n$ is its control input.

The problem of second-order consensus with a virtual leader is to design control input u_i , $i = 1, 2, \dots, N$, such that

$$\begin{aligned}\lim_{t \rightarrow \infty} \|q_i(t) - q_\gamma(t)\| &= 0, \\ \lim_{t \rightarrow \infty} \|p_i(t) - p_\gamma(t)\| &= 0,\end{aligned}$$

for all $i = 1, 2, \dots, N$, where q_γ and p_γ are respectively the position and velocity of the virtual leader, which does not have to be an actual agent but is specified by

$$\begin{aligned}\dot{q}_\gamma &= p_\gamma, \\ \dot{p}_\gamma &= f(p_\gamma).\end{aligned}\tag{4.59}$$

In this section, as in most existing works on synchronization problems on complex networks with nonlinear dynamics (see, e.g., [28, 29]) and second-order consensus-type problems with nonlinear agent dynamics (see, e.g., [30, 31]), all agents and the virtual leader share the same intrinsic dynamics.

Assumption 4.1 The vector field $f : \mathbf{R}^n \rightarrow \mathbf{R}^n$ satisfies

$$(x - y)^T [f(x) - f(y)] \leq (x - y)^T \Delta (x - y), \quad \forall x, y \in \mathbf{R}^n,$$

for some positive definite diagonal constant matrix Δ .

Assumption 4.1 is a Lipschitz-like condition, which is satisfied by, for example, all piecewise linear functions. As illustrated in [36], many well-known systems, such as the chaotic Chua circuit [37], satisfy this assumption.

4.3.2 Main Results

Assume that only a fraction of agents are informed with information about the virtual leader. Since some agents do not have any information of the virtual leader, certain connectivity conditions are required to guarantee the convergence of the coordinated motion. We will adopt the description of network connectivity from previous subsection.

The control input is designed as

$$\begin{aligned} u_i = & - \sum_{j \in \mathcal{N}_i(t)} \nabla_{q_i} \psi(\|q_{ij}\|) \\ & - \sum_{j \in \mathcal{N}_i(t)} m_{ij}(p_i - p_j) - h_i c_1(q_i - q_\gamma) - h_i c_2(p_i - p_\gamma), \\ \dot{m}_{ij} = & k_{ij}(p_i - p_j)^T(p_i - p_j), \\ \dot{c}_{2i} = & k_i(p_i - p_\gamma)^T(p_i - p_\gamma), \end{aligned} \quad (4.60)$$

where $q_{ij} = q_i - q_j$ and $\mathcal{N}_i(t)$ is the neighborhood of agent i at time t , defined as

$$\mathcal{N}_i(t) = \{j : \sigma(i, j)[t] = 1, j \neq i, j = 1, 2, \dots, N\}.$$

Here, the positive constant c_1 is the weight on the position navigational feedback and can take any fixed value, the adaptive parameters m_{ij} and c_{2i} represent the velocity coupling strengths and the weights on the velocity navigational feedbacks, respectively, and the positive constants $k_{ij} = k_{ji}$ and k_i are the corresponding weighting factors of their adaptation laws. If agent i is an informed agent, then $h_i > 0$; otherwise, $h_i = 0$. Without loss of generality, assume that the first M agents are informed, that is, $h_i > 0$ for $i = 1, 2, \dots, M$, and $h_i = 0$ for $i = M + 1, M + 2, \dots, N$.

Motivated by the specific potential function in [20], we propose a general potential function. The nonnegative-valued potential $\psi(\|q_{ij}\|)$ is defined to be a function of the distance $\|q_{ij}\|$ between agent i and agent j , differentiable with respect to $\|q_{ij}\| \in [0, r)$, such that

- (i) $\frac{\partial \psi(z)}{\partial z} > 0$ for $z \in (0, r)$.
- (ii) $\lim_{z \rightarrow 0} (\frac{\partial \psi(z)}{\partial z} \cdot \frac{1}{z})$ is nonnegative and bounded.
- (iii) $\psi(z) \rightarrow \infty$ as $z \rightarrow r$.

One example of such a potential function is the following:

$$\psi(\|q_{ij}\|) = \frac{\|q_{ij}\|^{l_1}}{(r - \|q_{ij}\|)^{l_2}}, \quad \|q_{ij}\| \in [0, r),$$

where integers $l_1 \geq 2$ and $l_2 \geq 1$. The potential function in [20] is another example. The potential function defined above differs from the potential function of [9] in that it is used to achieve position consensus.

Lemma 4.1 ([38]) *If G is a connected undirected graph, L is the symmetric Laplacian of the graph \mathcal{G} and the matrix $E = \text{diag}(e_1, e_2, \dots, e_N)$ with $e_i \geq 0$ for $i = 1, 2, \dots, N$, and at least one element in E is positive, then all eigenvalues of the matrix $L + E$ are positive.*

Lemma 4.2 ([39]) *Suppose that the eigenvalues of symmetric matrices $A, B \in \mathbf{R}^{N \times N}$ satisfy*

$$\lambda_1(A) \leq \lambda_2(A) \leq \cdots \leq \lambda_N(A),$$

and

$$\lambda_1(B) \leq \lambda_2(B) \leq \cdots \leq \lambda_N(B).$$

Then, the following inequalities hold:

$$\lambda_{i+j-1}(A+B) \geq \lambda_i(A) + \lambda_j(B), \quad i+j \leq N+1, 1 \leq i, j \leq N.$$

Lemma 4.3 *If G_1 is a connected undirected graph and G_2 is a graph generated by adding some edge(s) into the graph G_1 , then $\lambda_1(L_2 + E) \geq \lambda_1(L_1 + E) > 0$, where L_1 and L_2 are the symmetric Laplacians of graphs G_1 and G_2 , respectively.*

Proof Without loss of generality, assume that there is no edge between vertices 1 and 2 in graph G_1 , and graph G_2 is generated by adding a new edge between vertices 1 and 2 in graph G_1 , thus

$$L_2 = L_1 + \delta L,$$

where

$$\delta L = \begin{bmatrix} 1 & -1 & 0 & \cdots & 0 \\ -1 & 1 & 0 & \cdots & 0 \\ 0 & 0 & 0 & \cdots & 0 \\ \vdots & \vdots & \vdots & \ddots & \vdots \\ 0 & 0 & 0 & \cdots & 0 \end{bmatrix}.$$

From Lemma 4.2 it follows that

$$\lambda_1(L_2 + E) = \lambda_1(L_1 + \delta L + E) \geq \lambda_1(L_1 + E) + \lambda_1(\delta L) \geq \lambda_1(L_1 + E).$$

Thus, by Lemma 4.1, we have $\lambda_1(L_2 + E) \geq \lambda_1(L_1 + E) > 0$.

For notational convenience, denote $m = (m_{ij})_{N \times N}$, $q = [q_1^T \ q_2^T \ \cdots \ q_N^T]^T$, $p = [p_1^T \ p_2^T \ \cdots \ p_N^T]^T$ and $c_2 = [c_{21}^T \ c_{22}^T \ \cdots \ c_{2N}^T]^T$.

Let us define an energy function for the multi-agent system as

$$\begin{aligned} Q(q, p, q_\gamma, p_\gamma, m, c_2) = & \frac{1}{2} \sum_{i=1}^N [U_i(q, q_\gamma) + (p_i - p_\gamma)^T (p_i - p_\gamma)] \\ & + \frac{1}{2} \sum_{i=1}^N \left[\sum_{j \in \mathcal{N}_i(t)} \frac{(m_{ij} - \theta)^2}{2k_{ij}} + h_i \frac{(c_{2i} - \theta)^2}{k_i} \right], \quad (4.61) \end{aligned}$$

where

$$U_i(q, q_\gamma) = \sum_{j \in \mathcal{N}_i(t)} \psi(\|q_i - q_j\|) + h_i c_1 (q_i - q_\gamma)^T (q_i - q_\gamma),$$

and θ is a positive constant chosen such that

$$\theta \geq \frac{\lambda_{\max}(\Delta)}{\lambda_1(L(0) + H)}, \quad (4.62)$$

where $H = \text{diag}\{h_1, h_2, \dots, h_N\}$. Clearly, Q is a positive semi-definite function of its variables. \square

Theorem 4.6 Consider a system of N mobile agents with dynamics (4.58), each steered by protocol (4.60), and a virtual leader with dynamics (4.59). Suppose that the initial network $G(0)$ is connected, Assumption 4.1 holds, and the initial energy $Q_0 := Q(q(0), p(0), q_\gamma(0), p_\gamma(0), m(0), c_2(0))$ is finite. Then, the velocities and positions of all agents will converge to those of the virtual leader asymptotically.

Proof Denote the position difference and the velocity difference between agent i and the virtual leader as $q_{i\gamma} = q_i - q_\gamma$ and $p_{i\gamma} = p_i - p_\gamma$, respectively. Then, we have

$$\begin{aligned} \dot{q}_{i\gamma} &= p_{i\gamma}, \\ \dot{p}_{i\gamma} &= f(p_i) - f(p_\gamma) - \sum_{j \in \mathcal{N}_i(t)} \nabla_{q_{i\gamma}} \psi(\|q_{i\gamma} - q_{j\gamma}\|) \\ &\quad - \sum_{j \in \mathcal{N}_i(t)} m_{ij}(p_{i\gamma} - p_{j\gamma}) - h_i c_{1i} q_{i\gamma} - h_i c_{2i} p_{i\gamma}, \\ \dot{m}_{ij} &= k_{ij}(p_{i\gamma} - p_{j\gamma})^T (p_{i\gamma} - p_{j\gamma}), \\ \dot{c}_{2i} &= k_i p_{i\gamma}^T p_{i\gamma}, \end{aligned} \quad (4.63)$$

and the energy function (4.61) can be rewritten as

$$Q(\tilde{q}, \tilde{p}, m, c_2) = \frac{1}{2} \sum_{i=1}^N \left(U_i(\tilde{q}) + p_{i\gamma}^T p_{i\gamma} + \sum_{j \in \mathcal{N}_i(t)} \frac{(m_{ij} - \theta)^2}{2k_{ij}} + h_i \frac{(c_{2i} - \theta)^2}{k_i} \right), \quad (4.64)$$

where $\tilde{q} = [q_{1\gamma}^T \ q_{2\gamma}^T \ \dots \ q_{N\gamma}^T]^T$, $\tilde{p} = [p_{1\gamma}^T \ p_{2\gamma}^T \ \dots \ p_{N\gamma}^T]^T$, and

$$U_i(\tilde{q}) = \sum_{j \in \mathcal{N}_i(t)} \psi(\|q_{i\gamma} - q_{j\gamma}\|) + h_i c_{1i} q_{i\gamma}^T q_{i\gamma}.$$

Clearly, $Q(\tilde{q}, \tilde{p}, m, c_2)$ is a positive semi-definite function of \tilde{q} , \tilde{p} , m , and c_2 .

Assume that $G(t)$ switches at time t_k , $k = 1, 2, \dots$, and $G(t)$ is a fixed graph on each time-interval $[t_{k-1}, t_k)$. Note that Q_0 is finite and the time derivative of $Q(t)$ on $[t_0, t_1)$ satisfies

$$\begin{aligned} \dot{Q} &= \frac{1}{2} \sum_{i=1}^N \dot{U}_i + \sum_{i=1}^N p_{i\gamma}^T \dot{p}_{i\gamma} + \frac{1}{2} \sum_{i=1}^N \sum_{j \in \mathcal{N}_i(t)} (m_{ij} - \theta)(p_{i\gamma} - p_{j\gamma})^T (p_{i\gamma} - p_{j\gamma}) \\ &\quad + h_i \sum_{i=1}^N (c_{2i} - \theta) p_{i\gamma}^T p_{i\gamma} \end{aligned}$$

$$\begin{aligned}
&= \sum_{i=1}^N p_{i\gamma}^T \sum_{j \in \mathcal{N}_i(t)} \nabla_{q_{i\gamma}} \psi(\|q_{i\gamma} - q_{j\gamma}\|) \\
&\quad + \sum_{i=1}^N p_{i\gamma}^T \left[f(p_i) - f(p_\gamma) - \sum_{j \in \mathcal{N}_i(t)} m_{ij}(p_{i\gamma} - p_{j\gamma}) - h_i \theta p_{i\gamma} \right] \\
&\quad - \sum_{i=1}^N p_{i\gamma}^T \sum_{j \in \mathcal{N}_i(t)} \nabla_{q_{i\gamma}} \psi(\|q_{i\gamma} - q_{j\gamma}\|) \\
&\quad + \frac{1}{2} \sum_{i=1}^N \sum_{j \in \mathcal{N}_i(t)} (m_{ij} - \theta)(p_{i\gamma} - p_{j\gamma})^T (p_{i\gamma} - p_{j\gamma}) \\
&= \sum_{i=1}^N p_{i\gamma}^T \left[f(p_i) - f(p_\gamma) - \sum_{j \in \mathcal{N}_i(t)} \theta(p_{i\gamma} - p_{j\gamma}) - h_i \theta p_{i\gamma} \right] \\
&\leq -\tilde{p}^T [\theta(L(t) + H) \otimes I_n - I_n \otimes \Delta] \tilde{p}, \tag{4.65}
\end{aligned}$$

where, by Lemma 4.1, $(L(0) + H) \otimes I_n > 0$. It follows from (4.65) and (4.62) that

$$\dot{Q}(t) \leq 0, \quad \forall t \in [t_0, t_1),$$

which implies that

$$Q(t) \leq Q_0 < \infty, \quad \forall t \in [t_0, t_1).$$

By the definition of the potential function, one has $\lim_{\|q_{ij}(t)\| \rightarrow r} \psi(\|q_{ij}(t)\|) = \infty$. Therefore, the length of no existing edge will tend to r for $t \in [t_0, t_1)$, implying that no existing edge will be lost before time t_1 . Hence, new edges must be added to the evolving network at the switching time t_1 . Note that the hysteresis ensures that if a finite number of edges are added to $G(t)$, then the associated potential remains finite. Thus, $Q(t_1)$ is finite.

Similar to the above analysis, the time derivative of $Q(t)$ on every $[t_{k-1}, t_k)$ satisfies

$$\dot{Q}(t) \leq -\tilde{p}^T [\theta(L(t) + H) \otimes I_n - I_n \otimes \Delta] \tilde{p}. \tag{4.66}$$

By Lemma 4.3, it follows from (4.62) that

$$\theta \geq \frac{\lambda_{\max}(\Delta)}{\lambda_1(L(0) + H)} \geq \frac{\lambda_{\max}(\Delta)}{\lambda_1(L(t_{k-1}) + H)}. \tag{4.67}$$

Consequently, it follows from Lemma 4.1, (4.66) and (4.67) that

$$Q(t) \leq Q(t_{k-1}) < \infty, \quad \text{for } t \in [t_{k-1}, t_k), \quad k = 1, 2, \dots \tag{4.68}$$

Therefore, the length of no existing edge will tend to r for $t \in [t_{k-1}, t_k)$, implying that no edges will be lost before time t_k and so $Q(t_k)$ is finite. Since $G(0)$ is connected and no edges in $E(0)$ have been lost, $G(t)$ will remain connected for all $t \geq 0$.

Assume that there are m_k new edges added to the evolving network at time t_k . Clearly,

$$0 < m_k \leq \frac{(N-1)(N-2)}{2} \triangleq \bar{M}.$$

From (4.64) and (4.68), we have

$$Q(t_k) \leq Q_0 + (m_1 + m_2 + \cdots + m_k)\psi(\|r - \varepsilon\|) \triangleq Q_{\max}.$$

Since there are at most \bar{M} new edges that can be added to $G(t)$, one has $k \leq \bar{k} \leq \bar{M}$ and $Q(t) \leq Q_{\max}$ for all $t \geq 0$. Therefore, the number of switching times \bar{k} of system (4.63) is finite, which implies that the evolving network $G(t)$ eventually becomes fixed. Thus, the remaining discussions can be restricted on the time interval $(t_{\bar{k}}, \infty)$. Note that all the lengths of all edges are no greater than $\psi^{-1}(Q_{\max})$. Hence, the set

$$\Omega = \{\hat{q} \in D_g, \tilde{p} \in \mathbf{R}^{Nn} : Q(\hat{q}, \tilde{p}) \leq Q_{\max}\}$$

is positively invariant, where $\hat{q} = [q_{11}^T \ q_{12}^T \ \cdots \ q_{1N}^T \ \cdots \ q_{N1}^T \ q_{N2}^T \ \cdots \ q_{NN}^T]^T$ and

$$D_g = \{\hat{q} \in \mathbf{R}^{N^2n} : \|q_{i\gamma} - q_{j\gamma}\| \in [0, \psi^{-1}(Q_{\max})], \forall (i, j) \in E(t)\}.$$

Since $G(t)$ is connected for all $t \geq 0$, we have $\|q_{i\gamma} - q_{j\gamma}\| < (N-1)r$ for all i and j . Since $Q(t) \leq Q_{\max}$, one has $p_{i\gamma}^T p_{i\gamma} \leq 2Q_{\max}$, and thus $\|p_{i\gamma}\| \leq \sqrt{2Q_{\max}}$. Therefore, the set Ω satisfying $Q(t) \leq Q_{\max}$ is closed and bounded, and hence compact. Note that the closed-loop system (4.63) is an autonomous system on the concerned time interval $(t_{\bar{k}}, \infty)$. Therefore, the LaSalle Invariance Principle [11] can be applied. If the initial conditions of the system lie in Ω , then the corresponding trajectories will converge to the largest invariant set inside the region

$$S = \{\hat{q} \in D_g, \tilde{p} \in \mathbf{R}^{Nn} \mid \dot{Q} = 0\}.$$

From (4.66), $\dot{Q} = 0$ if and only if $p_1 = \cdots = p_N = p_\gamma$, which implies that the velocities of all agents will converge to that of the virtual leader asymptotically.

Since $p_1 = \cdots = p_N = p_\gamma$, from (4.63) we have

$$\dot{p}_{i\gamma} = - \sum_{j \in N_i(t)} \frac{\partial \psi(\|q_{ij}\|)}{\partial \|q_{ij}\|} \cdot \frac{1}{\|q_{ij}\|} (q_i - q_j) - h_i c_1 (q_i - q_\gamma) = 0. \quad (4.69)$$

Rewrite (4.69) in a matrix form as

$$-[(\hat{L}(t) \otimes I_n) + (c_1 H \otimes I_n)]\tilde{q} = 0, \quad (4.70)$$

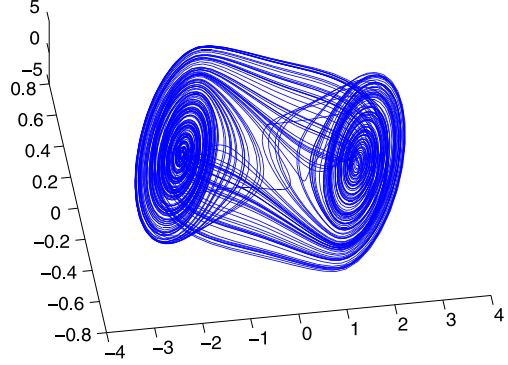
where $\hat{L}(t) = [\hat{l}_{ij}]$ is a matrix with

$$\hat{l}_{ij} = -\frac{\partial \psi(\|q_{ij}\|)}{\partial \|q_{ij}\|} \cdot \frac{1}{\|q_{ij}\|}, \quad i \neq j,$$

and

$$\hat{l}_{ii} = - \sum_{j=1, j \neq i}^N \hat{l}_{ij}.$$

Fig. 4.9 [40] The attractor of the Chua circuit



By the definition,

$$\frac{\partial \psi(\|q_{ij}\|)}{\partial \|q_{ij}\|} \cdot \frac{1}{\|q_{ij}\|}$$

is positive for $\|q_{ij}\| \in (0, r)$ and

$$\lim_{\|q_{ij}\| \rightarrow 0} \left(\frac{\partial \psi(\|q_{ij}\|)}{\partial \|q_{ij}\|} \cdot \frac{1}{\|q_{ij}\|} \right)$$

is nonnegative and bounded. From [10] and Lemma 4.1, $\hat{L}(t) \otimes I_n + c_1 H \otimes I_n$ is a positive-definite matrix and hence is nonsingular. Therefore, it follows from (4.70) that $\tilde{q} = 0$, namely, $q_1 = q_2 = \dots = q_N = q_\gamma$. \square

4.3.3 Simulation Study

In this subsection, simulation results are given to illustrate the theoretical results. In the simulation, the velocity of each agent is governed by the chaotic Chua circuit (see Fig. 4.9),

$$\begin{cases} \dot{p}_x = 10(-0.32p_x + p_y + 0.295(|p_x + 1| - |p_x - 1|)), \\ \dot{p}_y = p_x - p_y + p_z, \\ \dot{p}_z = -14.87p_y. \end{cases}$$

Shown in Fig. 4.10 are some results of simulation performed on a group of ten agents moving in a 3-dimensional space under the influence of the control protocol (4.60). Initial positions and initial velocities of the ten agents were chosen randomly from the cubes $[0, 10] \times [0, 10] \times [0, 10]$ and $[0, 3] \times [0, 3] \times [0, 3]$, respectively, and the initial position and velocity of the virtual leader were set at $q_\gamma(0) = [10 \ 10 \ 10]^T$ and $p_\gamma(0) = [3 \ 3 \ 3]^T$. The influencing/sensing radius was chosen as $r = 4$, with $\varepsilon = 0.5$, $m_{ij}(0) = 0$ for all i and j , $k_{ij} = 0.1$ for all i and j , $h_i = 1$ for the informed agent, $c_1 = 10$, $c_{2i}(0) = 0$ for all i and $k_i = 0.1$ for all i . The initial network was

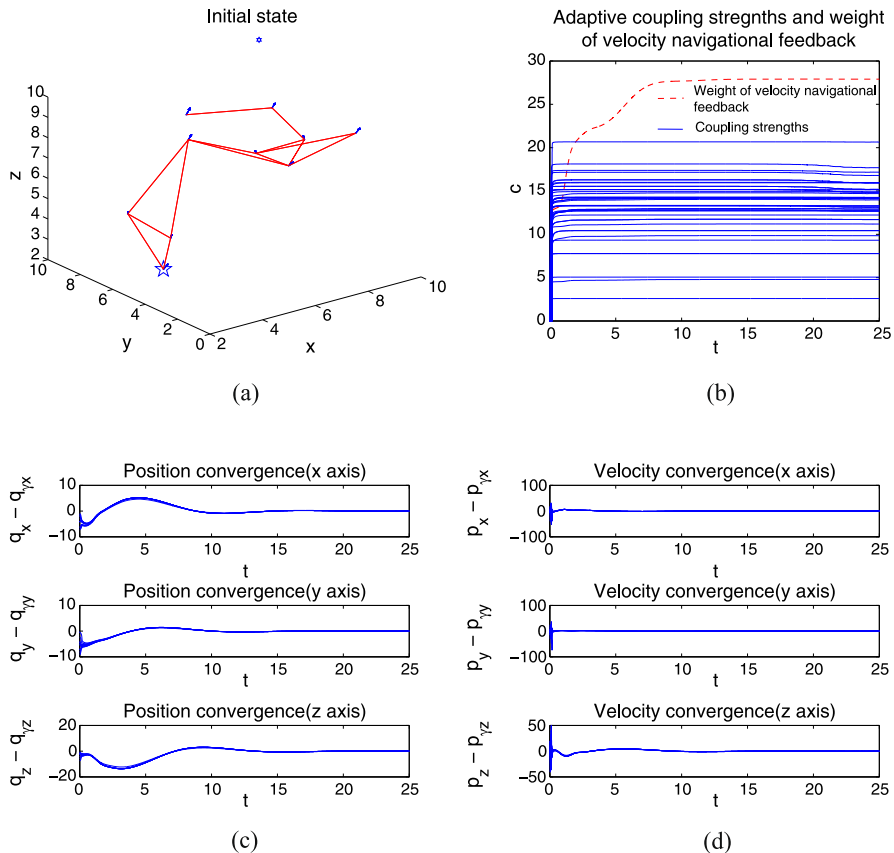


Fig. 4.10 [40] Second-order consensus of 10 agents with 1 informed agent under algorithm (4.60), and the informed agent is represented with a star in panel (a)

connected. There is one informed agent, which is chosen randomly from the group and marked with a star. In the figure, plot (a) shows the initial states of the agents, plot (b) shows the adaptive velocity coupling strengths and the adaptive weights on the informed agents, which all converge to constants, plot (c) shows the differences in positions on the x -axis, y -axis, and z -axis between all agents and the virtual leader, from which one can see that all agents eventually arrive at the same position as the virtual leader, and plot (d) shows the differences in velocities on the x -axis, y -axis, and z -axis between all agents and the virtual leader, from which one can see that all agents eventually move with the same velocity as the virtual leader.

Shown in Fig. 4.11 are more simulation results of the system described above, with the same initial positions and velocities, but different values of $m_{ij}(0)$ and $c_{2i}(0)$. It can be seen in the figure that, with the increase of $m_{ij}(0)$ and $c_{2i}(0)$, the maximum velocity coupling strength and the maximum weight on the velocity nav-

Fig. 4.11 [40] The maximum velocity coupling strength, the maximum weight on the velocity navigational feedback, the position convergence time, and the velocity convergence time as functions of $m_{ij}(0)$ and $c_{2i}(0)$, and the percentage set for the settling time of the position and the velocity is chosen as $c_{ts} = 0.04$

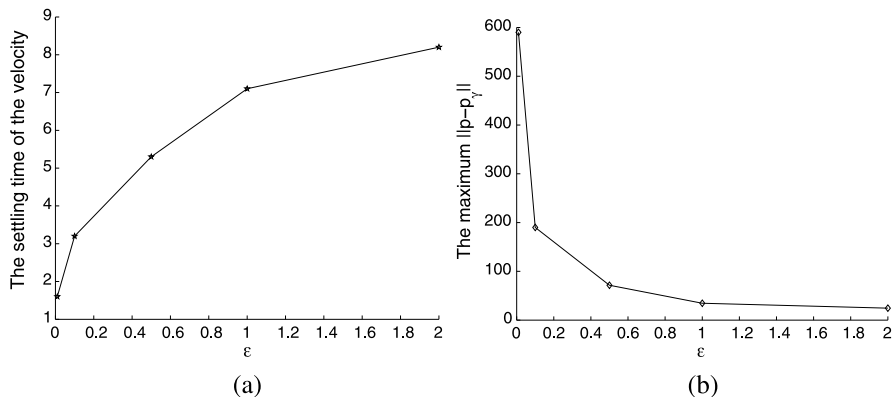
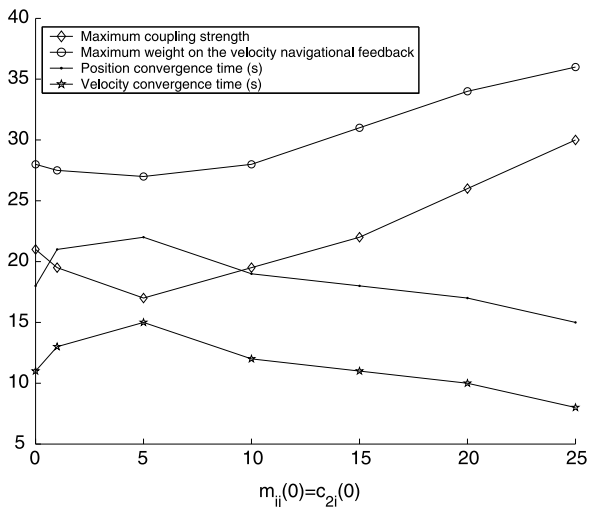


Fig. 4.12 [40] The settling time of the velocity and the maximum $\|p - p_Y\|$ as functions of ϵ , and the percentage set for the settling time of the velocity is chosen as $c_{ts} = 0.04$

igational feedback first decrease and then increase, while the position convergence time and the velocity convergence time first increase and then decrease.

Shown in Fig. 4.12 are simulation results with five informed agents, which were chosen randomly from the group. Under the same initial positions, initial velocities and informed agents, the simulation was performed with different values of ϵ . All other parameters were chosen as those in the simulation shown in Fig. 4.10. The figure shows that, the smaller the value of ϵ , the larger the maximum overshoot and the smaller the settling time of the velocity. Therefore, there exists a fundamental trade-off between the maximum overshoot and the settling time in choosing the value of the parameter ϵ . This is due to the fact that a smaller ϵ corresponds to a larger potential force, which also leads to earlier addition of edges.

4.4 Conclusions and Notes

In this chapter, we have investigated synchronization of coupled harmonic oscillators, both without and with a leader. By exploiting the inherent dynamical properties of the uncoupled systems, that is, the coupled harmonic oscillators will naturally exchange information with each other from time to time through the coupling, we were able to design control laws that achieve synchronization without requiring any connectivity assumption on the agents. This is in contrast with existing algorithms for the same problem where certain network connectivity assumptions are needed. In the situation when a leader is present, all agents in the group will track the leader in the absence of any connectivity assumption on the followers. We then have investigated the second-order consensus problem with connectivity preservation for double-integrator dynamics employing hysteresis for adding new links and using the potential function method. The hysteresis idea is adopted from [20] and [21]; yet, we found that there is a trade-off between the maximum overshoot and the settling time of velocity convergence for choosing the hysteresis parameter. We have constructed a class of bounded potential functions to guarantee the existing links not be lost, which is in some sense more practical than the two specific unbounded potential functions used in [20] and [21]. Moreover, we have investigated the coordinated control with a virtual leader and showed that all agents can asymptotically attain the desired velocity even if only one agent in the team has information about the virtual leader. Finally, we have investigated second-order consensus of multiple mobile agents with a virtual leader. Each agent was governed by nonlinear intrinsic dynamics. We proposed a connectivity-preserving second-order consensus algorithm and showed that, under the assumption that the initial network is connected and by introducing local adaptation strategies for both the weights on the velocity navigational feedback and the velocity coupling strengths, all agents in the group asymptotically synchronize with the virtual leader even when only one agent in the team has access to the information of the virtual leader, without requiring any knowledge of the agent dynamics. The results we have obtained in this chapter require weaker conditions than most corresponding results in the literature, and therefore are easier to apply.

References

1. Ren W (2008) Synchronization of coupled harmonic oscillators with local interaction. *Automatica* 44:3195–3200
2. Ren W, Atkins E (2007) Distributed multi-vehicle coordinated control via local information exchange. *Int J Robust Nonlinear Control* 17:1002–1033
3. Xie G, Wang L (2007) Consensus control for a class of networks of dynamic agents. *Int J Robust Nonlinear Control* 17:941–959
4. Ren W (2008) On Consensus algorithms for double-integrator dynamics. *IEEE Trans Autom Control* 53:1503–1509
5. Olfati-Saber R (2006) Flocking for multi-agent dynamic systems: algorithms and theory. *IEEE Trans Autom Control* 51:401–420

6. Tanner HG, Jadbabaie A, Pappas GJ (2007) Flocking in fixed and switching networks. *IEEE Trans Autom Control* 52:863–868
7. Su H, Wang X, Yang W (2008) Flocking in multi-agent systems with multiple virtual leaders. *Asian J Control* 10:238–245
8. Su H, Wang X, Lin Z (2009) Flocking of multi-agents with a virtual leader. *IEEE Trans Autom Control* 54:293–307
9. Su H, Wang X, Chen G (2009) A connectivity-preserving flocking algorithm for multi-agent systems based only on position measurements. *Int J Control* 82:1334–1343
10. Godsil C, Royle G (2001) Algebraic graph theory. Graduate texts in mathematics, vol 207. Springer, New York
11. Khalil HK (2002) Nonlinear systems, 3rd edn. Prentice Hall, Upper Saddle River
12. Su H, Wang X, Lin Z (2009) Synchronization of coupled harmonic oscillators in a dynamic proximity network. *Automatica* 45:2286–2291
13. Jadbabaie A, Lin J, Morse AS (2003) Coordination of groups of mobile agents using nearest neighbor rules. *IEEE Trans Autom Control* 48:988–1001
14. Lee D, Spong MW (2007) Stable flocking of multiple inertial agents on balanced graphs. *IEEE Trans Autom Control* 52:1469–1475
15. Cortes J, Martinez S, Bullo F (2006) Robust rendezvous for mobile autonomous agents via proximity graphs in arbitrary dimensions. *IEEE Trans Autom Control* 51:1289–1298
16. Degennaro MC, Jadbabaie A (2006) Decentralization control of connectivity for multi-agent systems. In: Proc of the 45th IEEE conference on decision and control, pp 3628–3633
17. Spanos DP, Murray RM (2004) Robust connectivity of networked vehicles. In: Proc of the 43rd IEEE conference on decision and control, pp 2893–2898
18. Dimarogonas DV, Kyriakopoulos KJ (2007) On the rendezvous problem for multiple non-holonomic agents. *IEEE Trans Autom Control* 52:916–922
19. Dimarogonas DV, Kyriakopoulos KJ (2007) Connectivity preserving distributed swarm aggregation for multiple kinematic agents. In: Proc of the 46th IEEE conference on decision and control, pp 2913–2918
20. Ji M, Egerstedt M (2007) Distributed coordination control of multiagent systems while preserving connectedness. *IEEE Trans Robot* 23:693–703
21. Zavlanos MM, Jadbabaie A, Pappas GJ (2007) Flocking while preserving network connectivity. In: Proc of the 46th IEEE conference on decision and control, pp 2919–2924
22. Su H, Wang X, Chen G (2010) Rendezvous of multiple mobile agents with preserved network connectivity. *Syst Control Lett* 59:313–322
23. Horn RA, Johnson CR (1987) Matrix analysis. Cambridge University Press, Cambridge
24. Fiedler M (1973) Algebraic connectivity of graphs. *Czechoslov Math J* 23:298–305
25. Couzin ID, Krause J, Franks NR, Levin SA (2005) Effective leadership and decision-making in animal groups on the move. *Nature* 433:513–516
26. Hong Y, Gao L, Cheng D, Hu J (2007) Lyapunov-based approach to multi-agent systems with switching jointly-connected interconnection. *IEEE Trans Autom Control* 52:943–948
27. Hui Q, Haddad WM (2008) Distributed nonlinear control algorithms for network consensus. *Automatica* 44:2375–2381
28. Wang X (2002) Complex networks: topology, dynamics, and synchronization. *Int J Bifur Chaos* 12:885–916
29. Wu CW (2002) Synchronization in coupled chaotic circuits and systems. World Scientific, Singapore
30. Yu W, Chen G, Cao M, Kurths J (2010) Second-order consensus for multi-agent systems with directed topologies and nonlinear dynamics. *IEEE Trans Syst Man Cybern, Part B, Cybern* 40:881–891
31. Zhou J, Yu W, Wu X, Small M, Lu J (2012) Flocking of multi-agent dynamical systems based on pseudo-leader mechanism. *Syst Control Lett* 61:195–202
32. Shi H, Wang L, Chu TG (2006) Virtual leader approach to coordinated control of multiple mobile agents with asymmetric interactions. *Physica D* 213:51–65

33. Shi H, Wang L, Chu TG (2009) Flocking of multi-agent systems with a dynamic virtual leader. *Int J Control* 82:43–58
34. Wang X, Chen G (2002) Pinning control of scale-free dynamical networks. *Physica A* 310:521–531
35. Li X, Wang X, Chen G (2004) Pinning a complex dynamical network to its equilibrium. *IEEE Trans Circuits Syst I, Fundam Theory Appl* 51:2074–2087
36. Yu W, Chen G, Lü J (2009) On pinning synchronization of complex dynamical networks. *Automatica* 45:429–435
37. Matsumoto T (1984) A chaotic attractor from Chua's circuit. *IEEE Trans Circuits Syst* 31:1055–1058
38. Hong Y, Hu J, Gao L (2006) Tracking control for multi-agent consensus with an active leader and variable topology. *Automatica* 42:1177–1182
39. Amir-Moez R (1956) Extreme properties of eigenvalues of a Hermitian transformation and singular values of the sum and product of linear transformations. *Duke Math J* 23:463–476
40. Su H, Chen G, Wang X, Lin Z (2011) Adaptive second-order consensus of networked mobile agents with nonlinear dynamics. *Automatica* 47:368–375

Chapter 5

Distributed Pinning-Controlled Consensus in a Heterogeneous Influence Network

Abstract This chapter introduces consensus algorithms in a heterogeneous influence network. We consider a dynamical network model in which a number of agents all move on the plane with the same constant absolute velocity. At each time step, each agent's direction is updated as the average of its direction plus the directions of other agents who can influence it. The influencing capability of each agent is represented by its influencing radius, which is randomly chosen according to a power law distribution with a scaling exponent between 2 and ∞ . As the value of the scaling exponent decreases, the radius distribution becomes more heterogeneous and the network becomes much easier to achieve direction consensus among agents due to the leading roles played by a few hub agents. Furthermore, almost all agents will finally move in the same desired direction in a strong heterogeneous influence network, if and only if a small fraction of hub agents can be controlled to move in the desired direction. These results also reflect the 'robust yet fragile' feature of a heterogeneous influence network.

Keywords Consensus · Heterogeneous influence network · Vicsek model · Power law distribution

5.1 Backgrounds and Problem Statement

Most of the researches in the distributed coordination of multiple autonomous agents assumed that each agent has the same sensing capability [1, 2]. A classical example of such completely homogeneous sensing models was proposed by Vicsek et al. [2]. In the Vicsek model, a number of agents move on the plane with the same absolute velocity but different directions. Each agent's direction is updated according to a local rule based on the average of its own direction plus the directions of its neighbors. Neighbors of an agent are those agents sensed by the agent and they are within a closed disk of the same sensing radius centered at the agent's current position [2]. Vicsek et al. provided a variety of simulation results to demonstrate that all agents may eventually move in the same direction, despite the absence of centralized coordination and the fact that each agent's set of nearest neighbors changes with time as the system evolves.

A completely homogeneous sensing model can equivalently be described as a completely homogeneous influencing model in which each agent adjusts its behavior based on the behaviors of those agents who can influence it. However, in many social networks, the distributions of the influencing capabilities of agents are heterogeneous. A typical example is consensus decision-making among a group of people. In the group, each person tries to persuade other people accept her or his opinion and at the same time tries to adjust her or his opinion based on the opinions of those people who can influence him. Clearly, different people may have different influence capabilities. A powerful leader may influence many people, while a little boy may influence only a few. Therefore, it is of practical importance to investigate collective behaviors in heterogeneous influencing networks.

Recently, the ability to synchronize in a complex dynamical network with respect to some kind of heterogeneity of the network (such as heterogeneous distribution of degree or intensity [3–8], parameter dispersion [9]) has been investigated. A basic assumption in these researches is that the topology of the network is fixed and a common result is that synchronizability is suppressed as the network becomes more heterogeneous [3–7, 9], with an exception that better synchronizability for the Watts–Strogatz small world network is induced as the heterogeneity of the degree distribution is increased [8].

In this chapter, we investigate the collective behavior in a heterogeneous influencing network model which is a modification of the homogeneous sensing Vicsek model. The influencing capability of an agent is represented by its influencing radius which is randomly chosen according to power law distribution $P(r) \sim r^{-\gamma}$ with a scaling exponent $\gamma \in [2, \infty]$. As the value of the scaling exponent decreases, the radius distribution becomes more heterogeneous. The aim of this chapter is to investigate the ability of the network to achieve global direction consensus among agents in the sense that most agents will eventually move in the same direction in terms of the influence heterogeneity of the network. The main conclusion is that agreement among a few powerful leaders in a heterogeneous influence network is the key to achieve global direction consensus for the whole system.

5.2 Consensus in a Heterogeneous Influence Network

As in the Vicsek model [2], we consider n autonomous agents, labeled 1 through n , all moving in a square shaped cell of linear size L with periodic boundary conditions. Each agent has the same absolute velocity v but with different directions θ , which are randomly distributed in $[0, 2\pi)$. Originally, agents are randomly distributed in the cell. In our model, we assume that agent i transmits its direction information to any other agents within a closed influencing disk of radius r_i centered at agent i . Each agent's direction is updated simultaneously based on the average of its own direction plus the directions of those agents whose influencing disks contain

it. Mathematically, agent i 's direction θ_i evolves in discrete-time in accordance with a model of the form

$$\theta_i(t+1) = \frac{1}{1+n_i(t)} \left(\theta_i(t) + \sum_{j \in N_i(t)} \theta_j(t) \right) \quad (5.1)$$

where $n_i(t)$ and $N_i(t)$ represent the number and set of agents who can influence agent i at time step t , respectively. The position of agent i is updated according to [2]

$$\mathbf{x}_i(t+1) = \mathbf{x}_i(t) + \mathbf{v}_i(t) \Delta t \quad (5.2)$$

where the velocity vector $\mathbf{v}_i(t)$ of agent i has an absolute value v and a direction given by the angle $\theta_i(t)$.

We further assume that each agent's influencing radius is chosen randomly according to the power-law distribution $P(r) \sim r^{-\gamma}$ with a scaling exponent $\gamma \in [2, \infty]$. When $\gamma = \infty$, the distribution of influencing radii is completely homogeneous, which implies that all agents have the same influencing radius. In this case, our model is equivalent to the Vicsek model. As the value of the exponent γ decreases, the network becomes more heterogeneous in the sense that fewer agents have evidently larger influencing radii, whereas more agents have the relatively smaller influencing radii.

To evaluate the degree of direction consensus among agents, we denote a cluster as a group of agents with the same direction. We are interested in the relative size S of the largest cluster, which is defined as the ratio of the number of agents within the largest cluster to the total number of agents of the network when the model evolves to a steady state, which means that all agents' directions keep invariant. Note that $0 \leq S \leq 1$, and a high value of S implies the high degree of direction consensus. If $S = 1$, complete direction consensus is achieved that all agents move in one direction.

To concentrate on the influence of heterogeneity represented by the scaling exponent parameter γ , we fix system parameters n , L and v . Suppose that there are $n = 1250$ agents moving in a square shaped cell of linear size $L = 50$ at the same absolute velocity $v = 0.1$. Figure 5.1(a) shows the relative size S of the largest cluster as a function of the average influencing radius $\langle r \rangle$ with different values of the scaling exponent γ . For a fixed exponent γ , we can see that S is an increasing function of $\langle r \rangle$, due to the fact that increasing $\langle r \rangle$ improves the connectivity of the network. Furthermore, for any value of γ , there exists a threshold $\bar{r}(\gamma)$ so that complete consensus can be achieved (i.e., $S = 1$) if $\langle r \rangle \geq \bar{r}(\gamma)$. We can see clearly that $\bar{r}(\gamma)$ is an increasing function of γ . In particular, in the most homogeneous case (i.e., $\gamma = \infty$), $\bar{r}(\infty) \approx 30$; while in the most heterogeneous case (i.e., $\gamma = 2$), $\bar{r}(2) \approx 3$, which is just about one tenth of $\bar{r}(\infty)$. This implies that it is much easier to achieve complete consensus as the network becomes more heterogeneous. Furthermore, for any given value of $\langle r \rangle$, S is a decreasing function of γ , implying that more agents will finally move in the same direction as the network becomes more heterogeneous.

We also compute the convergence time defined as the time required to arrive at the steady state. As shown in Fig. 5.1(b), the convergence time decreases when γ

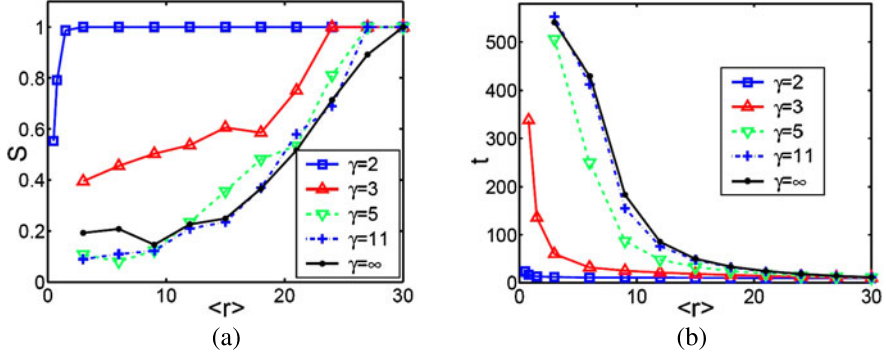


Fig. 5.1 [10] The relative size S of the largest cluster (a) and the convergence time (b) as functions of the average influencing radius $\langle r \rangle$ with various scaling exponents γ . System parameters are taken as $L = 50$, $n = 1250$ and $v = 0.1$. All quantities are averaged over 30 realizations

decreases or $\langle r \rangle$ increases. This implies that the required time to achieve consensus can also be shortened as the network becomes more heterogeneous or has better connectivity.

The heuristic reason for these phenomena lies in the fact that most agents in a strong heterogeneous network have very small influencing radii, but a few hub agents have very large influencing radii. In the ideal case, we can approximately assume that these hub agents form a complete subgraph, which can influence almost all other agents but cannot be influenced by those agents. Since a sufficient condition for consensus in a network of agents is that the network keeps strongly connected during the evolution process [11, 12], those hub agents will eventually move in the same direction, denoted as $\bar{\theta}$. Suppose that the number of hub agents is n_h , and each other agent i is influenced by at least one of the hub agents. Under these ideal assumptions, we have

$$\theta_i(t+1) = \frac{1}{1+n_i(t)}(\theta_i(t) + n_i(t)\bar{\theta}) \quad (5.3)$$

where $1 \leq n_i(t) \leq n_h$, which leads to

$$\theta_i(t+1) - \bar{\theta} = \frac{1}{1+n_i(t)}(\theta_i(t) - \bar{\theta}) \leq \frac{1}{2}(\theta_i(t) - \bar{\theta}). \quad (5.4)$$

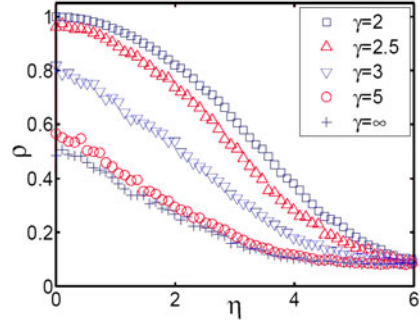
This implies that the direction of any other agents will also tend to $\bar{\theta}$.

The simulation results and heuristic analysis suggest that a few hub agents in a heterogeneous influence network play the leading roles during the system evolution process, and agreement among the hub agents is the key to achieve the nearly complete consensus in the whole network.

To investigate the influence of noise on our model, we rewrite the direction update equation (5.1) as follows:

$$\theta_i(t+1) = \frac{1}{1+n_i(t)}\left(\theta_i(t) + \sum_{j \in N_i(t)} \theta_j(t)\right) + \Delta\theta_i(t) \quad (5.5)$$

Fig. 5.2 [10] The order parameter ρ as a function of the noise amplitude η with various exponents γ . Other system parameters are taken as $\langle r \rangle = 3$, $n = 100$, $L = 31$ and $v = 1$. All estimates are the results of averaging over 100 realizations



where $\Delta\theta_i(t)$ is a random noise chosen with a uniform probability from the interval $[-\eta/2, \eta/2]$, $\eta \geq 0$. In this case, we cannot partition all the agents into different clusters accurately. Therefore, we adopt the order parameter ρ to evaluate the consensus degree which is defined as [2]:

$$\rho = \frac{1}{nv} \left| \sum_{i=1}^n \mathbf{v}_i \right|. \quad (5.6)$$

Clearly, as shown in Fig. 5.2, ρ is a decreasing function of η which implies that the consensus degree decreases as the noise amplitude increases. On the other hand, for any fixed value of η , ρ is a decreasing function of γ , which means that as the network becomes more heterogeneous, it is more robust to noise disturbance.

5.3 Pinning Controlled Consensus in a Heterogeneous Influence Network

Now suppose that we not only want to achieve the direction consensus but also want all agents to move in a given desired direction. Clearly, to achieve this goal, some kinds of control strategies need to be applied to the system. The leading role of the hub agents in an influence network motivate us to explore the possibility of achieving global consensus in a desired direction just by controlling a few leading agents.

Pinning control has been a common technique for the control of spatiotemporal chaos in regular dynamical networks and has recently been applied to scale-free dynamical networks [13–16]. Suppose that we want to achieve consensus in an influence network with a desired direction θ_p by pinning a fraction of agents. We compare two pinning control schemes. In the specifically pinning scheme, a fraction f of agents with the largest radii are pinned; while in the randomly pinning scheme, a fraction f of randomly selected agents are pinned. The pinned agents move at the same absolute velocity as other agents but with the fixed and desired direction θ_p . Other agents update their directions according to (5.1). To evaluate the degree of consensus in the desired direction, we define the relative size S_d of the

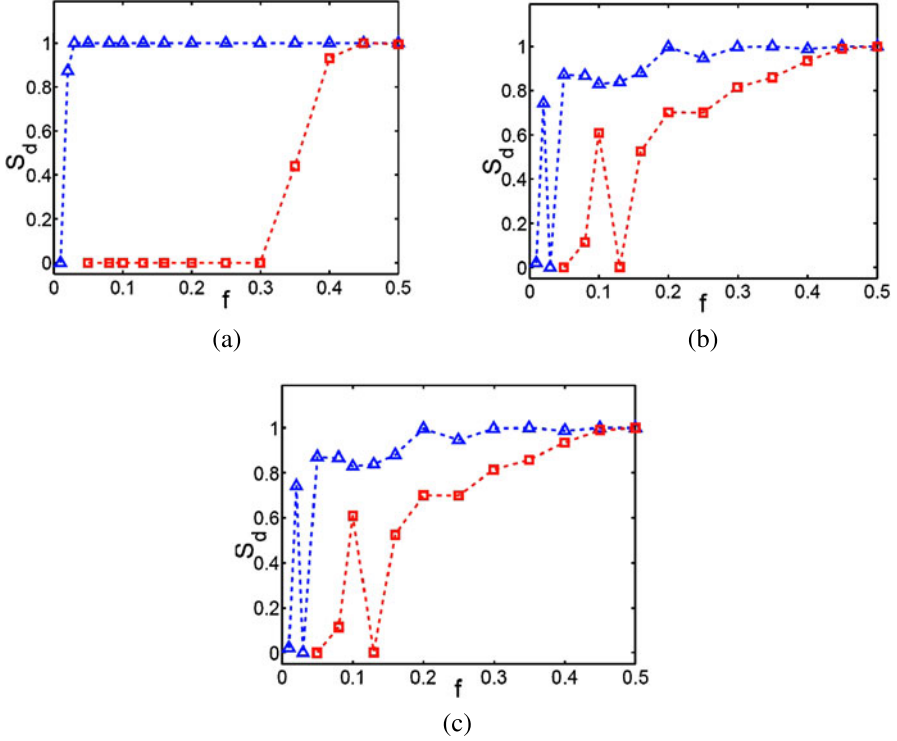
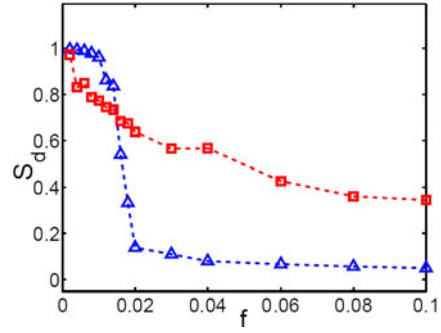


Fig. 5.3 [10] The relative size S_d of the largest desired cluster when a fraction f of randomly (\square) or specifically (\triangle) chosen agents are pinned at the desired direction: (a) $\gamma = 2$, (b) $\gamma = 3$, (c) $\gamma = 5$. Other system parameters are taken as $\langle r \rangle = 6$, $L = 50$, $n = 1250$, and $v = 0.1$. All estimates are the results of averaging over 30 realizations

largest desired cluster as the ratio of the largest number of agents moving in the desired direction θ_p to the total number of agents of the network when the system evolves to a steady state.

We compare the effects of specifically and randomly pinning control schemes on an influence network. The average influencing radius is taken as $\langle r \rangle = 6$. Figure 5.3 shows the relative size S_d of the largest desired cluster as a function of the fraction f of pinned agents with different scaling exponents γ . For each pinning control scheme and each value of γ , there exists a critical value of f above which all the agents will move in the desired direction (i.e., $S_d = 1$). In a highly homogeneous influence network with a relatively large scaling exponent (e.g., $\gamma = 5$), the difference between the critical values of two pinning control schemes is relatively small (see Fig. 5.3(c)). This is due to the fact that almost all the agents in the network have similar influencing abilities. On the other hand, there is a sharp difference between two critical values in a highly heterogeneous network. For example, in the case of $\gamma = 2$, the critical value corresponding to the randomly pinning control scheme is 0.43, which is about 10 times larger than the critical value 0.04 of the specifically

Fig. 5.4 [10] The relative size S_d of the largest cluster when the directions of a fraction f of randomly (\square) or specifically (\triangle) selected agents are randomly chosen and fixed through the evolution. System parameters are taken as $\langle r \rangle = 6$, $L = 50$, $n = 1250$, and $v = 0.1$. All estimates are the results of averaging over 30 realizations



pinning control scheme (see Fig. 5.3(a)). The origin of this sharp difference still lies in the heterogeneity feature: As explained before, if those hub agents with large radii move in the desired direction, then almost all other agents will also move in the desired direction. On the other hand, since most agents have small radii, the probability is very high that the small fraction of randomly chosen agents all have small radii, and pinning control of these agents cannot influence most of the other agents.

In the pinning control schemes, we assume that the directions of a small fraction of selected agents are fixed at the same direction. Now suppose that the directions of a small fraction of selected agents are fixed at different directions, can consensus still be achieved among other agents in the network? To investigate this question, we specifically or randomly choose a fraction f of agents. Directions of these agents are randomly chosen and fixed through the evolution process. Other agents update their directions according to (5.1). As shown in Fig. 5.4, in a high heterogeneous network with $\gamma = 2$, the relative size S of the largest cluster corresponding to the specific scheme decreases rapidly from $S = 1$ as f increases: the largest consensus cluster contains only about 10 % of the agents in the network if the directions of only 2 % of the agents with the largest influencing radii are fixed at different directions. This implies that agreement among hub agents is also a necessary condition for the emergence of global consensus. On the other hand, the relative size S of the largest cluster corresponding to the random scheme decreases very slowly from $S = 1$ as f increases: the largest consensus cluster contains nearly 40 % of the agents in the network even if the directions of 10 % of the random selected agents are fixed at different directions. This result demonstrates that the ability to achieve global consensus in a heterogeneous influence network is robust to random errors but fragile to specific attacks: Disagreement among a small number of specifically chosen hub agents with large radii can significantly destroy the emergence of global consensus, while disagreement among a small fraction of random selected agents with small radii cannot have a significant influence on consensus among other agents in the system. This conclusion is consistent with the recent discovery that the connectivity of a heterogeneous network is error tolerant but vulnerable to attacks [17].

5.4 Conclusions and Notes

Numerical simulations and heuristic analysis indicate that the ability to achieve direction consensus in an influence network is enhanced as the heterogeneity of the influencing radius distribution increases. In particular, global consensus with desired direction can be achieved in a heterogeneous influence network only if a small number of leading agents can be controlled to move along the desired direction. These results may shed some light on achieving desired consensus in social networks and other man-made multi-agent systems.

References

1. Reynolds CW (1987) Flocks, herds, and schools: a distributed behavioral model. *Comput Graph* 87(21):25–34
2. Vicsek T, Czir ok A, Ben-Jacob E, Cohen O, Shochet I (1995) Novel type of phase transition in a system of self-driven particles. *Phys Rev Lett* 75:1226–1229
3. Nishikawa T, Motter AE, Lai YC, Hoppensteadt FC (2003) Heterogeneity in oscillator networks: are smaller worlds easier to synchronize. *Phys Rev Lett* 91:014101
4. Motter AE, Zhou C, Kurths J (2005) Network synchronization, diffusion, and the paradox of heterogeneity. *Phys Rev E* 71:016116
5. Zhou C, Motter AE, Kurths J (2006) Universality in the synchronization of weighted random networks. *Phys Rev E* 96:034101
6. Donetti L, Hurtado PI, Munoz MA (2005) Entangled networks, synchronization, and optimal network topology. *Phys Rev Lett* 95:188701
7. Arenas A, Diaz-Guilera A, Perez-Vicente CJ (2006) Synchronization reveals topological scales in complex networks. *Phys Rev Lett* 96:114102
8. Hong H, Kim BJ, MY Choi, Park H (2004) Factors that predict better synchronizability on complex networks. *Phys Rev E* 69:067105
9. Assisi CG, Jirsa VK, Kelso JAS (2005) Synchrony and clustering in heterogeneous networks with global coupling and parameter dispersion. *Phys Rev Lett* 94:018106
10. Yang W, Cao L, Wang X, Li X (2006) Consensus in a heterogeneous influence network. *Phys Rev E* 74:037101
11. Olfati-Saber R, Murray RM (2004) Consensus problems in networks of agents with switching topology and time-delays. *IEEE Trans Autom Control* 49:1520–1533
12. Ren W, Beard RW (2005) Consensus seeking in multi-agent systems under dynamically changing interaction topologies. *IEEE Trans Autom Control* 50:655–661
13. Hu G, Xiao J, Gao J, Li X, Yao Y, Hu B (2000) Analytical study of spatiotemporal chaos control by applying local injections. *Phys Rev E* 62:3043–3046
14. Wang X, Chen G (2002) Pinning control of scale-free dynamical networks. *Physica A* 310:521–531
15. Li X, Wang X, Chen G (2004) Pinning a complex dynamical network to its equilibrium. *IEEE Trans Circuits Syst I, Fundam Theory Appl* 51:2074–2087
16. Wang X (2002) Complex networks: topology, dynamics, and synchronization. *Int J Bifurc Chaos* 12:885–916
17. Albert R, Jeong H, Barab si AL (2000) Error and attack tolerance of complex networks. *Nature* 406:378–482

Chapter 6

Distributed Pinning-Controlled Flocking with a Virtual Leader

Abstract This chapter introduces a flocking control problem in the presence of a virtual leader and only a fraction of informed agents. We solve the distributed collective tracking problem via pinning control approach. We first show that, even when only a fraction of agents are informed, the proposed flocking algorithm still enables all the informed agents to move with the desired constant velocity, and an uninformed agent to also move with the same desired velocity if it can be influenced by the informed agents from time to time during the evolution. In the situation where the virtual leader travels with a varying velocity, we propose a novel flocking algorithm and show that the proposed flocking algorithm enables the asymptotic tracking of the virtual leader. That is, the position and velocity of the center of mass of all agents will converge exponentially to those of the virtual leader. The convergent rate is also given. Numerical simulation demonstrates that a very small group of the informed agents can cause most of the agents to move with the desired velocity and the larger the informed group is the bigger portion of agents will move with the desired velocity.

Keywords Flocking · Informed agents · Virtual leader · Reynolds model · Multi-agent systems

6.1 Introduction

Flocking is the phenomenon in which large number of agents, using only limited environmental information and simple rules, organize into a coordinated motion. Flocking behavior exists in nature in the form of flocking of birds, schooling of fish, swarming of bacteria, and so on [1–13]. The classical flocking model proposed by Reynolds [3] in 1980s consists of three heuristic rules: (i) Separation: avoid collision with nearby flockmates; (ii) Alignment: attempt to match velocity with nearby flockmates; (iii) Cohesion: attempt to stay close to nearby flockmates. Over the years, many variants of these three rules and additional rules have been suggested, including obstacle avoidance and goal seeking. Many algorithms to realize these rules have also been proposed [14–26]. For example, graph theory [14, 15] and Lyapunov-based approach [16] have been used to investigate consensus (alignment) problem, local attractive/repulsive potential has been designed between neighbor-

ing agents to deal with separation and cohesion problem [17, 18], artificial potentials [19–21], and gyroscopic forces [22] have been used for obstacle avoidance, and (virtual) leader/follower approach have been investigated to goal seeking (tracking) problem [23–26].

Recently, flocking algorithms based on Reynolds flocking model were proposed by a combination of a velocity consensus component with a local artificial potential field [27–29]. In particular, Olfati-Saber [29] provided a theoretical and computational framework for design and analysis of scalable flocking algorithms. This framework includes three flocking algorithms. The first algorithm embodies the three rules of Reynolds and the third algorithm has obstacle avoidance capabilities. The second algorithm is the main flocking algorithm for a group of agents moving in a free space and is aimed at causing the group to track the path of a virtual leader by including a navigational feedback mechanism to every agent. It is assumed in the second algorithm that every agent in the group is an informed agent which has the information of the virtual leader. The benefit of this assumption is that it guarantees that all agents remain cohesive and asymptotically move with the same velocity. However, this assumption is in contrast with some phenomena in the nature and may be difficult to implement in engineering applications.

In some nature examples, few individuals have the pertinent information, such as knowledge of the location of a food source, or of a migration route. For example, few informed individuals within a fish school are known to be able to guide the school to navigate towards a target, and only about 5 % of the bees within a honeybee swarm can lead the group to a new nest site [30]. Recently, using a simple discrete-time model of group formation, Couzin et al. [30] revealed through simulation that only a very small proportion of informed individuals is required to achieve a great accuracy of group motion in a preferred motion.

The first objective of this chapter is to show that most agents will move with the desired velocity even when only a very small fraction of agents are informed agents in a large group of agents. In particular, under the assumption that the desired velocity is a constant vector, we will prove that the Olfati-Saber algorithm enables all the informed agents to move with the desired velocity, and an uninformed agent to also move with the same desired velocity if it can be influenced by the informed agents frequently enough during the evolution. This result may be similar with the convergent condition in consensus problems that the underlying topology of the network remaining connectivity frequently enough, which has been solved by graph theory and related stochastic matrix [15, 23] and Lyapunov-based approach [16]. However, due to the existing of nonlinear gradient-based term, these methods cannot be directly applied to the flocking problems. The challenge of the extension of Olfati-Saber's results is to show some uninformed agents can also approach the same desired velocity even when they cannot have constant access to one informed agent. This result will not only help to understand flocking behaviors in the nature, but also provide a framework for guiding the design of engineering multi-agent systems with a small fraction of agents being informed.

In the situation when the velocity of the virtual leader is not a constant vector, Olfati-Saber [29] has shown that his second algorithm is able to cause all the agents

in the group to eventually achieve the same velocity, which, however, is in general not equal to the velocity of the virtual leader. This motivates us to propose modification to the Olfati-Saber second algorithm so that the resulting algorithm will enable the asymptotic tracking of the virtual leader. That is, the position and velocity of the center of mass (COM) of all agents will converge exponentially to those of the virtual leader. In establishing this result, we will also obtain the rate of convergence.

6.2 Backgrounds and Problem Statement

We consider N agents moving in an n dimensional Euclidean space. The motion of each agent is described by two integrators as

$$\begin{cases} \dot{q}_i = p_i, \\ \dot{p}_i = u_i, \quad i = 1, 2, \dots, N, \end{cases} \quad (6.1)$$

where $q_i, p_i \in \mathbf{R}^n$ are respectively the position and velocity vectors of agent i , and $u_i \in \mathbf{R}^n$ is the (acceleration) control input acting on agent i . Each agent has a limited communication capability and it can only communicate with agents within its neighborhood region. The neighboring set of agents is the same as that in Sect. 4.1.

In his second algorithm, Olfati-Saber [29] proposes a distributed controller for each agent which only utilizes the information of other agents in its neighborhood and that of the virtual leader. Under his control scheme, agent i is steered via its acceleration input u_i that consists of three components

$$u_i = f_i^g + f_i^d + f_i^\gamma. \quad (6.2)$$

The first component of (6.2), f_i^g , is used to regulate position between agent i and its flockmates. This term is responsible for collision avoidance and cohesion in the group and is derived from the field produced by a collective potential function $V_i(q)$, which depends on the relative distance between agent i and its flockmates, and is defined as

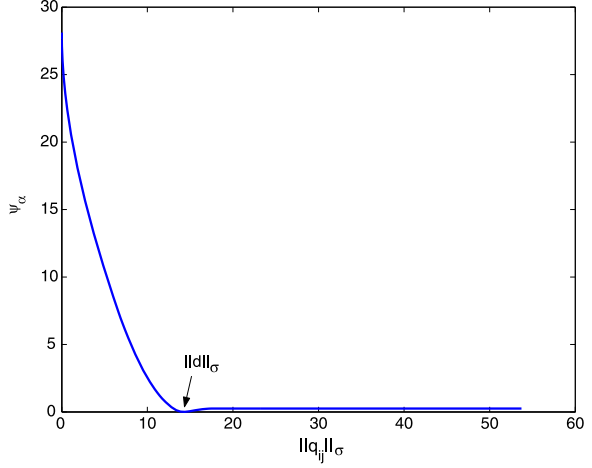
$$\begin{aligned} V_i(q) &= \sum_{j \in \mathcal{V} \setminus \{i\}} \psi_\alpha(\|q_i - q_j\|_\sigma) \\ &= \sum_{j \notin \mathcal{N}_i(t), j \neq i} \psi_\alpha(\|r\|_\sigma) + \sum_{j \in \mathcal{N}_i(t)} \psi_\alpha(\|q_i - q_j\|_\sigma), \end{aligned} \quad (6.3)$$

where the σ -norm $\|\cdot\|_\sigma$ of a vector is a map $\mathbf{R}^n \rightarrow \mathbf{R}_+$ defined as

$$\|z\|_\sigma = \frac{1}{\varepsilon} \left[\sqrt{1 + \varepsilon \|z\|^2} - 1 \right],$$

with a parameter $\varepsilon > 0$. Although $\|z\|$ is not differentiable at $z = 0$, the map $\|z\|_\sigma$ is differentiable everywhere, the property which is used to construct smooth collective potential functions for agents. The function $\psi_\alpha : \mathbf{R}_+ \rightarrow \mathbf{R}_+$ (see Fig. 6.1) is a non-negative smooth pairwise potential function of the distance $\|q_{ij}\|_\sigma$ between agents

Fig. 6.1 [31] Smooth pairwise potential function ψ_α



i and j , such that ψ_α reaches its maximum as $\|q_{ij}\|_\sigma \rightarrow 0$, attains its unique minimum when agents i and j are located at a desired distance $\|d\|_\sigma$, and is constant for $\|q_{ij}\|_\sigma \geq \|r\|_\sigma$.

The second component of (6.2), f_i^d , regulates the velocity of agent i to the weighted average velocity of its flockmates. This term is responsible for velocity alignment. The third component of (6.2), f_i^γ , is a navigational feedback term, which drives agent i to track the virtual leader with the following model of motion,

$$\begin{cases} \dot{q}_\gamma = p_\gamma, \\ \dot{p}_\gamma = f_\gamma(q_\gamma, p_\gamma), \end{cases} \quad (6.4)$$

where $q_\gamma, p_\gamma, f_\gamma \in \mathbf{R}^n$ are the position, velocity, and control input (acceleration) of the virtual leader with $(q_\gamma(0), p_\gamma(0)) = (q_d, p_d)$.

More specifically, the control protocol in the second Olfati-Saber flocking algorithm of [29] is given by

$$\begin{aligned} u_i = & - \sum_{j \in N_i(t)} \nabla_{q_i} \psi_\alpha(\|q_j - q_i\|_\sigma) + \sum_{j \in N_i(t)} a_{ij}(q)(p_j - p_i) \\ & - c_1(q_i - q_\gamma) - c_2(p_i - p_\gamma), \quad c_1, c_2 > 0, \end{aligned} \quad (6.5)$$

where $A(q) = (a_{ij}(q))$ is the adjacency matrix which is defined the same as in Sect. 4.1. It is then clear that $a_{ij}(q) = a_{ji}(q) > 0$ if $(j, i) \in \mathcal{E}(t)$ and $a_{ij}(q) = a_{ji}(q) = 0$ if $j \neq i$ but $(j, i) \notin \mathcal{E}(t)$. The two positive constants c_1 and c_2 represent the weights of the navigational feedback. We observe that the protocol (6.5) requires all agents have the knowledge of the virtual leader, (q_γ, p_γ) .

Under the reasonable assumption that the initial velocity mismatch and inertia are finite, Olfati-Saber proved that the three rules of Reynolds hold for a group of agents under the influence of the flocking algorithm (6.5). More specifically, it was established in [29] that the algorithm (6.5) enables a group of agents track a virtual leader moving at a constant velocity.

Motivated by these results of [29], we will examine in this chapter to what extent the algorithm (6.5) can still achieve flocking when not all agents have the knowledge of the virtual leader and how to modify the algorithm when the virtual leader moves at a varying velocity.

6.3 Flocking with a Fraction of Informed Agents

6.3.1 Algorithm Description and Main Results

In the flocking control algorithm (6.5), it is assumed that each agent is an informed agent who has the information about the virtual leader (i.e., its position and velocity). In this section, we assume that only some, but not all, of the agents are informed agents who are given the information about the virtual leader. Consequently, the control input for agent i , (6.5), is modified as

$$u_i = - \sum_{j \in \mathcal{N}_i(t)} \nabla_{q_i} \psi_\alpha(\|q_j - q_i\|_\sigma) + \sum_{j \in \mathcal{N}_i(t)} a_{ij}(q)(p_j - p_i) - h_i[c_1(q_i - q_\gamma) + c_2(p_i - p_\gamma)], \quad c_1, c_2 > 0, \quad (6.6)$$

where $h_i = 1$ if agent i is informed and $h_i = 0$ otherwise. Without loss of generality, we assume that the first M_0 ($1 \leq M_0 \leq N$) agents are informed agents, that is, $h_i = 1$ for $i = 1, 2, \dots, M_0$ and $h_i = 0$ for $i = M_0 + 1, M_0 + 2, \dots, N$. We further assume that the virtual leader moves along a fixed direction with a constant velocity p_d . Therefore, the dynamic equation (6.4) for the virtual leader can be simplified to

$$\dot{q}_\gamma = p_d, \quad q_\gamma(0) = q_d. \quad (6.7)$$

We are interested in the behavior of the whole group of agents in the situation when only a small fraction of the agents are informed agents (i.e., $1 \leq M_0 \ll N$). As an informed agent is not only influenced by the virtual leader but might also be influenced by some uninformed agents, it is not obvious that an informed agent will definitely track the virtual leader, not to mention those uninformed agents. A careful analysis will, however, show that not only all the informed agents but also some uninformed agents will track the virtual leader. Furthermore, we will carry out extensive simulation to reveal that the majority of the uninformed agents will indeed track the virtual leader even when only a small fraction of a large group of agents are informed agents.

Before stating the main results of this section, we need the following definition. Denote the union of all neighboring graphs across a nonempty finite time interval $[t_i, t_{i+1})$, $t_{i+1} > t_i$ as $\hat{\mathcal{G}}(t_i, t_{i+1})$, whose edges are the union of the edges of those neighboring graphs. For an uninformed agent, if there is a path between this agent and one informed agent in the union $\hat{\mathcal{G}}(t_i, t_{i+1})$, then we say that there exists a joint path between the uninformed agent and the informed agent across the finite time interval $[t_i, t_{i+1})$. We divide all the uninformed agents into two types. An uninformed

agent is called a type I uninformed agent if there exists an infinite sequence of contiguous, nonempty and uniformly bounded time-intervals $[t_i, t_{i+1})$, $i = 0, 1, 2, \dots$, such that across each time interval there exists a joint path between this agent and one informed agent. Otherwise, it is called a type II uninformed agent. Assume that there exists a sufficiently large $T > 0$ such that, for all $t \geq T$, there does not exist any joint path between any type II uninformed agent and any informed agent. This assumption implies that an uninformed agent that is disconnected from all informed agents for a long enough period of time will stay disconnected from them forever. Under this assumption, all the informed agents and type I uninformed agents cannot be influenced by type II uninformed agents directly or indirectly for all $t \geq T$. This assumption is reasonable in realism of a scenario. For example, if a bird did not get in touch with the flocks for a week, the probability of its coming back will be very low.

Define the sum of the total artificial potential energy and the total relative kinetic energy between all agents and the virtual leader as follows:

$$Q(q, p) = \frac{1}{2} \sum_{i=1}^N [U_i(q) + (p_i - p_\gamma)^T (p_i - p_\gamma)], \quad (6.8)$$

where

$$U_i(q) = \sum_{j=1, j \neq i}^N \psi_\alpha(\|q_i - q_j\|_\sigma) + h_i c_1 (q_i - q_\gamma)^T (q_i - q_\gamma). \quad (6.9)$$

Clearly, Q is a positive semi-definite function.

Our analysis results can then be summarized in the following theorem.

Theorem 6.1 *Consider a system of N mobile agents, each with dynamics (6.1) and steered by the control protocol (6.6). Suppose that the initial energy $Q_0 := Q(q(0), p(0))$ is finite. Then the following statements hold:*

- (i) *The distance between each informed agent and the virtual leader is not greater than $\sqrt{2Q_0/c_1}$ for all $t \geq 0$.*
- (ii) *The velocities of all informed agents and type I uninformed agents approach the desired velocity p_γ asymptotically.*
- (iii) *If the initial energy Q_0 of the group is less than $(\bar{k} + 1)c^*$, $c^* = \psi_\alpha(0)$, for some $\bar{k} \in \mathbf{Z}_+$, then at most \bar{k} distinct pairs of agents could possibly collide ($\bar{k} = 0$ guarantees a collision-free motion).*

The proof is carried out next in Sects. 6.3.2–6.3.4. Before we carry out this proof, we define the Laplacian of graph $\mathcal{G}(q)$ with adjacency matrix $A(q)$ as $L(q) = \Delta(A(q)) - A(q)$, where the degree matrix $\Delta(A(q))$ is a diagonal matrix with the i th diagonal element being $\sum_{j=1}^N a_{ij}(q)$. Denote the eigenvalues of $L(q)$ as $\lambda_1(L(q)) \leq \lambda_2(L(q)) \leq \dots \leq \lambda_N(L(q))$. Then, $\lambda_1(L(q)) = 0$ and $(1, 1, \dots, 1)^T \in \mathbf{R}^N$ is the corresponding eigenvector. Moreover, if $\mathcal{G}(q)$ is a connected graph, then $\lambda_2(L(q)) > 0$ [32]. The corresponding n dimensional graph Laplacian is defined as

$\hat{L}(q) = L(t) \otimes I_n$, where I_n is the identity matrix of order n and \otimes stands for the Kronecker product. This multi-dimensional Laplacian satisfies the following sum of squares property [29],

$$z^T \hat{L}(q) z = \frac{1}{2} \sum_{(i,j) \in \mathcal{E}} a_{ij}(q) \|z_j - z_i\|^2, \quad (6.10)$$

where

$$z = \begin{bmatrix} z_1 \\ z_2 \\ \vdots \\ z_N \end{bmatrix} \in \mathbf{R}^{Nn},$$

and $z_i \in \mathbf{R}^n$ for $i = 1, 2, \dots, N$.

6.3.2 Cohesive Analysis

We first carry out the cohesiveness analysis, which contains a proof of part (i) of Theorem 6.1.

Denote the position difference vector and the velocity difference vector between agent and the virtual leader as $\tilde{q}_i = q_i - q_\gamma$ and $\tilde{p}_i = p_i - p_\gamma$, respectively. We have

$$\begin{cases} \dot{\tilde{q}}_i = \tilde{p}_i, \\ \dot{\tilde{p}}_i = u_i, \end{cases} \quad i = 1, 2, \dots, N. \quad (6.11)$$

Let $q_{ij} = q_i - q_j$ and $\tilde{q}_{ij} = \tilde{q}_i - \tilde{q}_j$. Clearly, $\tilde{q}_{ij} = q_{ij}$, and the collective potential function (6.3) can be rewritten as

$$\begin{aligned} \tilde{V}_i(\tilde{q}_{ij}) &= V_i(q) = \sum_{j \in \mathcal{V} \setminus \{i\}} \psi_\alpha(\|\tilde{q}_{ij}\|_\sigma) \\ &= \sum_{j \notin \mathcal{N}_i(t), j \neq i} \psi_\alpha(\|r\|_\sigma) + \sum_{j \in \mathcal{N}_i(t)} \psi_\alpha(\|\tilde{q}_{ij}\|_\sigma). \end{aligned} \quad (6.12)$$

Similarly, the control protocol for agent i is rewritten as

$$\begin{aligned} u_i &= - \sum_{j \in \mathcal{N}_i(t)} \nabla_{\tilde{q}_i} \psi_\alpha(\|\tilde{q}_{ij}\|_\sigma) + \sum_{j \in \mathcal{N}_i(t)} a_{ij}(t) (\tilde{p}_j - \tilde{p}_i) \\ &\quad - h_i [c_1 \tilde{q}_i + c_2 \tilde{p}_i], \end{aligned} \quad (6.13)$$

and the positive semi-definite energy function (6.8) can be rewritten as

$$\mathcal{Q}(\tilde{q}, \tilde{p}) = \frac{1}{2} \sum_{i=1}^N (U_i(\tilde{q}) + \tilde{p}_i^T \tilde{p}_i), \quad (6.14)$$

where

$$\begin{aligned}
U_i(\tilde{q}) &= \sum_{j=1, j \neq i}^N \psi_\alpha(\|\tilde{q}_{ij}\|_\sigma) + h_i c_1 \tilde{q}_i^T \tilde{q}_i \\
&= \tilde{V}_i(\tilde{q}_{ij}) + h_i c_1 \tilde{q}_i^T \tilde{q}_i,
\end{aligned} \tag{6.15}$$

and

$$\tilde{q} = [\tilde{q}_1^T \quad \tilde{q}_2^T \quad \dots \quad \tilde{q}_N^T]^T, \quad \tilde{p} = [\tilde{p}_1^T \quad \tilde{p}_2^T \quad \dots \quad \tilde{p}_N^T]^T.$$

Due to the symmetry of the pairwise potential function ψ_α and the adjacency matrix $A(t)$, we have

$$\frac{\partial \psi_\alpha(\|\tilde{q}_{ij}\|_\sigma)}{\partial \tilde{q}_{ij}} = \frac{\partial \psi_\alpha(\|\tilde{q}_{ij}\|_\sigma)}{\partial \tilde{q}_i} = -\frac{\partial \psi_\alpha(\|\tilde{q}_{ij}\|_\sigma)}{\partial \tilde{q}_j}, \tag{6.16}$$

and by (6.11),

$$\frac{1}{2} \sum_{i=1}^N \dot{U}_i = \sum_{i=1}^N (\tilde{p}_i^T \nabla_{\tilde{q}_i} \tilde{V}_i(\tilde{q}_{ij}) + h_i c_1 \tilde{p}_i^T \tilde{q}_i), \tag{6.17}$$

where $\dot{U}_i = dU_i/dt$. Therefore, the derivative of Q along the trajectories of the agents and the virtual leader is given by

$$\begin{aligned}
\dot{Q} &= \frac{1}{2} \sum_{i=1}^N \dot{U}_i + \sum_{i=1}^N \tilde{p}_i^T \dot{\tilde{p}}_i \\
&= -\tilde{p}^T [(L(q) + c_2 H) \otimes I_n] \tilde{p},
\end{aligned} \tag{6.18}$$

where

$$H = \begin{bmatrix} h_1 & 0 & \dots & 0 \\ 0 & h_2 & \dots & 0 \\ \vdots & \vdots & \ddots & \vdots \\ 0 & 0 & \dots & h_N \end{bmatrix}.$$

Since $L(q)$ and H are both positive semi-definite matrices [33], $L(q) + c_2 H$ is also a positive semi-definite matrix. Therefore, $\dot{Q} \leq 0$, which implies that $Q(t)$ is a nonincreasing function of time t and thus $Q(t) \leq Q_0$ for all $t \geq 0$. It then follows from (6.14)–(6.15) that $c_1 \tilde{q}_i^T \tilde{q}_i \leq 2Q_0$ for any informed agent i . Hence, the distance between an informed agent i and the virtual leader is not greater than $\sqrt{2Q_0/c_1}$ for all $t \geq 0$.

6.3.3 Velocity Matching Analysis

We now continue with the asymptotic velocity matching analysis, which contains a proof of part (ii) of Theorem 6.1.

From part (i) of Theorem 6.1, the distance between any informed agent and the virtual leader is finite for all $t \geq 0$. It follows from (6.14) and (6.15) that

$\tilde{p}_i^T \tilde{p}_i \leq 2Q_0, i = 1, 2, \dots, N$, or equivalently, $\|\tilde{p}_i\| \leq \sqrt{2Q_0}, i = 1, 2, \dots, N$. That is, the velocity difference between any agent and the virtual leader is not greater than $\sqrt{2Q_0}$ for all $t \geq 0$. Since there exists a joint path between a type I uninformed agent and one informed agent in each finite time-interval $[t_i, t_{i+1}), i = 0, 1, 2, \dots$, the distance between any type I uninformed agent and virtual leader is also finite for all $t \geq 0$.

Let $M, M_0 \leq M \leq N$, be the total number of informed agents and type I uninformed agents in the group. Without loss of generality, we label type I uninformed agents from $M_0 + 1$ to M . From the earlier analysis, we know that all the informed agents and the type I uninformed agents cannot be influenced by a type II uninformed agents directly or indirectly for all $t \geq T$. For any $t \geq T$, we consider the positive semi-definite function

$$\check{Q}(\check{q}, \check{p}) = \frac{1}{2} \sum_{i=1}^M (\check{U}_i(\check{q}) + \check{p}_i^T \check{p}_i), \quad (6.19)$$

where

$$\check{U}_i(\check{q}) = \sum_{j=1, j \neq i}^M \psi_\alpha(\|\tilde{q}_{ij}\|_\sigma) + h_i c_1 \tilde{q}_i^T \tilde{q}_i, \quad (6.20)$$

where

$$\check{q} = [\tilde{q}_1^T \quad \tilde{q}_2^T \quad \dots \quad \tilde{q}_M^T]^T, \quad \check{p} = [\tilde{p}_1^T \quad \tilde{p}_2^T \quad \dots \quad \tilde{p}_M^T]^T.$$

From (6.14) and (6.19), it is clear that $\check{Q} \leq Q$. The derivative of \check{Q} along the trajectories of the agents and the virtual leader is given by

$$\dot{\check{Q}} = \frac{1}{2} \sum_{i=1}^M \dot{\check{U}}_i + \sum_{i=1}^M \check{p}_i^T \dot{\check{p}}_i = -\check{p}^T [(\check{L}(q) + c_2 \check{H}) \otimes I_n] \check{p}, \quad (6.21)$$

where $\check{L}(q) = [\check{l}_{ij}(q)]$ with

$$\check{l}_{ij}(q) = \begin{cases} -a_{ij}(q) & \text{if } i \neq j, \\ \sum_{j=1}^M a_{ij}(q) & \text{if } i = j, \end{cases}$$

and

$$\check{H} = \begin{bmatrix} h_1 & 0 & \dots & 0 \\ 0 & h_2 & \dots & 0 \\ \vdots & \vdots & \ddots & \vdots \\ 0 & 0 & \dots & h_M \end{bmatrix}.$$

Following a similar analysis that led to $\dot{Q} \leq 0$, we can obtain that $\dot{\check{Q}} \leq 0$ and consequently, $\check{Q} \leq \check{Q}_T \leq Q_T \leq Q_0$ for all $t \geq T$, where $\check{Q}_T = Q(\check{q}(T), \check{p}(T))$. Clearly, the set of all (\check{q}, \check{p}) such that $\check{Q} \leq Q_0$, that is,

$$\Omega = \{[\check{q}^T, \check{p}^T]^T \in \mathbf{R}^{2Mn} : \check{Q}(\check{q}, \check{p}) \leq Q_0\},$$

is an invariant set. We next show that it is also a compact set. By (6.19) and (6.20), $\tilde{p}_i^T \tilde{p}_i \leq 2Q_0$, for all $i = 1, 2, \dots, M$, and hence all $\tilde{p}_i, i = 1, 2, \dots, M$, are bounded. Similarly, all $\tilde{q}_i, i = 1, 2, \dots, M_0$, are bounded, that is, the positions of all informed agents are bounded. We next consider $\tilde{q}_i, i = M_0 + 1, M_0 + 2, \dots, M$. Each of these \tilde{q}_i is the position of a type I uninformed agent whose distance to an informed agent is, by the definition of the type I uninformed agents, bounded, due to the facts that the velocity of each agent is bounded and that the time intervals $[t_i, t_{i+1})$ are uniformly bounded. Consequently, the positions of all type I uninformed agents are also bounded. This concludes that the set Ω is compact.

It then follows from the LaSalle Invariance Principle [34] that all trajectories of the agents that start from Ω will converge to the largest invariant set inside the region

$$S = \{[\check{q}^T, \check{p}^T]^T \in \mathbf{R}^{2Mn} : \check{Q} = 0\}.$$

Denote the set of all the informed agents and type I uninformed agents as $\check{\mathcal{V}} = \{1, 2, \dots, M\}$. During the evolution, the graph $\check{\mathcal{G}}(t) = \{\check{\mathcal{V}}, \check{\mathcal{E}}(t)\}$, $\check{\mathcal{E}}(t) = \{(i, j) \in \check{\mathcal{V}} \times \check{\mathcal{V}} : i \sim j\}$, may not always be connected. Suppose that $\check{\mathcal{G}}(t)$ consists of $m(t)$, $1 \leq m(t) \leq M$, connected subgraphs for any $t \geq T$ and there are $M_k(t)$ agents in the k th, $1 \leq k \leq m(t)$, connected subgraph at time t . Clearly, $M = M_1(t) + M_2(t) + \dots + M_{m(t)}(t)$. A connected subgraph is called an informed subgraph if it includes at least one informed agent. We assume that the graph $\check{\mathcal{G}}(t)$ consists of $m_1(t)$, $1 \leq m_1(t) \leq M_0$, informed connected subgraphs.

As in the earlier analysis, we have that both $\check{L}(q) \otimes I_n$ and $\check{H} \otimes I_n$ are positive semi-definite. Thus, it follows from (6.21) that $\check{Q} = 0$ if and only if $\check{p}^T(\check{L}(q) \otimes I_n)\check{p} = 0$ and $\check{p}^T(\check{H} \otimes I_n)\check{p} = 0$.

Without loss of generality, we assume that the informed connected subgraphs are labeled from 1 to $m_1(t)$. For any time $t \geq T$, there exists an orthogonal permutation matrix $P(t) \in \mathbf{R}^{M \times M}$ such that $\check{L}(t)$ can be transformed into a block diagonal matrix of the form

$$\begin{aligned} \hat{L}(t) &= P(t)\check{L}(t)P^T(t) \\ &= \begin{bmatrix} \check{L}_1(t) & \dots & 0 & \dots & 0 \\ \vdots & \ddots & \vdots & \vdots & \vdots \\ 0 & \dots & \check{L}_{m_1(t)}(t) & \dots & 0 \\ \vdots & \vdots & \vdots & \ddots & \vdots \\ 0 & \dots & 0 & \dots & \check{L}_{m(t)}(t) \end{bmatrix}, \end{aligned}$$

where $\check{L}_k(t) \in \mathbf{R}^{M_k(t) \times M_k(t)}$ is the Laplacian matrix associated with the k th connected subgraph of the graph $\check{\mathcal{G}}(t)$. The indices of the state vector can be rearranged such that

$$\hat{\tilde{p}} = \begin{bmatrix} \check{\tilde{p}}^1 \\ \check{\tilde{p}}^2 \\ \vdots \\ \check{\tilde{p}}^{m(t)} \end{bmatrix} = (P(t) \otimes I_n) \check{\tilde{p}}, \quad \check{\tilde{p}}^k = \begin{bmatrix} \check{\tilde{p}}_1^k \\ \check{\tilde{p}}_2^k \\ \vdots \\ \check{\tilde{p}}_{M_k(t)}^k \end{bmatrix},$$

where $\check{\tilde{p}}^k$ is the velocity difference vector of the $M_k(t)$ agents within the k th connected subgraph. We have

$$\begin{aligned} & \hat{\tilde{p}}^T (\hat{L}(t) \otimes I_n) \hat{\tilde{p}} \\ &= ((P(t) \otimes I_n) \check{\tilde{p}})^T ((P(t) \check{L}(t) P^T(t)) \otimes I_n) (P(t) \otimes I_n) \check{\tilde{p}} \\ &= \check{\tilde{p}}^T (P^T(t) \otimes I_n) ((P(t) \check{L}(t) P^T(t)) \otimes I_n) (P(t) \otimes I_n) \check{\tilde{p}} \\ &= \check{\tilde{p}}^T ((P^T(t) P(t) \check{L}(t) P^T(t)) \otimes I_n) (P(t) \otimes I_n) \check{\tilde{p}} \\ &= \check{\tilde{p}}^T ((\check{L}(t) P^T(t) P(t)) \otimes I_n) \check{\tilde{p}} \\ &= \check{\tilde{p}}^T (\check{L}(t) \otimes I_n) \check{\tilde{p}}. \end{aligned} \tag{6.22}$$

Therefore,

$$\begin{aligned} & -\check{\tilde{p}}^T (\check{L}(t) \otimes I_n) \check{\tilde{p}} \\ &= - \begin{bmatrix} \check{\tilde{p}}^1 \\ \vdots \\ \check{\tilde{p}}^{m_1(t)} \\ \vdots \\ \check{\tilde{p}}^{m(t)} \end{bmatrix}^T \left(\begin{bmatrix} \check{L}_1(t) & \dots & 0 & \dots & 0 \\ \vdots & \ddots & \vdots & \vdots & \vdots \\ 0 & \dots & \check{L}_{m_1(t)}(t) & \dots & 0 \\ \vdots & \vdots & \vdots & \ddots & \vdots \\ 0 & \dots & 0 & \dots & \check{L}_{m(t)}(t) \end{bmatrix} \otimes I_n \right) \begin{bmatrix} \check{\tilde{p}}^1 \\ \vdots \\ \check{\tilde{p}}^{m_1(t)} \\ \vdots \\ \check{\tilde{p}}^{m(t)} \end{bmatrix}. \end{aligned} \tag{6.23}$$

Clearly, $-\check{\tilde{p}}^T (\check{L}(t) \otimes I_n) \check{\tilde{p}} = 0$ if and only if

$$(\check{\tilde{p}}^k)^T (\check{L}_k(t) \otimes I_n) \check{\tilde{p}}^k = 0, \quad k = 1, 2, \dots, m(t). \tag{6.24}$$

By the sum of squares property [29],

$$(\check{\tilde{p}}^k)^T (\check{L}_k(t) \otimes I_n) \check{\tilde{p}}^k = \frac{1}{2} \sum_{(i,j) \in \mathcal{E}(t)} a_{ij}(t) \|\check{\tilde{p}}_i^k - \check{\tilde{p}}_j^k\|^2.$$

Therefore, (6.24) is equivalent to

$$\check{\tilde{p}}_1^k = \check{\tilde{p}}_2^k = \dots = \check{\tilde{p}}_{M_k(t)}^k, \quad k = 1, 2, \dots, m(t). \tag{6.25}$$

Similarly, for any $t \geq T$, we have

$$\begin{aligned}
& -\check{\tilde{p}}^T (\check{H}(t) \otimes I_n) \check{\tilde{p}} \\
& = - \begin{bmatrix} \check{\tilde{p}}^1 \\ \vdots \\ \check{\tilde{p}}^{m_1(t)} \\ \vdots \\ \check{\tilde{p}}^{m(t)} \end{bmatrix}^T \left(\begin{bmatrix} \check{H}_1(t) & \dots & 0 & \dots & 0 \\ \vdots & \ddots & \vdots & \vdots & \vdots \\ 0 & \dots & \check{H}_{m_1(t)}(t) & \dots & 0 \\ \vdots & \vdots & \vdots & \ddots & \vdots \\ 0 & \dots & 0 & \dots & \check{H}_{m(t)}(t) \end{bmatrix} \otimes I_n \right) \begin{bmatrix} \check{\tilde{p}}^1 \\ \vdots \\ \check{\tilde{p}}^{m_1(t)} \\ \vdots \\ \check{\tilde{p}}^{m(t)} \end{bmatrix}, \tag{6.26}
\end{aligned}$$

where $\check{H}_k(t) \in \mathbf{R}^{M_k(t) \times M_k(t)}$ is the diagonal matrix associated with the k th connected subgraph with the i th diagonal element h_i^k , $i = 1, 2, \dots, M_k(t)$, which is equal to one for an informed agent and zero for an uninformed agent.

Clearly, $-\check{\tilde{p}}^T (\check{H}(t) \otimes I_n) \check{\tilde{p}} = 0$ if and only if

$$(\check{\tilde{p}}^k)^T (\check{H}_k(t) \otimes I_n) \check{\tilde{p}}^k = 0, \quad k = 1, 2, \dots, m(t), \tag{6.27}$$

which implies that the velocity difference between all informed agents and the virtual leader is zero. Since there is at least one informed agent in each informed connected subgraph, without loss of generality, we assume that the first agent in each informed connected subgraph is an informed agent. We have

$$\check{\tilde{p}}_1^k = 0, \quad k = 1, 2, \dots, m_1(t). \tag{6.28}$$

In view of (6.25), (6.27), and (6.28),

$$-\check{\tilde{p}}^T (\check{L}(t) \otimes I_n) \check{\tilde{p}} - \check{\tilde{p}}^T (c_2 \check{H}(t) \otimes I_n) \check{\tilde{p}} = 0 \tag{6.29}$$

if and only if

$$\check{\tilde{p}}_1^k = \check{\tilde{p}}_2^k = \dots = \check{\tilde{p}}_{M_k(t)}^k = 0, \quad k = 1, 2, \dots, m_1(t), \tag{6.30}$$

and

$$\check{\tilde{p}}_1^k = \check{\tilde{p}}_2^k = \dots = \check{\tilde{p}}_{M_k(t)}^k, \quad k = m_1(t) + 1, m_1(t) + 2, \dots, m(t), \tag{6.31}$$

which implies that the velocities of all agents in all informed connected subgroups approach the desired velocity p_γ asymptotically, and velocities of all agents in the same uninformed connected subgroup approach the same velocity.

We next show that, for $t \geq T$, all connected subgraphs are informed connected subgraphs, i.e., $m(t) = m_1(t)$ for t large enough. This would imply that the velocities of all informed agents and type I uninformed agents approach the desired velocity p_γ asymptotically. To this end, let us assume that the interaction network switches at time $t' \in [T, \infty)$, i.e., at time t' , either an agent i is disconnected from another agent j or an agent i is connected with another agent j . In either case, we have $\check{\tilde{p}}_i(t') \neq \check{\tilde{p}}_j(t')$. It then follows from (6.21), (6.23), and (6.26) that

$$\check{\dot{Q}}(t') < 0,$$

which contradicts the fact that $\dot{Q}(t) = 0$. Thus, we conclude that the interaction network will not switch for all $t \geq T$. By their definition, all type I uninformed agents must have a path to one informed agent in the fixed interaction network for all $t \geq T$. Consequently, $m(t) = m_1(t)$ for all $t \geq T$.

6.3.4 Collision Avoidance Analysis

Finally, we proceed to carry out the collision-avoidance analysis, which contains a proof of part (iii) of Theorem 6.1.

In view of (6.18), Q is a nonincreasing function of time t and thus $Q(t) \leq Q_0$ for all $t \geq 0$. The rest of the proof of this part is similar to that of part (iv) of Theorem 2 in [29]. Suppose that initial energy Q_0 is less than $(\bar{k} + 1)c^*$ and more than \bar{k} distinct pairs of agents collide at a given time $t^* > 0$, i.e., at least $\bar{k} + 1$ distinct pairs of agents collide at time $t^* > 0$. Then, at time $t^* > 0$, the collective potential of the system is at least $(\bar{k} + 1)\psi_\alpha(0)$. From $Q_0 \geq Q(t)$ for all $t \geq 0$, we have

$$Q_0 \geq Q(t^*) \geq (\bar{k} + 1)\psi_\alpha(0),$$

which contradicts the assumption that $Q_0 < (\bar{k} + 1)c^*$. This shows that no more than \bar{k} distinct pairs of agents can possibly collide at any time $t \geq 0$. Consequently, if $\bar{k} = 0$, no collision will occur.

6.4 Flocking with a Virtual Leader of Varying Velocity

6.4.1 Algorithm Description and Main Result

In the situation that all agents are informed agents and the virtual leader move with a constant velocity p_γ , Theorem 6.1 guarantees that all agents will finally move with the desired velocity p_γ . In the situation that the velocity $p_\gamma(t)$ of the virtual leader varies with time, even though it has been established in Theorem 2 of [29] that all agents in the group can finally achieve a common velocity, this common velocity in general does not match with $p_\gamma(t)$. In this section, we focus on the situation when the virtual leader move with a varying velocity. In order for the common velocity of all the agents to match that of a virtual leader of varying velocity, $p_\gamma(t)$, we propose to incorporate the information of acceleration of the virtual leader into the protocol (6.5) as follows:

$$\begin{aligned} u_i = & - \sum_{j \in \mathcal{N}_i(t)} \nabla_{q_i} \psi_\alpha(\|q_j - q_i\|_\sigma) + \sum_{j \in \mathcal{N}_i(t)} a_{ij}(q)(p_j - p_i) + f_\gamma(q_\gamma, p_\gamma) \\ & - c_1(q_i - q_\gamma) - c_2(p_i - p_\gamma), \quad c_1, c_2 > 0. \end{aligned} \quad (6.32)$$

Denote the position and velocity of the center of mass (COM) of all agents in the group as

$$\bar{q} = \frac{\sum_{i=1}^N q_i}{N}, \quad \bar{p} = \frac{\sum_{i=1}^N p_i}{N}.$$

The sum of the total artificial potential energy and the total relative kinetic energy between all agents and the virtual leader in this case is defined as follows:

$$Q(q, p) = \frac{1}{2} \sum_{i=1}^N (U_i(q) + (p_i - p_\gamma)^T (p_i - p_\gamma)), \quad (6.33)$$

where

$$U_i(q) = \sum_{j=1, j \neq i}^N \psi_\alpha(\|q_{ij}\|_\sigma) + c_1(q_i - q_\gamma)^T (q_i - q_\gamma). \quad (6.34)$$

Clearly, Q is a positive semi-definite function. Our main results on the tracking of the virtual leader can then be stated in the following theorem, whose proof will be carried out in next Sect. 6.4.2.

Theorem 6.2 *Consider a system of N mobile agents, each with dynamics (6.1) and steered by the control protocol (6.32). Suppose that the initial energy $Q_0 = Q(q(0), p(0))$ is finite. Then the following statements hold:*

- (i) *The distance between any agent and the virtual leader is not greater than $\sqrt{2Q_0/c_1}$ for all $t \geq 0$.*
- (ii) *The velocity of each agent approaches the desired velocity p_γ asymptotically.*
- (iii) *If both the initial velocity and position of the COM are equal to the initial velocity and position of the virtual leader, then the velocity (or position) of the COM will be equal to the velocity (or position) of the virtual leader for all $t \geq 0$; otherwise the velocity (or position) of the COM will converge exponentially to the velocity (or position) of virtual leader with a time constant τ , where*

$$\tau = \begin{cases} \frac{c_2}{2} & \text{if } c_2^2 \leq 4c_1, \\ \frac{c_2 - \sqrt{c_2^2 - 4c_1}}{2} & \text{if } c_2^2 > 4c_1. \end{cases}$$

- (iv) *Almost every configuration the system approaches is a local minimum of the total artificial potential energy $\frac{1}{2} \sum_{i=1}^N U_i(q)$.*
- (v) *If the initial energy Q_0 of the group of agents is less than $(\bar{k} + 1)c^*$, $c^* = \psi_\alpha(0)$, for some $\bar{k} \in \mathbf{Z}_+$, then at most \bar{k} distinct pairs of agents could possibly collide ($\bar{k} = 0$ guarantees a collision-free motion).*

6.4.2 Theoretical Analysis

We first prove part (i) of Theorem 6.2. Denote the position difference vector and the velocity difference vector between agent i and the virtual leader as $\tilde{q}_i = q_i - q_\gamma$ and $\tilde{p}_i = p_i - p_\gamma$, respectively. Then,

$$\begin{cases} \dot{\tilde{q}}_i = \tilde{p}_i, \\ \dot{\tilde{p}}_i = u_i - f_\gamma(q_\gamma, p_\gamma), \quad i = 1, 2, \dots, N. \end{cases} \quad (6.35)$$

We will also denote

$$\tilde{q} = \begin{bmatrix} \tilde{q}_1 \\ \tilde{q}_2 \\ \vdots \\ \tilde{q}_N \end{bmatrix}, \quad \tilde{p} = \begin{bmatrix} \tilde{p}_1 \\ \tilde{p}_2 \\ \vdots \\ \tilde{p}_N \end{bmatrix}.$$

Thus, the control protocol for agent i , (6.32), can be rewritten as

$$\begin{aligned} u_i = & - \sum_{j \in \mathcal{N}_i(t)} \nabla_{\tilde{q}_i} \psi_\alpha(\|\tilde{q}_{ij}\|_\sigma) + \sum_{j \in \mathcal{N}_i(t)} a_{ij}(q) (\tilde{p}_j - \tilde{p}_i) \\ & + f_\gamma(q_\gamma, p_\gamma) - c_1 \tilde{q}_i - c_2 \tilde{p}_i. \end{aligned} \quad (6.36)$$

From the previous analysis, we recall that the collective potential function (6.3) can be rewritten as

$$\begin{aligned} \tilde{V}_i(\tilde{q}_{ij}) &= V_i(q) \\ &= \sum_{j \in \mathcal{V} \setminus \{i\}} \psi_\alpha(\|\tilde{q}_{ij}\|_\sigma) \\ &= \sum_{j \notin \mathcal{N}_i(t), j \neq i} \psi_\alpha(\|r\|_\sigma) + \sum_{j \in \mathcal{N}_i(t)} \psi_\alpha(\|\tilde{q}_{ij}\|_\sigma). \end{aligned} \quad (6.37)$$

Also, the positive definite function (6.33) can be rewritten as

$$Q(\tilde{q}, \tilde{p}) = Q(q, p) = \frac{1}{2} \sum_{i=1}^N (U_i(\tilde{q}) + \tilde{p}_i^T \tilde{p}_i), \quad (6.38)$$

where

$$U_i(\tilde{q}) = \sum_{j=1, j \neq i}^N \psi_\alpha(\|\tilde{q}_{ij}\|_\sigma) + c_1 \tilde{q}_i^T \tilde{q}_i = \tilde{V}_i(\tilde{q}_{ij}) + c_1 \tilde{q}_i^T \tilde{q}_i. \quad (6.39)$$

Due to the symmetry of the pairwise potential function ψ_α and the adjacency matrix $A(t)$,

$$\frac{1}{2} \sum_{i=1}^N \dot{U}_i = \sum_{i=1}^N (\tilde{p}_i^T \nabla_{\tilde{q}_i} \tilde{V}_i(\tilde{q}_{ij}) + c_1 \tilde{p}_i^T \tilde{q}_i). \quad (6.40)$$

Therefore, the derivative of Q along the trajectories of the agents and the virtual leader is given by

$$\dot{Q} = \frac{1}{2} \sum_{i=1}^N \dot{U}_i + \sum_{i=1}^N \tilde{p}_i^T \dot{\tilde{p}}_i = -\tilde{p}^T [(L(q) + c_2 I_N) \otimes I_n] \tilde{p}. \quad (6.41)$$

Recalling that $L(t)$ is a positive semi-definite matrix [33], we have $\dot{Q} \leq 0$, which implies that $Q(t) := Q(\tilde{q}, \tilde{p})$ is a nonincreasing function of time t and thus $Q(t) \leq Q_0$ for all $t \geq 0$. From (6.38) and (6.39), we have $c_1 \tilde{q}_i^T \tilde{q}_i \leq 2Q_0$ for any agent i . Therefore, the distance between any agent and the virtual leader is not greater than $\sqrt{2Q_0/c_1}$ for all $t \geq 0$.

We now prove parts (ii) and (iii) of Theorem 6.2.

Since Q is positive definite and $\dot{Q} \leq 0$, the set

$$\Omega = \{[\tilde{q}^T, \tilde{p}^T]^T \in \mathbf{R}^{2Nn} : Q \leq Q_0\}$$

is a compact invariant set. It then follows from the LaSalle Invariance Principle that all trajectories of the agents that start from Ω converge to the largest invariant set inside the region

$$S = \{[\tilde{q}^T, \tilde{p}^T]^T \in \mathbf{R}^{2Nn} : \dot{Q} = 0\}.$$

From (6.41), we have

$$\dot{Q} = -\tilde{p}^T [(L(q) + c_2 I_N) \otimes I_n] \tilde{p} = -\tilde{p}^T (L(q) \otimes I_n) \tilde{p} - c_2 \tilde{p}^T \tilde{p}. \quad (6.42)$$

Hence $\dot{Q} = 0$ is equivalent to

$$\tilde{p}_1 \equiv \tilde{p}_2 \equiv \cdots \equiv \tilde{p}_N = 0,$$

which occurs only when

$$p_1 \equiv p_2 \equiv \cdots \equiv p_N \equiv p_\gamma. \quad (6.43)$$

This proves part (ii).

It follows from the control protocol (6.32) and the symmetry of ψ_α and $A(t)$ that

$$\begin{aligned} \bar{u} &= \frac{\sum_{i=1}^N u_i}{N} \\ &= f_\gamma(q_\gamma, p_\gamma) - \frac{1}{N} \sum_{i=1}^N \left(\sum_{j \in \mathcal{N}_i(t)} \nabla_{q_i} \psi_\alpha(\|q_j - q_i\|_\sigma) \right. \\ &\quad \left. + \sum_{j \in \mathcal{N}_i(t)} a_{ij}(q)(p_i - p_j) + c_1(q_i - q_\gamma) + c_2(p_i - p_\gamma) \right) \\ &= f_\gamma(q_\gamma, p_\gamma) - c_1(\bar{q} - q_\gamma) - c_2(\bar{p} - p_\gamma), \end{aligned}$$

which in turn implies that

$$\begin{cases} \dot{\bar{q}} = \bar{p}, \\ \dot{\bar{p}} = \dot{p}_\gamma - c_1(\bar{q} - q_\gamma) - c_2(\bar{p} - p_\gamma). \end{cases} \quad (6.44)$$

The solution of (6.44) can be obtained in three separate cases. For $c_2^2 > 4c_1$,

$$\left\{ \begin{array}{l} \bar{q}(t) = q_\gamma(t) - \frac{1}{\sqrt{c_2^2 - 4c_1}}(\bar{p}(0) - p_\gamma(0)) \\ \quad + \frac{c_2 - \sqrt{c_2^2 - 4c_1}}{2}(\bar{q}(0) - q_\gamma(0))e^{-\frac{c_2 - \sqrt{c_2^2 - 4c_1}}{2}t} \\ \quad + \frac{1}{\sqrt{c_2^2 - 4c_1}}(\bar{p}(0) - p_\gamma(0)) \\ \quad + \frac{c_2 + \sqrt{c_2^2 - 4c_1}}{2}(\bar{q}(0) - q_\gamma(0))e^{-\frac{c_2 + \sqrt{c_2^2 - 4c_1}}{2}t}, \\ \bar{p}(t) = p_\gamma(t) + \frac{c_2 + \sqrt{c_2^2 - 4c_1}}{2\sqrt{c_2^2 - 4c_1}}(\bar{p}(0) - p_\gamma(0)) \\ \quad + \frac{c_2 - \sqrt{c_2^2 - 4c_1}}{2}(\bar{q}(0) - q_\gamma(0))e^{-\frac{c_2 - \sqrt{c_2^2 - 4c_1}}{2}t} \\ \quad + \frac{-c_2 + \sqrt{c_2^2 - 4c_1}}{2\sqrt{c_2^2 - 4c_1}}(\bar{p}(0) - p_\gamma(0)) \\ \quad + \frac{c_2 + \sqrt{c_2^2 - 4c_1}}{2}(\bar{q}(0) - q_\gamma(0))e^{-\frac{c_2 + \sqrt{c_2^2 - 4c_1}}{2}t}, \end{array} \right. \quad (6.45)$$

for $c_2^2 = 4c_1$,

$$\left\{ \begin{array}{l} \bar{q}(t) = q_\gamma(t) + (\bar{q}(0) - q_\gamma(0) + (\bar{p}(0) - p_\gamma(0) + \frac{2c_1}{c_2}(\bar{q}(0) - q_\gamma(0)))t)e^{-\frac{c_2}{2}t}, \\ \bar{p}(t) = p_\gamma(t) + (\bar{p}(0) - p_\gamma(0) + (-\frac{c_2}{2}(\bar{p}(0) - p_\gamma(0)) - c_1(\bar{q}(0) \\ \quad - q_\gamma(0)))t)e^{-\frac{c_2}{2}t}, \end{array} \right. \quad (6.46)$$

and for $c_2^2 < 4c_1$,

$$\left\{ \begin{array}{l} \bar{q}(t) = q_\gamma(t) + ((\bar{q}(0) - q_\gamma(0)) \cos \frac{\sqrt{4c_1 - c_2^2}}{2}t + \frac{2}{\sqrt{4c_1 - c_2^2}}(\frac{c_2}{2}(\bar{q}(0) - q_\gamma(0)) \\ \quad + \bar{p}(0) - p_\gamma(0)) \sin \frac{\sqrt{4c_1 - c_2^2}}{2}t)e^{-\frac{c_2}{2}t}, \\ \bar{p}(t) = p_\gamma(t) + ((\bar{p}(0) - p_\gamma(0)) \cos \frac{\sqrt{4c_1 - c_2^2}}{2}t - (\frac{\sqrt{4c_1 - c_2^2}}{2}(\bar{q}(0) - q_\gamma(0)) \\ \quad + \frac{2}{\sqrt{4c_1 - c_2^2}}(\frac{c_2}{2}(\bar{q}(0) - q_\gamma(0)) + \bar{p}(0) - p_\gamma(0))) \sin \frac{\sqrt{4c_1 - c_2^2}}{2}t)e^{-\frac{c_2}{2}t}, \end{array} \right. \quad (6.47)$$

where $\bar{q}(0)$ and $\bar{p}(0)$ are the initial position and velocity of the COM of the group, and $q_\gamma(0)$ and $p_\gamma(0)$ are the initial position and velocity of the virtual leader. The solution (6.45)–(6.47) indicates that, if $\bar{q}(0) = q_\gamma(0)$ and $\bar{p}(0) = p_\gamma(0)$, then the position and velocity of the COM will be equal to those of the virtual leader for all

$t \geq 0$, otherwise they will converge exponentially to those of the virtual leader with a time constant of $\frac{c_2}{2}$ when $c_2^2 \leq 4c_1$, or $\frac{c_2 - \sqrt{c_2^2 - 4c_1}}{2}$ when $c_2^2 > 4c_1$.

We now prove part (iv) of Theorem 6.2. From (6.43), we see that, in steady state,

$$\dot{p}_1 = \dot{p}_2 = \cdots = \dot{p}_N = \dot{p}_\gamma = f_\gamma(q_\gamma, p_\gamma),$$

which implies that $u_i = f_\gamma(q_\gamma, p_\gamma)$. It thus follows from (6.36) and (6.39) that

$$\nabla_q \left(\frac{1}{2} \sum_{i=1}^N U_i(q) \right) = 0. \quad (6.48)$$

Thus, the configuration converges asymptotically to a fixed configuration that is an extremum of $\frac{1}{2} \sum_{i=1}^N U_i(q)$. If the solution of (6.48) starts at the an equilibrium, which is a local maximum or a saddle point, the solution will be invariant for all time. Then, not all solutions of (6.48) converge to local minima. However, anything but a local minimum is an unstable equilibrium [29]. Thus, almost every configuration the system approaches is a local minimum of the total artificial potential energy $\frac{1}{2} \sum_{i=1}^N U_i(q)$.

Finally, we prove part (v) of Theorem 6.2. From the earlier analysis, we recall that $Q \leq Q_0$. The results then follow the same arguments as used in the proof of part (v) of Theorem 6.1. This completes the proof of Theorem 6.2.

6.5 Simulation Study

6.5.1 Flocking with a Fraction of Informed Agents

Simulation was performed on 100 agents moving in a 2-dimensional space under the influence of the control protocol (6.6). Initial positions and initial velocities of the 100 agents were chosen randomly from the boxes $[0, 55] \times [0, 55]$ and $[0, 0.01] \times [0, 0.01]$, respectively, and the initial position and velocity of the virtual leader were set at $q_\gamma(0) = [10, 10]^T$ and $p_\gamma(0) = [1, 1]^T$. The influencing/sensing radius was chosen as $r = 4$, the desired distance $d = 3.3$, $\varepsilon = 0.1$ for the σ -norm, $h = 0.9$ for the bump function $\rho_h(\cdot)$, and $c_1 = c_2 = 0.5$.

Some simulation results are shown in Fig. 6.2. In the figure, the solid lines represent the neighboring relations, the solid lines with arrows represent the velocities, and the hexagram represents the desired position, which is where the virtual leader is. There are ten informed agents which are chosen randomly from the group and marked with circles. Figure 6.2(a) shows the group initial state which is highly disconnected. As time evolves, the size of the largest cluster increases and more and more agents move with the same velocity. Eventually, 86 of the 100 agents move with the desired velocity (see plot (f)).

To further substantiate the results shown in Fig. 6.2, we ran extensive simulations on groups of different size N . In order for the comparison to be reasonable, initial positions of the agents were chosen randomly from the $[0, L] \times [0, L]$ box so that the

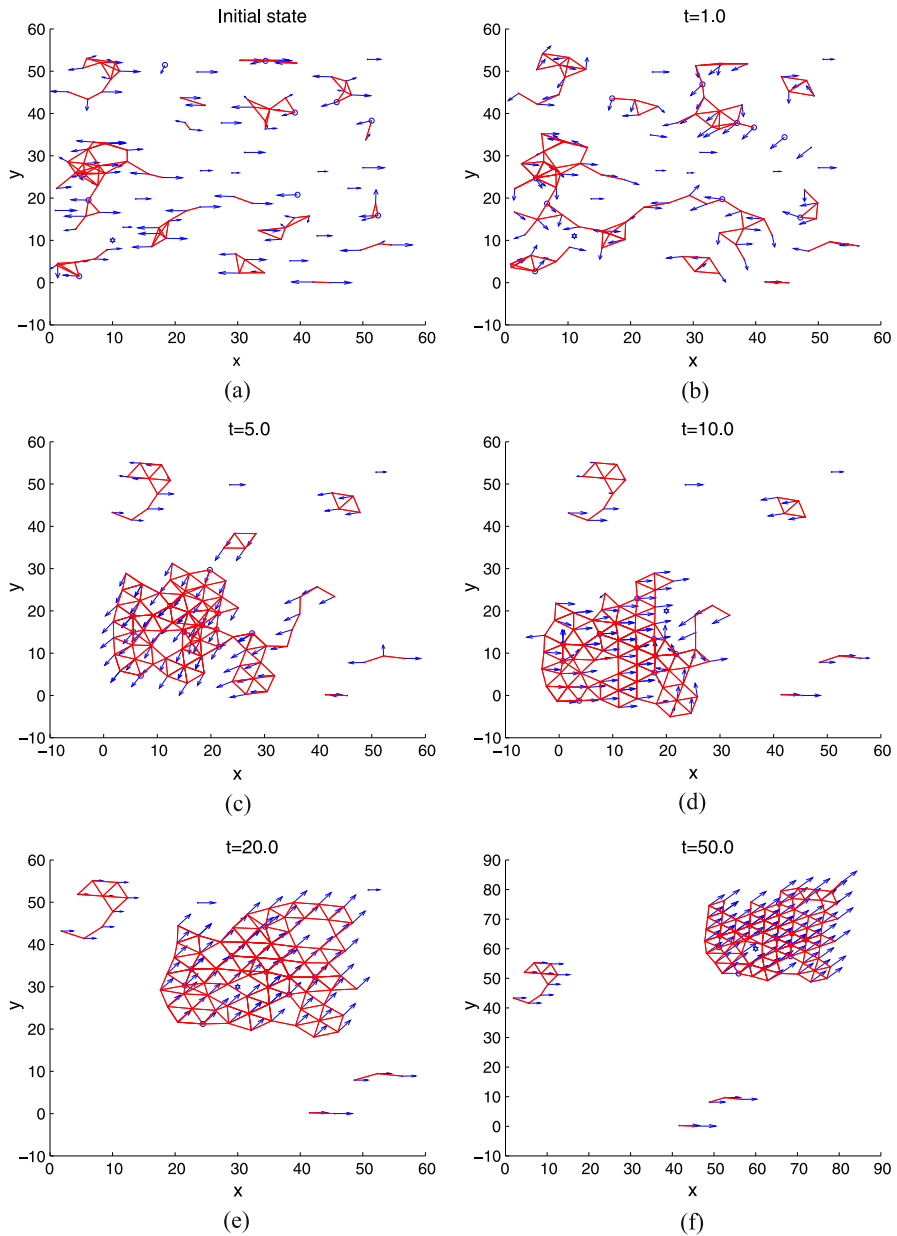
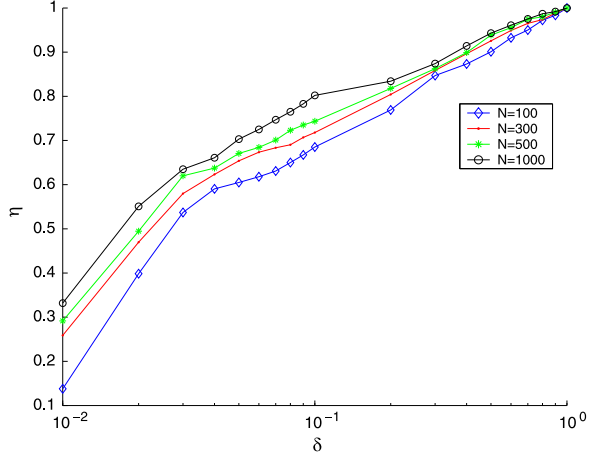


Fig. 6.2 [31] 2-D flocking for 100 agents applying algorithm (6.6) with 10 informed agents

density is fixed at $\rho = N/L^2 = 0.05$. Initial velocities of the N agents were chosen randomly from $[0, 4] \times [0, 4]$, and the initial position and velocity of the virtual leader were set at $q_\gamma(0) = [10, 10]^T$ and $p_\gamma(0) = [3, 3]^T$. The influencing/sensing

Fig. 6.3 [31] Fraction of agents with the desired velocity as a function of informed agents. All estimates are the results of averaging over 50 realizations



radius was set at $r = 3$, the desired distance $d = 2.5$, $\varepsilon = 0.1$ for the σ -norm, $h = 0.2$ for the bump function $\rho_h(\cdot)$, and $c_1 = c_2 = 0.5$.

We randomly select a fraction δ of the N agents as the informed agents. Figure 6.3 shows the relationship between the fraction η of the agents that eventually move with the desired velocity and the fraction δ of the informed agents with $N = 100, 300, 500$, and 1000 , respectively. All estimates are the results of averaging over 50 realizations. Obviously, for any given group size N , the fraction η of agents that move with the desired velocity is an increasing function of the fraction δ of informed agents. Furthermore, the larger the group, the smaller the fraction δ of informed agents is needed to guide the group with a given fraction η . For example, in order for 80 % of the agents to move with the same desired velocity, about 27 % of the agents should be informed agents when the group size is $N = 100$, but only about 10 % of the agents need to be the informed agents when the group has $N = 1000$ agents. Thus, for sufficiently large groups, only a very small fraction of informed agents will guide most agents in the group.

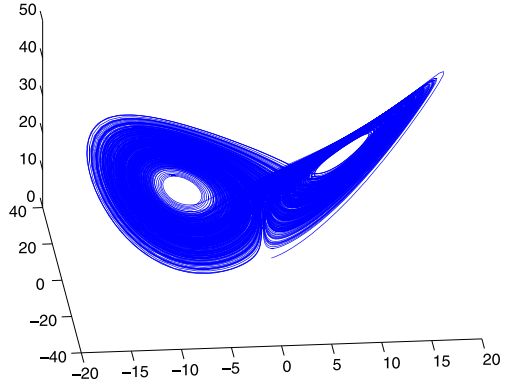
6.5.2 Flocking with a Virtual Leader of Varying Velocity

Simulations for protocol (6.5) (Algorithm 2 in [29]) and protocol (6.32) were performed with ten agents moving in a 3-dimensional space, and a virtual leader whose acceleration function $f_\gamma(q_\gamma, p_\gamma)$ satisfies the Lorenz equation (see Fig. 6.4),

$$\begin{cases} \dot{p}_{\gamma x} = 10(p_{\gamma y} - p_{\gamma x}), \\ \dot{p}_{\gamma y} = 28p_{\gamma x} - p_{\gamma x}p_{\gamma z} - p_{\gamma y}, \\ \dot{p}_{\gamma z} = p_{\gamma x}p_{\gamma y} - \frac{8}{3}p_{\gamma z}. \end{cases}$$

Simulation results are shown in Figs. 6.5 and 6.6. In the simulation, initial positions and velocities of the ten agents were chosen randomly from the same cube

Fig. 6.4 [31] The attractor of Lorenz system



$[0, 15] \times [0, 15] \times [0, 15]$, and the initial position and velocity of the virtual leader were set at $q_\gamma(0) = [10, 10, 10]^T$ and $p_\gamma(0) = [3, 3, 3]^T$. The influencing/sensing radius was chosen at $r = 4.8$, the desired distance $d = 4$, $\varepsilon = 0.1$ for the σ -norm, $h = 0.2$ for the bump function $\rho_h(\cdot)$, and $c_1 = c_2 = 0.5$. The solid lines in the figures represent the neighboring relations, the dotted lines with arrows represent the agent velocities, and the hexagram represents the desired position. In both Figs. 6.5 and 6.6, plot (a) shows the initial states of the agents; plot (b) presents the configuration and velocities of the group of agents at $t = 30$ seconds; plot (c) depicts the motion trajectories of all agents from $t = 0$ to 30 seconds; plot (d) shows the convergence of velocity, from which we can see that all the agents eventually achieve the same velocity; plots (e) and (f) depict the position and velocity difference between the COM and the desired position $q_\gamma(t)$ and velocity $p_\gamma(t)$, respectively.

It is obvious from Figs. 6.5 and 6.6 that both control protocols (6.5) and (6.32) are capable of achieving stable flocking motion. Under the protocol (6.5), the position and velocity of the COM fluctuate around those of the virtual leader (see Fig. 6.5, plots (e) and (f)). However, under the protocol (6.32), the position and velocity of the COM converge exponentially to those of the virtual leader (see Fig. 6.6, plots (e) and (f)).

6.5.3 Flocking with a Fraction of Informed Agents and a Virtual Leader of Varying Velocity

This section presents simulation results for the situation when only a fraction of agents are informed agent and in the same time, the velocity of the virtual leader is varying with time. The control protocol for agent i is naturally chosen as

$$u_i = - \sum_{j \in \mathcal{N}_i(t)} \nabla_{q_i} \psi_\alpha(\|q_j - q_i\|_\sigma) - \sum_{j \in \mathcal{N}_i(t)} a_{ij}(p_i - p_j) + h_i[f_\gamma(q_\gamma, p_\gamma) + c_1(q_\gamma - q_i) + c_2(p_\gamma - p_i)], \quad (6.49)$$

where $h_i = 1$ if agent i is an informed agent, and $h_i = 0$ otherwise. Simulation results are shown in Fig. 6.7. In the simulation, the acceleration vector of the virtual

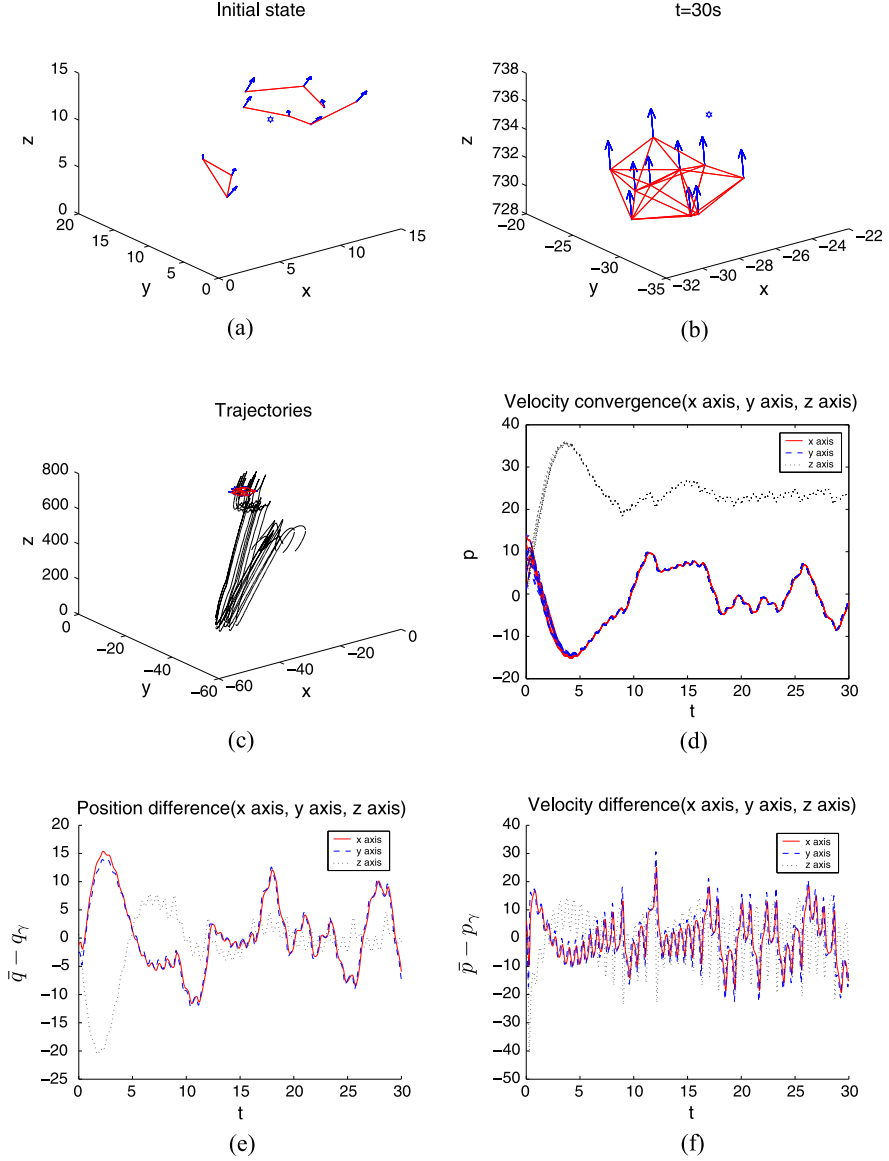


Fig. 6.5 [31] 3-D flocking for 10 agents applying algorithm 2 in [29]

leader was selected as $f_\gamma = [-0.3, 0.3]^T$ and all other parameters were chosen the as those in the simulation shown in Fig. 6.2. Plot (a) shows the group initial state, which is highly disconnected. As time evolves, the size of the largest cluster increases and more and more agents move with the same velocity. Finally, 89 agents move with the desired velocity (see plot (f)).

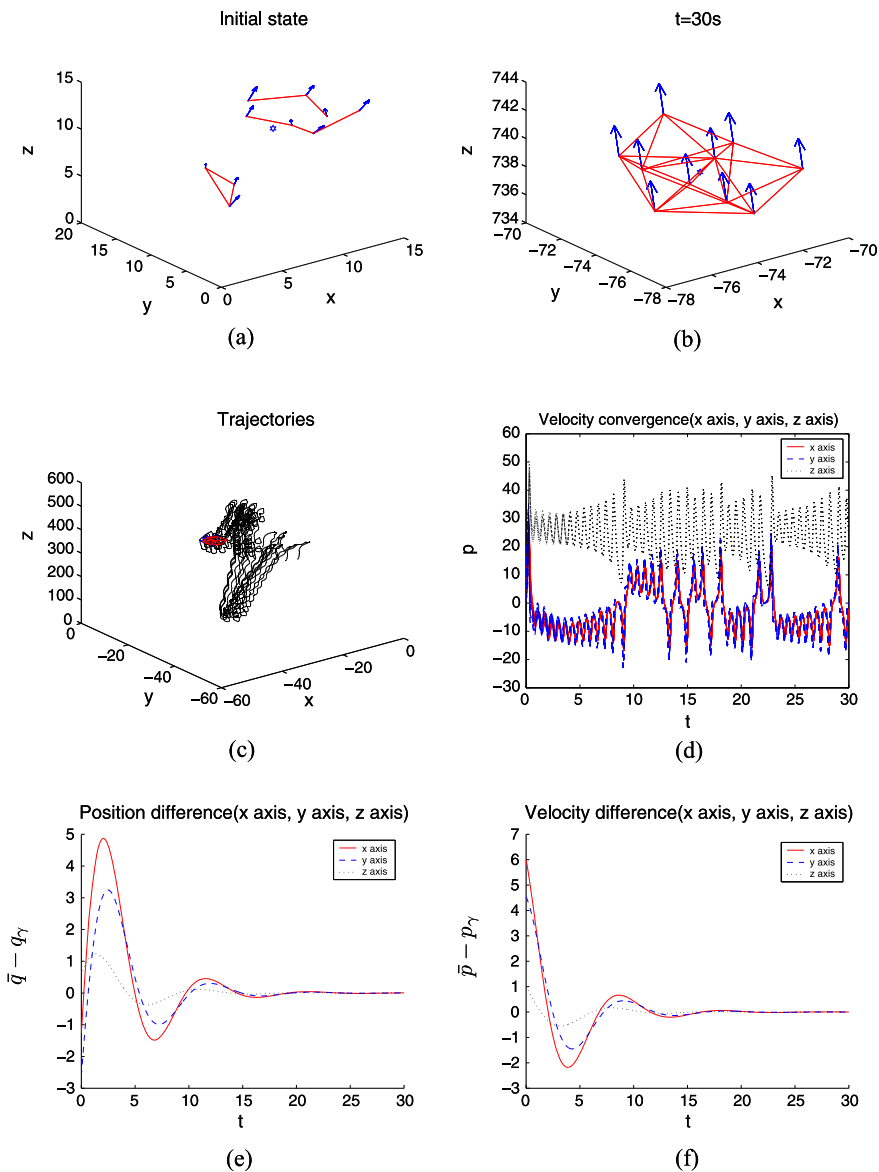


Fig. 6.6 [31] 3-D flocking for 10 agents applying algorithm (6.32)

6.6 Conclusions and Notes

In this chapter, a flocking algorithm proposed by Olfati-Saber for a group of agents to track a virtual leader is extended in two directions. First, the flocking algorithm is generalized to the case that only a fraction of agents are informed agents. We estab-

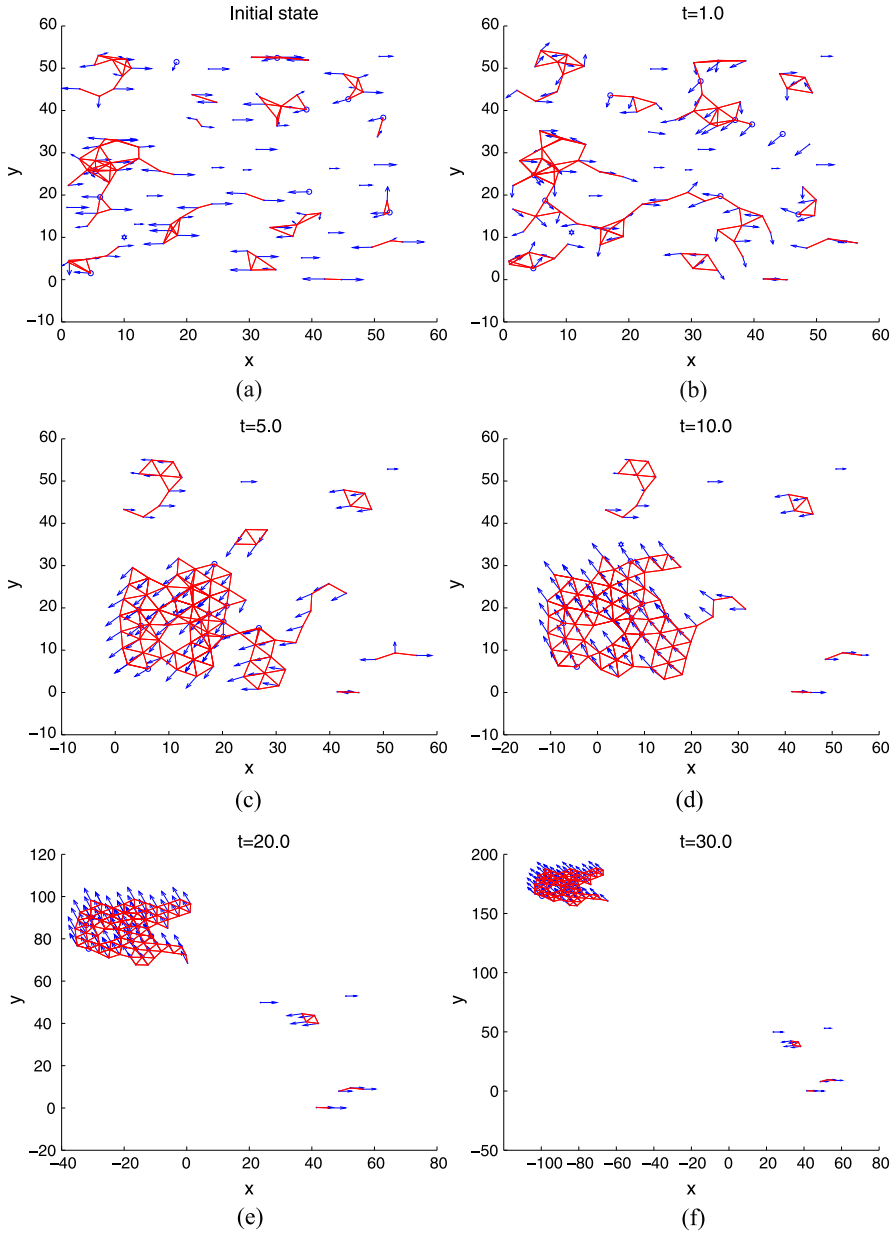


Fig. 6.7 [31] 2-D flocking for 100 agents with 10 informed agents and a virtual leader of varying velocity

lished that all the informed agents will move with the desired velocity. Furthermore, if an uninformed agent can be influenced by the informed agents from time to time

during the evolution, this uninformed agent will also move with the desired velocity. We demonstrate numerically that a very small proportion of informed agents can make most of agents move with the desired velocity, and the larger the group, the higher the proportion of agents that will eventually move with the desired velocity. Second, we modified the algorithm for a group of agents in order to track a virtual leader of varying velocity. Moreover, we established that the position and velocity of the COM will converge exponentially to those of virtual leader. The convergent rate was also given. See [35] for flocking with both a virtual leader of varying velocity and a minority of informed agents via a variable structure approach.

References

1. Shaw E (1975) Fish in schools. *Nat Hist* 84:40–45
2. Okubo A (1986) Dynamical aspects of animal grouping: swarms, schools, flocks and herds. *Adv Biophys* 22:1–94
3. Reynolds CW (1987) Flocks, herds, and schools: a distributed behavioral model. *Comput Graph* 21:25–34
4. Vicsek T, Cziro'ok A, Ben-Jacob E, Cohen O, Shochet I (1995) Novel type of phase transition in a system of self-driven particles. *Phys Rev Lett* 75:1226–1229
5. Levine H, Rappel WJ (2001) Self organization in systems of self-propelled particles. *Phys Rev E* 63:208–211
6. Shimoyama N, Sugawara K, Mizuguchi T, Hayakawa Y, Sano M (1996) Collective motion in a system of motile elements. *Phys Rev Lett* 76:3870–3873
7. Mogilner A, Edelstein-Keshet L (1996) Spatio-temporal order in populations of self-aligning objects: formation of oriented patches. *Physica D* 89:346–367
8. Mogilner A, Edelstein-Keshet L (1999) A non-local model for a swarm. *J Math Biol* 38:534–570
9. Toner J, Tu Y (1998) Flocks, herds, and schools: a quantitative theory of flocking. *Phys Rev E* 58:4828–4858
10. Toner J, Tu Y (2005) Hydrodynamics and phases of flocks. *Ann Phys* 318:170–244
11. Akylidiz I, Su W, Sankarasubramniam Y, Cayirci E (2002) A survey on sensor networks. *IEEE Commun Mag* 40:102–114
12. Crowther B (2003) Flocking of autonomous unmanned air vehicles. *Aeronaut J* 107:99–109
13. Balch T, Arkin RC (1998) Behavior-based formation control for multirobot teams. *IEEE Trans Robot Autom* 14:926–939
14. Olfati-Saber R, Murray RM (2004) Consensus problems in networks of agents with switching topology and time-delays. *IEEE Trans Autom Control* 49:1520–1533
15. Ren W, Beard RW (2005) Consensus seeking in multi-agent systems under dynamically changing interaction topologies. *IEEE Trans Autom Control* 50:655–661
16. Hong Y, Gao L, Cheng D, Hu J (2007) Lyapunov-based approach to multi-agent systems with switching jointly-connected interconnection. *IEEE Trans Autom Control* 52:943–948
17. Gazi V, Passino KM (2003) Stability analysis of swarms. *IEEE Trans Autom Control* 48:692–697
18. Liu Y, Passino KM, Polycarpou MM (2003) Stability analysis of M -dimensional asynchronous swarms with a fixed communication topology. *IEEE Trans Autom Control* 48:76–95
19. Khatib O (1986) Real-time obstacle avoidance for manipulators and mobile robots. *Int J Robot Res* 5:90–98
20. Tanner H (2004) Flocking with obstacle avoidance in switching networks of interconnected vehicles. In: *IEEE international conference robotics and automation*, pp 3006–3011

21. Olfati-Saber R, Murray RM (2003) Flocking with obstacle avoidance: cooperation with limited communication in mobile networks. In: Proc of the 42nd IEEE conference on decision and control, pp 2022–2028
22. Chang DE, Shadden S, Marsden J, Olfati-Saber R (2003) Collision avoidance for multiple agent systems. In: Proc of the 42nd IEEE conference on decision and control, pp 539–543
23. Jadbabaie A, Lin J, Morse AS (2003) Coordination of groups of mobile agents using nearest neighbor rules. *IEEE Trans Autom Control* 48:988–1001
24. Shi H, Wang L, Chu TG (2006) Virtual leader approach to coordinated control of multiple mobile agents with asymmetric interactions. *Physica D* 213:51–65
25. Ogren P (2002) Formation with a mission: stable coordination of vehicle group maneuvers. In: Symposium on mathematical theory of network and systems, pp 1–22
26. Leonard N, Frierelli E (2001) Virtual leaders, artificial potentials and coordinated control of groups. In: Proc of the 40th IEEE conference on decision and control, pp 2968–2973
27. Tanner HG, Jadbabaie A, Pappas GJ (2003) Stable flocking of mobile agents, part I: fixed topology. In: Proc of the 42nd IEEE conference on decision and control, pp 2010–2015
28. Tanner HG, Jadbabaie A, Pappas GJ (2003) Stable flocking of mobile agents, part II: dynamic topology. In: Proc of the 42nd IEEE conference on decision and control, pp 2016–2021
29. Olfati-Saber R (2006) Flocking for multi-agent dynamic systems: algorithms and theory. *IEEE Trans Autom Control* 51:401–420
30. Couzin ID, Krause J, Franks NR, Levin SA (2005) Effective leadership and decision-making in animal groups on the move. *Nature* 433:513–516
31. Su H, Wang X, Lin Z (2009) Flocking of multi-agents with a virtual leader. *IEEE Trans Autom Control* 54:293–307
32. Godsil C, Royle G (2001) Algebraic graph theory. Graduate texts in mathematics, vol 207. Springer, New York
33. Horn RA, Johnson CR (1987) Matrix analysis. Cambridge University Press, Cambridge
34. Khalil HK (2002) Nonlinear systems, 3rd edn. Prentice Hall, Upper Saddle River
35. Cao Y, Ren W (2012) Distributed coordinated tracking with reduced interaction via a variable structure approach. *IEEE Trans Autom Control* 57:33–48

Chapter 7

Distributed Pinning-Controlled Flocking with Preserved Network Connectivity

Abstract This chapter introduces distributed pinning-controlled flocking of multi-agent systems with preserved network connectivity. Most existing flocking algorithms rely on information about both relative position and relative velocity among neighboring agents. We first propose a connectivity-preserving flocking algorithm for multi-agent systems based only on position measurements. Under the assumption that the initial interactive network is connected, the flocking algorithm not only can steer a group of agents to a stable flocking motion, but also can preserve the connectivity of the interactive network during the dynamical evolution. Moreover, we investigate the flocking algorithm with a virtual leader and show that all agents can asymptotically attain a desired velocity even if only one agent in the team has access to the information of the virtual leader. We then investigate the flocking problem of multiple nonlinear dynamical mobile agents with a virtual leader in a dynamic proximity network. We assume that only a fraction of agents in the network are informed and propose a connectivity-preserving flocking algorithm. Under the assumption that the initial network is connected, we introduce local adaptation strategies for both the weights on the velocity navigational feedback and the coupling strengths that enable all agents to track the virtual leader, without requiring the knowledge of the agent dynamics. The resulting flocking algorithm works even for the case where only one agent is informed.

Keywords Flocking · Network connectivity · Nonlinear dynamics · Multi-agent systems

7.1 Flocking Based only on Position Measurements

Existing flocking algorithms rely on information about both the relative position and the relative velocity information among neighboring agents. However, not all the agents (robots, air vehicles, manipulators, and so on) in practice are equipped with speed sensors. Furthermore, an algorithm using only position measurements has the advantage of decreasing equipment cost and network traffic. In this chapter, therefore, we study the flocking problem based only on position measurements. We modify the passivity approach in [1–3] and use it for the proposed flocking algorithm to produce an output vector, which can replace the roles of the velocity.

Our proposed control input has the same function as that in [3] while a nonlinear gradient-based term is used to replace the linear one in [3]. Moreover, we extend the results in [3] to the case of switching topology. In addition, we propose two rules that a potential function should obey in order to preserve the connectivity of the network as long as the initial network is connected. We prove the global asymptotic stability by applying the LaSalle Invariance Principle. Furthermore, we investigate the flocking algorithm with a virtual leader and show that all agents can asymptotically attain the desired velocity even if only one agent in the team has access to the information of the virtual leader.

7.1.1 Background and Problem Statement

We consider N agents moving in an n -dimensional Euclidean space. The motion of each agent is described by a double-integrator system of the form

$$\begin{aligned}\dot{q}_i &= p_i, \\ \dot{p}_i &= u_i, \quad i = 1, \dots, N,\end{aligned}\tag{7.1}$$

where $q_i \in \mathbf{R}^n$ is the position vector of agent i , $p_i \in \mathbf{R}^n$ is its velocity vector and $u_i \in \mathbf{R}^n$ is the (force) control input acting on agent i .

Our objective is to design control inputs $u_i \in \mathbf{R}^n$ so that all agents move with a common velocity while avoiding collisions among agents based only on position measurements, under the assumption that the initial network is connected in the usual sense of a connected graph. In the situation that there is a virtual leader in the group of agents, the flocking algorithm should be designed to enable all agents to asymptotically track the virtual leader, in the sense that all agents asymptotically move with the same velocity as the virtual leader.

7.1.2 Fundamental Flocking Algorithm

Motivated by the flocking algorithms developed in [4–6] and the passivity approach used in [1–3], we present a new flocking algorithm using only position measurements, which is described as follows:

$$\begin{cases} u_i = -\sum_{j \in N_i(t)} (\nabla_{q_i} \psi(\|q_{ij}\|) - w_{ij}(y_i - y_j)), \\ y_i = PT\hat{x}_i + P \sum_{j \in N_i(t)} w_{ij}q_{ij}, \\ \dot{\hat{x}}_i = T\hat{x}_i + \sum_{j \in N_i(t)} w_{ij}q_{ij}, \end{cases}\tag{7.2}$$

where $\hat{x}_i, y_i \in \mathbf{R}^n$, $y = [y_1^T, \dots, y_N^T]^T$, $q_{ij} = q_i - q_j$, $T \in \mathbf{R}^{n \times n}$ is a Hurwitz matrix, $P \in \mathbf{R}^{n \times n}$ is a symmetric positive-definite matrix such that $T^T P + PT = -Q$ is a symmetric positive-definite matrix, the constant $w_{ij} = w_{ji} > 0$ for all $i, j \in V$, ∇

is the gradient operator, $\psi(\cdot)$ is a potential function to be specified below in (7.4), $N_i(t)$ is the neighborhood of agent i at time t which is the same as that in Sect. 4.2, and

$$N_i(t) = \{j \mid \sigma(i, j)[t] = 1, j \neq i, j = 1, \dots, N\}. \quad (7.3)$$

In the proposed flocking algorithm (7.2), the output vector y is produced by distributed filters based only on relative position measurements. The gradient-based term of control input u_i is responsible for collision avoidance and for maintaining the connectivity of the network. Every output vector, which regulates the velocity of each agent, tends to zero if all agents attain a common velocity. Note that the form of the proposed control input is not the same as that in [3]. The control input in [3] cannot perform the function in this chapter, even if the linear gradient-based term in [3] is replaced by the proposed nonlinear one in this chapter. This is because the negative semi-definiteness of the derivative of the Lyapunov function relies on the linear property of gradient-based term. However, our proposed control input has the same function as that in [3] when the proposed nonlinear gradient-based term is reduced to the linear one in [3].

The nonnegative potential $\psi(\|q_{ij}\|)$ is a function of the distance $\|q_{ij}\|$ between agent i and agent j , which is differentiable for $\|q_{ij}\| \in (0, r)$, satisfying

- (i) $\psi(\|q_{ij}\|) \rightarrow \infty$ as $\|q_{ij}\| \rightarrow 0$ or $\|q_{ij}\| \rightarrow r$.
- (ii) $\psi(\|q_{ij}\|)$ attains its unique minimum when $\|q_{ij}\|$ equals a desired distance.

The main difference between the potential function $\psi(\|q_{ij}\|)$ here and the potential function in [5] is that $\psi(\|q_{ij}\|)$ tends to infinity when the distance between agent i and agent j tends to r . This property can guarantee that no initial connections will be lost. Note that the potential function in [6] is an example which satisfies the above definition of the potential function $\psi(\|q_{ij}\|)$. Another example is as follows (see Fig. 7.1):

$$\psi(\|q_{ij}\|) = \begin{cases} +\infty, & \|q_{ij}\| = 0, \\ \frac{r}{\|q_{ij}\|(r-\|q_{ij}\|)}, & \|q_{ij}\| \in (0, r), \\ +\infty & \|q_{ij}\| = r. \end{cases} \quad (7.4)$$

The adjacency matrix $A(t)$ of a graph $G(t)$ is defined as

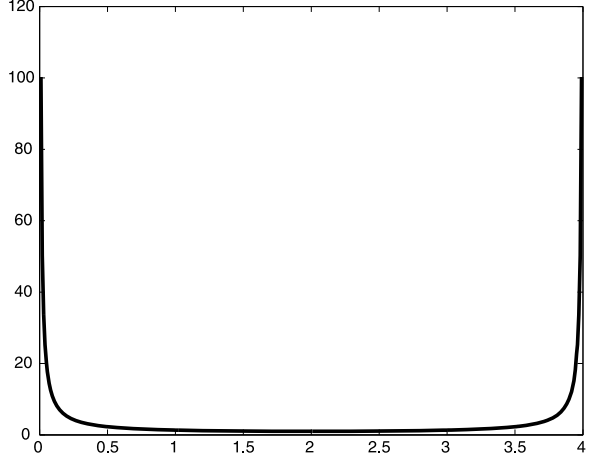
$$a_{ij}(t) = \begin{cases} w_{ij}, & (i, j) \in E(t), \\ 0, & \text{otherwise.} \end{cases} \quad (7.5)$$

The energy function for the system is defined as follows:

$$W = \frac{1}{2} \sum_{i=1}^N \left(\sum_{j \in N_i(t)} \psi(\|q_{ij}\|) + p_i^T p_i \right) + \frac{1}{2} \dot{\hat{x}}^T (I_N \otimes P) \dot{\hat{x}}. \quad (7.6)$$

Clearly, $W = W(\hat{q}(t), p(t), \hat{x}(t)) = W(t)$ is a positive semi-definite function, where $\hat{q} = [q_{11}^T, \dots, q_{1N}^T, \dots, q_{N1}^T, \dots, q_{NN}^T]^T$ and $\hat{x} = [\hat{x}_1^T, \dots, \hat{x}_N^T]^T$. We state the main result in the following.

Fig. 7.1 [7] An example of the potential function $\psi(\|q_{ij}\|)$



Theorem 7.1 Consider a system of N mobile agents with dynamics (7.1), each being steered by protocol (7.2). Suppose that the initial network $G(0)$ is connected and the initial energy $W_0 = W(\hat{q}(0), p(0), \hat{x}(0))$ is finite. Then, the following hold:

- (i) $G(t)$ will remain connected for all $t \geq 0$.
- (ii) All agents asymptotically move with the same velocity.
- (iii) Almost every final configuration locally minimizes each agent's global potential $\sum_{j \in N_i(t)} \nabla_{q_i} \psi(\|q_{ij}\|)$.
- (iv) Collisions between the agents are avoided.

Proof Proof of part (i)

Assume that $G(t)$ switches at time t_k ($k = 1, 2, \dots$), which implies that $G(t)$ is a fixed graph in each time-interval $[t_{k-1}, t_k)$. Note that W_0 is finite and the time derivative of $W(t)$ in $[t_0, t_1)$ is

$$\begin{aligned}
 \dot{W}(t) &= \frac{1}{2} \sum_{i=1}^N \sum_{j \in N_i} \dot{\psi}(\|q_{ij}\|) + \sum_{i=1}^N p_i^T u_i + \frac{1}{2} \ddot{x}^T (I_N \otimes P) \dot{x} + \frac{1}{2} \dot{x}^T (I_N \otimes P) \ddot{x} \\
 &= \sum_{i=1}^N p_i^T \sum_{j \in N_i} \nabla_{q_i} \psi(\|q_{ij}\|) \\
 &\quad - \sum_{i=1}^N p_i^T \left(\sum_{j \in N_i(t)} \nabla_{q_i} \psi(\|q_{ij}\|) + \sum_{j \in N_i(t)} w_{ij} (y_i - y_j) \right) \\
 &\quad + \frac{1}{2} \dot{x}^T (I_N \otimes T^T) (I_N \otimes P) \dot{x} + \frac{1}{2} p^T (L^T \otimes I_n) (I_N \otimes P) \dot{x} \\
 &\quad + \frac{1}{2} \dot{x}^T (I_N \otimes P) (I_N \otimes T) \dot{x} + \frac{1}{2} \dot{x}^T (I_N \otimes P) (L \otimes I_n) p
 \end{aligned}$$

$$\begin{aligned}
&= -p^T(L \otimes I_n)y + p^T(L \otimes I_n)(I_N \otimes P)\dot{\hat{x}} - \frac{1}{2}\dot{\hat{x}}^T(I_N \otimes Q)\dot{\hat{x}} \\
&= -\frac{1}{2}\dot{\hat{x}}^T(I_N \otimes Q)\dot{\hat{x}} \leq 0,
\end{aligned} \tag{7.7}$$

where $p = [p_1^T, \dots, p_N^T]^T$ and \otimes stands for the Kronecker product, which implies that

$$W(t) \leq W_0 < \infty \quad \text{for } t \in [t_0, t_1).$$

From the definition of the potential function, we have $\lim_{\|q_{ij}(t)\| \rightarrow r} \psi(\|q_{ij}(t)\|) = \infty$. Therefore, no distance of existing edges will tend to r for $t \in [t_0, t_1)$, which also implies that no existing edges will be lost before time t_1 . Hence, new edges must be added in the interaction network at switching time t_1 . Note that the hysteresis ensures that if a finite number of links are added to $G(t)$, then the associated potentials remains to be finite. Thus, $W(t_1)$ is finite.

Similar to the above analysis, the time derivative of $W(t)$ in every $[t_{k-1}, t_k)$ is

$$\dot{W}(t) = -\frac{1}{2}\dot{\hat{x}}^T(I_N \otimes Q)\dot{\hat{x}} \leq 0, \tag{7.8}$$

which implies that

$$W(t) \leq W(t_{k-1}) < \infty \quad \text{for } t \in [t_{k-1}, t_k), \quad k = 1, 2, \dots \tag{7.9}$$

Therefore, no distance of existing edges will tend to r for $t \in [t_{k-1}, t_k)$, which also implies that no edges will be lost before time t_k and $W(t_k)$ is finite.

Since $G(0)$ is connected and no edges in $E(0)$ was lost, $G(t)$ will remain to be connected for all $t \geq 0$.

Proof of parts (ii) and (iii)

Assume that m_k new edges are added to the network at time t_k . Clearly, we have

$$0 < m_k \leq \frac{N(N-1)}{2} - (N-1) \triangleq M.$$

From (7.6) and (7.9), we have $W(t_k) \leq W_0 + (m_1 + \dots + m_k)\psi(\|r - \varepsilon\|)$. Since there are at most M new edges that can be added to $G(t)$, we have $k \leq M$, $m_1 + \dots + m_k \leq M$ and $W(t) \leq W_0 + M\psi(\|r - \varepsilon\|) \triangleq W_{\max}$ for all $t \geq 0$. Therefore, the number of switching times k of the system (7.1) is finite, which implies the interaction network $G(t)$ eventually becomes fixed. Thus, the rest discussions can be restricted on the time interval (t_k, ∞) . Note that the distance of edge is not longer than $\max\{\psi^{-1}(W_{\max})\}$, or not shorter than $\min\{\psi^{-1}(W_{\max})\}$. Hence, the set

$$\Omega = \{\hat{q} \in D_g, p, \hat{x} \in \mathbf{R}^{Nn} \mid W(\hat{q}, p, \hat{x}) \leq W_{\max}\}, \tag{7.10}$$

is positively invariant on the time interval (t_k, ∞) , where

$$D_g = \{\hat{q} \in \mathbf{R}^{N^2n} \mid \|q_{ij}\| \in [\min\{\psi^{-1}(W_{\max})\}, \max\{\psi^{-1}(W_{\max})\}], \forall (i, j) \in E(t)\}.$$

Since $G(t)$ is connected for all $t \geq 0$, $\|q_{ij}\| \leq (N-1)r$ for any i and j . Because $W(t) \leq W_{\max}$, we have $p_i^T p_i \leq 2W_{\max}$ and $\lambda_{\max}(P)\hat{x}_i^T \hat{x}_i \leq 2W_{\max}$, where $\lambda_{\max}(P)$ is the largest eigenvalue of matrix P , which implies that \hat{x}_i from (7.2)

is also bounded. Therefore, the set Ω such that $W(t) \leq W_{\max}$ is closed and bounded, hence is compact. Note that system (7.1) with control input (7.2) is an autonomous system, at least on the concerned time interval (t_k, ∞) . It follows from LaSalle's invariance principle [8] that if the initial conditions of the system (7.1) lie in Ω , its trajectories will converge to the largest invariant set inside the region $S = \{\hat{q} \in D_g, p, \hat{x} \in \mathbf{R}^{Nn} \mid \dot{W} = 0\}$. From (7.8), $\dot{W} = 0$ if and only if $\dot{\hat{x}} = 0$, which implies that $\ddot{\hat{x}} = 0$. From (7.2), we have

$$\ddot{\hat{x}}_i = T \dot{\hat{x}}_i + \sum_{j \in N_i(t)} w_{ij}(p_i - p_j), \quad i = 1, \dots, N, \quad (7.11)$$

which implies that $(L \otimes I_n)p = 0$. Since the dynamic network is connected all the time, from the property of the Laplacian matrix $L \otimes I_n$ [9], p converges asymptotically to $1_N \otimes \beta$, for some constant vector $\beta \in \mathbf{R}^n$, which implies that $\|p_i - p_j\| \rightarrow 0$ for all i, j as $t \rightarrow \infty$.

Since $(L \otimes I_n)p = 0$, we have $(L \otimes I_n)u = 0$, which implies that $u = 1_N \otimes \alpha$, for some constant vector $\alpha \in \mathbf{R}^n$. From (7.2) and $\dot{\hat{x}} = 0$, we have $y = 0$, which implies that

$$u = - \begin{bmatrix} \sum_{j \in N_1(t)} \nabla_{q_1} \psi(\|q_{1j}\|) \\ \vdots \\ \sum_{j \in N_N(t)} \nabla_{q_N} \psi(\|q_{Nj}\|) \end{bmatrix}. \quad (7.12)$$

It follows from (7.12) and $\psi(\|q_{ij}\|) = \psi(\|q_{ji}\|)$ that

$$\begin{aligned} \nabla_{q_i} \psi(\|q_{ij}\|) &= -\nabla_{q_j} \psi(\|q_{ij}\|) = -\nabla_{q_j} \psi(\|q_{ji}\|), \\ \sum_{j \in N_1(t)} \nabla_{q_1} \psi(\|q_{1j}\|) + \dots + \sum_{j \in N_N(t)} \nabla_{q_N} \psi(\|q_{Nj}\|) &= 0, \\ (1_N \otimes \alpha)^T u &= 0, \end{aligned} \quad (7.13)$$

which implies that u is orthogonal to $1_N \otimes \alpha$. Since $u = \{1_N \otimes \alpha\} \cap \{1_N \otimes \alpha\}^\perp$, we have $u = 0$. From (7.12), we have

$$\begin{bmatrix} -\sum_{j \in N_1(t)} \nabla_{q_1} \psi(\|q_{1j}\|) \\ \vdots \\ -\sum_{j \in N_N(t)} \nabla_{q_N} \psi(\|q_{Nj}\|) \end{bmatrix} = 0. \quad (7.14)$$

Thus, the configuration converges asymptotically to a fixed configuration that is an extremum of all agent global potentials. If the solution of (7.14) starts at an equilibrium, which is a local maximum or saddle point, the solution will be invariant at all times. Then, not all solutions of (7.14) converge to local minima. However, every point but local minima is an unstable equilibrium [4]. Thus, almost every final configuration locally minimizes each agent's global potential $\sum_{j \in N_i(t)} \nabla_{q_i} \psi(\|q_{ij}\|)$.

Proof of part (iv)

In view of (7.10), $W(\hat{q}, p, \hat{x}) \leq W_{\max}$ for all $t \geq 0$. However, from the definition of potential function, we have $\lim_{\|q_{ij}\| \rightarrow 0} \psi(\|q_{ij}\|) = \infty$. Therefore, collisions among agents are avoided. \square

7.1.3 Flocking with a Virtual Leader

In this subsection, we investigate the flocking algorithm with a virtual leader. We assume that the virtual leader moves along a fixed direction with a constant velocity p_γ , which is the same as the investigation in [10]. We assume that only one agent is being informed about the virtual leader. This assumption is of practical value since it requires only one agent to know the global moving target. Certainly, the result can be generalized to the case with multiple informed agents [11]. The control input for agent i is designed as

$$\begin{cases} u_i = -\sum_{j \in N_i(t)} (\nabla_{q_i} \psi(\|q_{ij}\|) - w_{ij}(y_i - y_j)) - h_i y_i, \\ y_i = PT\hat{x}_i + P \sum_{j \in N_i(t)} w_{ij} q_{ij} + Ph_i(q_i - q_\gamma), \\ \dot{\hat{x}}_i = T\hat{x}_i + \sum_{j \in N_i(t)} w_{ij} q_{ij} + h_i(q_i - q_\gamma), \end{cases} \quad (7.15)$$

where q_γ is the position of the virtual leader. If agent i is the informed agent, then $h_i = 1$; otherwise, $h_i = 0$. Without loss of generality, we assume that the first agent is the informed agent, that is, $h_i = 1$ for $i = 1$ and $h_i = 0$ for all the others.

The energy function for the system is defined as follows:

$$U = \frac{1}{2} \sum_{i=1}^N \left(\sum_{j \in N_i(t)} \psi(\|q_{ij}\|) + (p_i - p_\gamma)^T (p_i - p_\gamma) \right) + \frac{1}{2} \dot{\hat{x}}^T (I_N \otimes P) \dot{\hat{x}}. \quad (7.16)$$

Clearly, $U = U(\hat{q}(t), p(t), \hat{x}(t)) = U(t)$ is a positive semi-definite function. Our second main result on tracking the virtual leader is stated in the following theorem.

Theorem 7.2 *Consider a system of N mobile agents with dynamics (7.1), each being steered by protocol (7.15). Suppose that the initial network $G(0)$ is connected and the initial energy $U_0 = U(\hat{q}(0), p(0), \hat{x}(0))$ is finite. Then, the following hold:*

- (i) $G(t)$ will remain to be connected for all $t \geq 0$.
- (ii) All agents asymptotically move with the desired velocity p_γ .
- (iii) almost every final configuration locally minimizes each agent's global potential $\sum_{j \in N_i(t)} \nabla_{q_i} \psi(\|q_{ij}\|)$.
- (iv) Collisions between the agents are avoided.

Proof We first prove part (i) of Theorem 7.2.

Denote the position difference vector and the velocity difference vector between agent i and the virtual leader as $\tilde{q}_i = q_i - q_\gamma$ and $\tilde{p}_i = p_i - p_\gamma$, respectively. Then

$$\begin{aligned} \dot{\tilde{q}}_i &= \tilde{p}_i, \\ \dot{\tilde{p}}_i &= u_i, \quad i = 1, \dots, N. \end{aligned} \quad (7.17)$$

By the definition of $\psi(\|q_{ij}\|)$, we have

$$\psi(\|q_{ij}\|) = \psi(\|\tilde{q}_{ij}\|), \quad (7.18)$$

where $\tilde{q}_{ij} = \tilde{q}_i - \tilde{q}_j$. Thus, the control input (7.15) for agent i can be rewritten as

$$\begin{cases} u_i = -\sum_{j \in N_i(t)} (\nabla_{\tilde{q}_i} \psi(\|\tilde{q}_{ij}\|) - w_{ij}(y_i - y_j)) - h_i y_i, \\ y_i = PT\hat{x}_i + P\sum_{j \in N_i(t)} w_{ij}\tilde{q}_{ij} + Ph_i\tilde{q}_i, \\ \dot{\hat{x}}_i = T\hat{x}_i + \sum_{j \in N_i(t)} w_{ij}\tilde{q}_{ij} + h_i\tilde{q}_i, \end{cases} \quad (7.19)$$

and the positive semi-definite energy function (7.16) can be rewritten as

$$U = \frac{1}{2} \sum_{i=1}^N \left(\sum_{j \in N_i(t)} \psi(\|\tilde{q}_{ij}\|) + \tilde{p}_i^T \tilde{p}_i \right) + \frac{1}{2} \dot{\hat{x}}^T (I_N \otimes P) \dot{\hat{x}}. \quad (7.20)$$

Similar to the proof of part (i) of Theorem 7.1, the time derivative of $U(t)$ in $[t_{k-1}, t_k)$ is obtained as

$$\begin{aligned} \dot{U}(t) &= \frac{1}{2} \sum_{i=1}^N \sum_{j \in N_i} \dot{\psi}(\|\tilde{q}_{ij}\|) + \sum_{i=1}^N \tilde{p}_i^T u_i + \frac{1}{2} \ddot{\hat{x}}^T (I_N \otimes P) \dot{\hat{x}} + \frac{1}{2} \dot{\hat{x}}^T (I_N \otimes P) \ddot{\hat{x}} \\ &= \sum_{i=1}^N \tilde{p}_i^T \sum_{j \in N_i} \nabla_{\tilde{q}_i} \psi(\|\tilde{q}_{ij}\|) \\ &\quad - \sum_{i=1}^N \tilde{p}_i^T \left(\sum_{j \in N_i(t)} \nabla_{\tilde{q}_i} \psi(\|\tilde{q}_{ij}\|) + \sum_{j \in N_i(t)} w_{ij}(y_i - y_j) + h_i y_i \right) \\ &\quad + \frac{1}{2} \dot{\hat{x}}^T (I_N \otimes T^T) (I_N \otimes P) \dot{\hat{x}} + \frac{1}{2} \tilde{p}^T (L^T \otimes I_n) (I_N \otimes P) \dot{\hat{x}} \\ &\quad + \frac{1}{2} \tilde{p}^T (H_N^T \otimes I_n) (I_N \otimes P) \dot{\hat{x}} + \frac{1}{2} \dot{\hat{x}}^T (I_N \otimes P) (I_N \otimes T) \dot{\hat{x}} \\ &\quad + \frac{1}{2} \dot{\hat{x}}^T (I_N \otimes P) (L \otimes I_n) \tilde{p} + \frac{1}{2} \dot{\hat{x}}^T (I_N \otimes P) (H_N \otimes I_n) \tilde{p} \\ &= -\tilde{p}^T ((L + H_N) \otimes I_n) y + \tilde{p}^T ((L + H_N) \otimes I_n) (I_N \otimes P) \dot{\hat{x}} \\ &\quad - \frac{1}{2} \dot{\hat{x}}^T (I_N \otimes Q) \dot{\hat{x}} \\ &= -\frac{1}{2} \dot{\hat{x}}^T (I_N \otimes Q) \dot{\hat{x}} \leq 0, \end{aligned} \quad (7.21)$$

where $H_N = \text{diag}(h_1, \dots, h_N)$, which implies that

$$U(t) \leq U(t_{k-1}) < \infty \quad \text{for } t \in [t_{k-1}, t_k), \quad k = 1, 2, \dots \quad (7.22)$$

Therefore, no distance of existing edges will tend to r for $t \in [t_{k-1}, t_k)$, which also implies that no existing edges will be lost before time t_k , and $U(t_k)$ is finite. Since $G(0)$ is connected and no edges in $E(0)$ will be lost, $G(t)$ will remain to be connected for all $t \geq 0$.

We now prove parts (ii) and (iii) of Theorem 7.2.

Similar to the proof of part (ii) of Theorem 7.1, the set

$$\Omega = \{\tilde{q} \in D_g, \tilde{p}, \hat{x} \in \mathbf{R}^{Nn} \mid U(\tilde{q}, \tilde{p}, \hat{x}) \leq U_{\max}\}, \quad (7.23)$$

is compact on the time interval (t_k, ∞) , where $\widehat{\tilde{q}} = [\tilde{q}_{11}^T, \dots, \tilde{q}_{1N}^T, \dots, \tilde{q}_{N1}^T, \dots, \tilde{q}_{NN}^T]^T$, $\tilde{p} = [\tilde{p}_1^T, \tilde{p}_2^T, \dots, \tilde{p}_N^T]^T$, $U_{\max} \triangleq U_0 + (\frac{N(N-1)}{2} - (N-1))\psi(\|r - \varepsilon\|)$ and $D_g = \{\widehat{\tilde{q}} \in \mathbf{R}^{N^2n} \mid \|\tilde{q}_{ij}\| \in [\min\{\psi^{-1}(U_{\max})\}, \max\{\psi^{-1}(U_{\max})\}], \forall (i, j) \in E(t)\}$. Therefore, from LaSalle's invariance principle [8], we have

$$\dot{U} = -\frac{1}{2}\dot{\hat{x}}^T(I_N \otimes Q)\dot{\hat{x}} = 0, \quad (7.24)$$

which implies that $\dot{\hat{x}} = 0$ and $\ddot{\hat{x}} = 0$. From (7.15), we have

$$\ddot{\hat{x}}_i = T\dot{\hat{x}}_i + \sum_{j \in N_i(t)} w_{ij}(\tilde{p}_i - \tilde{p}_j) + h_i \tilde{p}_i, \quad i = 1, \dots, N, \quad (7.25)$$

which implies that $((L + H_N) \otimes I_n)\tilde{p} = 0$. Since the dynamic network is connected all the time and one agent is the informed agent, from Lemma 3 in [12], the symmetric matrix $(L + H_N) \otimes I_n$ is positive definite, which implies $\|\tilde{p}_i\| \rightarrow 0$ for all i as $t \rightarrow \infty$, hence $\|p_i - p_\gamma\| \rightarrow 0$ for all i as $t \rightarrow \infty$.

From the previous analysis, we can see that, in steady state,

$$\dot{p}_i = \dot{p}_\gamma = 0, \quad i = 1, \dots, N, \quad (7.26)$$

which implies that $u = 0$. Similar to the proof of part (iii) of Theorem 7.1, we have

$$u = - \begin{bmatrix} \sum_{j \in N_1(t)} \nabla_{q_1} \psi(\|q_{1j}\|) \\ \vdots \\ \sum_{j \in N_N(t)} \nabla_{q_N} \psi(\|q_{Nj}\|) \end{bmatrix} = 0. \quad (7.27)$$

Thus, almost every final configuration locally minimizes each agent's global potential $\sum_{j \in N_i(t)} \nabla_{q_i} \psi(\|q_{ij}\|)$.

Finally, we prove part (iv) of Theorem 7.2. From the earlier analysis, we recall that $U(\widehat{\tilde{q}}, \tilde{p}, \hat{x}) \leq U_{\max}$. The results then follow by the same arguments as that used in the proof of part (iv) of Theorem 7.1. This completes the proof of Theorem 7.2. \square

7.1.4 Simulation Study

All the simulations are performed with ten agents moving in the plane whose initial positions and velocities are randomly chosen within $[0, 7] \times [0, 7]$ and $[0, 1] \times [0, 1]$, respectively. We restrict the initial interaction network be connected. In simulations, we choose the influencing/sensing radius $r = 4$, the parameter $\varepsilon = 0.5$, the weights $w_{ij} = 1$ for all $i, j \in V$, the matrices

$$T = -0.5 \begin{bmatrix} 1 & 0 \\ 0 & 1 \end{bmatrix}, \quad P = \begin{bmatrix} 1 & 0 \\ 0 & 1 \end{bmatrix},$$

and the potential function (7.4) for flocking algorithm (7.2).

In Fig. 7.2, we compare the flocking algorithm (7.2) proposed in this work with the flocking algorithm in [5]. Figure 7.2(a) shows the initial states of the agents;

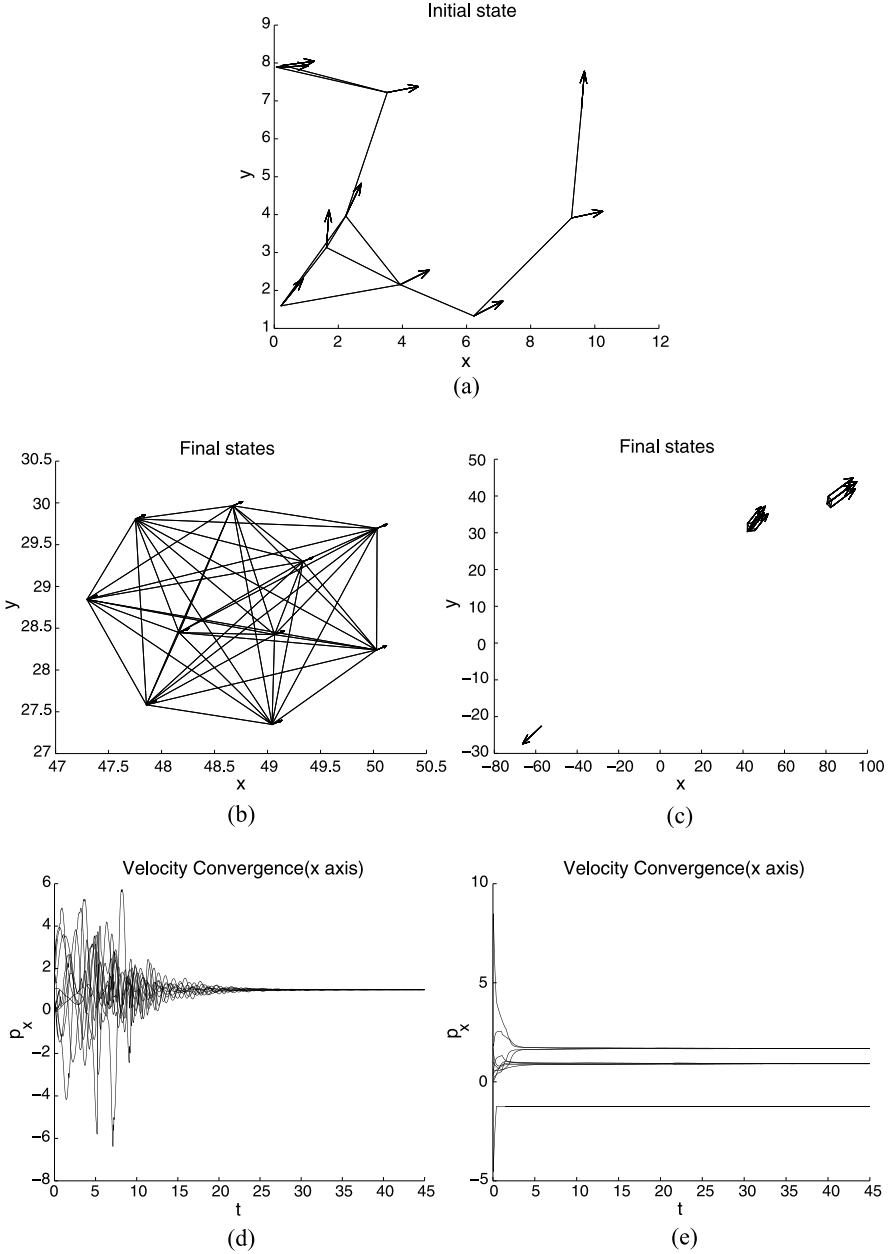


Fig. 7.2 [7] Flocking of ten agents applying the algorithm (7.2) and the algorithm in [5]

Figures 7.2(b)–(c) depict the configuration and velocities of the group of agents at $t = 45$ obtained by the algorithm (7.2) and the algorithm in [5], respectively; Figures 7.2(d)–(e) show the curves of velocities for the x -axis by the algorithm (7.2)

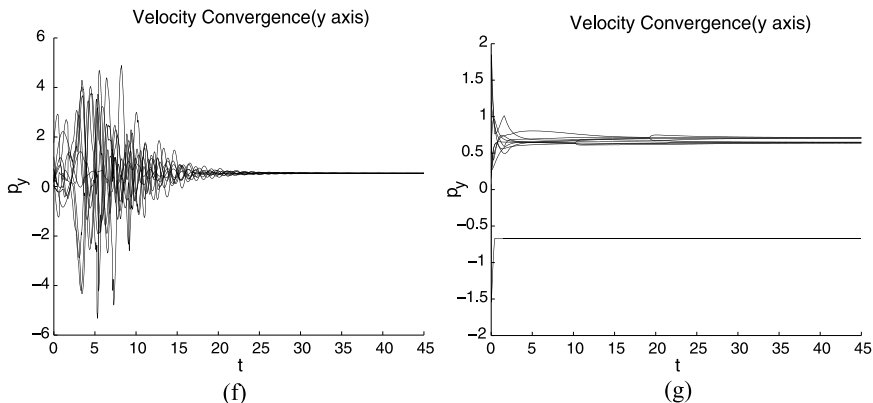


Fig. 7.2 (Continued)

here and the algorithm in [5], respectively; Figures 7.2(f)–(g) show the curves of velocities for the y -axis by the algorithm (7.2) here and the algorithm in [5], respectively. We can see that algorithm (7.2) here produces flocking behavior, while the algorithm in [5] leads to fragmentation. This is due to the fact that the connectivity of the initial network cannot guarantee the connectivity of the network during the evolution by using the algorithm in [5].

If we directly use the algorithm (7.2) about without the estimate vector y to control a group of mobile autonomous agents, the control inputs can be simply written as follows:

$$u_i = - \sum_{j \in N_i(t)} \nabla_{q_i} \psi(\|q_{ij}\|), \quad i = 1, \dots, N. \quad (7.28)$$

Under the same initial states of the ten agents, simulation results for the flocking algorithm (7.2), the flocking algorithm (7.15), and the control inputs (7.28) are shown in Fig. 7.3. The initial position and velocity of the virtual leader are set at $q_\gamma(0) = [0, 0]^T$ and $p_\gamma(0) = [2, 2]^T$. Figure 7.3(a) shows the initial states of the agents; Figures 7.3(b)–(d) depict the configuration and velocities of the group of agents at $t = 45$ obtained by the algorithm (7.2), the algorithm (7.15), and the control inputs (7.28), respectively; Figures 7.3(e)–(g) show the curves of velocities for the x -axis by the algorithm (7.2), the algorithm (7.15), and the control inputs (7.28), respectively; Figures 7.3(h)–(j) show the curves of velocities for the y -axis by the algorithm (7.2), the algorithm (7.15), and the control inputs (7.28), respectively. We can see that all agents reach a common velocity by using the flocking algorithm (7.2), and attain a desired velocity by using the flocking algorithm (7.15). However, without the estimate vector y , the agents may not achieve velocity consensus.

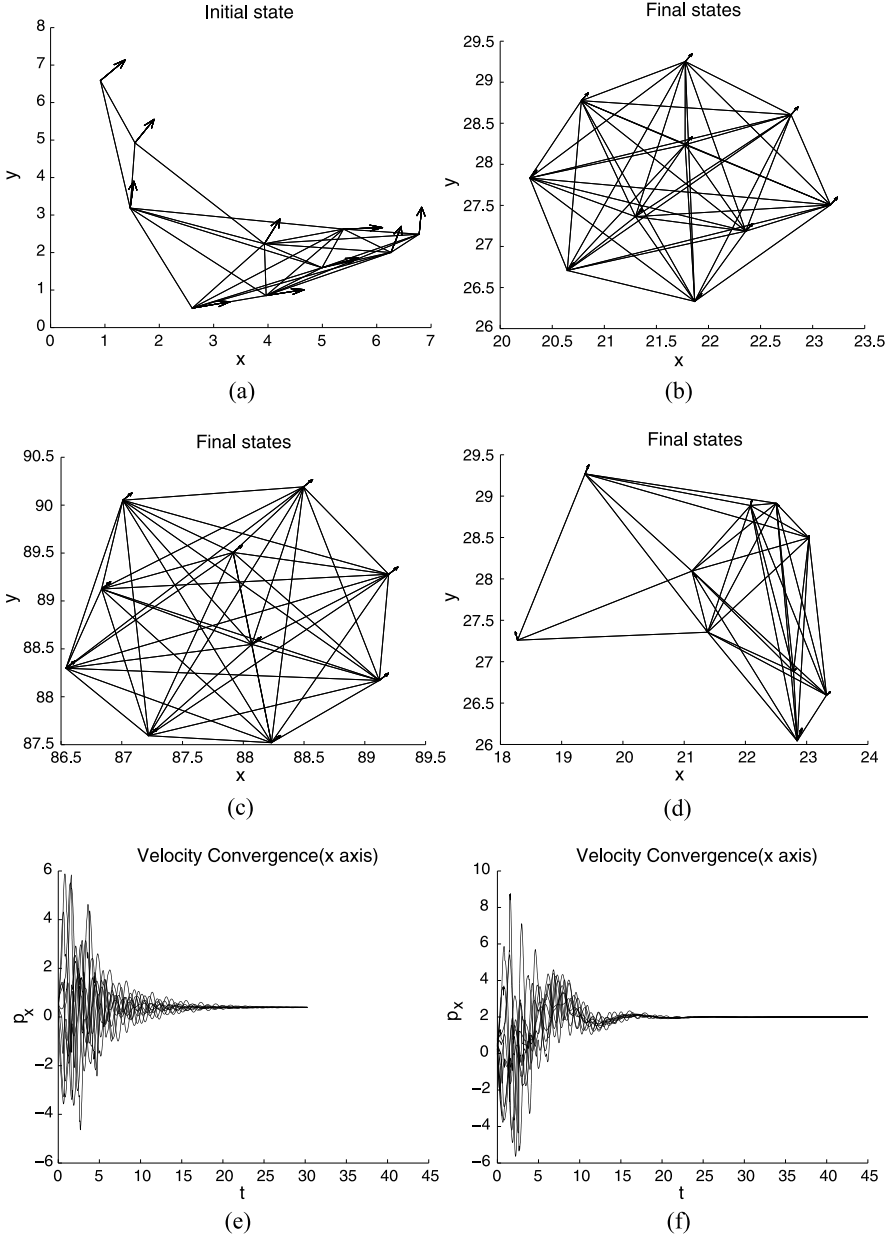


Fig. 7.3 [7] Flocking of ten agents applying the algorithm (7.2), the algorithm (7.15) and the control inputs (7.28)

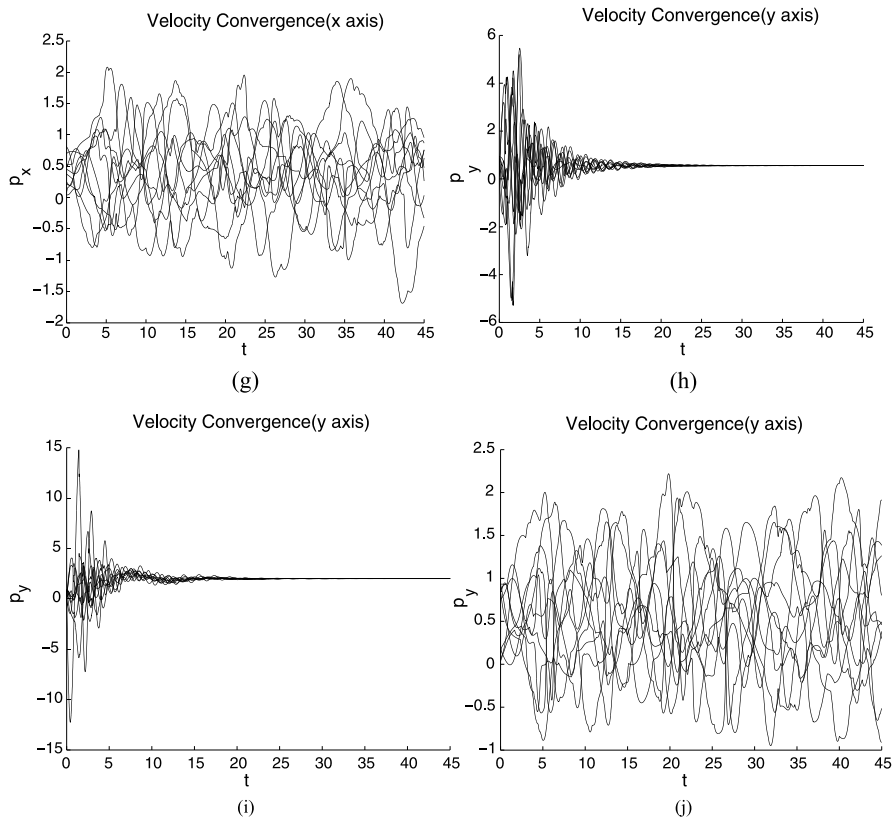


Fig. 7.3 (Continued)

7.2 Adaptive Flocking of Multiple Agents Governed by Nonlinear Dynamics

Recently, more and more works turned to studying the flocking of multiple agents governed by nonlinear dynamics because this situation is more realistic. In [13], a flocking algorithm for multi-agent systems with fixed topologies and nonlinear dynamics based on pseudo-leader mechanism was proposed. In [14], a flocking problem for multiple agents governed by nonlinear dynamics with a virtual leader was investigated, and an adaptive flocking algorithm was proposed. Under the assumption that the initial network is connected, all the agents in multi-agent systems can asymptotically synchronize with the virtual leader. In some existing works, such as [13, 14], second-order systems with nonlinear intrinsic dynamics depending only on velocity information for the agent were investigated. In [13–15], a global Lipschitz-like condition was used to explore the flocking problem, and for the second-order consensus problem [16, 17] such a condition was also used.

However, the nonlinear intrinsic dynamics of a system depending on both position and velocity information is more rational in reality. For the generality of systems, in this subsection, a system consisting of agents whose dynamics depends on both position and velocity information is taken into consideration. Moreover, many nonlinear systems cannot satisfy the global Lipschitz-like condition, and they are only locally Lipschitz, for example the Lorenz system and the Chen system. In this section, a local Lipschitz condition is presented for multi-agent systems with local Lipschitz nonlinearity. And then, an adaptive flocking algorithm is proposed to achieve the control objective without any information on the dynamics of the agents.

7.2.1 Preliminaries and Problem Statement

Consider a multi-agent system with N agents, labeled as $1, \dots, N$. The dynamics of each agent is characterized by

$$\begin{aligned}\dot{q}_i &= p_i \\ \dot{p}_i &= f(p_i, q_i) + u_i, \quad i = 1, \dots, N,\end{aligned}\tag{7.29}$$

where $q_i \in \mathbf{R}^n$, $p_i \in \mathbf{R}^n$ are the position vector and the velocity vector of the i th agent, respectively, $f(q_i, p_i) = (f_1(q_i, p_i), f_2(q_i, p_i), \dots, f_n(q_i, p_i))^T \in \mathbf{R}^n$ is the i th agent's intrinsic nonlinear dynamics, and $u_i \in \mathbf{R}^n$ is the control input.

A virtual leader is taken into consideration in our approach, and its dynamics is characterized by

$$\begin{aligned}\dot{q}_r &= p_r, \\ \dot{p}_r &= f(q_r, p_r),\end{aligned}\tag{7.30}$$

where $q_r, p_r \in \mathbf{R}^n$ are respectively the leader's position and velocity vector. An assumption has been made in this paper that the virtual leader and the agents have the same intrinsic dynamics.

Remark 7.1 It should be noted that we choose the dynamics in the form of $f(q_i, p_i)$ instead of $f(p_i)$ selected in some existing works, and obviously, this is more general and rational.

In this flocking problem for multi-agent systems, the aims of designing the control law are stated as follows:

- (i) $\lim_{t \rightarrow \infty} \|p_i(t) - p_r(t)\| = 0$ for any $i = 1, 2, \dots, N$.
- (ii) The distance between any two agents is stabilized asymptotically.
- (iii) There are no collisions among the systems.

Assumption 7.1 The nonlinear function f in system (7.29) is locally Lipschitz, that is, for any compact set $S \in \mathbf{R}^{Nn}$, there exist a positive constant matrix $B(S, N(0))$ whose elements depend on the space and the initial network $N(0)$, and a constant $\delta(S) > 0$ whose values depend on the space S such that

$$\begin{aligned}\tilde{y}^T \tilde{f}(x, y) &\leq \tilde{y}^T (B(S, N(0)) \otimes I_n) \tilde{x} + \delta(S) \|\tilde{y}\|^2, \\ \forall \tilde{x} = x - x_r, \tilde{y} = y - y_r \in S,\end{aligned}\quad (7.31)$$

where $\tilde{f}(x, y) = f(x, y) - f(x_r, y_r)$ and $B(S, N(0))$ is an $N \times N$ matrix whose element b_{ij} satisfies that when $i \neq j$, $b_{ij} < 0$ if there is an edge between agent i and agent j in the initial network, while $b_{ij} = 0$ otherwise. $b_{ii} = -\sum_{j=1, j \neq i}^N b_{ij}$.

Remark 7.2 The local Lipschitz condition is weaker than the global Lipschitz condition. However, for some specific systems, the global Lipschitz condition may not hold. It is clear that if the Jacobian matrix of $f(x, y)$ is continuous for any $x \in \mathbf{R}^n$, $y \in \mathbf{R}^{Nn}$, $f(x, y)$ is at least locally Lipschitz. Accordingly, the local Lipschitz condition is more reasonable.

Assumption 7.2 The virtual leader's signal (q_r, p_r) is bounded, that is, there exists a compact set $S = S(q_r(0), p_r(0)) \subset \mathbf{R}^n \times \mathbf{R}^n$ such that the trajectory of system (7.30) starting from $(q_r(0), p_r(0))$ is always in the set S .

In this section, the connectivity-preserving rules of the network and the potential function $\Psi(\|q_i - q_j\|)$ are the same as those in Sect. 7.1, and we choose $\varepsilon = R$.

7.2.2 Main Results

Let

$$\begin{aligned}d_0 &= \frac{1}{2} \sum_{i=1}^N \sum_{j \in N_i(0)}^N \Psi(\|q_i(0) - q_j(0)\|), \\ \tilde{d}_0 &= \frac{1}{2} \sum_{i=1}^N \|p_r(0) - p_i(0)\|^2,\end{aligned}$$

and say a space is formed:

$$\begin{aligned}S(d_0, \tilde{d}_0, q_r, p_r) &= \left\{ q, p \in \mathbf{R}^{nN} \left| \frac{1}{2} \sum_{i=1}^N \sum_{j \in N_i(t)}^N \Psi(\|q_i - q_j\|) + \frac{1}{2} \sum_{i=1}^N \|q_r - q_i\|^2 \right. \right. \\ &\quad \left. \left. \leq \sigma_1 d_0 + \sigma_2 \tilde{d}_0 \right\},\end{aligned}$$

where $q = (q_1^T, q_2^T, \dots, q_N^T)^T$, $p = (p_1^T, p_2^T, \dots, p_N^T)^T$, and σ_1, σ_2 are scalars to be chosen later. Then, the local Lipschitz condition is that there exist a constant matrix $B(S, G(0))$ whose elements depend on both the space S and the initial network $G(0)$ and constant $\delta(S) > 0$ depending on the space S such that, for any $\tilde{q} = q_i - q_r \in S(d_0, \tilde{d}_0, q_r, p_r)$ and $\tilde{p} = p_i - p_r \in S(d_0, \tilde{d}_0, q_r, p_r)$, $\tilde{p}^T(\tilde{f}(q, p)) \leq \tilde{p}^T(B(S, G(0)) \otimes I_n) \tilde{q} + \delta(S) \|\tilde{p}\|^2$, where $\tilde{f}(q, p) = f(q, p) -$

$f(q_r, p_r)$, $B(S, G(0))$ is an $N \times N$ matrix whose element b_{ij} satisfies that when $i \neq j$,

$$b_{ij} \begin{cases} < 0 & \text{if } (i, j) \in E(0), \\ = 0, & \text{otherwise,} \end{cases}$$

while $b_{ii} = -\sum_{j=1, j \neq i}^N b_{ij}$.

The control law is designed as:

$$\begin{aligned} u_i &= - \sum_{j \in N_i(t)} \nabla_{q_i} \Psi(\|q_i - q_j\|) - \sum_{j \in N_i(t)} m_{ij}(q_i - q_j) \\ &\quad - \sum_{j \in N_i(t)} \tilde{m}_{ij}(p_i - p_j) - h_i c_i(q_i - q_r) - h_i \tilde{c}_i(p_i - p_r), \\ \dot{m}_{ij} &= k_{ij}(p_i - p_j)^T(q_i - q_j), \\ \dot{\tilde{m}}_{ij} &= \tilde{k}_{ij}(p_i - p_j)^T(p_i - p_j), \\ \dot{c}_i &= w_i(p_i - p_r)^T(q_i - q_r), \\ \dot{\tilde{c}}_i &= \tilde{w}_i(p_i - p_r)^T(p_i - p_r), \end{aligned} \quad (7.32)$$

where $N_i(t)$ is the set of agents that can connect with agent i at time t , $m_{ij} > 0$ and $\tilde{m}_{ij} > 0$ respectively represent the position and velocity coupling strengths satisfying $m_{ij} = m_{ji}$, $\tilde{m}_{ij} = \tilde{m}_{ji}$, and c_i, \tilde{c}_i are the position and velocity navigation feedback weights, respectively. Suppose that there are only a small fraction of agents that can get the information on the virtual leader, and $h_i = 1$ if the i th agent is informed, while $h_i = 0$ otherwise.

An energy function $V(t)$ is proposed to demonstrate the flocking results:

$$\begin{aligned} V(q, p, q_r, p_r, m, \tilde{m}, c, \tilde{c}) &= \frac{1}{2} \sum_{i=1}^N \sum_{j \in N_i(t)} \Psi(\|q_i - q_j\|) + \frac{1}{2} \sum_{i=1}^N (p_i - p_r)^T(p_i - p_r) \\ &\quad + \frac{1}{2} \sum_{i=1}^N \sum_{j \in N_i(t)} \frac{(m_{ij} - \theta_{ij})^2}{2k_{ij}} + \frac{1}{2} \sum_{i=1}^N \sum_{j \in N_i(t)} \frac{(\tilde{m}_{ij} - \tilde{\theta})^2}{2\tilde{k}_{ij}} \\ &\quad + \frac{1}{2} \sum_{i=1}^N h_i \frac{(c_i - \sum_{j \in N_i(t)} \theta_{ij})^2}{k_i} + \frac{1}{2} \sum_{i=1}^N h_i \frac{(\tilde{c}_i - \tilde{\theta})^2}{\tilde{k}_i}, \end{aligned} \quad (7.33)$$

where θ_{ij} is the element of the $N \times N$ matrix Θ , which satisfies that when $i \neq j$, $\theta_{ij} = \theta_{ji} \begin{cases} > 0 & \text{if } (i, j) \in E(0), \\ = 0, & \text{otherwise} \end{cases}$ and $\theta_{ii} = 0$, $L(\Theta) = D(\Theta) - \Theta$, where $D(\Theta) = \text{diag}(D_1, D_2, \dots, D_N)$ with $D_i = \sum_{j=1, j \neq i}^N \theta_{ij}$, and $L(\Theta) + H D(\Theta) = B(S, G(0))$.

Theorem 7.3 Consider a system of N agents with dynamics (7.29) and a virtual leader with dynamics (7.30), and the controller (7.32) is applied. Suppose that Assumptions 7.1 and 7.2 hold, and the initial network $G(0)$ is connected.

- (i) $G(t)$ will not change for all $t \geq 0$.
(ii) For all $t \in [0, +\infty)$, the combined trajectories of the agents and the control parameters $(q, p, m, \tilde{m}, c, \tilde{c})$ in (7.29), (7.30), and (7.32) belong to a compact hyper-ellipsoid

$$\begin{aligned} & \Omega(\sigma_1 d_0, \sigma_2 \tilde{d}_0, \theta, \tilde{\theta}, p_r, q_r) \\ &= \{(q, p, m, \tilde{m}, c, \tilde{c}) \in \mathbf{R}^{Nn} \times \mathbf{R}^{Nn} \times \mathbf{R}^{NN} \times \mathbf{R}^{NN} \times \mathbf{R}^N \times \mathbf{R}^N | \\ & \quad V < \sigma_1 d_0 + \sigma_2 \tilde{d}_0\}, \end{aligned} \quad (7.34)$$

where σ_1 and σ_2 are scalars satisfying $\sigma_1 > 1$, $\sigma_2 > 1$, if the initial value is selected from

$$\begin{aligned} & \Omega_0(\sigma_1 d_0, \sigma_2 \tilde{d}_0, \theta, \tilde{\theta}, p_r, q_r) \\ &= \{(q, p, m, \tilde{m}, c, \tilde{c}) \in \mathbf{R}^{Nn} \times \mathbf{R}^{Nn} \times \mathbf{R}^{NN} \times \mathbf{R}^{NN} \times \mathbf{R}^N \times \mathbf{R}^N | \\ & \quad V(0) < \sigma_1 d_0 + \sigma_2 \tilde{d}_0\}. \end{aligned} \quad (7.35)$$

Proof Let $q_{ir} = q_i - q_r$, $p_{ir} = p_i - p_r$, $q_{ij} = q_i - q_j = q_{ir} - q_{jr}$, $p_{ij} = p_i - p_j = p_{ir} - p_{jr}$. Then (7.32) can be rewritten as

$$\begin{aligned} u_i &= - \sum_{j \in N_i(t)} \nabla_{q_{ir}} \Psi(\|q_{ij}\|) - \sum_{j \in N_i(t)} m_{ij}(q_{ir} - q_{jr}) \\ & \quad - \sum_{j \in N_i(t)} \tilde{m}_{ij}(p_{ir} - p_{jr}) - h_i c_i q_{ir} - h_i \tilde{c}_i p_{ir}, \\ \dot{m}_{ij} &= k_{ij}(p_{ir} - p_{jr})^T (q_{ir} - q_{jr}), \\ \dot{\tilde{m}}_{ij} &= \tilde{k}_{ij}(p_{ir} - p_{jr})^T (p_{ir} - p_{jr}), \\ \dot{c}_i &= w_i p_{ir}^T q_{ir}, \\ \dot{\tilde{c}}_i &= \tilde{w}_i p_{ir}^T p_{ir}. \end{aligned} \quad (7.36)$$

Then, the energy function (7.33) can be rewritten as

$$\begin{aligned} & V(q, p, q_r, p_r, m, \tilde{m}, c, \tilde{c}) \\ &= \frac{1}{2} \sum_{i=1}^N \sum_{j \in N_i(t)} \Psi(\|q_{ij}\|) + \frac{1}{2} \sum_{i=1}^N p_{ir}^T p_{ir} \\ & \quad + \frac{1}{2} \sum_{i=1}^N \sum_{j \in N_i(t)} \frac{(m_{ij} - \theta_{ij})^2}{2k_{ij}} + \frac{1}{2} \sum_{i=1}^N \sum_{j \in N_i(t)} \frac{(\tilde{m}_{ij} - \tilde{\theta})^2}{2\tilde{k}_{ij}} \\ & \quad + \frac{1}{2} \sum_{i=1}^N h_i \frac{(c_i - \sum_{j \in N_i(t)} \theta_{ij})^2}{w_i} + \frac{1}{2} \sum_{i=1}^N h_i \frac{(\tilde{c}_i - \tilde{\theta})^2}{\tilde{w}_i}. \end{aligned} \quad (7.37)$$

Suppose that the graph $G(t)$ switches at time $t_k (k = 1, 2, \dots)$ which means that $G(t)$ is a fixed graph in each time interval $[t_{k-1}, t_k)$. Note that $V(0)$ is finite and time derivative of $V(t)$ in $[t_0, t_1)$ is shown as follows

$$\begin{aligned}
\dot{V} &= \sum_{i=1}^N p_{ir}^T \sum_{j \in N(t)} \nabla_{q_{ir}} \Psi(\|q_{ij}\|) + \sum_{i=1}^N p_{ir}^T (f(q_i, p_j) - f(q_r, p_r)) \\
&\quad - \sum_{i=1}^N p_{ir}^T \sum_{j \in N_i(t)} \nabla_{q_{ir}} \Psi(\|q_{ij}\|) - \sum_{i=1}^N p_{ir}^T \sum_{j \in N_i(t)} m_{ij} (q_{ir} - q_{jr}) \\
&\quad - \sum_{i=1}^N p_{ir}^T \sum_{j \in N_i(t)} \tilde{m}_{ij} (p_{ir} - p_{jr}) - \sum_{i=1}^N p_{ir}^T h_i c_i q_{ir} - \sum_{i=1}^N p_{ir}^T h_i \tilde{c}_i p_{ir} \\
&\quad + \frac{1}{2} \sum_{i=1}^N \sum_{j \in N_i(t)} (m_{ij} - \theta_{ij}) (p_{ir} - p_{jr})^T (q_{ir} - q_{jr}) \\
&\quad + \frac{1}{2} \sum_{i=1}^N \sum_{j \in N_i(t)} (\tilde{m}_{ij} - \tilde{\theta}) (p_{ir} - p_{jr})^T (p_{ir} - p_{jr}) \\
&\quad + \sum_{i=1}^N h_i \left(c_i - \sum_{j \in N_i(t)} \theta_{ij} \right) p_{ir}^T q_{ir} + \sum_{i=1}^N h_i (\tilde{c}_i - \tilde{\theta}) p_{ir}^T p_{ir} \\
&= \sum_{i=1}^N p_{ir}^T (f(q_i, p_j) - f(q_r, p_r)) - \sum_{i=1}^N p_{ir}^T \sum_{j \in N_i(t)} \theta_{ij} (q_{ir} - q_{jr}) \\
&\quad - \sum_{i=1}^N p_{ir}^T \sum_{j \in N_i(t)} \tilde{\theta} (p_{ir} - p_{jr}) - \sum_{i=1}^N h_i \sum_{j \in N_i(t)} \theta_{ij} p_{ir}^T q_{ir} - \sum_{i=1}^N h_i \tilde{\theta} p_{ir}^T p_{ir} \\
&\leq -\tilde{p}^T ((L(\Theta) + HD(\Theta) - B(S, G(0))) \otimes I_n) \tilde{q} \\
&\quad - \tilde{p}^T ((\tilde{\theta}(L(t) + H) - \delta(S)I_N) \otimes I_n) \tilde{p} \\
&= -\tilde{p}^T ((\tilde{\theta}(L(t) + H) - \delta(S)I_N) \otimes I_n) \tilde{p}.
\end{aligned}$$

Since $L(0) + H > 0$ [12], and with the condition $\tilde{\theta} \geq \frac{\delta(S)}{\lambda_{\min}(L(0)+H)}$, one has $\dot{V}(t) \leq 0$; therefore, the energy function $V(t)$ is non-increasing on $[t_0, t_1]$, which implies that $V(t) \leq V(0) < \infty$ for $t \in [t_0, t_1]$.

From the definition of the potential function, we have $\lim_{\|q_i - q_j\| \rightarrow R} \Psi \times (\|q_i - q_j\|) = +\infty$. Therefore, no distance of existing edges will tend to R for $t \in [t_0, t_1]$, which also implies that no existing edges will be lost before time t_1 . According to the network connectivity-preserving rules and the definition of the potential function, since we choose $\varepsilon = R$, if $\varphi(i, j)(t^-) = 0$, it is impossible to add a new edge between agent i and j , so no new edge will be added to the network, and then the associated potentials remain finite. Thus, $V(t_1)$ is finite.

Like in the above analysis, the time derivative of $V(t)$ in every $[t_{k-1}, t_k]$ is

$$V(t) \leq -\tilde{p}^T ((\tilde{\theta}(L(t) + H) - \delta(S)I_N) \otimes I_n) \tilde{p}.$$

By Lemma 4.3, it follows from $\tilde{\theta} \geq \frac{\delta(S)}{\lambda_{\min}(L(0)+H)}$ that

$$\tilde{\theta} \geq \frac{\delta(S)}{\lambda_{\min}(L(0)+H)} \geq \frac{\delta(S)}{\lambda_{\min}(L(t_{k-1})+H)}.$$

Then, it can be obtained that

$$V(t) \leq V_{k-1} < \infty \quad \text{for } t \in [t_{k-1}, t_k), k = 1, 2, \dots$$

Thus, no distance of existing edges will tend to R for $t \in [t_{k-1}, t_k)$ and no edges will be lost before t_k and $V(t_k)$ is finite.

Since $G(0)$ is connected, while no edge in $E(0)$ will be lost and no new edge can be added to $E(0)$, $G(t)$ will not change for all $t \geq 0$; then $G(t) = G(0)$, $L(t) = L(0)$.

Since $V(t) \leq V(0) < \infty$, we can draw the conclusion that if the initial value is selected from $\Omega_0(\sigma_1 d_0, \sigma_2 \tilde{d}_0, \theta, \tilde{\theta}, p_r, q_r)$, the combined trajectories of the agents and the control parameters $(q, p, m, \tilde{m}, c, \tilde{c})$ in (7.29), (7.30), and (7.32) belong to a compact hyper-ellipsoid $\Omega(\sigma_1 d_0, \sigma_2 \tilde{d}_0, \theta, \tilde{\theta}, p_r, q_r)$.

To ensure that the set $\Omega_0(\sigma_1 d_0, \sigma_2 \tilde{d}_0, \theta, \tilde{\theta}, p_r, q_r)$ is well defined, we choose $\sigma_1 > 1$ and $\sigma_2 > 1$. \square

Theorem 7.4 Consider a system of N agents with dynamics (7.29) and a virtual leader with dynamics (7.30). Suppose that the initial network $G(0)$ is connected, Assumptions 1 and 2 hold, and the initial value is as defined in (7.35). Then, when the controller (7.32) is applied, the following statements hold:

- (i) All agents move asymptotically move with the same velocity.
- (ii) Almost every final configuration locally minimizes each agent's global potential.
- (iii) Collisions among agents are avoided.

Proof All the lengths of edges are not longer than $\Psi^{-1}(V(0))$. Therefore, the set

$$\Omega' = \{(q, p, m, \tilde{m}, c, \tilde{c}) \in \Omega(\sigma_1 d_0, \sigma_2 \tilde{d}_0, \theta, \tilde{\theta}, p_r, q_r) \mid V \leq V(0)\}$$

is positively invariant.

Since $G(t)$ is connected and unchanged for all $t \geq 0$, it is clear that $\|q_{ir} - q_{jr}\| < (N-1)R$ for all i and j . Because $V(t) \leq V(0)$, one has $p_{ir}^T p_{ir} \leq 2V(0)$, $\|p_{ir}\| \leq \sqrt{2V(0)}$. Therefore, the set Ω is closed and bounded, and hence compact. In view of the fact that system (7.29) with control input (7.32) is an autonomous system for all $t \geq 0$, the LaSalle Invariance Principle [8] can be applied, so the corresponding trajectories will converge to the largest invariant set inside the region:

$$\Omega_f = \{(q, p, m, \tilde{m}, c, \tilde{c}) \in \Omega(\sigma_1 d_0, \sigma_2 \tilde{d}_0, \theta, \tilde{\theta}, p_r, q_r) \mid \dot{V} = 0\}.$$

From Lemma 4.1 and the fact that $\dot{V}(t) \leq 0$, $\dot{V} = 0$ if and only if $\tilde{p} = 0$, that is, $p_1 = p_2 = \dots = p_N = p_r$, so $\lim_{t \rightarrow \infty} \|p_i(t) - p_r(t)\| = 0$, all the agents move asymptotically with the same velocity.

Hence, one has

$$\begin{aligned}
\dot{p}_{ir} &= - \sum_{j \in N_i(t)} \nabla_{q_{ir}} \Psi(\|q_{ij}\|) - \sum_{j \in N_i(t)} m_{ij}(q_{ir} - q_{jr}) \\
&\quad - h_i c_i q_{ir} \\
&= - \sum_{j \in N_i(t)} \frac{\partial \Psi(\|q_{ij}\|)}{\partial \|q_{ij}\|} \frac{1}{\|q_{ij}\|} (q_i - q_j) \\
&\quad - \sum_{j \in N_i(t)} m_{ij}(q_{ir} - q_{jr}) - h_i c_i q_{ir} \\
&= 0.
\end{aligned}$$

Generally, unless the initial configuration of the agents is close enough to the global minimum, almost every final configuration locally minimizes each agent's global potential. From the definition of the potential function, it is obvious that

$$\lim_{\|q_{ij}(t)\| \rightarrow 0} \Psi(\|q_{ij}\|) = +\infty.$$

Although $V(t) \leq V(0)$ for all $t \geq 0$, collisions among agents are avoided. \square

7.2.3 Simulation Study

In this section, a numerical example is given to illustrate the effectiveness of our theoretical results. We take a group of ten agents which move in a three-dimensional space in this example. Consider the intrinsic nonlinear dynamic term $f(q, p)$ given as

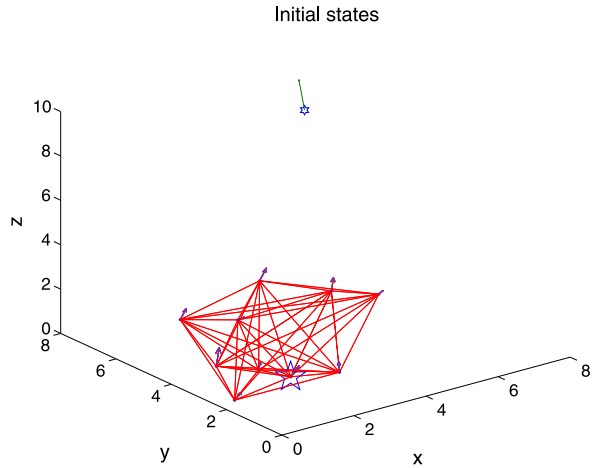
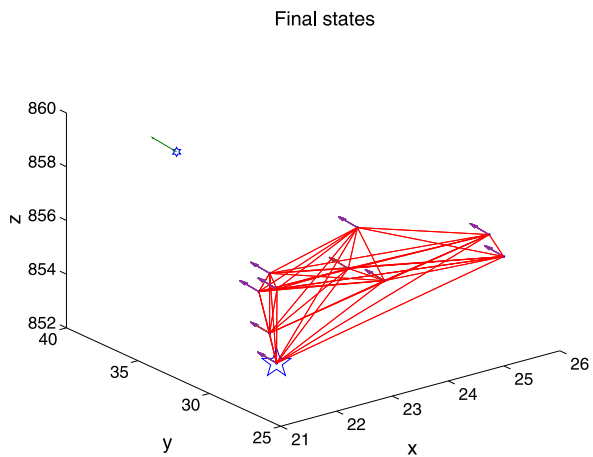
$$f(q, p) = \begin{pmatrix} \xi_1(p_y - p_x) - q_x \\ \xi_2 p_x - p_x p_z - p_y - q_y \\ p_x p_y - \xi_3 p_z - q_z \end{pmatrix},$$

where the parameters q, p are respectively defined as $q = [q_x, q_y, q_z]^T$, $p = [p_x, p_y, p_z]^T$. In particular, the parameters are chosen as $\xi_1 = 10$, $\xi_2 = 28$ and $\xi_3 = \frac{8}{3}$.

The initial positions and initial velocities of the ten agents are generated from $[0, 5] \times [0, 5] \times [0, 5]$ and $[0, 3] \times [0, 3] \times [0, 3]$ cubes, respectively. The initial position of the virtual leader is chosen as $q_r(0) = [6, 7, 8]^T$, while its initial velocity is $p_r(0) = [1, 2, 3]^T$. The initial edges are generated by $E(0) = \{(i, j) : \|q_i(0) - q_j(0)\| < r, i, j \in V\}$, where r is chosen as $r = 5$. Let $\varepsilon = R = 10$. The potential function is chosen as

$$\Psi(\|q_{ij}\|) = \begin{cases} +\infty, & \|q_{ij}\| = 0, \\ \frac{R}{\|q_{ij}\|(R - \|q_{ij}\|)}, & \|q_{ij}\| \in (0, R), \\ +\infty, & \|q_{ij}\| = R. \end{cases}$$

The initial value of the position coupling strengths is chosen as $m_{ij}(0) = 0$, with $k_{ij} = 0.1$ for all i and j , while the initial value of the velocity coupling strengths

Fig. 7.4 [18] Initial states**Fig. 7.5** [18] Final states

is selected as $\tilde{m}_{ij}(0) = 0$, with $\tilde{k}_{ij} = 0.1$ for all i and j . The initial weights on the position and velocity navigational feedbacks are chosen as $c_i(0) = 0$, $\tilde{c}_i(0) = 0$, respectively, with $w_i = 0.1$, $\tilde{w}_i = 0.1$ for all i . Suppose that there is only one agent that can get the information on the virtual leader, and without loss of generality, we assume that the first agent is informed and marked with a star, that is, $h_1 = 1$, and $h_i = 0$ for $i = 2, 3, \dots, 10$. The initial network is connected. Figure 7.4 shows the initial states of the ten agents and the virtual leader. Figure 7.5 depicts the final state of the network after 50 seconds with the control law (7.32). Figure 7.6 describes the velocity differences between every agent and the virtual leader on the x -axis, y -axis, and z -axis. In Fig. 7.6, it is illustrated that each agent finally moves with the same velocity as the virtual leader. Figures 7.7 and 7.8 show the weights of navigational feedbacks and coupling strengths of the position and velocity, respectively, and all converge to constants.

Fig. 7.6 [18] Velocity convergence

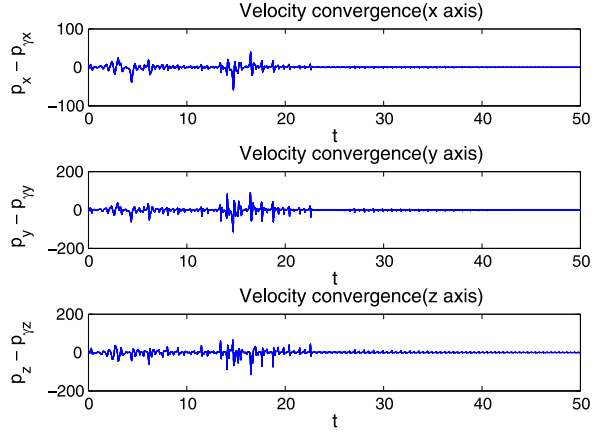
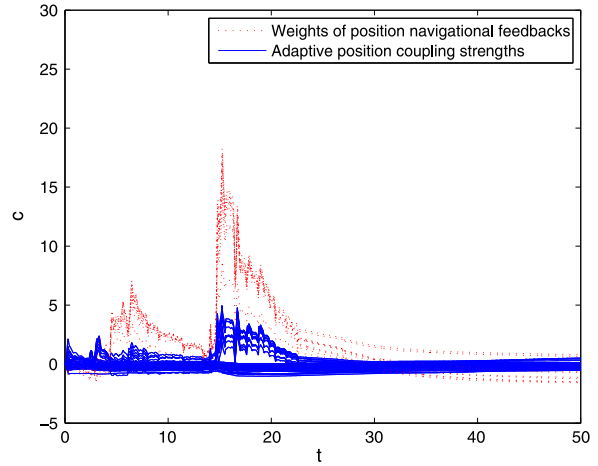


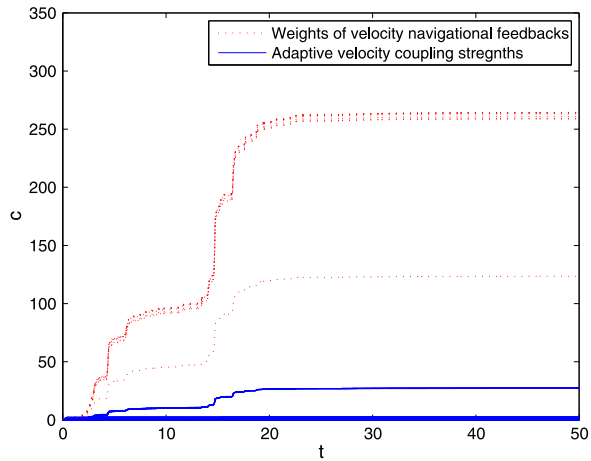
Fig. 7.7 [18] Weights of position navigational feedbacks and adaptive position coupling strengths



7.3 Conclusions and Notes

In this chapter, we have presented a connectivity-preserving flocking algorithm using only position measurements. Under the assumption that the initial network is connected, we have theoretically proved that the network remains connected all the time, all the agents asymptotically move with the same velocity, collision can be avoided between agents, and the final formation minimizes all agents' global potentials. Moreover, we have investigated the flocking algorithm with a virtual leader and shown that all agents can asymptotically attain a desired velocity even if only one agent in the team has access to the information about the virtual leader. Furthermore, we have investigated a flocking problem of multiple mobile agents with a virtual leader. Unlike most existing flocking algorithms, each agent here is subject to nonlinear dynamics. We have proposed a connectivity-preserving flocking algorithm, and showed that, under the assumption that the initial network is connected

Fig. 7.8 [18] Weights of velocity navigational feedbacks and adaptive velocity coupling strengths



and by introducing local adaptation strategies for both the weights on the velocity navigational feedback and the coupling strengths, all agents in the group can asymptotically synchronize with the virtual leader even if only one agent in the team has access to the information of the virtual leader, without requiring any knowledge of the agent dynamics.

References

1. Lizarralde F, Wen JT (1996) Attitude control without angular velocity measurements: a passivity approach. *IEEE Trans Autom Control* 41:468–472
2. Lawton JR, Beard RW (2002) Synchronized multiple spacecraft rotations. *Automatica* 38:1359–1364
3. Ren W (2008) On consensus algorithms for double-integrator dynamics. *IEEE Trans Autom Control* 53:1503–1509
4. Olfati-Saber R (2006) Flocking for multi-agent dynamic systems: algorithms and theory. *IEEE Trans Autom Control* 51:401–420
5. Tanner HG, Jadbabaie A, Pappas GJ (2007) Flocking in fixed and switching networks. *IEEE Trans Autom Control* 52:863–868
6. Zavlanos MM, Jadbabaie A, Pappas GJ (2007) Flocking while preserving network connectivity. In: *Proc the 46th IEEE conference on decision and control*, pp 2919–2924
7. Su H, Wang X, Chen G (2009) A connectivity-preserving flocking algorithm for multi-agent systems based only on position measurements. *Int J Control* 82:1334–1343
8. Khalil HK (2002) *Nonlinear systems*, 3rd edn. Prentice Hall, Upper Saddle River
9. Godsil C, Royle G (2001) *Algebraic graph theory*. Graduate texts in mathematics, vol. 207. Springer, New York
10. Shi H, Wang L, Chu TG (2006) Virtual leader approach to coordinated control of multiple mobile agents with asymmetric interactions. *Physica D* 213:51–65
11. Couzin ID, Krause J, Franks NR, Levin SA (2005) Effective leadership and decision-making in animal groups on the move. *Nature* 433:513–516
12. Hong Y, Hu J, Gao L (2006) Tracking control for multi-agent consensus with an active leader and variable topology. *Automatica* 42:1177–1182

13. Zhou J, Yu W, Wu X, Small M, Lu J (2012) Flocking of multi-agent dynamical systems based on pseudo-leader mechanism. *Syst Control Lett* 61:195–202
14. Su H, Chen G, Wang X, Lin Z (2010) Adaptive flocking with a virtual leader of multiple agents governed by nonlinear dynamics. In: The 29th Chinese control conference, pp 5827–5832
15. Yu W, Chen G, Cao M (2010) Distributed leader-follower flocking control for multi-agent dynamical systems with time-varying velocities. *Syst Control Lett* 59:543–552
16. Yu W, Chen G, Cao M, Kurths J (2010) Second-order consensus for multi-agent systems with directed topologies and nonlinear dynamics. *IEEE Trans Syst Man Cybern, Part B, Cybern* 40:881–891
17. Su H, Chen G, Wang X, Lin Z (2011) Adaptive second-order consensus of networked mobile agents with nonlinear dynamics. *Automatica* 47:368–375
18. Su H, Zhang N, Chen MZQ, Wang H, Wang X (2013) Adaptive flocking with a virtual leader of multiple agents governed by locally Lipschitz nonlinearity. *Nonlinear Anal, Real World Appl* 14:798–806

Index

A

Adaptive control, 1, 3, 45
Adaptive strategy, 8, 45–49, 52, 53
Adjacency matrix, 28, 38, 63, 64, 75, 114, 116, 118, 125, 139
Artificial potential function, 9
Asymptotic stability, 3, 138
Automatic control, 1
Average path length, 2, 54, 56

B

BA scale-free network, 17, 19, 29, 31
Barbalat's lemma, 49
Betweenness centrality, 7, 8
Bump function, 63, 128, 130, 131

C

Chaotic Chen's oscillator, 32
Chaotic Chua Circuit, 53, 90, 96
Chaotic Lorenz oscillator, 39
Cluster synchronization, vii, 2, 5–8, 45, 46, 52, 59
Clustering coefficient, 2, 54, 56
Cohesion, 111–113
Communication technology, 1
Complete synchronization, vii, 2, 4, 8, 17, 20, 45, 52
Complex dynamical networks, vii, 1–8, 17, 20, 27, 45, 46, 52, 59, 61, 89
Complex network theory, 2
Complex networked systems, vii, 1, 11
Computer technology, 1
Connectivity maintenance, 3, 10
Consensus vii, 1, 3, 6, 9–11, 61, 63, 67, 71–73, 78, 84, 86–91, 97, 99, 103–107, 109–112
Containment control, 10

Controllability, 8, 11, 39
Controllable regions, 2, 3, 8
ControlRank, 7, 17, 20, 21, 37, 42
Cooperative control, 1
Coordinated control, 1–3, 9, 99
Coupled harmonic oscillators, 61–63, 67, 70, 99
Coupled systems, 2
Coupling strengths, 4, 6, 8, 34, 35, 38, 45, 55–59, 61, 89, 91, 97, 99, 137, 152, 156–159

E

Eigenvalue, 8, 22, 23, 38, 39, 71, 78, 81, 141
Eigenvector, 22, 38, 39, 64, 116
Equilibrium point, 33, 34
ER random network, 17, 18, 29, 31

F

Finite-time control, 3
First-order dynamics, 89
Fixed topology, 112
Flocking, vii, 1, 3, 9–11, 61, 71, 89, 111, 112, 114, 115, 123, 128–135, 137–139, 143, 145–152, 158
Fragmentation, 71, 89, 147

G

Global Lipschitz condition, 149, 151
Global stability condition, 4

H

Heterogeneous
 influence network, vii, 103–107, 109, 110
 stationary states, 6, 45, 49, 52, 54, 59
Hierarchical control, 1
Homogeneous influence network, 108

Homogeneous stationary state, 4, 23, 26, 27, 38, 53, 56

Hub agents, 103, 106, 107, 109

Hurwitz matrix, 25, 138

Hysteresis, 10, 71, 72, 75, 94, 99, 141

I

Impulsive control, 3

Informed agent, 2, 3, 9, 11, 78–81, 86, 89–91, 96–98, 111, 112, 115, 116, 118–120, 122, 123, 128–131, 133–135, 143, 145

Inhibitory coupling, 6, 46, 47

Input saturation, 10

Intelligent control, 1

Intermittent control, 3

Intrinsic dynamics, 3, 4, 8, 89, 90, 99, 149, 150

Irreducible, 22, 23, 28, 39, 47, 48

J

Joint path, 115, 116, 119

K

Kronecker product, 22, 23, 75, 117, 141

L

Laplacian matrix, 38, 65, 71, 78, 120, 142

Largest desired cluster, 108

Lasalle Invariance Principle, 65, 67, 68, 95, 120, 126, 138, 155

Leader–follower approach, 89

Linear matrix inequalities, 5

Lipschitz constant, 21, 22, 25, 33

Lipschitz-like condition, 90, 149, 150

Local information, 1

Local stability conditions, 5, 25

Locally Lipschitz condition, 150, 151

Lyapunov

exponent, 25

function, 24, 64, 68, 139

M

Master stability function approach, 8

Maximum

overshoot, 61, 72, 73, 83, 85, 98, 99

positive LE, 26, 33

Mean square errors, 54, 56

Methodologies, 2, 3, 8

theory, 1

Minor matrix, 28, 38

Mobile sensor networks, 1

Multi-agent systems vii, 1–3, 9–11, 61, 89, 110–112, 137, 149, 150

Multiple interconnected systems, 1

N

Navigational feedback, 2, 61, 73, 89, 91, 98, 99, 112, 114, 137, 159

Neighborhood nonlinear dynamics, 10, 89, 90, 149, 150, 158

Network connectivity vii, 10, 11, 61, 63, 67, 70–72, 91, 99, 137, 154

Network theory, 1, 2

Network topology vii, 7, 8

Node-degree, 32

Nonnegative smooth pairwise potential function, 113

O

Obstacle avoidance, 111, 112

Opinion formation, 11

Optimal control, 1

Out-degree, 7, 17, 20, 21, 37–42

P

PageRank, 37–39

Passivity approach, 137, 138

Pinning control, vii, 1–11, 17, 23, 27, 28, 30–33, 35, 37, 42, 45, 46, 52, 55–59, 89, 107–109, 111

Pinning strategy, 3, 7, 37–42

Positive definite, 21–26, 64, 68, 90, 125, 126, 145

Positive semi-definite, 22–25, 75, 76, 79, 80, 93, 116–120, 124, 126, 139, 143, 144

Primitive power-law distribution, 19, 105

R

Radially unbounded single integrator dynamics, 64, 68

Random dynamical network, 7, 17, 31, 35

Randomly pinning scheme, 17, 107

Reducible Reynolds flocking model, 112

Rendezvous, 1, 10, 11, 71

Robust control, 1

S

Scale-free directed dynamical network, 7

Scale-free network, 2, 7, 17, 19, 20, 23, 29, 31, 32, 39, 40, 42

Schur complement, 38

Second-order consensus vii, 9, 10, 61, 71, 89, 90, 97, 99, 149

Second-order dynamics, 89

Selective strategies, 2, 3, 7, 32

Self-organization swarming, 1

Sensing radius, 63, 67, 70, 72, 74, 83, 96, 103, 128, 131, 145

Separation, 111, 112

Settling time, 61, 72, 73, 83, 85, 98, 99

Small-world network, 2, 54, 56
 Social learning, 11
 Social networks, 6, 11, 104, 110
 Specifically pinning scheme, 107
 Stochastic
 control, 1, 3
 matrix, 39, 112
 switching topology matrix, 3
 Strongly connected, 20, 37–39, 42, 106
 Subgraph, 65, 68, 69, 106, 120–122
 Surrounding control, 10
 Symmetric matrix, 22, 23, 25, 47, 145
 Synchronization, vii, 1–9, 17, 20, 29, 35, 38,
 41, 45, 46, 52, 58, 59, 61–63, 67, 70,
 71, 89, 90, 99

T

Time delays, 3, 5

U

Uniformly bounded, 66, 67, 70, 78, 116, 120
 Uniformly continuous, 49, 51

V

Velocity alignment, 11, 71, 114
 Vicsek model, 103–105
 Virtual control, 2, 7, 17, 27–31, 42
 Virtual leader, 9, 10, 61, 72, 73, 78, 79, 81,
 89–91, 93, 95–97, 99, 111–119,
 122–131, 133–135, 137, 138, 143,
 149–152, 155–159